UNCLASSIFIED

AD NUMBER

ADB006891

NEW LIMITATION CHANGE

TO

Approved for public release, distribution unlimited

FROM

Distribution authorized to U.S. Gov't. agencies only; Test and Evaluation; 22 April 1975. Other requests shall be referred to Manufacturing Technology Division LTM, Air Force Materials Laboratory, Wright-Patterson Air Force Base, Ohio 45433.

AUTHORITY

AFWAL1 ltr, 9 Aug 1984.

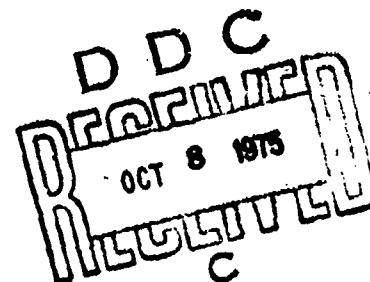## THIS PAGE IS UNCLASSIFIED

AD Boo 6891

AUTHORITY.

AFWAL

ltr: 9 Aug 84

ADB006891

SUPERPLASTIC FORMING OF TITANIUM STRUCTURES

ROCKWELL INTERNATIONAL CORPORATION
LOS ANGELES AIRCRAFT DIVISION
LOS ANGELES INTERNATIONAL AIRPORT
LOS ANGELES, CALIFORNIA 90009

D D C

OCT 8 1975

C

APRIL 1975

TECHNICAL REPORT AFML-TR-65-62

FINAL REPORT FOR PERIOD 1 FEBRUARY 1973 - 30 APRIL 1975

This final report was submitted by Rockwell International Corporation, Los Angeles Aircraft Division, Los Angeles, California, under Contract F33615-73-C-5005, Manufacturing Methods Project 194-3, "Superplastic Forming of Titanium Structures." Mr. John R. Williamson, AFML/LTM, was the laboratory monitor.

This technical report has been reviewed and is approved for publication.

John R. Williamson

JOHN R. WILLIAMSON
Project Monitor

FOR THE DIRECTOR

H. A. Johnson

H. A. JOHNSON
Chief, Metals Branch
Manufacturing Technology Division

SECURITY CLASSIFICATION OF THIS PAGE (When Data Entered)

REPORT DOCUMENTATION PAGE	READ INSTRUCTIONS BEFORE COMPLETING FORM

1. REPORT NUMBER	2. GOVT ACCESSION NO.	3. RECIPIENT'S CATALOG NUMBER
AML-TR-75-62		

4. TITLE (and Subtitle)	5. TYPE OF REPORT & PERIOD COVERED
SUPERPLASTIC FORMING OF TITANIUM STRUCTURES	Final Report 1 Feb 1973-30 Apr 1975
	6. PERFORMING ORG. REPORT NUMBER

7. AUTHOR(s)	8. CONTRACT OR GRANT NUMBER(s)
C. H. Hamilton J. A. Mills G. W. Stacher H. W. Li	F33615-73-C-5005

9. PERFORMING ORGANIZATION NAME AND ADDRESS	10. PROGRAM ELEMENT, PROJECT, TASK AREA & WORK UNIT NUMBERS
Rockwell International Corp Los Angeles Aircraft Division	78011F

11. CONTROLLING OFFICE NAME AND ADDRESS	12. REPORT DATE
Air Force Materials Laboratory Manufacturing Technology Division Wright-Patterson Air Force Base, Ohio	April 1975
	13. NUMBER OF PAGES 234 Plus Appendix

14. MONITORING AGENCY NAME & ADDRESS(if different from Controlling Office)	15. SECURITY CLASS. (of this report)
	Unclassified
	15a. DECLASSIFICATION/DOWNGRADING SCHEDULE

16. DISTRIBUTION STATEMENT (of this Report)

Distribution limited to U.S. Government Agencies only; Test and Evaluation Data; 22 April 1975. Other requests for this document must be referred to the Manufacturing Technology Division (LTM), Air Force Materials Laboratory, Wright-Patterson Air Force Base, Ohio 45433

17. DISTRIBUTION STATEMENT (of the abstract entered in Block 20, If different from Report)

18. SUPPLEMENTARY NOTES

19. KEY WORDS (Continue on reverse side if necessary and identify by block number)

Forming, superplastic, process parameters, titanium alloys, Sheet Metal, elevated Temperature, argon gas, pressure forming, strain-rate sensitivity, high-temperature tooling, die inserts, surface enrichment, superplastic forming dies, titanium fabrication

20. ABSTRACT (Continue on reverse side if necessary and identify by block number)

This program was directed at the establishment of superplastic forming of Ti-6Al-4V and Ti-6Al-2Sn-4Zr-2Mo alloys as a production process. Forming studies were pursued to evaluate the process parameters of superplastic forming and to extend the process to forming aircraft structural components.

(cont)

DD FORM 1 JAN 73 1473   EDITION OF 1 NOV 65 IS OBSOLETE

UNCLASSIFIED

SECURITY CLASSIFICATION OF THIS PAGE (When Data Entered)

20. ABSTRACT (Continued)

A detailed study was carried out on the effect of forming parameter variations with the two titanium alloys and two configurations. It was found that the degree of forming was directly related to time at pressure at elevated temperatures.

Optimum sealing techniques to eliminate atmospheric contamination of the titanium sheet material were established. Concurrently, low-cost tooling materials were evaluated with respect to their reaction with titanium.

In addition, 23 parts were formed in six different configurations to assess the forming parameters needed to fabricate components of varying shapes and dimensions. Each configuration was evaluated with respect to dimensional variation and surface enrichment due to tooling pickup and/or contaminated environment, and an evaluation was made of tensile, compression, and fatigue properties of the formed part as compared to as-received material.

The process was then extended to superplastic forming of Ti-6Al-4V and Ti-6Al-2Sn-4Zr-2Mo sheet metal alloys through the fabrication of full-scale complex structural configurations. A total of 20 full-scale formed parts was produced utilizing gas pressure forming at elevated temperatures. Variation in part configuration caused attendant variations in process parameters, but both titanium alloys on the same configuration utilized similar processing. Structural testing was accomplished on each configuration and alloy showing the compatibility of superplastic formed parts with aircraft structural integrity requirements.

Substantial cost savings were shown to be possible through the use of superplastic forming of titanium sheet metal by reducing overall fabrication time and by providing the capability to eliminate assemblies and producing simpler, more efficient, monolithic structure.

SUMMARY

This was a 24-month manufacturing methods program to establish superplastic forming as a titanium production process. It was demonstrated that superplastic forming can be used to fabricate complex titanium parts requiring large tensile elongations that could not be formed by conventional processes.

The purpose of this program was to establish production material/process interrelationships for the superplastic process and to optimize these parameters in relation to manufacturing producibility, cost, and structural performance. The metallurgical and mechanical property variations permitted by commercially available titanium sheet and their relationship to process parameters, effects of the process or the material, forming capabilities and limits, process techniques and control requirements, and techniques for establishing and accurately predciting parameters for specific part configurations have been established.

The program was developed and conducted in three phases.

PHASE I - PRODUCTION PARAMETERS

The phase I activity was directed toward understanding the range of superplastic properties available in commercial Ti-6Al-4V sheet, relationship to the metallurgical condition, part configurations producible, resulting characteristics, and mechanical properties. In addition, other process factors such as tooling compatibility and surface protection methods were also developed.

Six different heats of Ti-6Al-4V (MIL-T-9046) were evaluated for metallurgical condition, and the stress versus strain rate properties of these materials were established in the superplastic temperature range (1550° F to below the beta transus). From these data, it was observed that four of the heats were highly superplastic, one was borderline (being highly superplastic in only one direction), and one was questionable (being more superplastic than conventional materials, but considerably inferior to the other heats). The microstructure was correlated with these results, and metallographic guidelines were established for selecting a superplastic material. From these data, processing temperature was selected to be 1,700° F, with a significant latitude in usable temperature range (e.g., 1,650° to 1,750° F).

Tooling compatibility studies were conducted, and a range of iron-base alloys low in nickel content and containing moderate carbon were demonstrated to be suitable for use with Ti-6Al-4V at the process temperatures used. Environmental control methods were developed to protect the titanium alloy

surfaces from atmospheric contamination during the high-temperature processing. Sealing methods between the titanium and tooling were evaluated in conjunction with the use of vacuum and/or argon gas to achieve the required protection. The simplest, most effective, method established was the use of an integral machined lip in the tooling to seat into the titanium, and the use of argon gas over both surfaces throughout the process.

The process capability was demonstrated and evaluated by fabrication of numerous parts to six different configurations. These configurations included rectangular and circular pan sections, stepped side walls, beads, joggles, and multiple parts formed at one time. These parts were formed from three different heats of the Ti-6Al-4V alloy which represented a range in superplastic properties. The parts were subsequently evaluated for thickness profile characteristics and tested to establish tensile, fatigue, and compression properties.

The results of the phase I activities provided the basis for conducting phase II in which full-scale parts were subsequently fabricated by the process.

PHASE II - STRUCTURAL COMPONENTS

Two titanium sheet metal configurations were produced by the superplastic process during this phase of the program. One configuration, the nacelle forward center beam frame, was a completely redesigned part combining several members of an existing aircraft assembly. The second configuration, a nacelle aft center beam frame, was not redesigned since the original design lent itself to the superplastic forming process. A total of 11 of the foward frame Ti-6Al-4V alloy parts and 10 of the aft frame Ti-6Al-4V parts was produced. The first configuration, a sheet metal beaded part with return flanges, was fabricated in a female, multiple-piece, steel die. The latter parts were fabricated in an existing male steel die. All parts were produced using argon gas pressure on a titanium sheet diaphragm at a temperature of 1,700° F. The 21 parts fabricated all exhibited the capability of being formed to a complex configuration with well-formed beads and joggles, tight bend radii, and 90-degree return flanges.

Since titanium exhibits an affinity for contaminants at elevated temperatures, a sealed die, with argon gas as the forming medium, was used to eliminate or at least minimize surface enrichment of the part. Enrichment of the surface did occur in depths of 0.004 inch to 0.010 inch on the bottom of the part only. Graphite lubricant was applied to the tooling prior to forming, and this in conjunction with direct tooling contact of the sheet bottom side contributed to the surface enrichment. This was later completely, removed by chemical milling.

Dimensional inspection of the parts produced revealed a thickness profile conforming to analytical predictions. Thinning of the forming diaphragm sheet occurs until die contact is made, at which time only the free-standing or remaining unformed material continues to thin. This mechanism produces thick and thin sections where the radii is the thinnest. The parts fabricated demonstrated this thinning mechanism as anticipated and as predicted. Constant section thicknesses were obtained through subsequent chemical milling. Dimensional changes occurred over the range of 10 parts of each configuration in the order of 0.009 inch to 0.038 inch depending on location. These changes were attributed to the material movement over the 10 forming cycles for each configuration. The cause of the dimensional changes is believed to be primarily due to thermal gradients in the die developing during heat-up and cool-down. A change to higher hot strength alloys for tooling would minimize this condition during production.

During metallurgical examination after forming, it was noted that no acicular or blocky alpha in a uniform average grain size of 7 to 12 occurred indicating the superplastic characteristics of the selected material.

Superplastic forming of the titanium sheet used resulted in a reduction of tensile ultimate and yield strengths due to texturizing of the microstructure. When the mechanical property data were reduced to MIL-HDBK-5A and S values and compared to diffusion bonded data, which uses similar thermal cycles, a good correlation existed showing tensile property equivalency. No degradation in fatigue properties was observed on the same formed material.

Static structural testing of two each of both configurations was accomplished by subjecting the formed frames to static structural loading to evaluate buckling and crippling characteristics of the designs. In all cases, buckling and failure modes were as anticipated, indicating the suitability of the designs.

A cost comparison study was made of both fabricated frames showing the cost difference between superplastic forming and the conventional hot sizing methods. Since the forward frame redesign for superplastic forming eliminated a mechanically fastened assembly, the cost reduction of this part superplastically formed in one piece was approximately 50 percent compared to the hot sizing of the individual assembly parts. This represents a substantial and significant economic savings over a large production run. A cost reduction by superplastically forming the aft frame was also shown when compared with the hot size method; however, the savings was an order of magnitude less than that calculated for the forward frame.

PHASE III - PROCESS EXTENSION

The capability of accurately predetermining process parameters and forming capability for application to one other titanium alloy was established in this phase. The Ti-6Al-2Sn-4Zr-2Mo alloy was superplastically formed into the forward frame configuration of phase II. Superplastic characteristics and high-temperature flow properties were determined and found to be similar to the Ti-6Al-4V alloy. Therefore, the same parameters and procedures established in phase II were utilized in phase III. Three parts of the Ti-6Al-2Sn-4Zr-2Mo alloy were successfully formed in the forward frame die. Two parts were subjected to a static structural test.

The results from structural testing the phase III frames showed a similar behavior as with the phase II frames and substantiated the fact that superplastic forming extended to the new alloy can produce structural elements capable of carrying static loads equivalent to that displayed by parts conventionally formed. Surface enrichment, dimensional characteristics, and m mechanical property evaluations on one part were accomplished similar to the phase II effort. The results substantiated and demonstrated that the superplastic forming process can be extended to other titanium alloys.

PREFACE

This final engineering report covers the work performed under contract
F33615-73-C-5005 from 1 February 1973 through 30 April 1975. This contract
with the Rockwell International Corporation was initiated under Manufacturing
Methods Project 794-3, "Superplastic Forming of Titanium Structures." It was
under the technical direction of Mr. J. R. Williamson, Metals Processing
Branch (LTM), Manufacturing Technology Division, Air Force Materials
Laboratory, Wright-Patterson Air Force Base, Ohio.

This program was accomplished by Materials and Producibility Engineering
of the Los Angeles Aircraft Division of Rockwell International Corporation,
Los Angeles, California, with Dr. C. H. Hamilton as the Program Manager and
Mr. G. W. Stacher, Project Engineer. Phase I studies were under the direction
of Mr. J. A. Mills. Mr. H. W. Li performed the metallurgical and mechanical
properties studies of phases II and III. Structural design and structural
analysis effort was accomplished under the direction of L. Ascani and E. Rosen-
thal, respectively. The high-temperature process parameter studies were con-
ducted by the Rockwell International Science Center under the direction of
Dr. N. E. Paton. The performance of the program was under the general direc-
tion of Mr. N. Klimmek, Manager, Materials and Producibility, and Mr. W. D.
Padian, Supervisor, Fabrication Development.

The program was undertaken to establish superplastic forming as a
qualified method for production of sheet metal titanium parts. Superplastic
forming offers considerable relief to current sheet metal design and forming
limitations. Extensive tensile elongation and low forming stresses are the
primary characteristics of the process which will permit the forming of many
titanium sheet metal configurations beyond the forming capabilities of
current state-of-the-art methods.

This report was released by the author in April 1975.

TABLE OF CONTENTS

Contents   Page

LIST OF ILLUSTRATIONS

xiii

xvii

xix

INTRODUCTION

The objective of this program was to establish superplastic forming as a qualified method for production of complex, sheet metal titanium parts that could not be fabricated by the existing conventional forming processes.

Titanium alloys are being used increasingly on high-performance aircraft for sheet metal parts as well as for primary load-carrying structures. However, the limitations and costs of conventional titanium forming methods often required the use of other more formable (and heavier) alloys, forming of smaller assemblies which must subsequently be joined or require that the desired part be machined from heavy starting material such as plate or bar. The forming of complex configurations in titanium sheet metal poses distinct manufacturing limitations, particularly where large tensile elongations are required. Problems such as limited tensile elongation, excessive springback, and compression wrinkling require elevated-temperature creep sizing, after room temperature forming, in the temperature range of 1,200° to 1,450° F. This is necessary in order to increase the allowable deformation and minimize springback and sizing problems, even though an expensive, integrally heated, double-action forming die would be involved. Even with these advanced techniques, the forming of titanium alloys is still severely limited, and compromises in the design of structures are necessary. Due to the forming limitations of conventional methods, and the ever-increasing requirements for and use of titanium alloys in aircraft structures, the need for an advancement in manufacturing forming technology to circumvent these problems is apparent.

Superplastic forming, developed at the Rockwell International Los Angeles Aircraft Division (LAAD), has demonstrated the capability for improving the fabricability of titanium parts and eliminating the problems discussed. The unique superplastic forming method, using differential pressure across a titanium alloy sheet, has been shown to offer substantial increases in formability, reduction of working forces, elimination of residual stresses and the Bauschinger effect, and control of microstructure and properties in postformed parts. Additionally, a single male or female tool of an inexpensive alloy is sufficient for forming parts because of the low working forces.

Superplastic forming is a sheet metal fabrication process which uses the extensive tensile elongation and deformation stresses uniquely available in a superplastic material to form parts requiring high tensile elongations. The term "superplasticity" is used to describe the capability of a material to develop unusually high tensile elongations, a capability exhibited by only a few metals and alloys and within a limited temperature and strain rate range. Titanium and titanium alloys, including Ti-6Al-4V, have been observed to exhibit superplastic characteristics equal to or greater than those of any other metals.

1

Superplasticity has been demonstrated on commercial titanium alloys, and now this unique characteristic has been applied to the high rate production of formed sheet metal parts. This program has resulted in a proven detail processing baseline and analysis methods which demonstrate good correlation between predicted forming parameters and hardware results. Rockwell has demonstrated that complex titanium parts requiring extreme elongations and sharp bend radii can be fabricated by the superplastic forming process. The parts produced show that limitations imposed by state-of-the-art forming techniques are not significant when superplastic forming techniques are used. An entirely new set of titanium forming capabilities have been defined for this process and indicate that titanium forming capabilities can be advanced by orders of magnitude.

This program establishes the technological bridge required to assure an orderly transfer from the laboratory to the manufacturing environment for the superplastic forming process. The effort necessary to accomplish this transfer is defined, along with the elements of fundamental understanding and process definition necessary to assure a solid foundation for the manufacturing capability.

This phase of the program was conducted to evaluate material characteristics and process techniques and procedures, and to integrate these into a superplastic forming (SPF) method for fabrication of Ti-6Al-4V alloy sheet materials. This activity was conducted in three tasks as follows:

- Task 1, Process Parameters - Evaluation of commercially available Ti-6Al-4V alloy as to its suitability for superplastic forming

- Task 2, Other Process Factors - Evaluation of tooling materials and methods for minimizing surface enrichment during processing

- Task 3, Processing Capability - Evaluation of the material/process combination to evaluate the capability for producing various test configurations.

The definition of material and process parameters used in phase II in the fabrication of full-scale structural parts was based on phase I activity.

PROCESS PARAMETER STUDY (TASK 1)

This task was conducted to evaluate commercially available Ti-6Al-4V alloy sheet (MIL-T-9046), both for effects of SPF processing on properties as well as for the superplastic characteristic and resulting suitability for forming complex configurations by this process.

MATERIAL SELECTION

Six different heats of Ti-6Al-4V sheet material with a range of chemistries and representing two thicknesses (four heats of 0.056-inch sheet and two heats of 0.100-inch sheet) were selected within MIL-T-9046 specifications. The selection was made to provide a representative sampling of commercially available titanium sheet material having a potential variance in superplastic characteristics. Table 1 lists the alloy composition and dimensions of each of the six heats of Ti-6Al-4V.

These materials were evaluated to characterize their microstructure and mechanical properties, and to establish superplastic properties in the process temperature range. The microstructural characterization was conducted to provide a basis for the relating of metallurgical conditions of the material with its propensity to undergo superplastic forming since the microstructure strongly influences the superplastic properties. Past studies of this

3

TABLE 1. CHEMICAL COMPOSITION OF Ti-6Al-4V
ALLOY SHEET RECEIVED FOR PHASE I

Heat No.	Dimensions (in.)	Al	V	O	N	C	Fe	H (ppm)	β transus (°F)
G51126	0.097 x 36 x 96	6.20	3.90	0.132	0.016	0.024	0.12	67	1,860
3C3182	0.108 x 36 x 103	6.20	4.30	0.128	0.007	0.020	0.15	29	1,850
295405	0.054 x 38 x 94	6.40	4.20	0.143	0.012	0.020	0.17	28	1,850
K6838	0.061 x 48 x 93.5	5.80	4.10	0.140	0.009	0.022	0.22	-	1,825
304488	0.060 x 48 x 95	6.10	4.10	0.116	0.009	0.020	0.20	43	1,836
301715	0.058 x 34-3/8 x 83-7/8	6.40	4.20	0.103	0.007	0.020	0.16	36	1,825

4

correlation have been conducted on laboratory-controlled variations in microstructure, but little data have been available which show the variability to be expected in commercially available material.

Since the SPF process involves the exposure of the titanium alloy to temperatures of nominally 1,700° F, it was anticipated that the strength of the mill-annealed product used would decrease somewhat consistent with the full anneal resulting from the processing. The mechanical properties were, therefore, evaluated to assess the extent of this effect.

MICROSTRUCTURE

The microstructure of the three basic orthogonal directions of the six heats are presented in Figure 1. The characterization of this as received material involved a determination of grain size, uniformity of grain size, volume fraction of acicular and blocky alpha, grain aspect ratio, and degree of recrystallization. The grain size measurements were made by counting the number of phase boundaries encountered in the circumference of a circle overlaid on 500X photomicrographs for each orientation. The volume fractions were established by the standard point count method in which an overlay grid was placed on 500X photomicrographs, and the grid points within the phase of interest were established. The textures of the titanium alloy sheets were established by generating $(10\bar{1}0)$ and (0002) polar projections using standard X-ray techniques. The results of the microstructural analyses are summarized in Table 2.

Of the six heats procured, two (No. 295405 and No. 304488) exhibited a refined grain structure with uniform, equiaxed grains. A wide variation in both extent and orientation of preferred (0002) texture is apparent among these materials. Heat G51126 exhibited the least refined microstructure, including heavy banding of acicular and blocky alpha and a high degree of texture. The range of microstructures provided an excellent basis for evaluating the corresponding superplastic properties.

The degree of recrystallization was established by optical and electron microscopy analyses. This was used on titanium material that was thermally cycled at 1,700° F for 3 hours. This analysis showed that the materials were fully recrystallized.

SUPERPLASTIC PROPERTIES

The data which were developed to describe the high-temperature superplastic behavior of Ti-6Al-4V are flow stress (σ) as a function of strain rate ($\dot{\epsilon}$), and the corresponding strain-rate sensitivity m (m = $d\ln\sigma/d\ln\dot{\epsilon}$). The method used to establish superplastic properties is illustrated in Figure 2. It is the flow stress versus strain rate data which determine the propensity
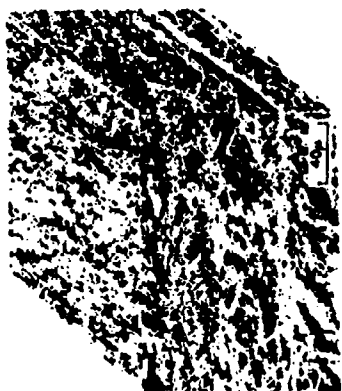
Figure 1. Microstructures of three orthogonal planes of the six heats of Ti-6Al-4V evaluated in phase I.

6

TABLE 2. SUMMARY OF MICROSTRUCTURAL CHARACTERISTICS

Heat No.	Grain Size (μ)				Grain Aspect Ratio	Uniform Grain Size	Volume fraction (percent)		Texture $\left(\text{Ratio} \frac{I^L_{0002}}{I^{LT}_{0002}} \right)$	Comments
	Rw	RT	Wt	Avg			Blocky Alpha	Acicular Alpha		
G51126	6.5	6.5	6.5	6.5	~6	No	0	29	0.10	Banded, lamelar alpha.
295405	8.2	8.5	7.7	8.1	~1	Yes	0	0	0.07	Few large primary alpha grains.
301715	8.9	8.8	8.6	8.7	~3	No	11	11	8.0	Lamellar alpha grains.
303182	10.0	11.2	8.2	9.8	~3	Yes	9	0	0.30	Uniform alpha.
K6838	7.5	7.9	7.5	7.6	~4	No	21	0	4.0	Many large blocky primary alpha grains.
304488	6.5	9.9	9.6	8.6	~1	Yes	0	0	2.0	Uniform alpha.
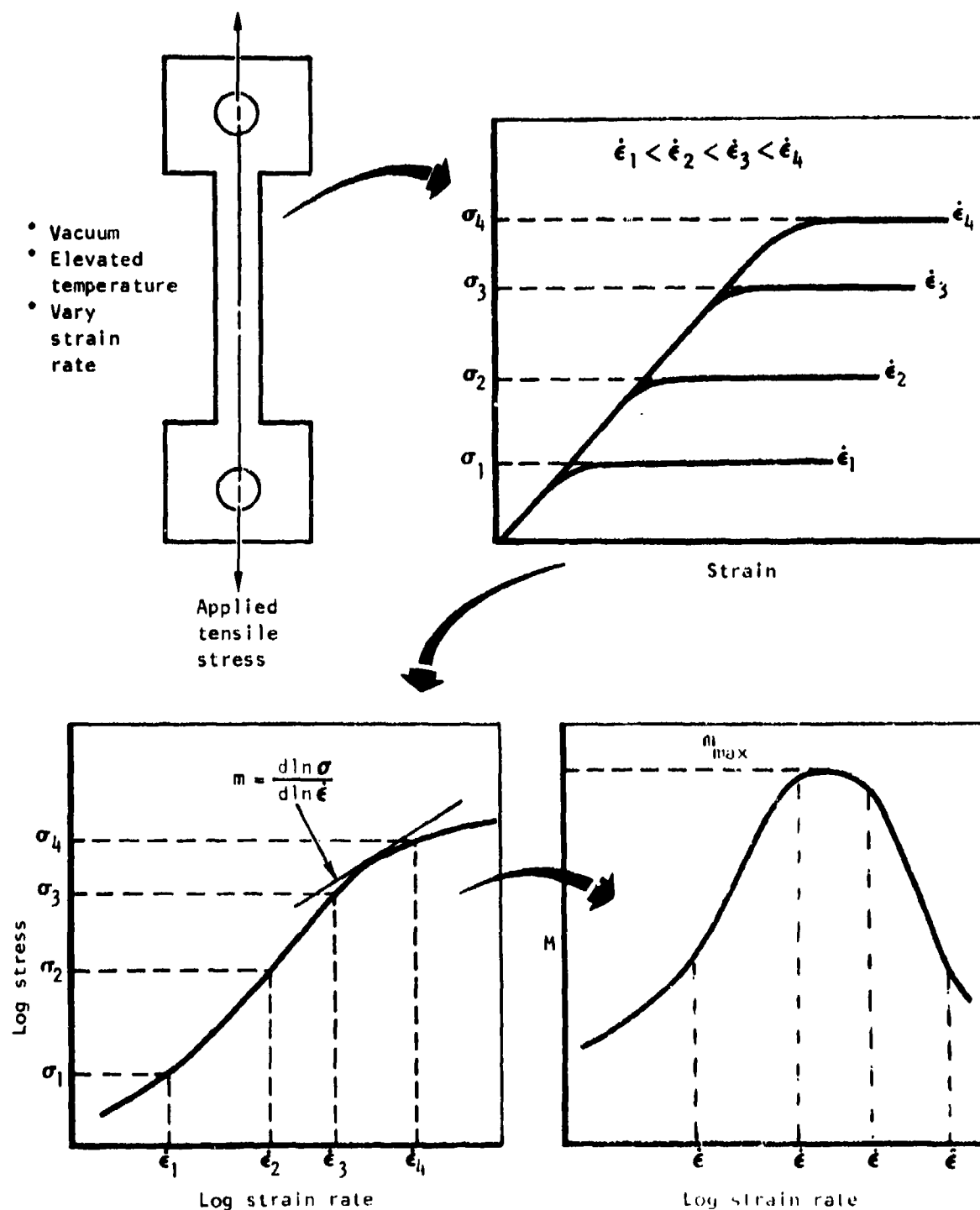
Figure 2. Method used for development of superplastic properties.

8

for superplasticity, available elongation, and ease of deformation under given pressures. The determination of this data for establishing the process parameters and correlating with metallurgical variables are the objectives of this aspect of the program.

The technique employed to establish the flow stress as a function of applied strain-rate is one of tensile loading a test specimen, at the temperature of interest, varying the crosshead speed of the tensile machine to impose various strain rates, and measuring the corresponding stress. Since the material does not undergo strain hardening, the resistance to deformation (as a flow stress) is a function only of the rate of straining, and is virtually independent of the extent of straining. The resulting data provide the stress/strain rate relationship necessary to compute m, the strain rate sensitivity index.

In this program, the stress/strain rate data were evaluated with the aid of a computer to determine the constants providing the best fit to a constitutive equation established by Paton (Reference 1) of the form:

$$\dot{\epsilon} = K_1 (\sigma - \sigma_0) + K_2 \sigma^n$$

where

$\dot{\epsilon}$ = strain rate

σ = flow stress

K_1, K_2, σ_0, and n = constants

The excellent fit of the data to the aforementioned relation observed in this program allows the computation of an accurate, continuous plot of strain rate sensitivity index, m, as a function of strain rate.

The results of the superplastic property tests of the six heats for 1700°F are presented in Table 3, and Figures 3 through 6.

The strain rate sensitivity index varies from 0.51 (heat G51126) to as high as 0.94 (heat K6838).

From these data, and considerations of the microstructural characteristics, three heats were selected for more detailed evaluation. The heats were purposefully selected to represent the widest range of superplastic forming

9

TABLE 3. MINIMUM FLOW STRESS AND MAXIMUM STRAIN-RATE SENSITIVITY
INDEX IN LONGITUDINAL AND LONG TRANSVERSE DIRECTIONS OF
THE SIX HEATS OF TITANIUM 6A1-4V SELECTED FOR PHASE I

Heat No.	σ_0 (ksi)		Maximum m	
	L	LT	L	LT
G51126	0.116	0.189	0.63	0.51
295405	0.124	0.133	0.92	0.92
K6838	0.260	0.216	0.94	0.94
304488	0.111	0.252	0.84	0.79
303182	0.130	0.160	0.84	0.88
301715	0.298	0.225	0.61	0.84

capabilities, including the worst case as well as the best. The heats
selected are:

- Heat No. 295405 - best case

- Heat No. 301715 - intermediate case

- Heat No. G51126 - worst case

This is summarized in Table 4.

These three heats were tested to determine superplastic properties as
functions of temperatures, grain orientation, and extended hold times. Tests
were conducted under vacuum over a range of strain rates from 1.6×10^{-6} in./
in./sec to 1×10^{-2} in./in./sec, which brackets the range in which maximum
superplasticity is observed. The results of these tests are presented in
Figures 7 through 18.

The effect of temperature on the flow stress and m values of the materials
is shown in Figures 7 through 12. The flow stresses decrease for a given
strain rate as the temperature is increased from 1,500°F to 1,700°F; little
change is observed between 1,700°F and the beta transus -10°F except that the
flow stresses at low strain rates are higher for the beta transus -10°F.
However, the m values near the beta transus are reduced, indicating that the
superplastic capability is reduced at these higher temperatures. Since flow

10

TABLE 4. THREE HEATS OF Ti-6Al-4V SELECTED FOR FURTHER FORMING STUDIES

Heat	Gage (in.)	Comments	
G51126	0.100	Worst Case:	Heaviest gage; superplastic index (m) = 0.51-0.63; strong texture with $(10\bar{1}0)$ 25 times random in the rolling direction
301715	0.056	Intermediate Case:	Thinner gage; superplastic index (m) = 0.61-0.84; weak texture with $(10\bar{1}0)$ 4 times random in the transverse direction
295405	0.056	Best Case:	Thinner gage; superplastic index (m) = 0.92-0.92; moderate texture with $(10\bar{1}0)$ 14 times random in the rolling direction

stress data relate directly to the ease and rate of forming parts, it is apparent that 1,700°F offers significant advantages over 1,500°F and 1,600°F for the production of parts.

As an example of the effect of temperature, the variations of strain rate at a flow stress of 1,000 psi for heat No. 301715 can be considered. The strain-rates corresponding to 1,500°F, 1,600°F, and 1,700°F are 3×10^{-5} and 1.2×10^{-4} in./in./sec, respectively. For this stress and the corresponding strain rates, forming will proceed more than twice as fast at 1,700°F than at 1,600°F, and nearly 10 times as fast at 1,700°F than at 1,500°F.

The variations of flow stresses and m values at 1,700°F among the three heats can be seen in Figures 3 through 6 for the longitudinal and long transverse directions, respectively. It is apparent from these curves that heat No. 295405 exhibits the greatest degree of strain-rate sensitivity of these materials as well as the lowest flow stresses at the lower strain rates (i.e., for less than about 10^{-3} in./in./sec) where maximum superplastic characteristics are generally observed. These data of flow stress and the observed high m values indicate that heat No. 295405 should be the best of the three selected heats for superplastic forming.

Table 5 gives values of σ_0, m_{max} values, and σ and $\dot{\epsilon}$ at m_{max} value for the three heats tested at 1,500°F, 1,600°F, 1,700°F and β transus.-10°F.
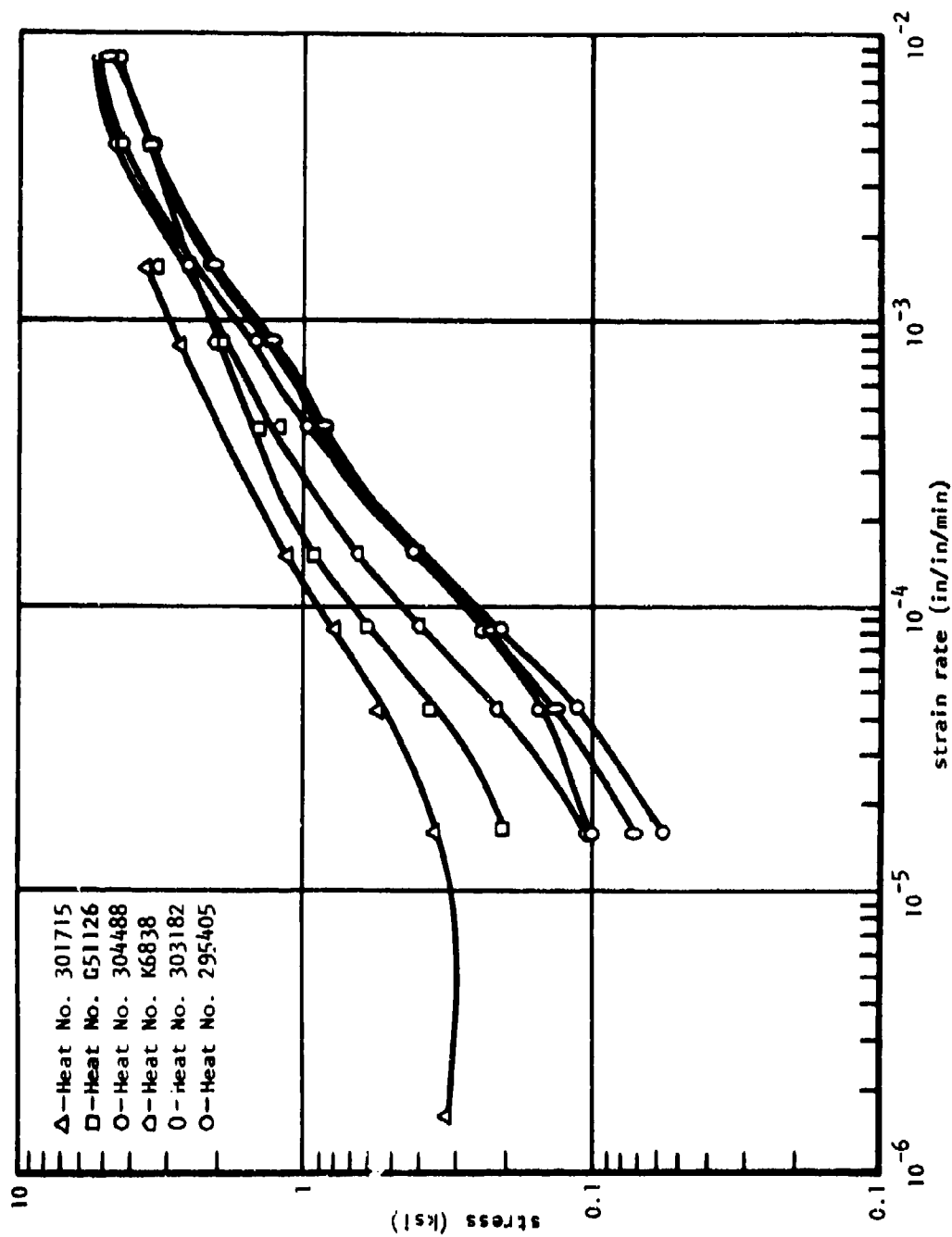
11

Figure 5. Log Stress versus log strain rate of phase I 6Al-4V titanium sheet material at 1,700°F in longitudinal direction.

△—Heat No. 301715
◻—Heat No. G51126
◯—Heat No. 304488
◇—Heat No. K6838
◯—Heat No. 303182
◯—Heat No. 295405

strain rate (in/in/min)

stress (ksi)

12
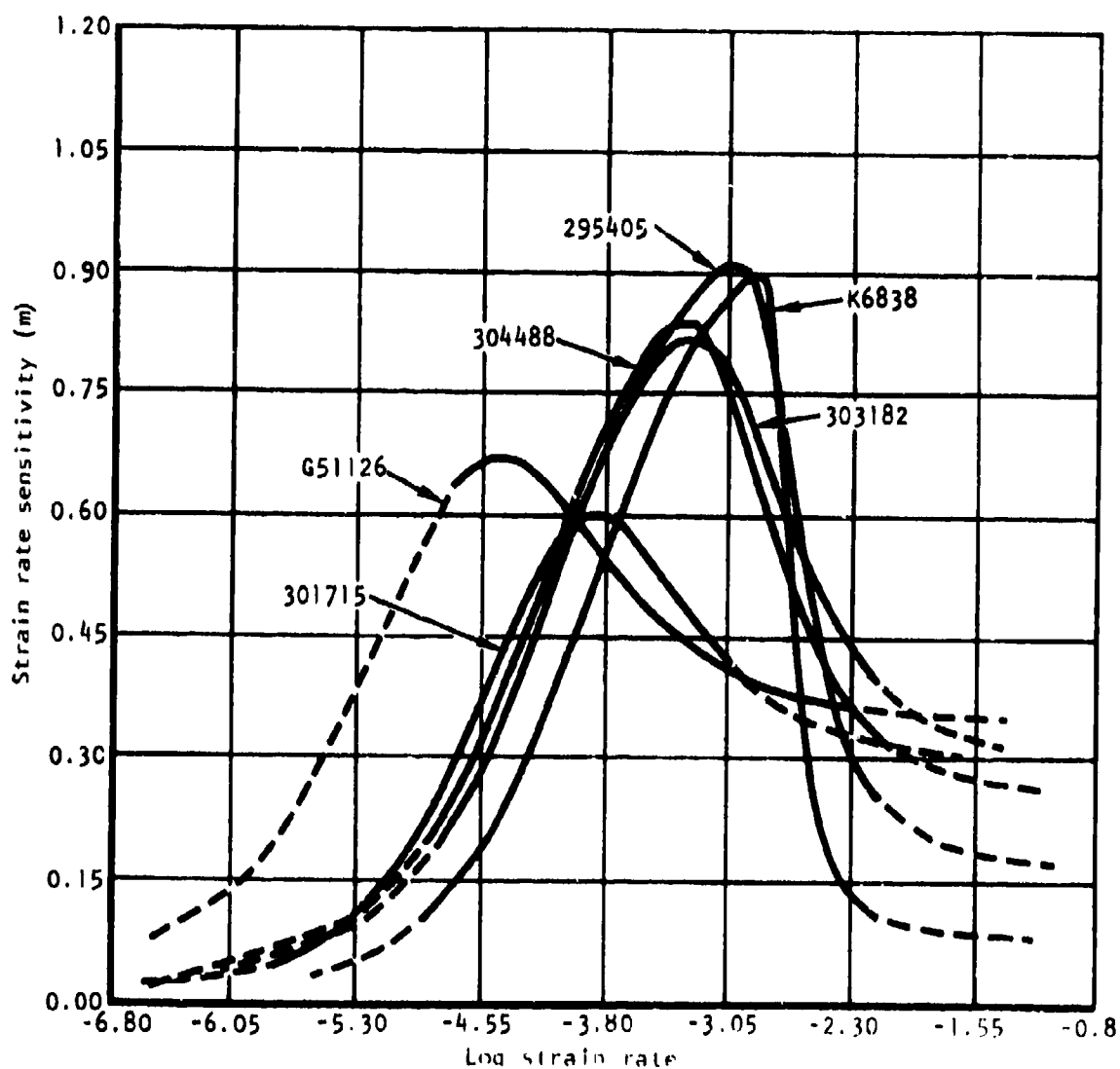
Figure 1. Strain rate sensitivity versus log strain rate curves of phase I material at 1,700°/F in longitudinal direction.

Figure 5. Log stress versus log strain rate of phase I 6Al-4V titanium sheet material at 1,700°F in long transverse direction.

14
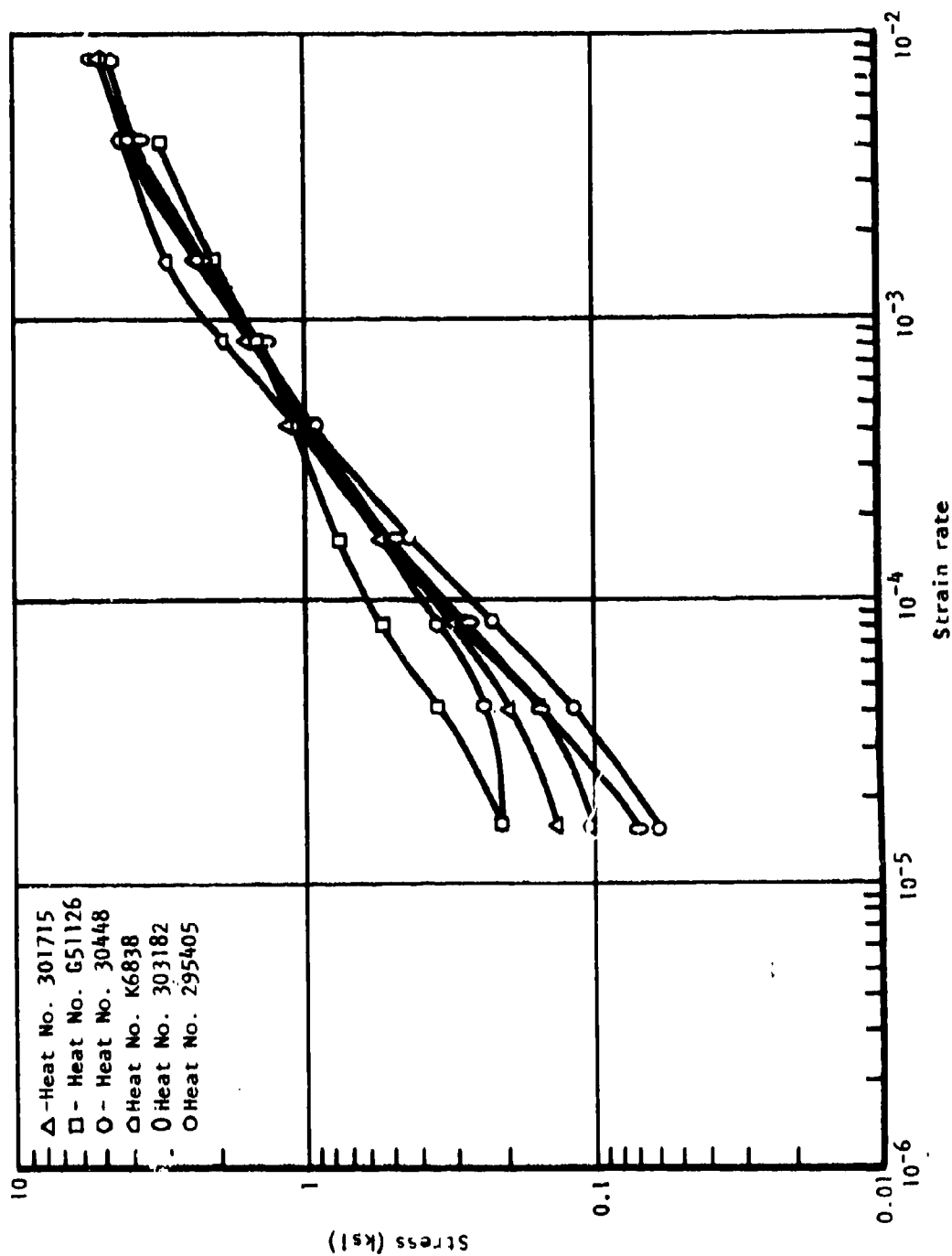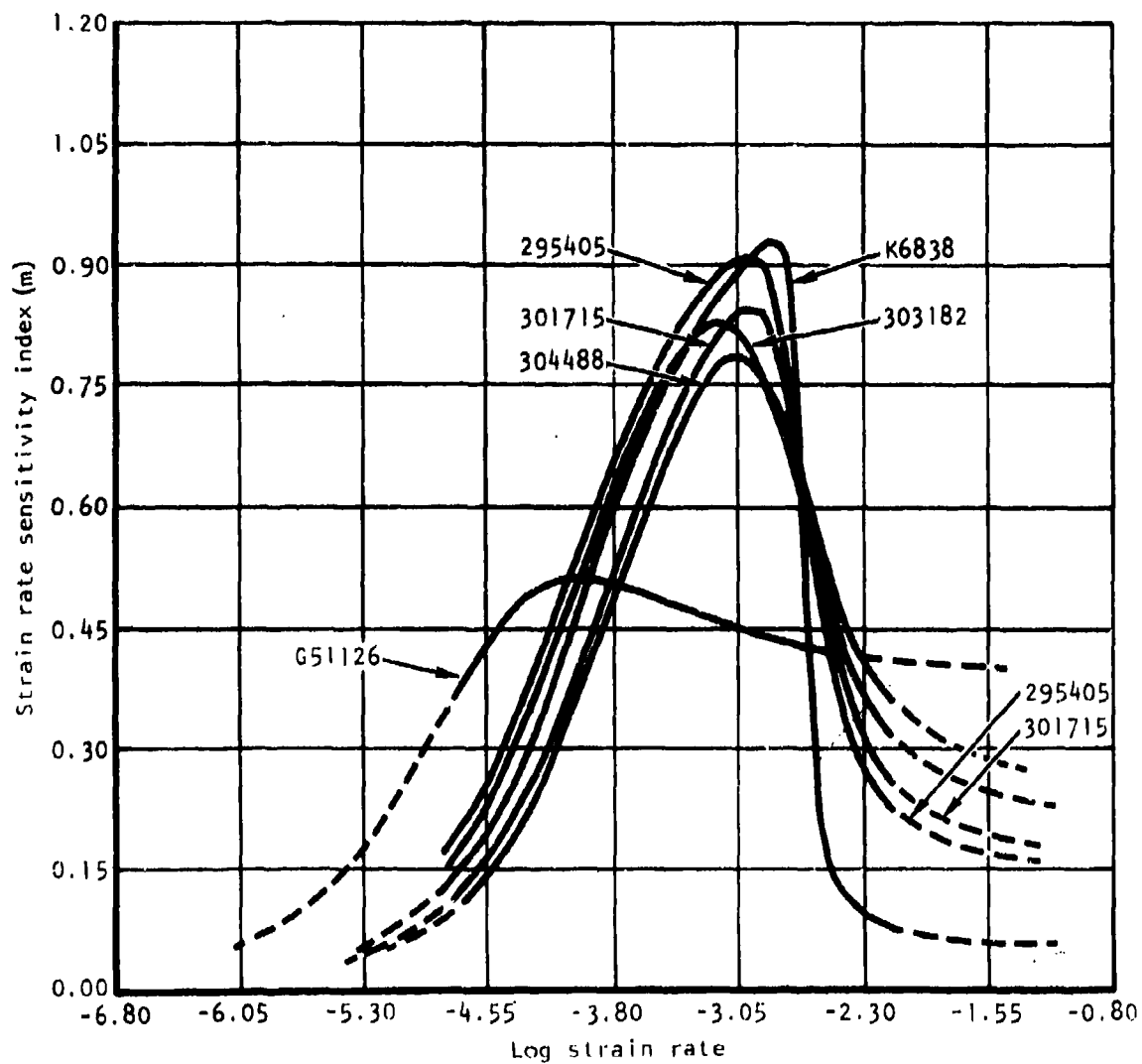
Figure 6. Strain rate sensitivity versus log strain rate curves of phase I material at 1,700° F in long transverse direction.

15
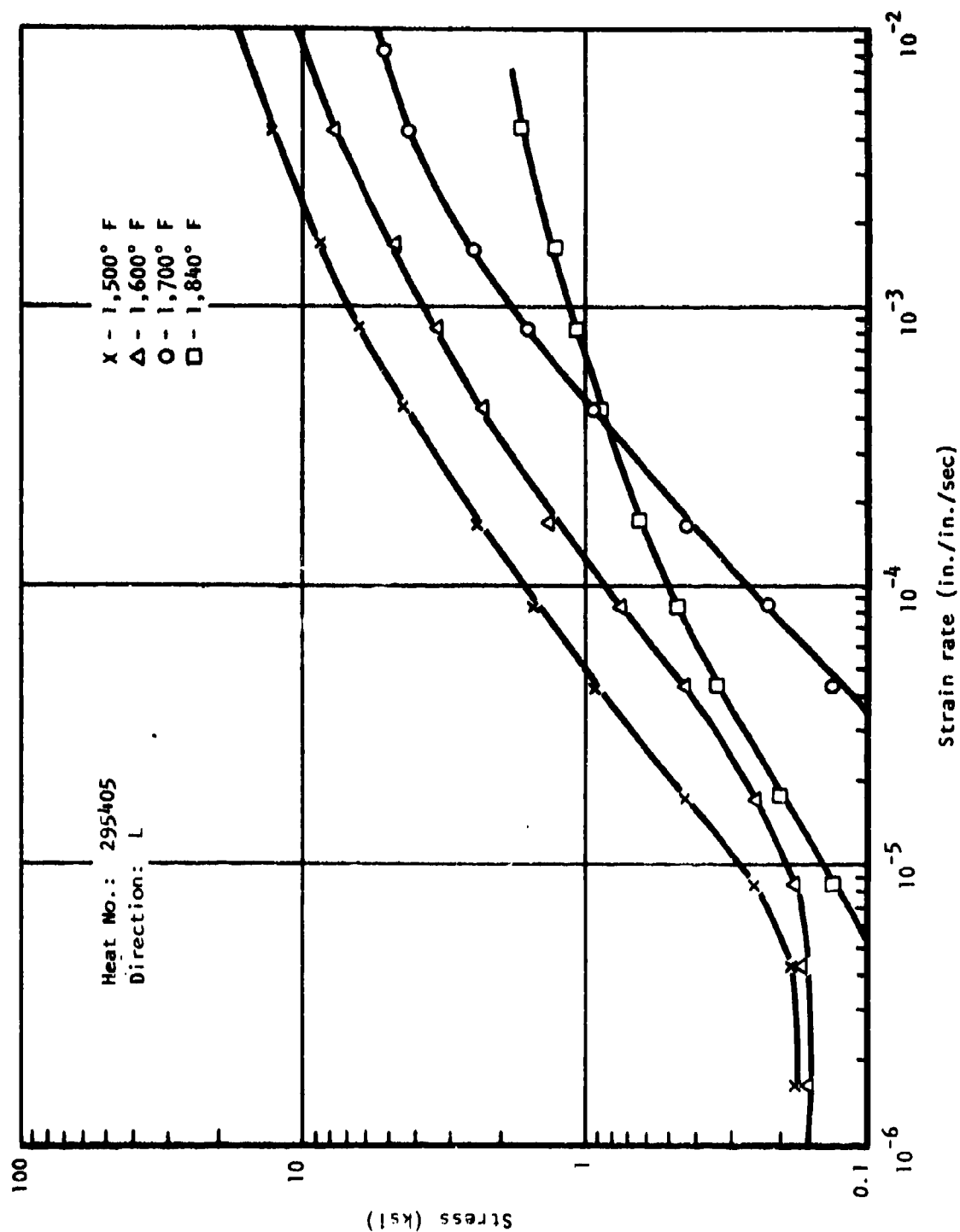
Figure 7.   Effect of temperature flow stress versus strain rate for heat 295405.

16
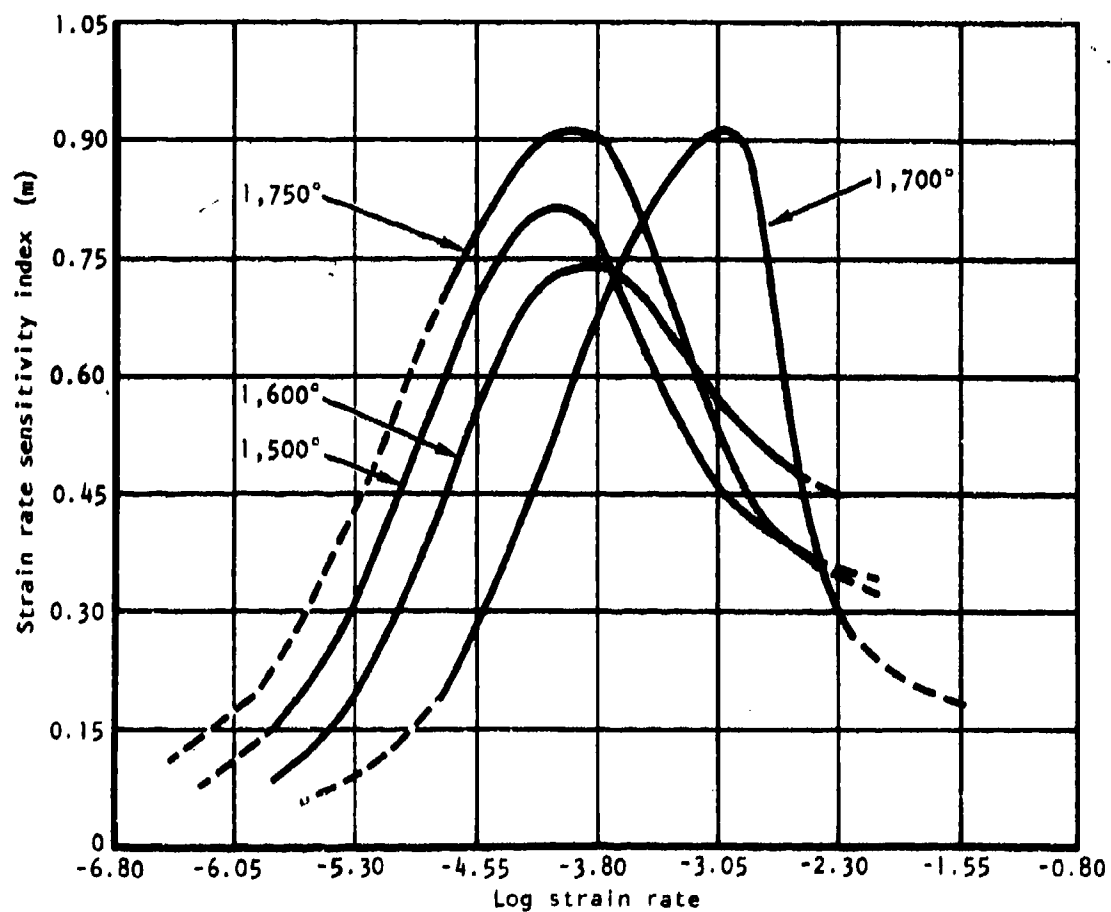
Figure 8. Comparison of strain rate sensitivity index versus log strain rate of heat No. 295405 at various temperatures in longitudinal direction.
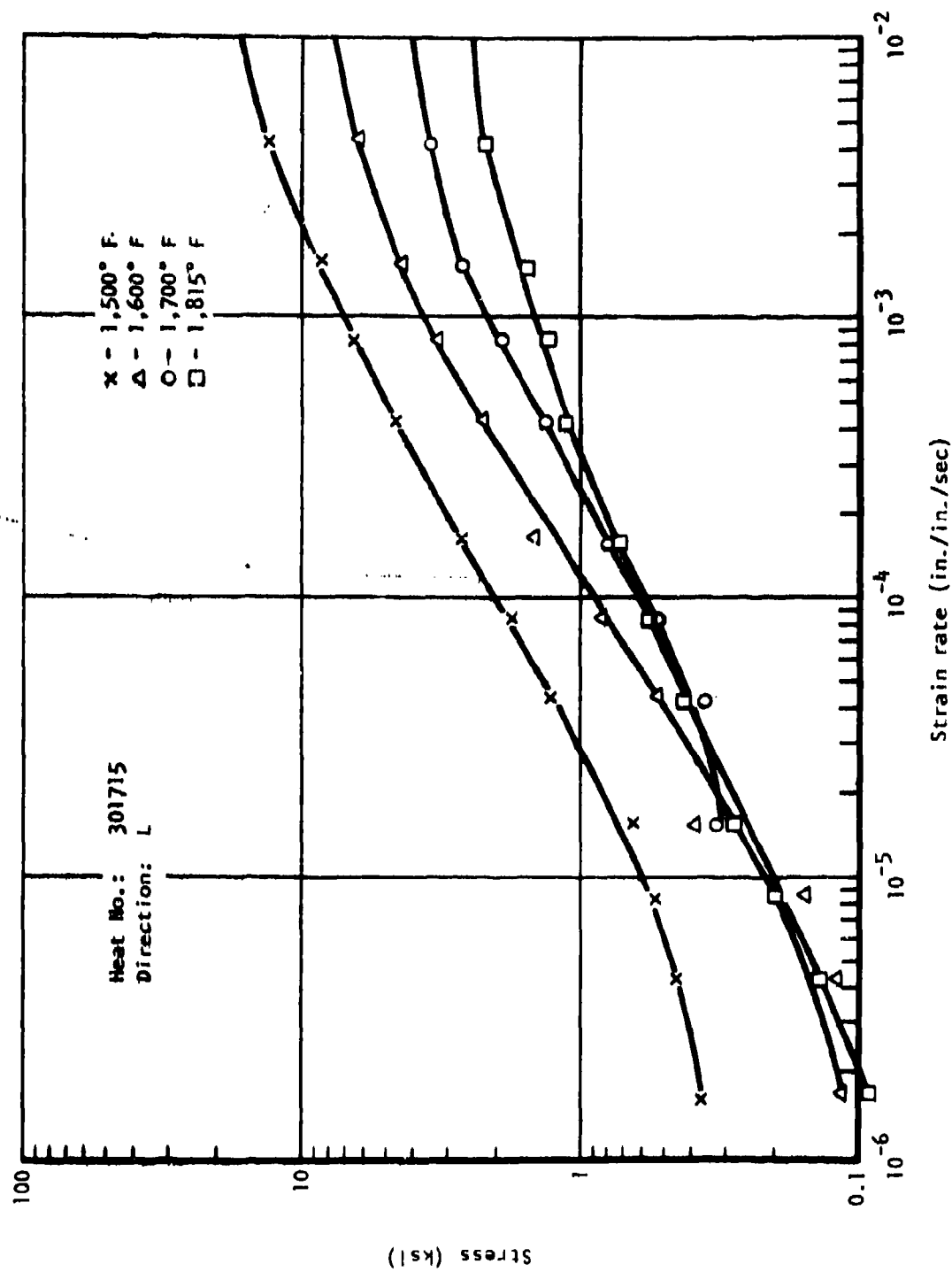
Figure 9. Effect of temperature on flow stress versus strain rate for heat 301715.

18
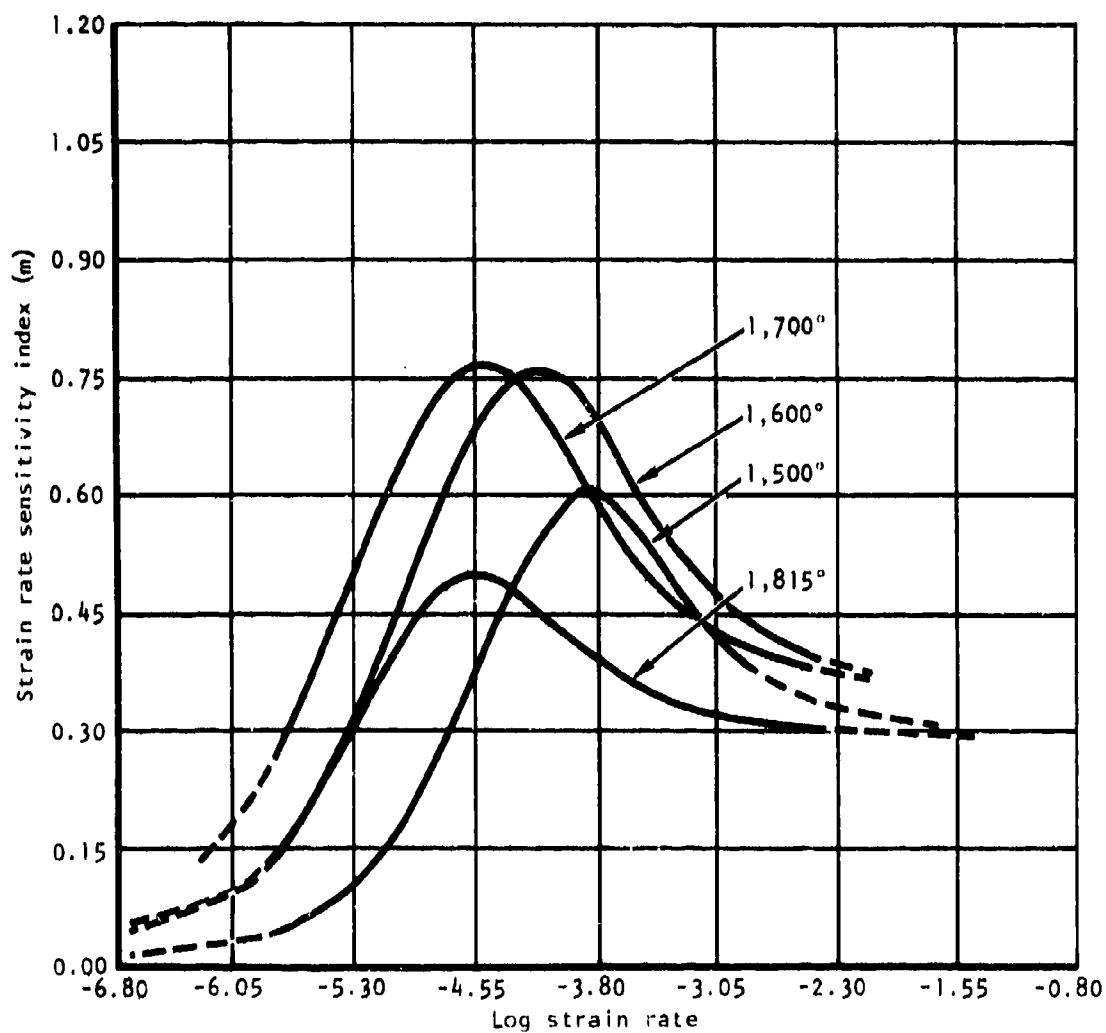
Figure 10. Comparison of strain rate sensitivity index versus log strain rate of heat No. 301715 at various temperatures in longitudinal direction.

19
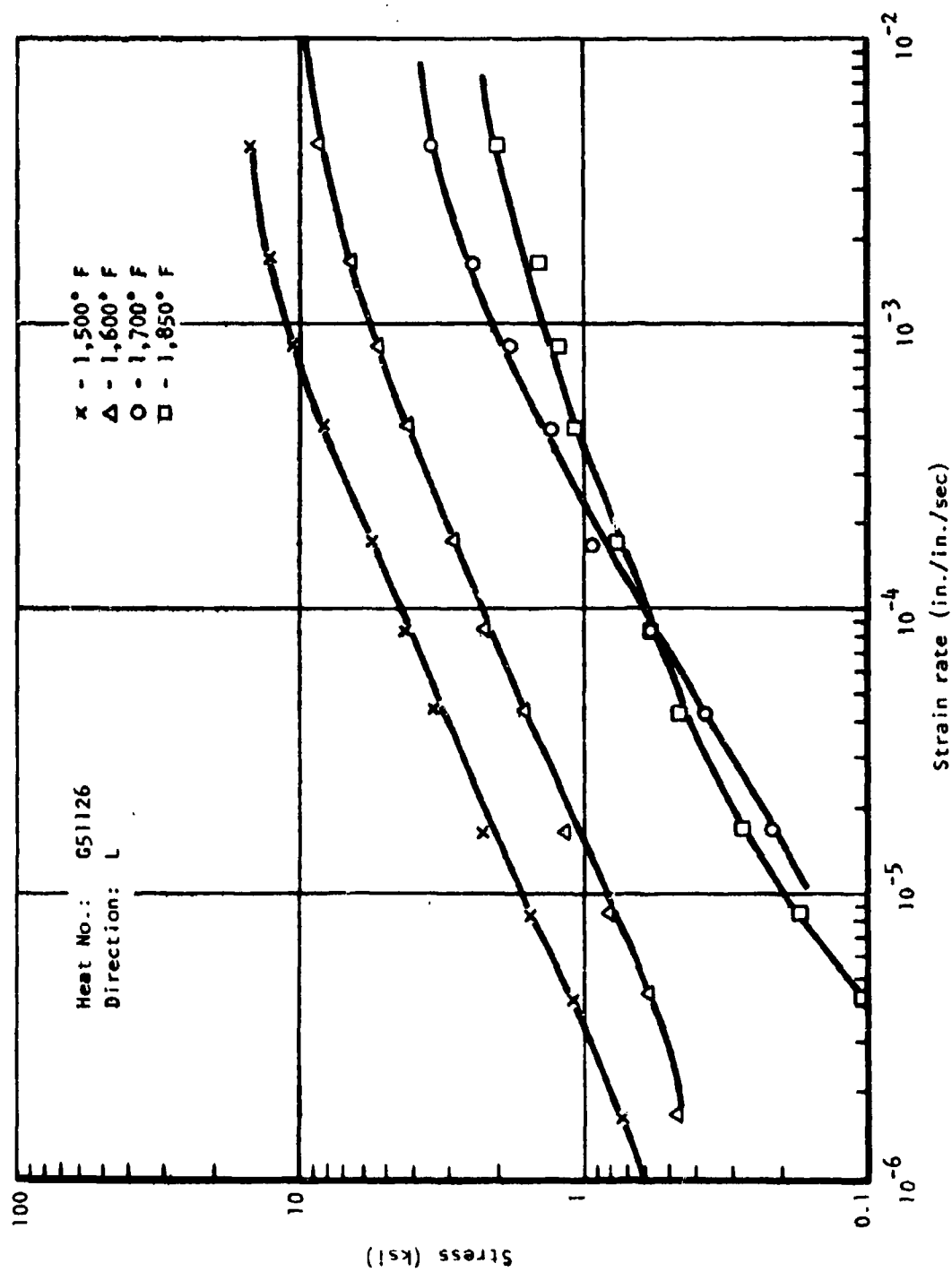
Figure 11. Effect of temperature on flow stress versus strain rate for heat G51126.

20
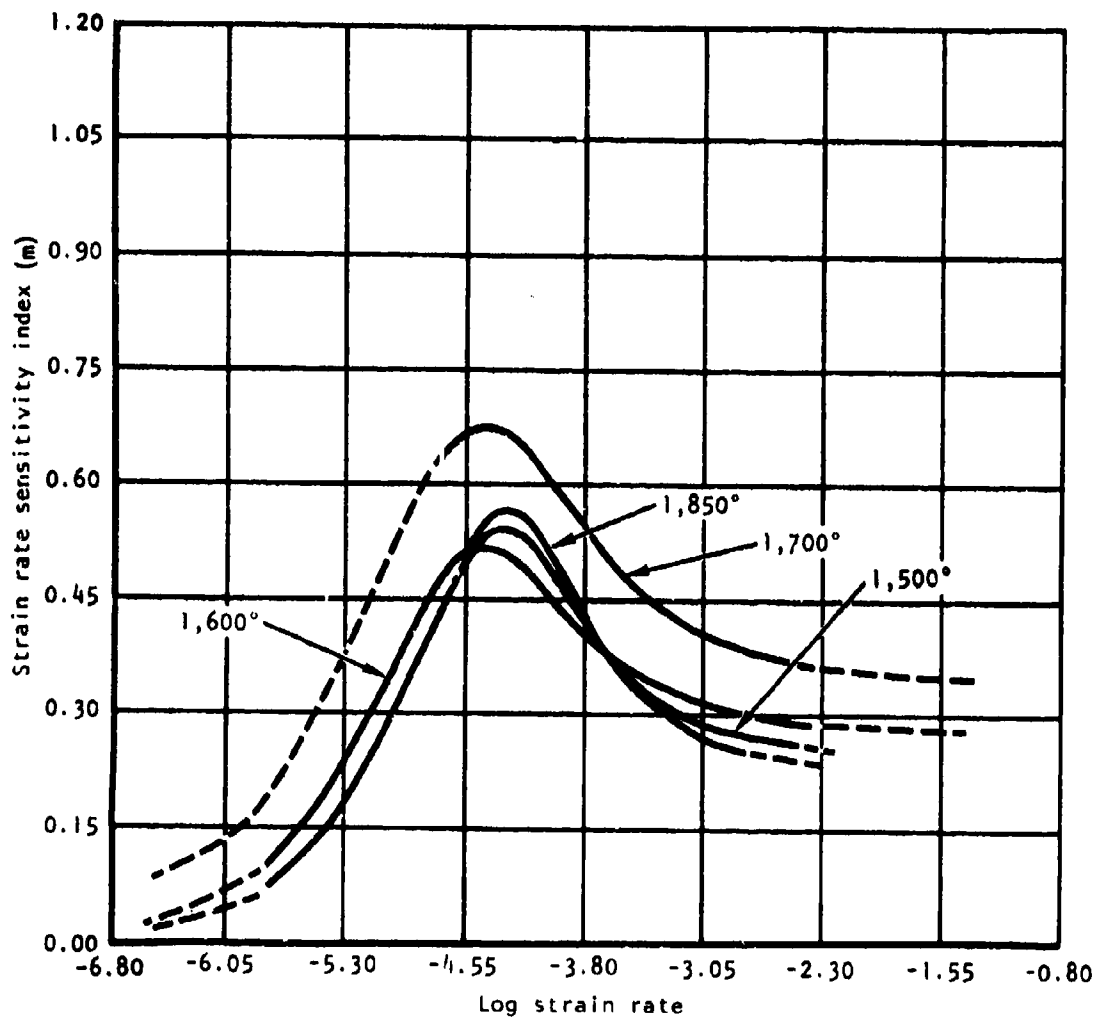
Figure 12. Comparison of strain rate sensitivity index versus log strain rate of heat No. G51126 at various temperatures in longitudinal direction.

21
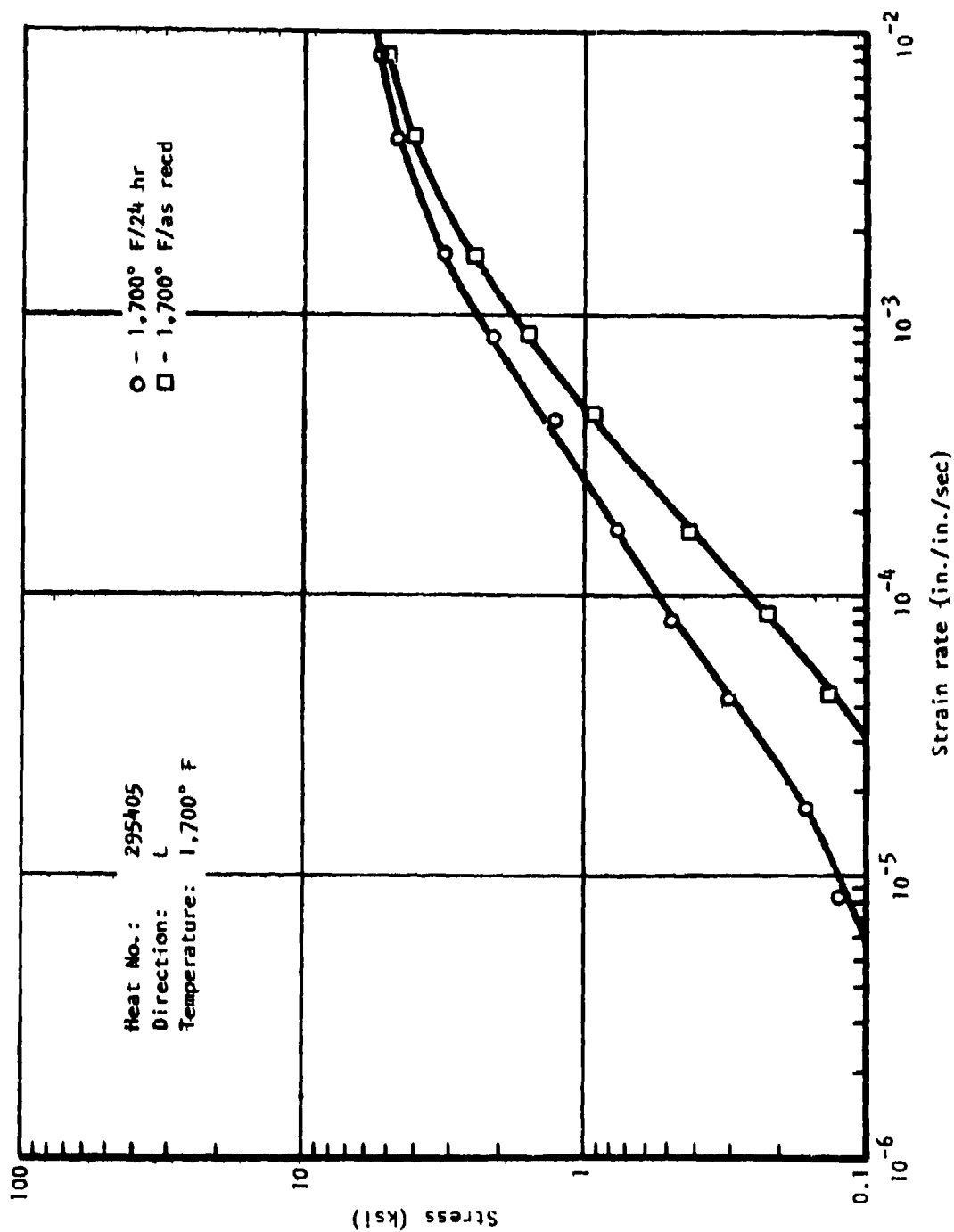
Figure 13. Effect of 24-hour exposure at 1,700° F on flow stress versus strain rate for heat 295405.

22
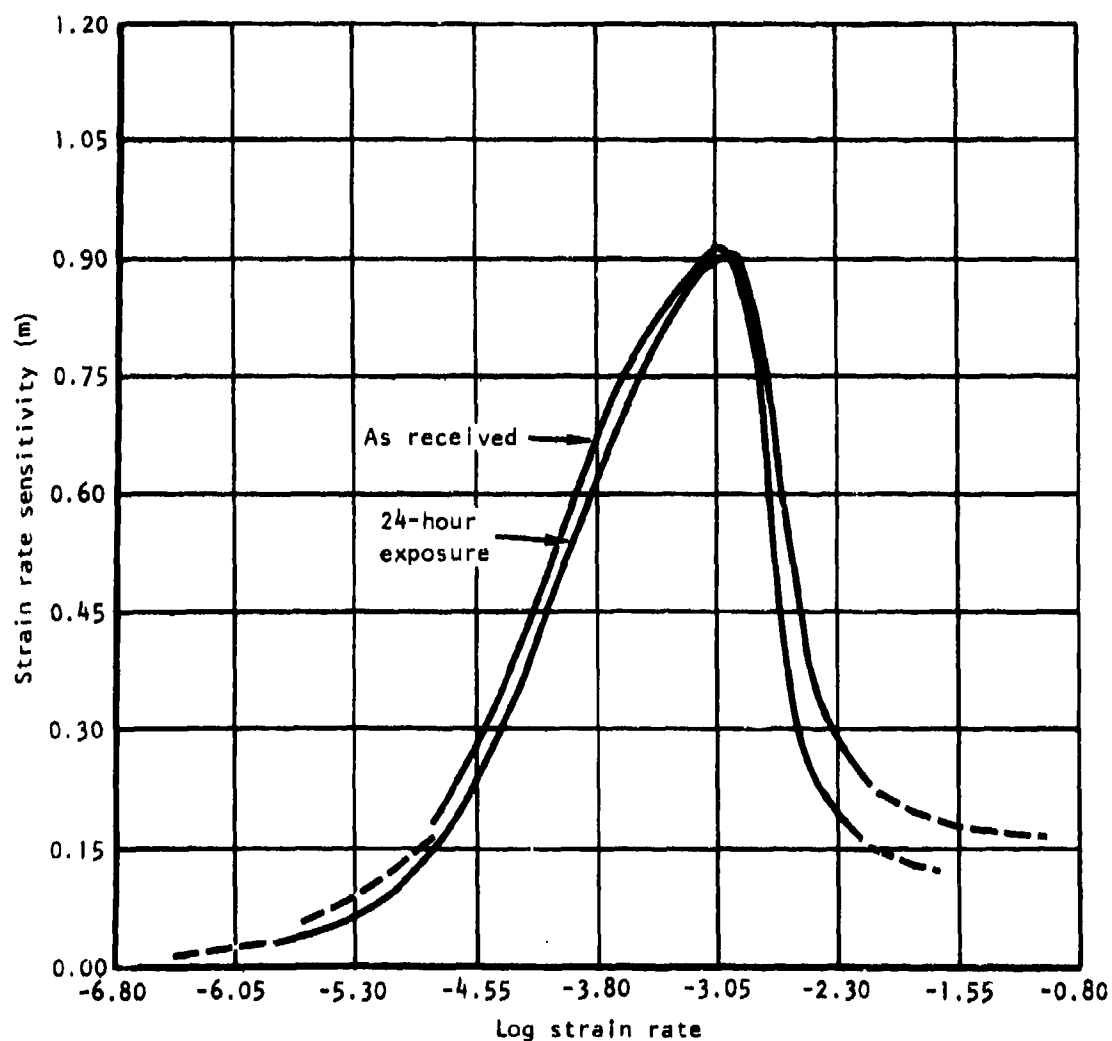
Figure 14. Comparison of strain rate sensitivity index versus log strain rate of heat No. 295405 at 1,700° F in the longitudinal direction for the as-received and 24 hour exposure conditions.

23
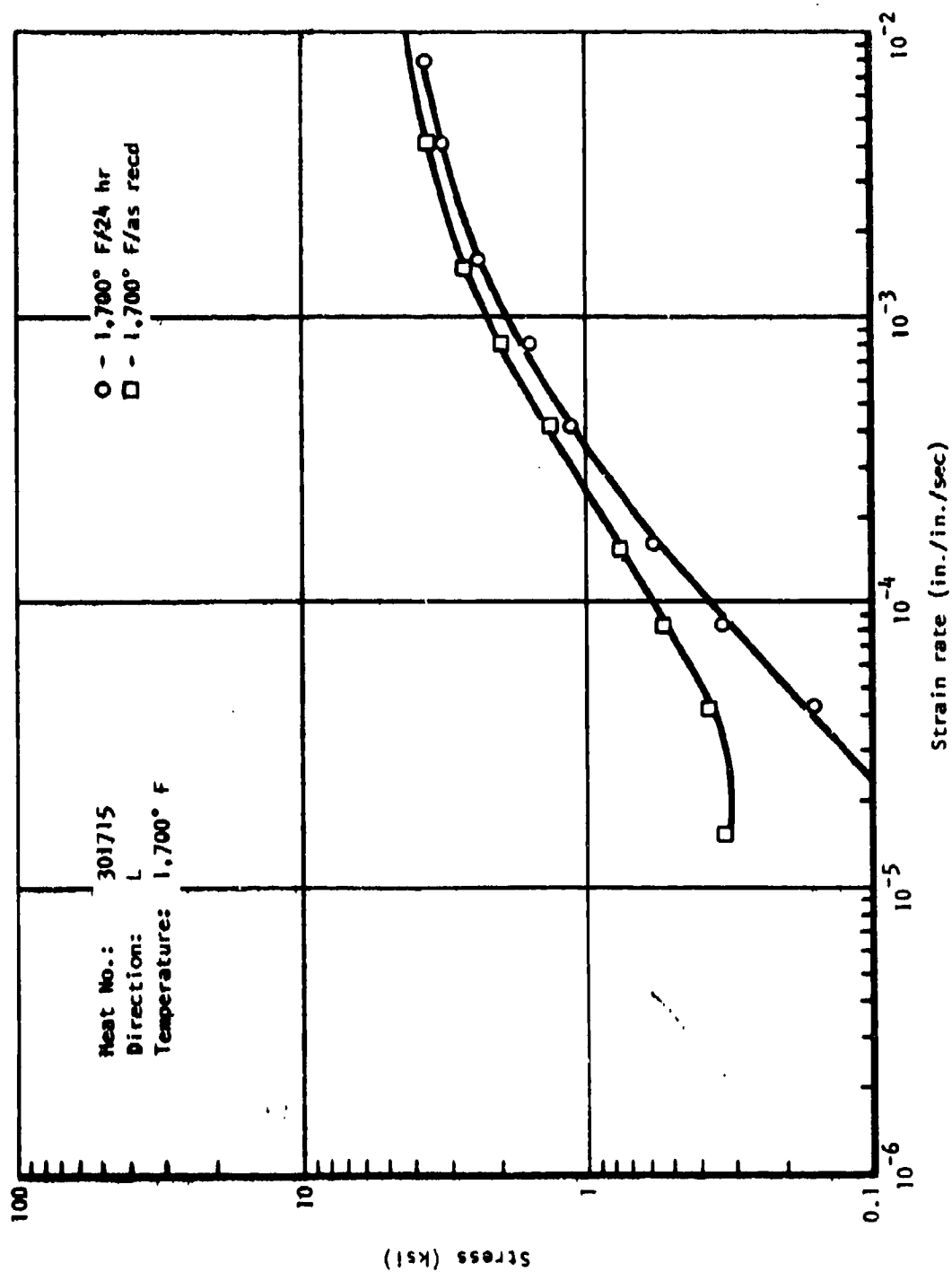
Figure 15. Effect of 24-hour exposure at 1,700° F on flow stress versus strain rate for heat 301715.

24
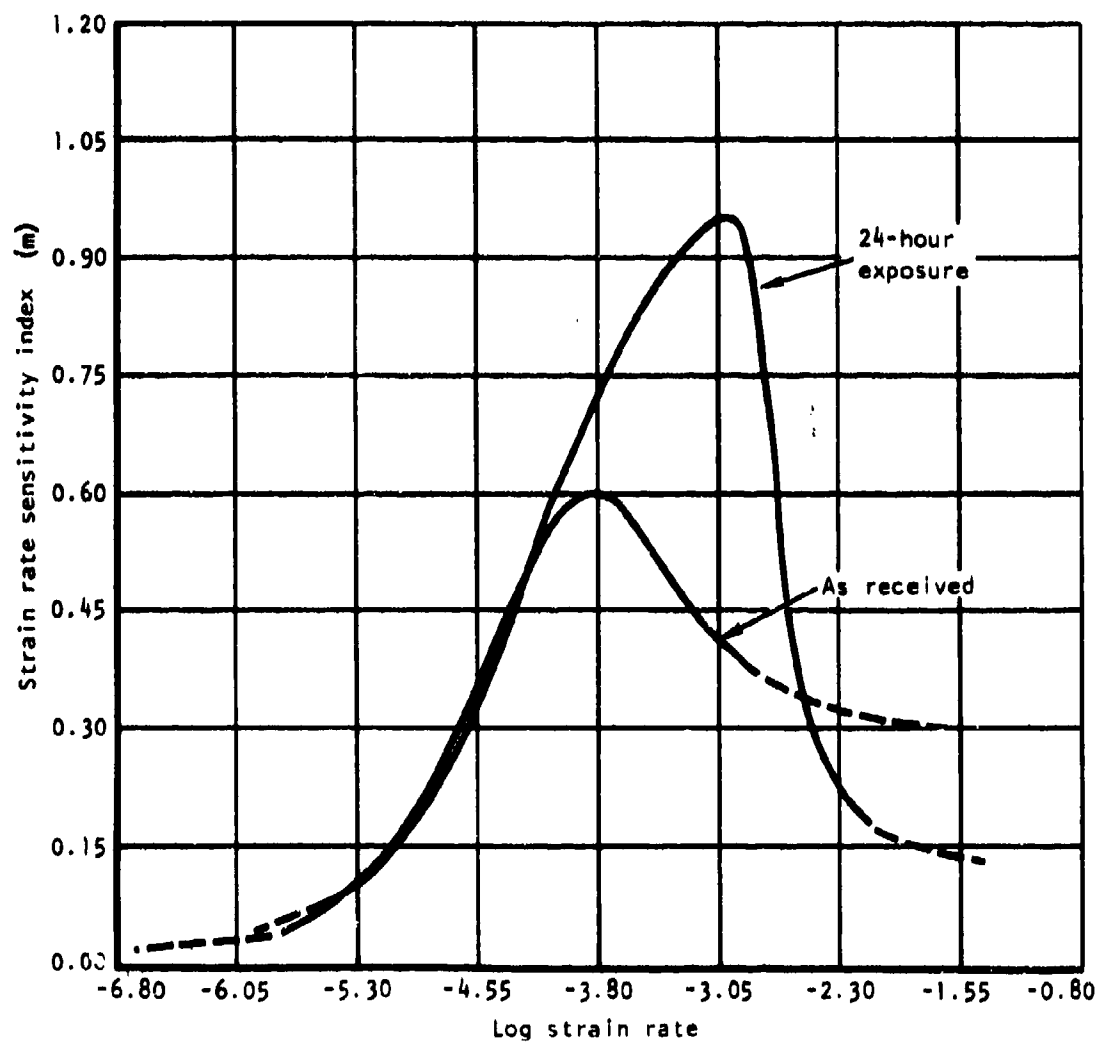
Figure 16. Comparison of strain rate sensitivity index versus log strain rate of heat No. 301715 at 1,700° F in longitudinal direction for as-received and 24-hour exposure conditions.
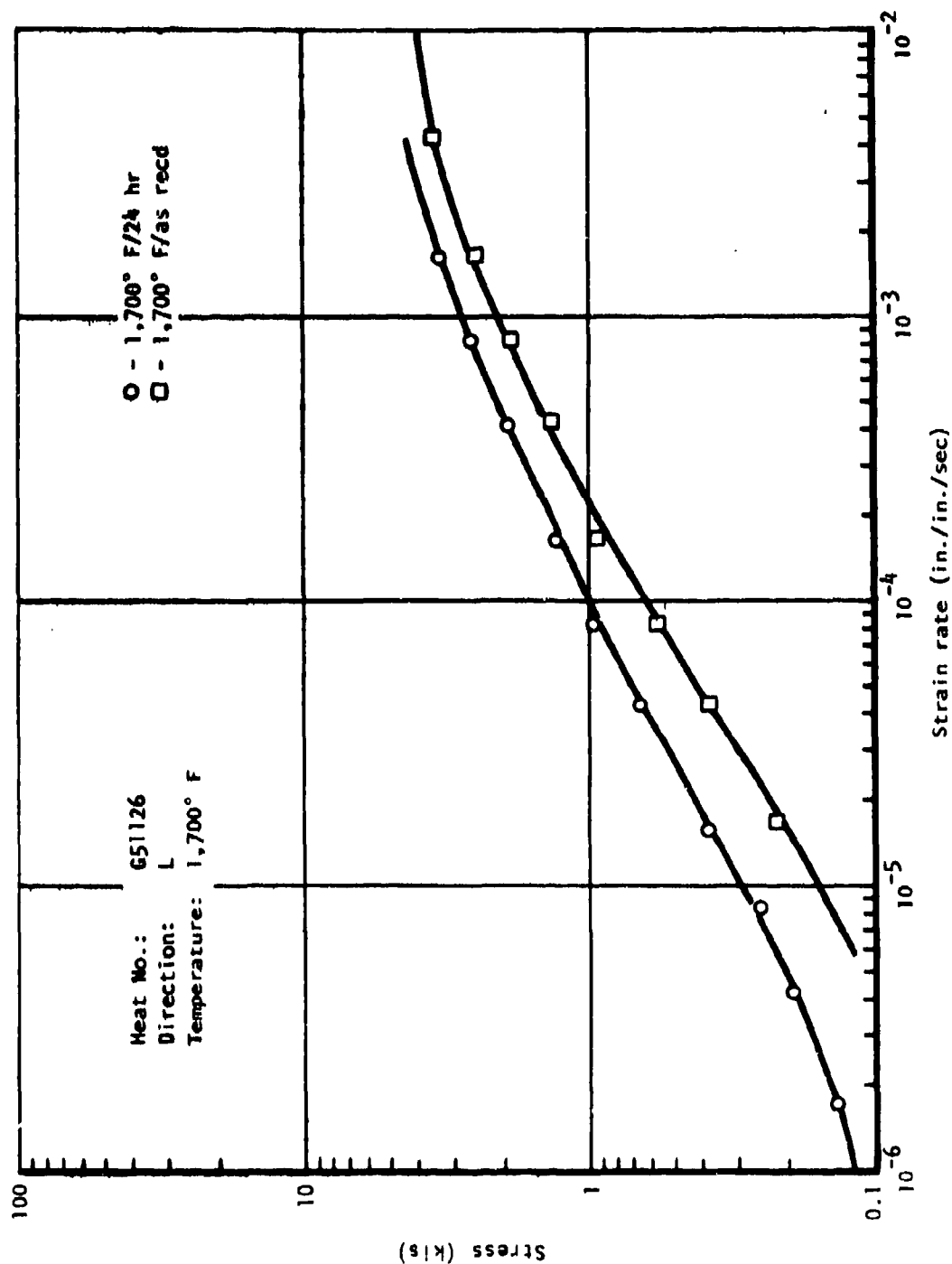
Figure 17. Effect of 24-hour exposure at 1,700° F on flow stress versus strain rate for heat G51126.
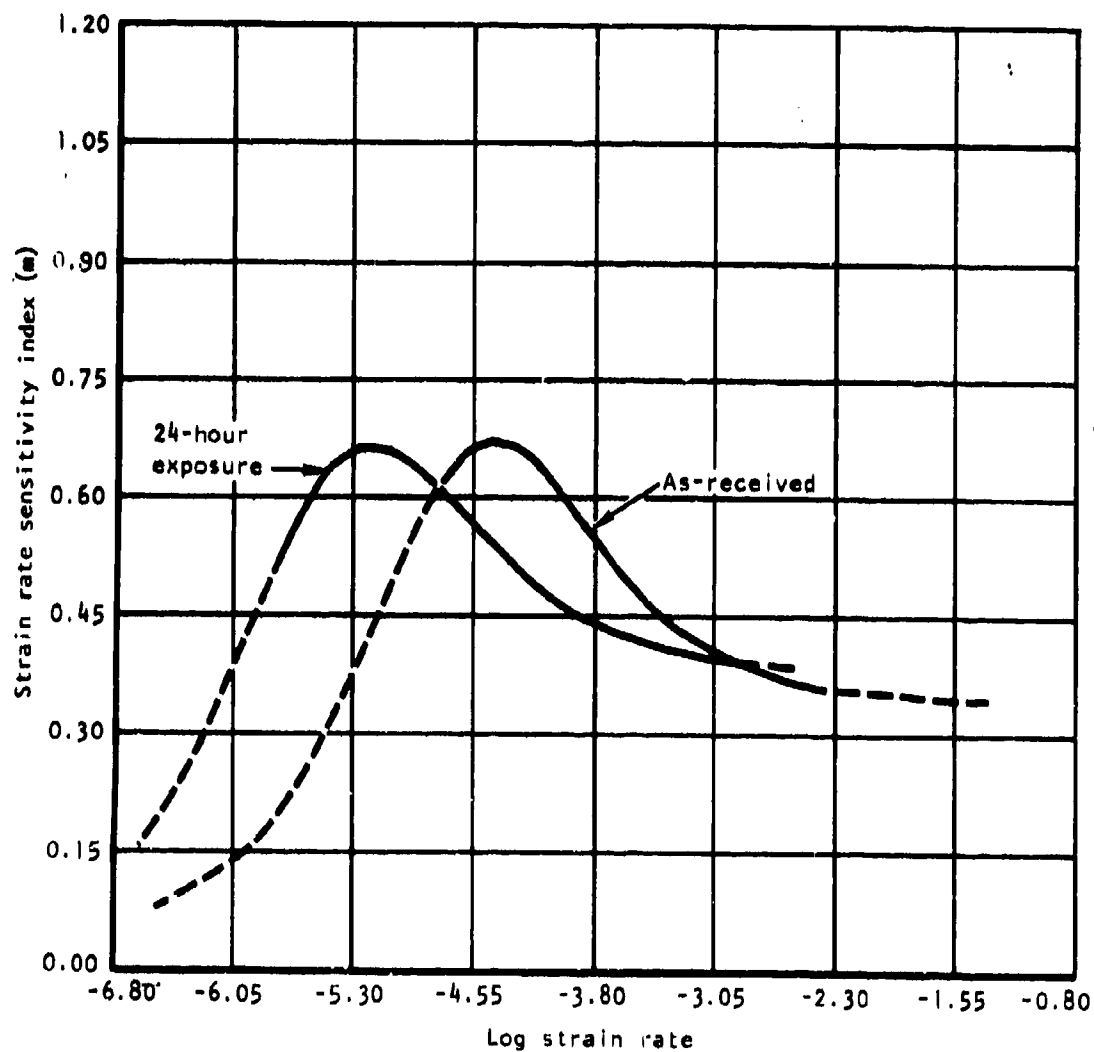
Figure 18. Comparison of strain rate sensitivity index versus log strain rate
of heat No. G51126 at 1,700° F in longitudinal direction for
as-received and 24-hour exposure conditions.

27

TABLE 5. SUPERPLASTIC FORMING PARAMETERS OF Ti-6Al-4V

Heat No.	Temperature (°F)	σ_o (KSI)		$m_{(max)}$		σ at $m_{(max)}$ (ksi)		$\dot{\varepsilon}$ at $m_{(max)}$ $\times 10^{-5}$ sec^{-1}	
		L	LT	L	LT	L	LT	L	LT
GS1125	1,500	1.14	0.869	0.538	0.607	3.25	3.16	4.8	6.01
	1,600	0.514	0.84	0.52	0.53	1.47	2.47	3.48	4.76
	1,700	0.07	0.16	0.685	0.511	0.33	0.53	3.2	9.0
301715	1,500	0.147	0.531	0.775	0.663	0.9	2.26	2.98	8.27
	1,600	0.119	0.069	0.756	0.740	0.71	0.42	7.06	3.5
	1,700	0.31	0.22	0.699	0.843	1.28	1.67	44	103
295405	1,500	0.184	0.185	0.819	0.811	1.35	1.38	7.92	7.15
	1,600	0.165	0.078	0.737	0.848	0.98	0.74	1.31	1.04
	1,700	0.124	0.132	0.909	0.908	1.57	1.62	93	100

From these data, it can be seen that increasing the temperature does not necessarily increase the m_{max} value markedly, but does increase the strain rate at which maximum m occurs, as the temperature is raised from 1,600°F to 1,700°F.

Unusual behavior was observed with material from heat G51126. The m_{max} was lowest at all temperatures on heat G51126 which necked in a very non-uniform manner at 1,500°F and 1,600°F. This is illustrated for the case at 1,500°F in Figure 19a where the surface of both the longitudinal (L) and long transverse (LT) samples are seen to be severely corrugated and nonuniform. In the LT sample, the deformation resulted in nonuniform thinning of the sheet. In the L sample, however, the cross section became corrugated as illustrated in Figure 19b. Figure 19c shows that the microstructure of this heat of acicular material was severely banded with acicular alpha in the plane of the sheet.

Since the superplastic forming process requires that the titanium be exposed to the forming temperature for a prolonged time, possibly as long as several hours for some parts, the effect of time at temperature on the super-plastic properties was considered.

To determine the effect of hold time on properties at temperature before load (or pressure) application, samples were held at 1,500° F, 1,600° F, 1,700°F, and 10°F below the transus for 24 hours. This excessive time was selected for evaluation to insure that the extreme effects of time at temperature were established — effects which exceed any encountered in an actual forming operation. It was expected that some grain growth might occur, particularly at the higher temperatures, resulting in increased flow stresses and possibly decreased formability, as measured by m values.

The samples were tested at the hold temperature by the standard strain rate change method as described previously to determine flow stress and m-value as a function of strain rate. Although increases were observed, no substantial change in flow stress properties was found at the various temperatures for any of the three heats tested.

The effect of the 24-hour exposure on longitudinal flow stresses and m-values is shown for the three heats at 1,700°F in Figures 13 through 18, where stress versus strain rate is plotted for as-received and 24-hour expo-sure at temperature. Heats 295405 and G51126 exhibited a slight increase in flow stresses after the 24-hour exposure, while heat 301715 showed a reduction of flow stress, accompanied by an increase in m-value from 0.699 to 0.930, for the long exposure. The cause of this change was not investigated, but may be due to a change of the anisotropy which was so pronounced for this heat of material, or variability of structure from area to area of the sheet. Further tests were not conducted to establish the cause of this anomalous result since the minor variation of properties observed for this prolonged
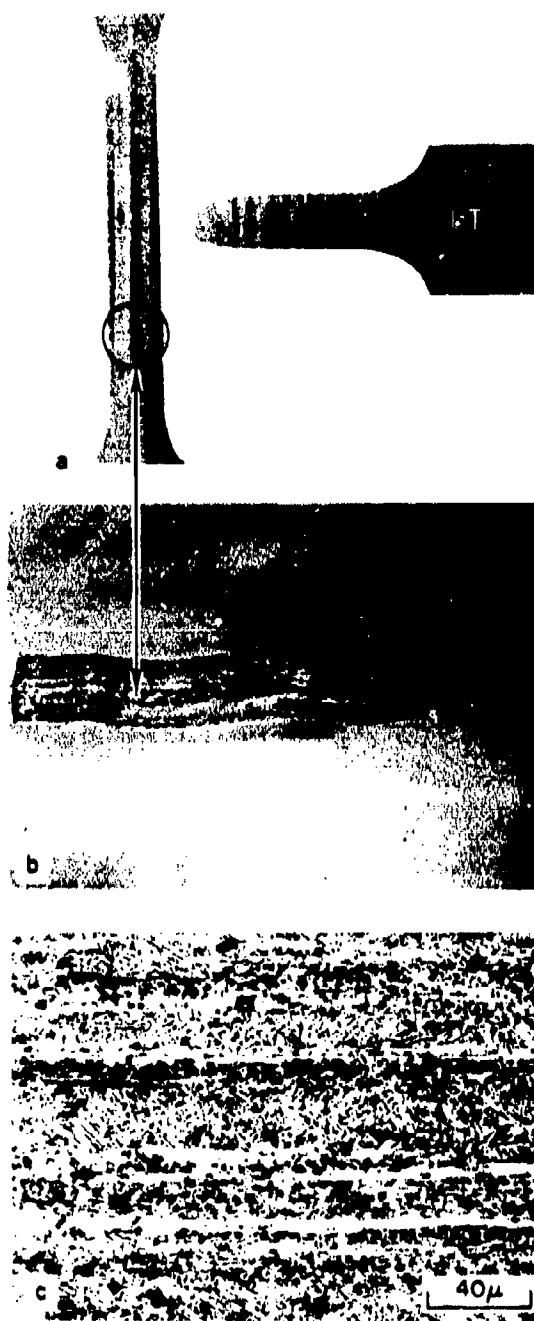
Figure 19. Example of nonuniform deformation in heat No. G51126.

exposure time are not considered to significantly impact the forming parameters for producing structural parts.

The results of these tests are encouraging, since no significant degradation in SPF ability was indicated even with the extreme hold time of 24 hours, a time which far exceeds that which would be encountered in a practical forming situation.

MECHANICAL PROPERTIES

The tensile properties of the L and LT directions for the six heats were determined for the as-received condition. The evaluation of process cycle effects was conducted on three of the heats which were selected to provide a range of superplastic characteristics and which were utilized in subsequent SPF studies. The three selected heats (G51126, 295405, and 301715) were subjected to a range of simulated SPF process cycles and subsequently tested to determine tensile, fatigue, and compression properties.

The samples were processed in a stainless steel retort which was filled with high purity argon to protect the surfaces. The six cycles are as follows:

1. 1/2 hr/1,700°F/furnace cool

2. 3 hr/1,700°F/furnace cool

3. 3 hr/1,750°F/furnace cool

4. 3 hr/1,650°F/furnace cool

5. 3 hr/1,500°F/furnace cool

6. 5 hr/1,700°F/furnace cool

The test specimen configurations were for the determination of the mechanical properties of the titanium sheet as shown in Figure 20.

The tensile and fatigue properties of the as-received material are presented in Tables 6 and 7, respectively, and the tensile, compression, and fatigue properties for the process cycled material are presented in Tables 8 through 15. The effect of increasing temperature (3-hour) exposure, as shown in Figures 21 and 22, is to reduce tensile properties somewhat in the 1,650°F to 1,750°F temperature range, although the change of properties within this range is slight. No drop in properties is observed for the 1,500°F/3 hr exposure, and no appreciable drop in the compressive yield properties is observed at any of the test temperatures as shown in figure 23.

31

8.0

0.50

1.25

Tensile

0.5010

t

1.0

Compression

3.0

7

3-1/2

1-1/8

0.50 ± 0.005

Smooth fatigue

7

2-1/4

50°
(typ)

0.25

Notched fatigue

R = 0.0212
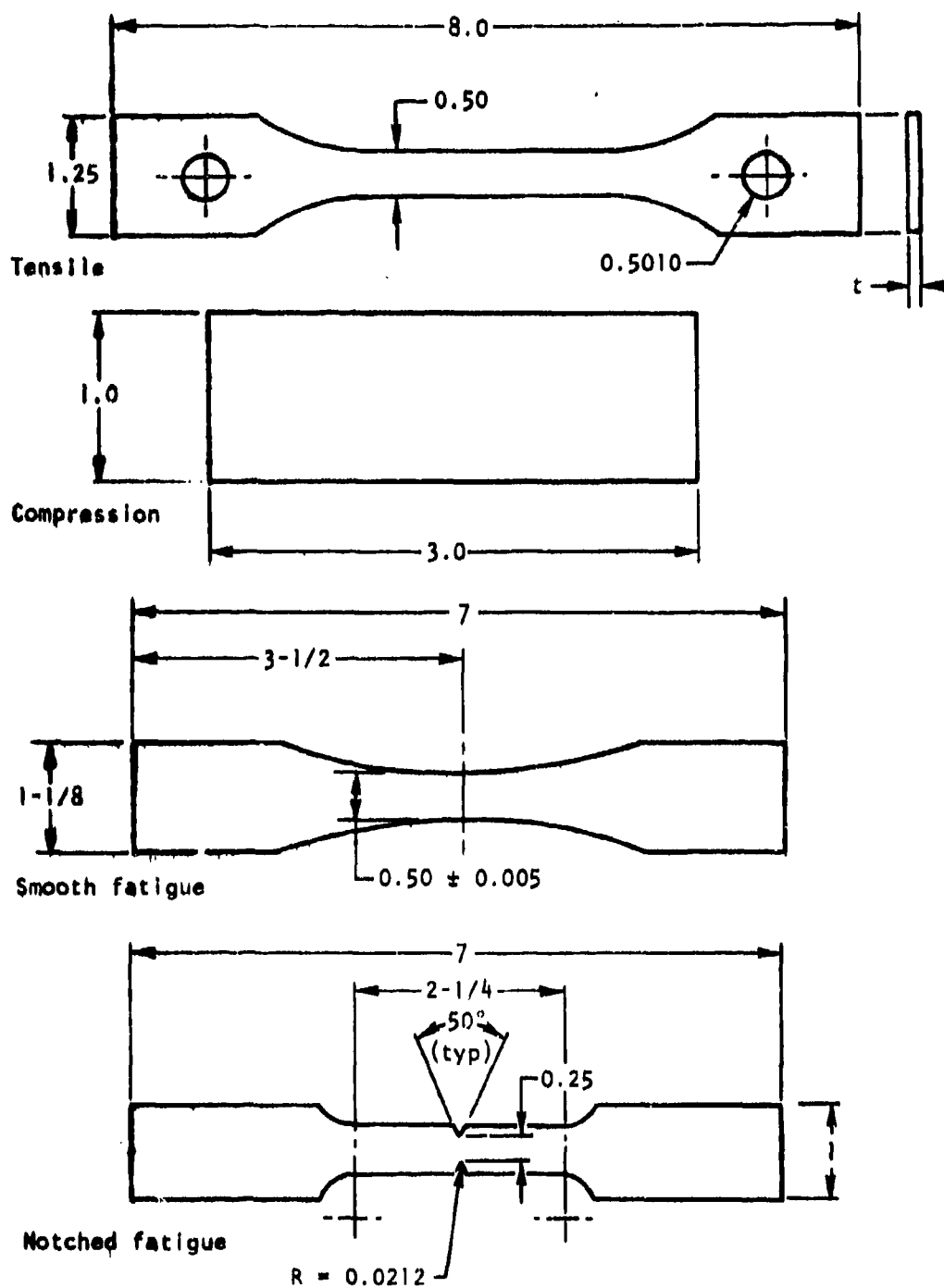
Figure 20. Test specimen configurations used to evaluate as-received
and thermally cycled Ti-6Al-4V sheet material.

Heat No.	Thickness (in.)	Test dir	Specimen No.	F_{tu} (ksi)	0.2% Yield (ksi)	% Elong (2 in. gage)
G51126	0.097	L	T11	148.2	130.4	10.0
		L	T115	142.3	126.4	9.5
		LT	T118	157.5	150.1	10.0
		LT	T131	157.6	150.6	9.5
295405	0.054	L	T21	144.1	141.1	13.0
		L	T215	143.7	139.9	11.5
		LT	T218	141.5	131.2	13.5
		LT	T231	143.8	133.5	14.5
K6838	0.061	L	T31	143.8	130.4	12.0
		L	T315	145.3	131.3	11.5
		LT	T318	150.0	144.0	13.0
		LT	T331	152.5	145.1	13.0
304488	0.060	L	T41	145.3	143.0	14.0
		L	T415	145.5	142.8	13.5
		LT	T418	142.6	137.6	14.0
		LT	T431	142.2	138.1	13.0
303182	0.108	L	T51	145.6	140.7	11.5
		L	T515	145.1	139.5	12.5
		LT	T518	154.7	152.7	13.0
		LT	T531	154.9	153.4	12.0
301715	0.058	L	T61	141.3	138.5	13.5
		L	T615	141.2	139.4	11.5
		LT	T618	138.9	132.6	13.5
		LT	T631	138.4	133.2	13.0

TABLE 7. SMOOTH FATIGUE & NOTCHED PROPERTIES OF AS-RECEIVED Ti-6Al-4V SHEET MATERIAL FOR PHASE I

Heat No.	Thickness (in.)	K_t	Test direction	Specimen No.	% F_{tu}^a	Cycles to failure	Comments
G51126	0.096	1	L	F13	62.0	4,001,080	No failure
					75.7	205,000	Retest
		1	L	F114	75.7	69,000	
		3	L	FL38	50.0	8,000	
		1	LT	F124	70.0	1,517,000	
		1	LT	F126	73.0	92,000	
		3	LT	F139	50.0	4,000	
295405	0.054	1	L	F23	76.4	2,400,000	No failure
					79.9	756,000	Retest
		1	L	F214	80.6	3,434,000	No failure
					83.4	1,497,000	Retest
		3	L	T22	50.0	11,000	
		1	LT	F224	84.1	23,000	
		1	LT	F226	84.1	96,000	
		3	LT	F243	50.0	9,000	
301715	0.058	1	L	F63	79.9	558,000	
		1	L	F614	81.4	Not Certain	
		3	L	T62	50.0	7,000	
		1	LT	F624	82.9	44,000	
		1	LT	F626	82.9	11,000	
		3	LT	F643	50.0	8,000	

$^a R = +0.05$

34

TABLE 8. TENSILE PROPERTIES OF PHASE I Ti-6Al-4V SHEET
MATERIAL PROCESSED THROUGH THERMAL CYCLES OF 1,500°,
1,650°, AND 1,750° F FOR 3 HOURS

Heat No.	Thickness (in.)	Time/temperature cycle (°F)	Test dir	Specimen No.	F_{tu} (ksi)	0.2% Yield (ksi)	% Elong (2 in. gage)
G51126	0.100	3 hr/1,500	L	T14	147.0	136.5	10.0
			LT	T117	160.0	153.8	12.0
		3 hr/1,650	L	T17	135.1	125.1	11.0
			LT	T120	154.4	145.4	12.0
		3 hr/1,750	L	T110	127.0	118.3	10.5
			LT	T122	152.8	142.2	11.5
295405	0.056	3 hr/1,500	L	T24	146.4	142.7	14.5
			LT	T217	144.4	132.9	13.5
		3 hr/1,650	L	T27	147.0	138.9	15.7
			LT	T22	139.1	124.8	13.5
		3 hr/1,750	L	T210	150.0	138.5	13.0
			LT	T222	137.3	125.2	10.0
301715	0.056	3 hr/1,500	L	T64	142.7	139.5	14.5
			LT	T617	139.3	131.6	13.5
		3 hr/1,650	L	T67	136.8	130.8	14.5
			LT	T620	135.6	125.0	14.0
		3 hr/1,750	L	T610	139.0	129.4	15.0
			LT	T622	132.0	118.2	13.0

TABLE 9. TENSILE PROPERTIES OF PHASE I Ti-6Al-4V SHEET
MATERIAL PROCESSED THROUGH THREE DIFFERENT
THERMAL CYCLES AT 1,700° F

Heat No.	Thickness (in.)	Time/ temperature cycle (°F)	Test dir	Specimen No.	F_{tu} (ksi)	0.2% Yield (ksi)	% Elong (2 in. gage)
G51126	0.100	1/2 hr/1,700	L	T133	134.6	125.9	11.5
		1/2 hr/1,700	L	T134[a]	134.3	126.1	12.0
		3 hr/1,700	L	A11	132.2	122.6	11.5
		3 hr/1,700	LT	E11	151.8	143.9	11.0
		5 hr/1,700	L	A12	135.4	127.1	11.0
		5 hr/1,700	LT	E12	155.4	150.1	6.5
295405	0.056	1/2 hr/1,700	L	T233	142.3	136.9	15.0
		1/2 hr/1,700	LT	T238	138.5	126.6	14.5
		3 hr/1,700	L	A21	141.7	134.5	14.0
		3 hr/1,700	LT	E21	136.6	123.3	14.5
		5 hr/1,700	L	A22	146.4	137.8	14.0
		5 hr/1,700	LT	E22	143.6	128.7	11.0
301715	0.056	1/2 hr/1,700	L	T633	136.3	122.1	14.5
		1/2 hr/1,700	LT	T638	134.6	125.0	15.5
		3 hr/1,700	L	A6	138.8	131.7	14.5
		3 hr/1,700	LT	I61	131.7	121.2	12.0
		5 hr/1,700	L	B6	146.2	137.5	14.5
		5 hr/1,700	LT	I62	136.5	124.0	13.0

TABLE 10. COMPRESSION PROPERTIES OF PHASE I Ti-6A1-4V SHEET
MATERIAL PROCESSED THROUGH THERMAL CYCLES OF 1,500°,
1,650°, AND 1,750° F FOR 3 HOURS

Heat No.	Thickness (in.)	Time/ temperature cycle (°F)	Test dir	Specimen No.	0.2% F_{cy} (ksi)	Modulus (10^6)
G51126	0.100	3 hr/1,500	L	C113	127.5	16.1
			LT	C125	188.0	20.9
		3 hr/1,650	L	C18	120.2	16.3
			LT	C127	183.9	21.3
		3 hr/1,750	L	C16	116.2	16.7
			LT	C129	186.8	20.7
295405	0.056	3 hr/1,500	L	C213	152.7	18.7
			LT	C225	135.5	17.0
		3 hr/1,650	L	C28	149.8	18.7
			LT	C227	126.7	17.0
		3 hr/1,750	L	C26	151.5	18.8
			LT	C229	123.4	16.4
301715	0.056	3 hr/1,500	L	C613	147.9	18.6
			LT	C625	132.2	17.0
		3 hr/1,650	L	C68	144.8	19.0
			LT	C627	125.3	16.6
		3 hr/1,750	L	C66	142.2	18.9
			LT	C629	120.7	16.9

TABLE 11. COMPRESSION PROPERTIES OF PHASE I Ti-6Al-4V SHEET MATERIAL PROCESSED THROUGH THREE DIFFERENT THERMAL CYCLES OF 1,700° F

Heat No.	Thickness (in.)	Time/ temperature cycle (°F)	Test dir	Specimen No.	0.2% F_{cy} (ksi)	Modulus (10^6)
G51126	0.100	1/2 hr/1,700	L	C121	126.2	16.5
		1/2 hr/1,700	LT	C138	186.4	20.8
		3 hr/1,700	L	C11	119.6	16.4
		3 hr/1,700	LT	H11	184.9	20.7
		5 hr/1,700	L	C122	125.2	16.2
		5 hr/1,700	LT	H12	190.7	21.7
295405	0.056	1/2 hr/1,700	L	C236	147.5	19.0
		1/2 hr/1,700	LT	C240	129.3	17.0
		3 hr/1,700	L	C21	148.8	19.4
		3 hr/1,700	LT	H21	128.1	17.2
		5 hr/1,700	L	C22	154.2	20.0
		5 hr/1,700	LT	H22	131.4	16.6
301715	0.056	1/2 hr/1,700	L	C636	142.5	18.3
		1/2 hr/1,700	LT	C640	125.2	17.2
		3 hr/1,700	L	G6	144.6	18.6
		3 hr/1,700	LT	L61	122.1	16.3
		5 hr/1,700	L	H6	150.6	18.7
		5 hr/1,700	LT	L62	126.7	16.8

TABLE 12. SMOOTH FATIGUE PROPERTIES OF PHASE I Ti-6A1-4V SHEET
MATERIAL PROCESSED THROUGH THERMAL CYCLES OF 1,500°, 1,650°,
AND 1,750° F FOR 3 HOURS

Heat No.	Thickness (in.)	Time/ temperature cycle (°F)	Test dir	Specimen No.	$\%^a$ F_{tu}	Cycles to failure	Applied stress (ksi)
GS1126	0.096	3 hr/1,500	L LT	F15 F119	78.2 65.6	40,000 663,000	115 105
		3 hr/1,650	L LT	F19 F121	85.1 68.0	53,000 446,000	115 105
		3 hr/1,750	L LT	F116 F132	90.5 68.7	39,000 80,000	115 105
295405	0.054	3 hr/1,500	L LT	F25 F219	75.1 76.2	565,000 71,000	110 110
		3 hr/1,650	L LT	F29 F221	74.8 79.1	82,000 264,000	110 110
		3 hr/1,750	L LT	F216 F232	73.3 80.1	109,000 67,000	110 110
301715	0.058	3 hr/1,500	L LT	F65 F619	73.6 75.4	570,000 120,000	105 105
		3 hr/1,650	L LT	F69 F621	76.8 77.4	77,000 84,000	105 105
		3 hr/1,750	L LT	F616 F632	75.5 79.5	110,000 49,000	105 105

$^a R = +0.05$

39

TABLE 13. SMOOTH FATIGUE PROPERTIES OF PHASE I Ti-6A1-4V SHEET
MATERIAL PROCESSED THROUGH THREE DIFFERENT
THERMAL CYCLES AT 1,700° F

Heat No.	Thickness (in.)	Time/ temperature cycle (°F)	Test dir	Specimen No.	$\%^{a}$ F_{tu}	Cycles to failure	Applied stress (ksi)
G51126	0.096	1/2 hr/1,700	L	F135	78.0	98,000	105
		1/2 hr/1,700	LT	F136	78.2	89,000	105
		3 hr/1,700	LT	D11	79.4	67,000	105
		3 hr/1,700	LT	G11	69.2	310,000	105
		5 hr/1,700	L	D12	77.5	60,000	105
		5 hr/1,700	LT	G12	67.6	114,000	105
295405	0.054	1/2 hr/1,700	L	F234	77.3	56,000	110
		1/2 hr/1,700	LT	F237	79.4	43,000	110
		3 hr/1,700	LT	G21	80.5	23,000	110
		3 hr/1,700	LT	G21	80.5	23,000	110
		5 hr/1,700	L	D22	75.1	33,000	110
		5 hr/1,700	LT	G22	76.6	12,000	110
301715	0.058	1/2 hr/1,700	L	F634	77.0	97,000	105
		1/2 hr/1,700	LT	F637	78.0	76,000	105
		3 hr/1,700	L	E6	75.0	90,000	105
		3 hr/1,700	LT	K61	79.7	61,000	105
		5 hr/1,700	L	F6	71.8	53,000	105
		5 hr/1,700	LT	K62	76.9	47,000	105

$^{a}R = +0.05$

TABLE 14. NOTCHED FATIGUE ($K_t = 3$) PROPERTIES OF PHASE I Ti-6Al-4V SHEET MATERIAL PROCESSED THROUGH THERMAL CYCLES OF 1,500°, 1,650°, AND 1,750° F FOR 3 HOURS

Heat No.	Thickness (in.)	Time/ temperature cycle (°F)	Test dir	Specimen No.	%[a] F_{tu}	Cycles to failure	Applied stress (ksi)
G51126	0.096	3 hr/1,500	L	F1123	50.0	11,000	73.5
		3 hr/1,500	LT	F1303		10,000	80.0
		3 hr/1,650	L	F1173		16,000	67.6
		3 hr/1,650	LT	F1283		7,000	77.2
		3 hr/1,750	L	F1183		40,000	63.5
		3 hr/1,750	LT	F1233		11,000	76.4
295405	0.054	3 hr/1,500	L	F2123	50.0	10,000	73.0
		3 hr/1,500	LT	F2303		14,000	72.2
		3 hr/1,650	L	F2173		15,000	73.5
		3 hr/1,650	LT	F2283		17,000	69.6
		3 hr/1,750	L	F2183			75.0
		3 hr/1,750	LT	F2233		17,000	68.7
301715	0.058	3 hr/1,500	L	F6123	50.0	16,000	71.4
		3 hr/1,500	LT	F6303		8,000	69.7
		3 hr/1,650	L	F6173		20,000	68.4
		3 hr/1,650	LT	F6283		17,000	67.8
		3 hr/1,750	L	F6183		12,000	69.5
		3 hr/1,750	LT	F6233		24,000	66.0

[a]$R = +0.05$

41

TABLE 15. NOTCHED FATIGUE ($K_t=3$) PROPERTIES OF PHASE I Ti-6A1-4V SHEET
MATERIAL PROCESSED THROUGH THREE DIFFERENT
THERMAL CYCLES AT 1,700° F

Heat No.	Thickness (in.)	Time/ temperature cycle (°F)	Test dir	Specimen No.	F_{tu}[a]	Cycles to failure	Applied stress (ksi)
G51126	0.096	1/2 hr/1,700	L	F1373	52.0	24,000	70
		1/2 hr/1,700	LT	F1113	52.1	13,000	70
		3 hr/1,700	L	B11	53.0	14,000	70
		3 hr/1,700	LT	F11	46.1	9,000	70
		5 hr/1,700	L	B12	51.7	16,000	70
		5 hr/1,700	LT	F12	45.0	8,000	70
295405	0.054	1/2 hr/1,700	L	F2353	49.2	9,000	70
		1/2 hr/1,700	LT	F2393	50.5	14,000	70
		3 hr/1,700	L	B21	49.4	13,000	70
		3 hr/1,700	LT	F21	51.2	9,000	70
		5 hr/1,700	L	B22	47.8	10,000	70
		5 hr/1,700	LT	F22	48.7	11,000	70
301715	0.058	1/2 hr/1,700	L	F6353	51.4	10,000	70
		1/2 hr/1,700	LT	F6393	52.0	11,000	70
		3 hr/1,700	L	C6	50.4	10,000	70
		3 hr/1,700	LT	J61	53.2	10,000	70
		5 hr/1,700	L	D6	47.9	11,000	70
		5 hr/1,700	LT	J62	51.3	9,000	70

[a] $R = +0.05$
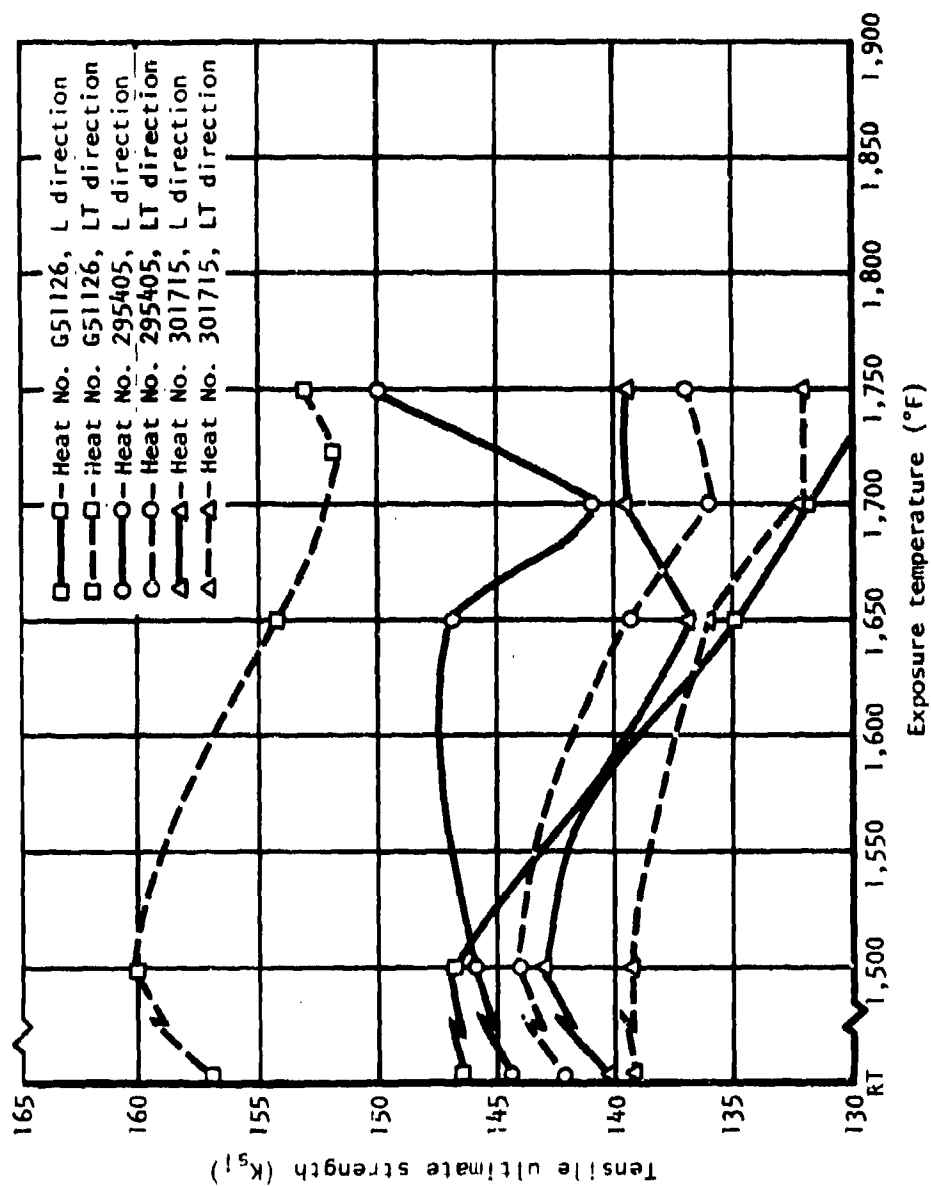
Figure 21. Tensile ultimate strengths as a function of temperature at which material was exposed for 3 hours.
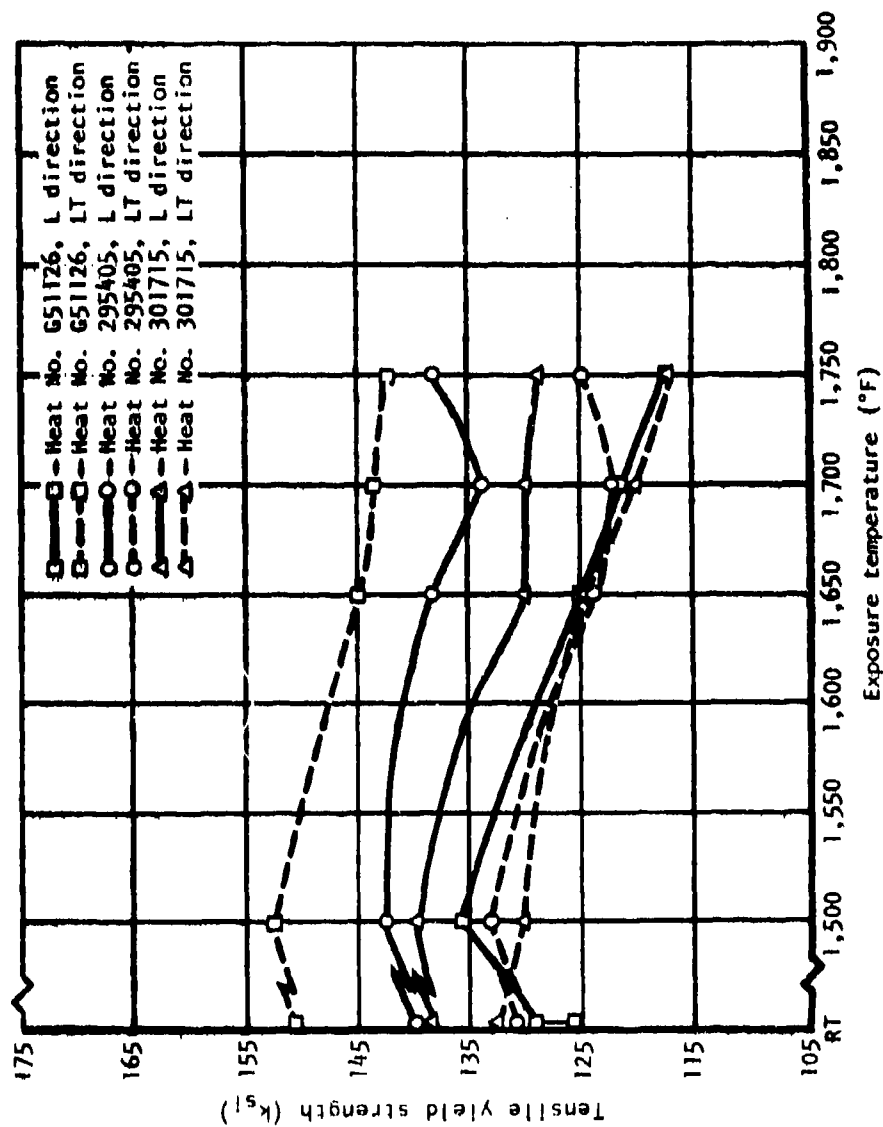
Figure 22. Tensile yield strengths as a function of temperature at which material was exposed for 3 hours.

44
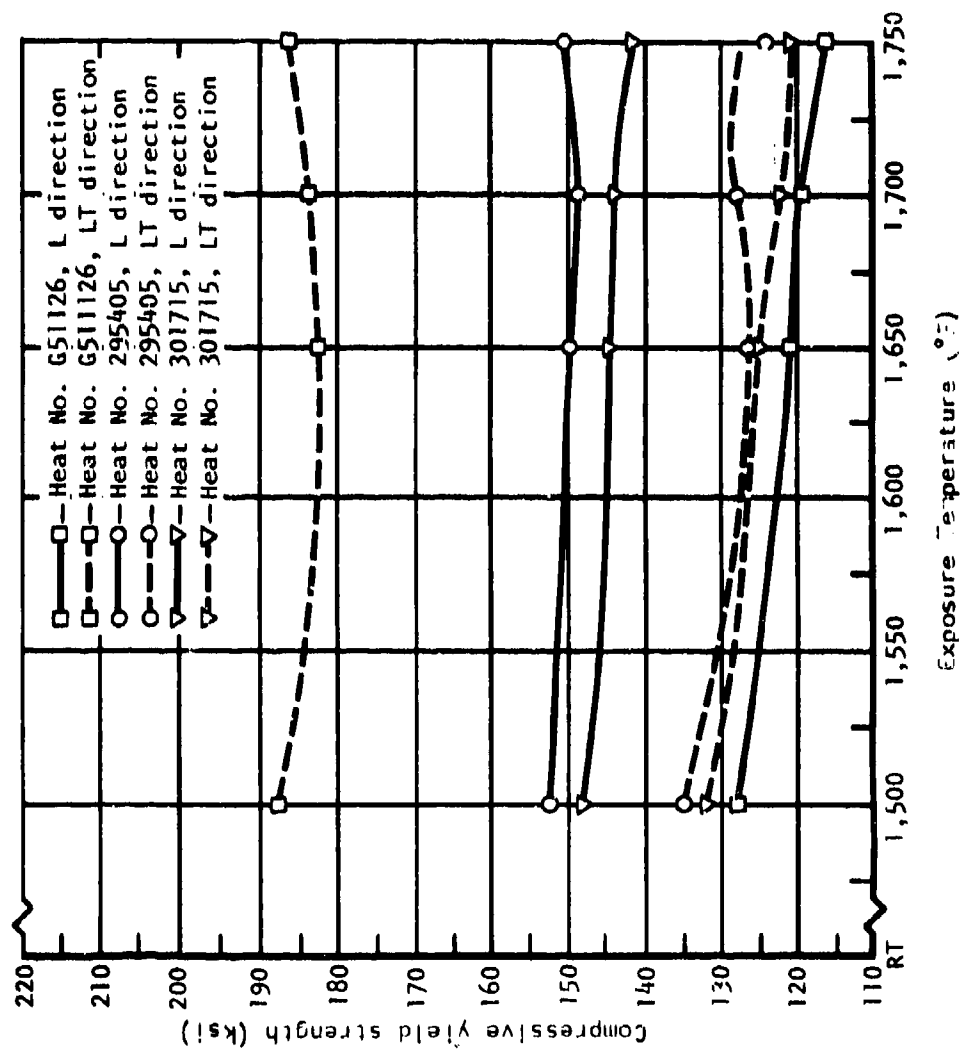
Figure 23. Compressive yield strength as a function of temperature at which materials were exposed for 3 hours.

45

Heat G51126 exhibited unusual anistrostropic properties. A high degree
of anistropy in mechanical properties was observed in this material for the
as-received condition, and this anisotropy was maintained after the exposure
to the various thermal cycles. This characteristic was most pronounced for
the compression yield strength and compression modulus as shown in Tables 10
and 11. These anisotropic properties are traceable to the high degree
crystallographic texture and banding observed for this particular heat of
material. The highest modulus and highest strength both are observed in the
long transverse direction, the direction coincident with the highest concen-
tration of basal (0002) poles.

The variation of time from 1/2 to 5 hours at 1,700°F does not cause a
noticeable change in resulting tensile ultimate or yield strength (refer to
Table 9). The compression yield strengths follow the same trend with
exposure as the tensile yield.

No effect of the temperature or time exposure combinations on fatigue life
is observed where the fatigue cycles to failure is considered as a function
of applied stress expressed as a percent of ultimate strength.

CORRELATION BETWEEN MICROSTRUCTURE AND SUPERPLASTICITY

From the six heats of material evaluated, one of these materials (G51126)
is, at best, a borderline superplastic material and is not considered desirable
for the process. Thus, although most commercially available material is
expected to be suitable for superplastic forming, it is desirable to have a
correlation between microstructure and superplastic properties. Such a
correlation could be valuable in screening material or in establishing pro-
curement requirements.

The six heats evaluated under contract were examined in detail for micro-
structural characteristics, superplastic properties, and the correlation of
these characteristics with the m_{max} values at 1,700°F. These results are
summarized in Table 16. The major result of this effort is the observation
that a "refined" grain structure will consistently produce high m_{max} values
(e.g., greater than about 0.70) and corresponding high tensile elongations
(e.g., greater than about 500 percent elongation). A refined grain structure
referred to here is as follows:

* No blocky alpha

* No acicular alpha

46

TABLE 16. MICROSTRUCTURE AND PROPERTIES OF Ti-6Al-4V SHEET

Heat No.	Orientation	max m-value[a]	Elongation[a] percent	Flow stress (Ksi)	Volume Percent		Grain size (μ)	Uniform grain size	Grain Aspect ratio	Comment
					Acicular	Blocky				
K6838	L	.926	230	3.1	0	21	7.6	No	~4	
K6838	LT	.895	310	2.98						
301715	L	.699	511	2.65	11	11	8.7	No	~3	
301715	LT	.843	535	2.36						
303182	L	.816	675	2.26	0	9	9.8	Yes	~3	
303182	LT	.825	512	2.18						
304488	L	.836	512	2.17	0	0	8.6	Yes	~1	
30448	LT	.784	500	2.24						
295405	L	.909	550	2.47	0	0	8.1	Yes	~1	
295405	LT	.908	475	2.40						
G51126	L	.685	612	2.47	29	0	6.5	No	~6	Heavily banded structure
G51126	LT	.511	412	2.08						

a at 1,700° F

b $\dot{\epsilon}$ = 1.67 x 10^{-3} sec^{-1}

47

- Uniform grain size

- Grain aspect ratio ≅ 1

- No banded structure

- Grain size less than about 10 μ diameter

This is supported also by Lee and Backofen (Reference 2). In their tests, the Ti-6Al-4V basic material was of "refined" structure which was processed to increase grain size as well as to transform the structure (i.e., exceed beta transus temperature). For this material with a grain diameter less than 11.4 μ, maximum m values of 0.7 and above were observed.

On the other extreme of the microstructural spectrum is the beta transformed and heavily banded structure with high acicular alpha concentration which develop reduced m_{max} values and little or no capability for SPF. For transformed Ti-6Al-4V, Lee and Backofen show m values less than 0.35. Heat G51126 evaluated in this program was heavily banded with a high concentration of acicular alpha, nonuniform grain size, and with a grain aspect ratio approximately = 6. Even though the average grain size for this heat was 6.5 μ, the m_{max} value was low (0.511 to 0.685).

The most difficult correlation to obtain is for intermediate microstructural characteristics; that is, for grain aspect ratios in the range of 3 to 6, uniform or nonuniform grain size, concentrations of blocky alpha (to 21 volume percent), concentrations of acicular alpha (to 11 volume percent), with grain diameters less than about 10 μ, as shown in Table   . For these microstructural conditions, m_{max} values of from 0.699 to 0.926 were determined.

The data of Table 16 suggest that some concentrations of blocky alpha are less detrimental to m_{max} properties than corresponding concentrations of acicular alpha. However, data in these ranges of microstructure are limited and, until a greater volume of data are available and a more solid correlation established, a high-temperature mechanical property test is considered necessary to confirm that a material with questionable microstructure is highly superplastic.

No consistent correlation was found between the m_{max} and elongations measured, but subsequent forming studies conducted in phase I of this program demonstrated that m_{max} is a better measure of the capability of the material for SPF than the total elongation measured.

The reason for this is that the forming problems encountered were tearing over a die edge and is related to plastic instability which m_{max} measures, and not limited elongation. The total elongation available in the materials tested, however, is more than sufficient to meet the total stretch requirements of the parts fabricated in this program (and probably most structural configurations).

OTHER PROCESS FACTORS (TASK 2)

This effort was conducted to evaluate nonmaterial-dependent processing variables including tooling and surface enrichment control techniques.

This activity was concentrated on establishing tool alloy compositions compatible with Ti-6Al-4V at SPF temperatures, and techniques for controlling the environment surrounding the titanium sheet during processing to minimize enrichment from gaseous interstitials such as oxygen and nitrogen.

TOOLING

Since the forming pressures necessary for superplastic forming titanium are typically low, it was considered that relatively low-strength alloys would be suitable for forming most parts. The primary consideration was that of compatibility with the tooling material at the processing temperature and, therefore, candidate tooling materials were evaluated for their interactions with Ti-6Al-4V at 1,700°F.

A list of 25 potential tooling materials was compiled on the basis of a literature survey and prior experience in diffusion bonding processing of titanium. Fifteen of these materials were selected for subsequent reaction studies with Ti-6Al-4V on the basis of their availability, machinability, available forms, coefficient of thermal expansion, alloy content, and cost. The established list of 15 candidate materials contains carbon and alloy steels, graphite, and ceramic. (Refer to Table 17). All of these materials were expected to be acceptable for use as tooling in the SPF of titanium when compared to the two baseline tooling materials, 4130 and 4340 steels, previously used in SPF and diffusion bonding studies.

Studies at Rockwell have shown that the diffusion depth in Ti-6Al-4V is a function of the C/Ni ratio. Consequently, the candidate iron-base materials have moderate to high carbon and low nickel contents. Each of the 15 candidates was subjected to intimate contact with Ti-6Al-4V in an argon environment with 250 psi applied pressure at 1,700°F for 3 hours. This pressure, which is higher than that anticipated for SPF, was deliberately applied to achieve simplicity in the test setup and to insure that the results of the tests would be conservative. The exposed titanium was subsequently subjected to metallographic analysis to evaluate the extent of surface reaction.

TABLE 17.   CHEMICAL COMPOSITION OF CANDIDATE TOOLING MATERIALS EVALUATED

Tooling Material	Composition (%)							
	C	Ni	Cr	Mn	Si	Mo	V	W
C1022	0.20	-	-	0.45	-	-	-	-
Graphite	-	-	-	-	-	-	-	-
6150	0.50	0.11	0.96	0.79	0.29	0.04	0.19	-
440C	1.01	0.27	16.73	0.35	0.36	0.53	-	-
431	0.15	2.44	15.86	0.64	0.28	0.16	-	-
H11	0.39	0.04	4.83	0.24	0.90	1.31	0.43	-
300M	0.42	1.74	0.90	0.87	1.62	0.40	-	-
D6AC	0.46	0.56	1.04	0.75	0.22	1.00	-	-
4130	0.30	-	0.95	0.50	0.30	0.20	-	-
4340	0.40	1.80	0.75	0.85	0.20	0.25	-	-
01	0.90	-	0.50	1.00	-	-	-	0.50
SiO_2	-	-	-	-	-	-	-	-
CA40	0.30	1.00	13.00	1.00	-	0.50	-	-
52100	1.02	0.11	1.45	0.39	0.28	0.06	-	-
A10	1.35	1.85	-	1.80	1.20	1.50	-	-

(a)
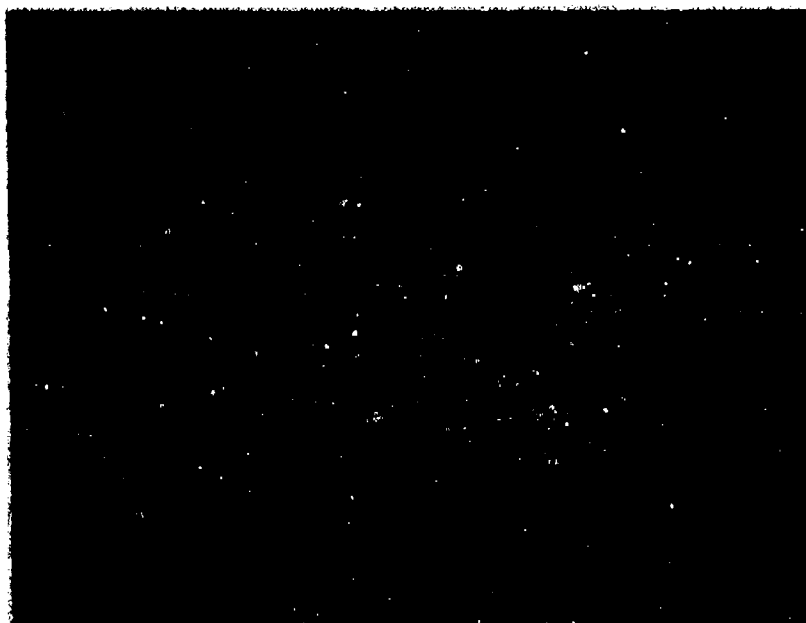
Effect of 4130   500X

(b)
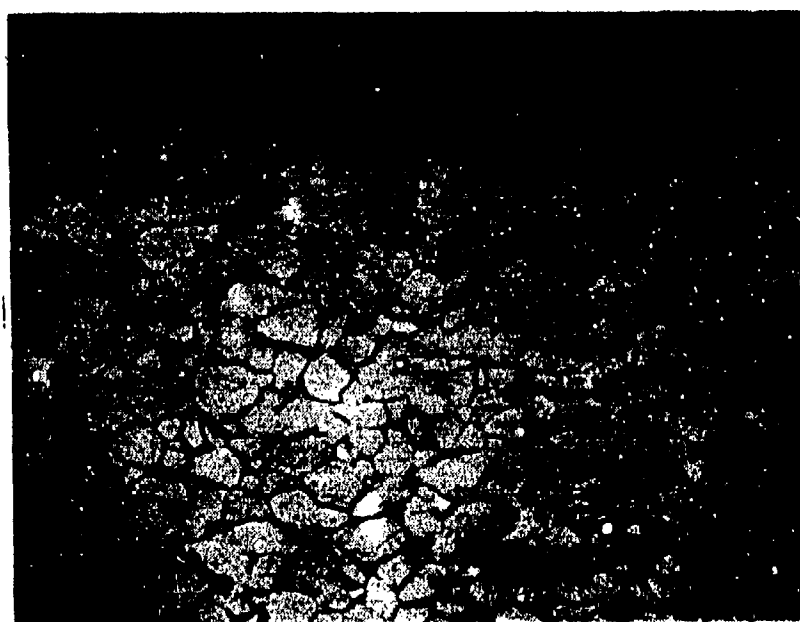
Effect of 4340   500X

Figure 24.   Effect of candidate tooling material placed in contact
             with Ti-6Al-4V at 1,700° F.

51

(a)

Effect of 440C   500X

(b)

Effect of 431   500X

Figure 25.   Effect of candidate tooling material placed in contact with
Ti-6Al-4V at 1,700° F

52

(a)

Effect of C1020   500X

(b)
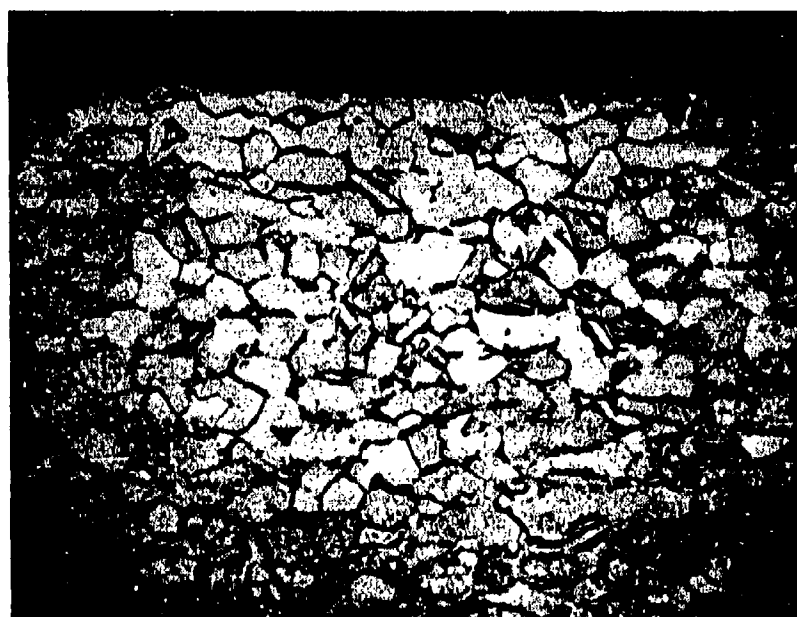
Effect of graphite   500X

Figure 26.   Effect of candidate tooling material placed in contact
with Ti-6A1-4V at 1,700° F.

53

(a)

Effect of D6AC   500X

(b)
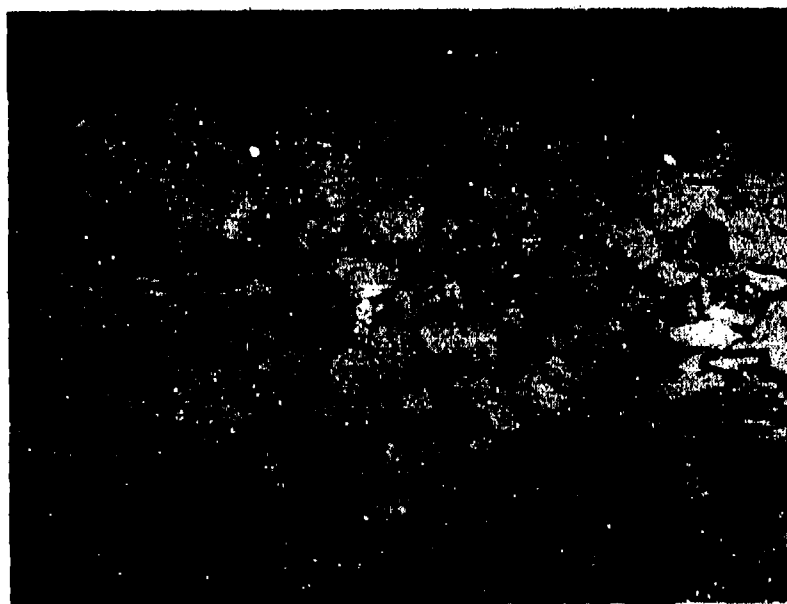
Effect of 300M   500X

Figure 27.   Effect of candidate tooling material placed in contact
with Ti-6Al-4V at 1,700° F.

(a)
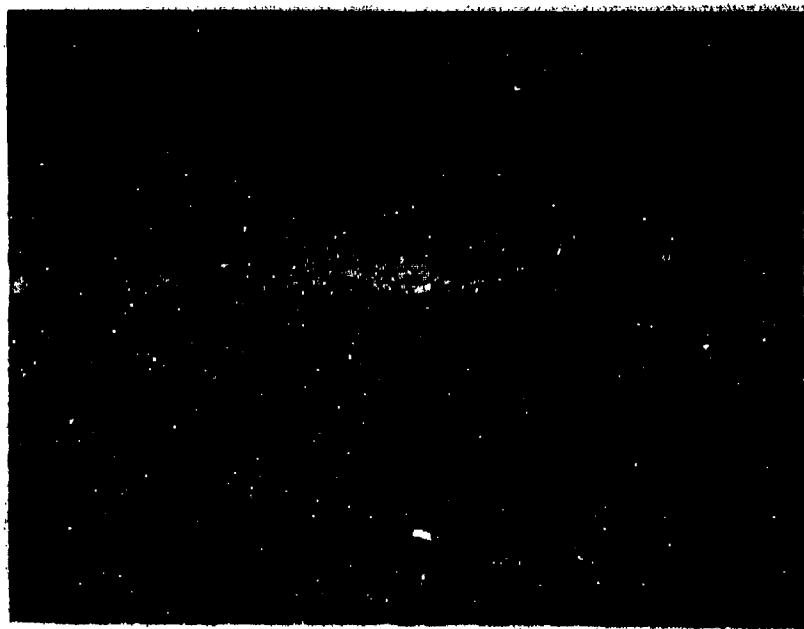
Effect of 01   500X

(b)
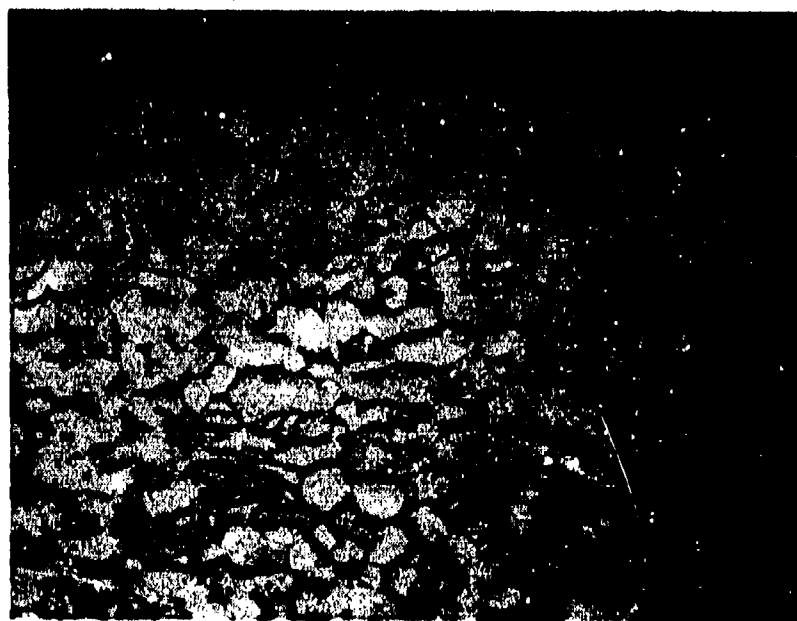
Effect of H11   500X

Figure 28.   Effect of candidate tooling material placed in contact
with Ti-6Al-4V at 1,700° F.

55

(a)

Effect of 321   100X

(b)

Effect of 6150   500X

Figure 29. Effect of candidate tooling material placed in contact with Ti-6Al-4V at 1,700° F.
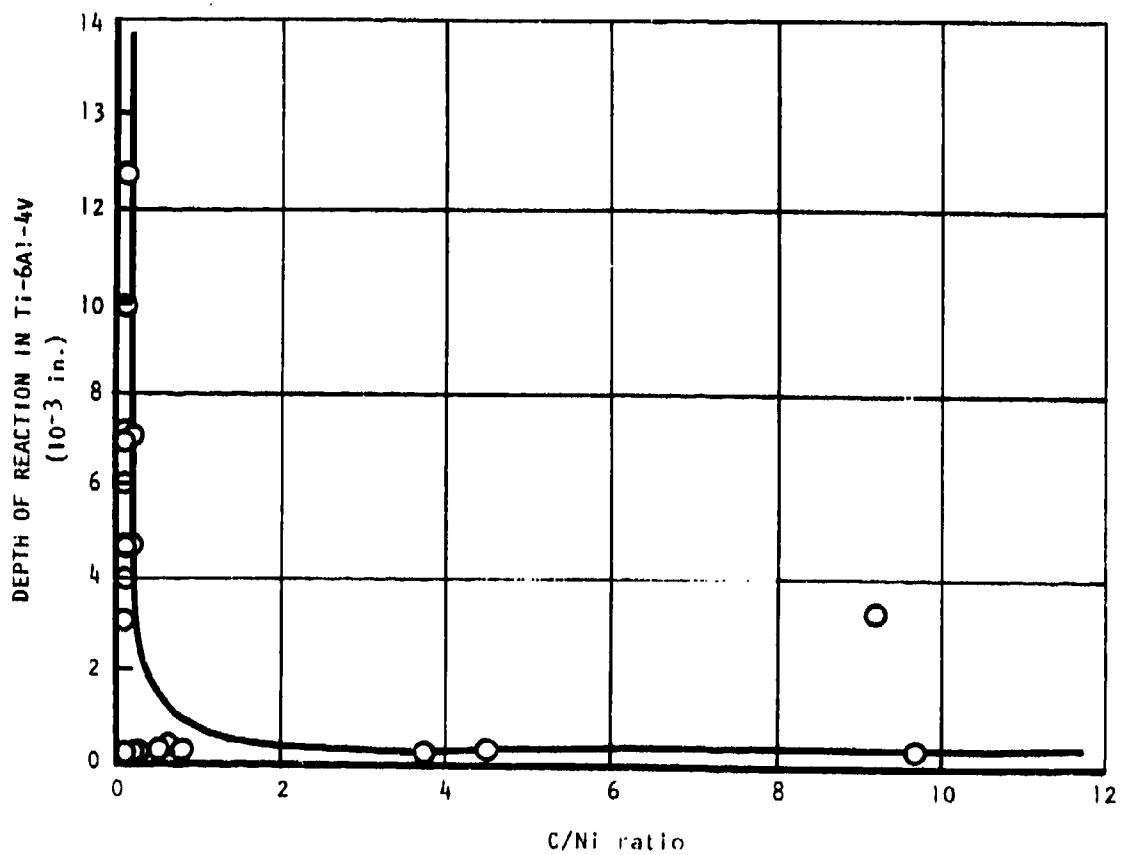
Figure 30. Effect of C/Ni ratio of iron base tool alloys on depth of reaction with Ti-6Al-4V after exposure to 1,700° F.

TABLE 18. DEPTH OF REACTION IN Ti-6Al-4V RESULTING FROM CONTACT WITH TOOL MATERIAL INDICATED[a]

Tooling candidate	Depth of Reaction		
	First run	Second run	Third run
C1020	<0.0001 in.	<0.0001 in.	None observed[b]
SiO2	<0.0001 in.	None observed	None observed[b]
Graphite	<0.0001 in.	<0.0001 in.	- - - - - - - - -
CA40	<0.0001 in.	-	
431	<0.0001 in.	0.0027 in.	
440C	<0.0001 in.	<0.0001 in.	None observed[b]
4130	0.00015 in.	-	- - - - - - -
H11	0.00015 in.	<0.0001 in.	None observed[b]
4340	0.00020 in.	-	
6150	0.00018 in.	-	
300M	0.00023 in.	-	
D6AC	0.00025 in.	-	
01	0.00030 in.	-	
A10	0.00037 in.	-	
52100	0.00270 in.		

[a] Exposure: 1,700° F, 250 psi, 3 hours (simulated forming run)

[b] Included in actual forming operation

The effect of the candidate tooling on the Ti-6Al-4V material that was placed in contact with the tooling is shown in Figures 24 through 29. The effect of increased Ni content and low carbon content is shown in Figure 30 which shows the significant surface diffusion resulting from titanium content with 321 stainless steel.

The materials which exhibited a smaller reaction layer than either 4130 or 4340 steel are C1020, SiO_2, graphite, 431, CA40, 440C, and H11 which were exposed to a additional compatibility tests to assess their characteristics when subjected to multiple runs. After testing, the 431 stainless steel was eliminated from further consideration as it showed an increase in the reaction layer of exposed titanium by approximately 3 mils. The ceramic, SiO_2, was not considered to be a suitable tooling material for most applications as it cracked and chipped around the edges. The remaining tooling candidates, C1020, graphite, 440, and H11 were subjected to a simulated forming process under 30 psi pressure. After this exposure, no measurable reaction layer in the titanium exposed to the tooling materials was observed. The results of the compatibility tests are presented in Table 18.

The materials which showed best compatibility with titanium are the alloy and carbon steels. The least expensive of the materials is 1020 low carbon steel. Other low-cost, readily available materials which are compatible with Ti-6Al-4V are 4130, 4340, H11, 6150, and other similar materials which are low in nickel (e.g., less than about 2 percent) and contain more than about 0.20 percent carbon. The extent of reaction between the Ti-6Al-4V and candidate tooling materials is minimal for all cases, being less than 0.0001-inch deep, as shown in Table 18, and should be easily removed by pickling or chem-milling. This limited extent of reaction is contrasted by the much heavier reaction encountered with steels of much higher nickel content, for example 321 stainless steel, with which the reaction depth exceeds 0.014 inch (Figure 29a).

A 4340 steel tool which was fabricated for use in subsequent forming studies was subjected to multiple forming runs, and was evaluated periodically for increased reaction with the titanium and for distortion or change in dimensions. No increase in reaction depth in the area of forming was observed, although sticking between the tool and titanium at the seal area was encountered after six forming runs. This problem was corrected by spraying graphite on the tool sealing surfaces prior to forming. The graphite coating prevented further sticking, and subsequent tests indicated that this spray coating can be used as a stop-off on internal tooling surfaces as well. (See Figure 31). No significant dimensional changes were observed in this small tool.

Figure 31. As-formed Ti-6Al-4V surface in contact with tooling sprayed with graphite coating (oxalic acid etchant)

SURFACE ENRICHMENT

The superplastic effect in Ti-6Al-4V has been demonstrated for temperatures in the range of 1,550°F to 1,750°F, the range at which surface enrichment by air proceeds at a rapid rate. Consequently, environmental control methods are necessary, and a series of forming tests were conducted to evaluate techniques to minimize the titanium surface enrichment.

The tests conducted involved evaluating the use of argon cover gas, vacuum, and edge sealing configurations to contain these environments. In these tests, small part configurations (pans) were superplastically formed and the enrichment control methods employed during the forming. The three basic techniques evaluated were:

1. Argon on the top surface, vacuum on the bottom surface. Sealing techniques were evaluated for maximizing vacuum tightness.

2. Argon-pressurized top surface, and argon on the bottom surface, with exit vents to allow its removal as the sheet forms into the cavity. This procedure would use only argon pressure and would preclude the need for a vacuum-tight seal.

3. Argon on the top surface and vacuum on the bottom surface, with low pressure argon flow superimposed on the vacuum (bottom) side.

The forming tools used were 2 inches deep by 8 inches wide by 11 inches long. Two tools were fabricated for this series of forming tests. The first was constructed of 22Cr-4Ni-9Mn tool steel bar welded to a base plate to form the lower cavity. The second tool was fabricated by machining the lower forming cavity in a 3-inch-thick plate of 4340 steel. The lower tool is shown in Figure 32. The SPF tool arrangement used is shown in Figure 33, and a typical formed part is shown in Figure 34.

Sealing between the tool and titanium sheet was accomplished by imposing pressure with a hydraulic press to create the necessary clamping forces on the seal and thereby prevent influx of air into the forming chamber. Several sealing methods were evaluated for attaining a vacuum seal between the titanium sheet and lower tool. These methods include the use of 0.063-inch-diameter titanium wire (both single and double) as an O-ring; a single integral lip (approximately 0.030-inch wide and 0.030-inch high) machined on the sealing surface of the lower tool and a double integral lip machined on the sealing surface with a continuous channel machined between the two lips for argon flow, as shown in Figure 35.

Figure 32. Lower tooling chamber for superplastic forming studies.

62
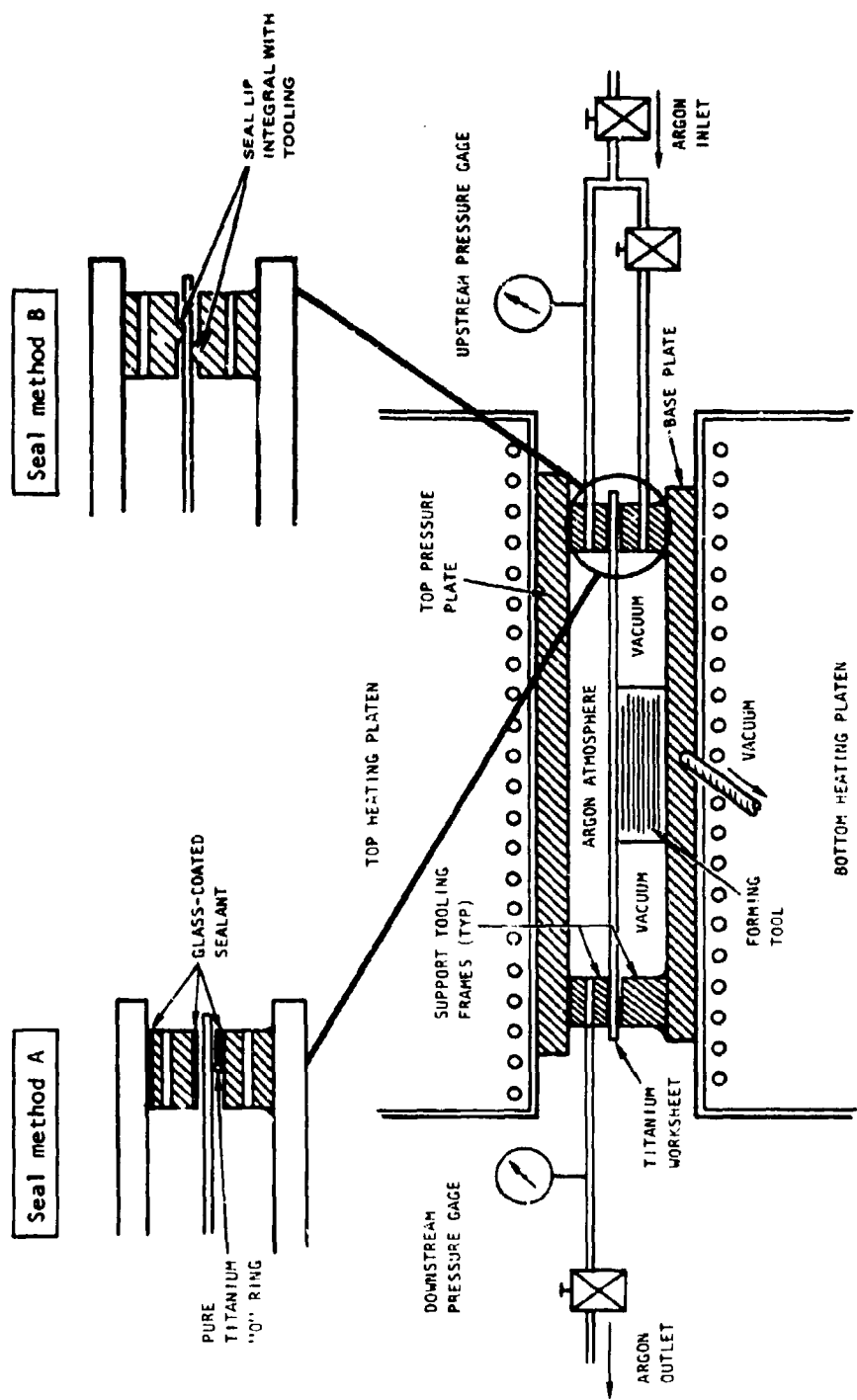
Figure 33. Schematic drawing of forming assembly.
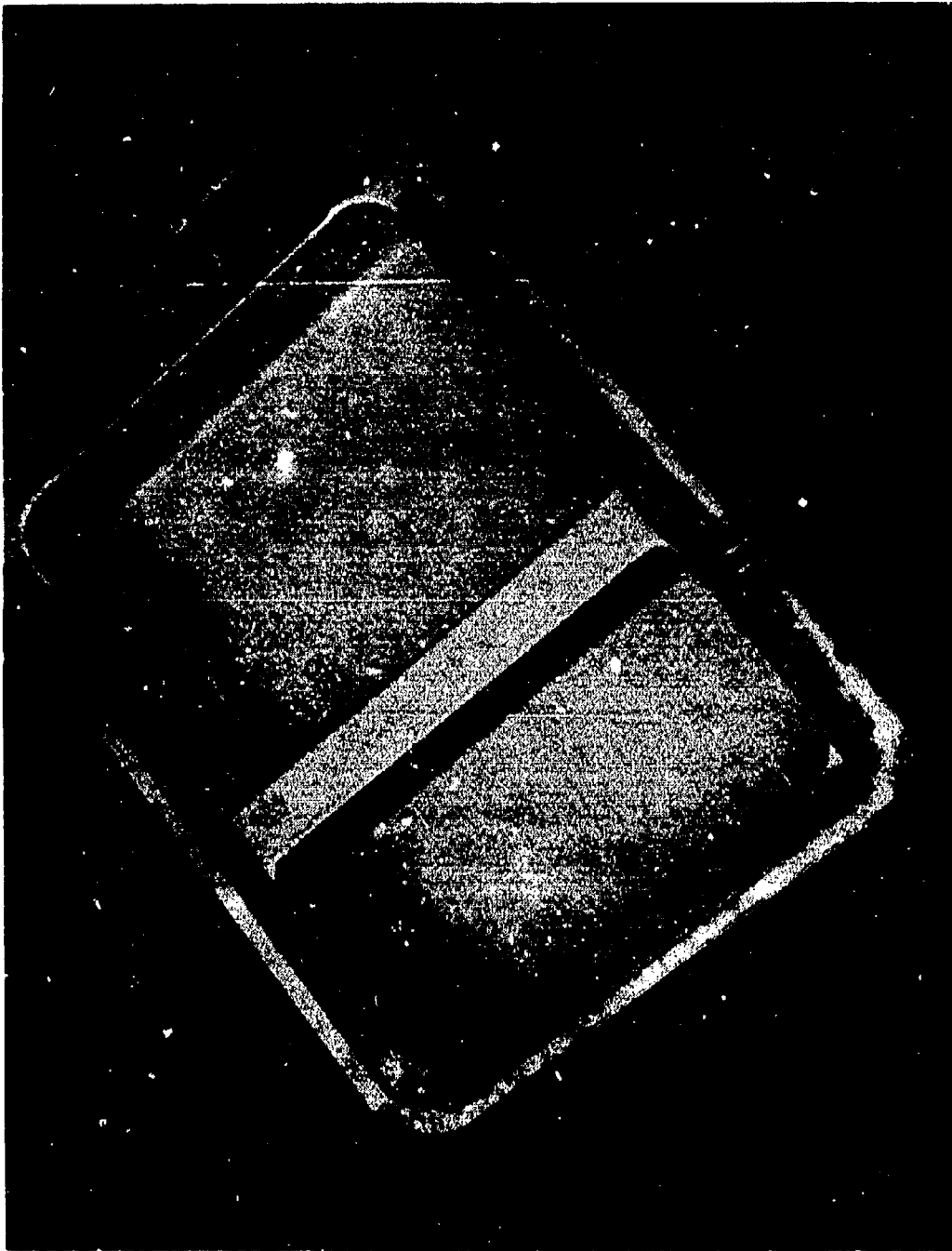
Figure 34. Typical formed part for environment control testing.

64
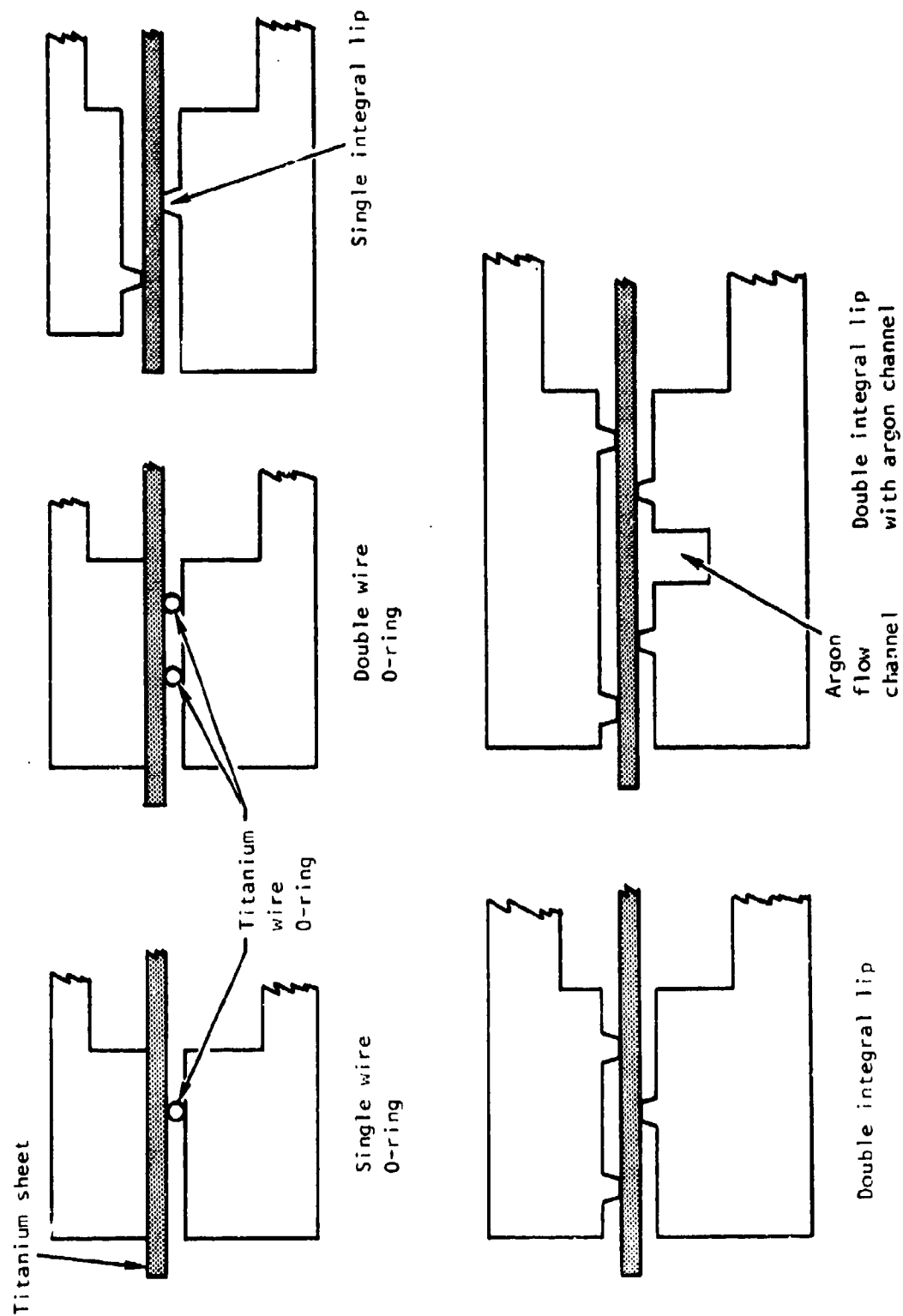
Figure 35. Sealing methods evaluated.

Forming pressure was developed across the titanium sheet by the applied vacuum, or by the imposition of increased argon pressure in the upper chamber. The forming conditions used were as follows: argon cover gas maintained over top and bottom surfaces during heat-up, forming was conducted at 1,700°F under increased argon pressure in the top cavity and/or vacuum in the lower cavity, differential forming pressure of 30 psi was maintained for 2 hours, and the part was cooled under argon.

After forming, metallographic examinations were conducted on the formed parts to establish the extent of surface enrichment resulting from each forming run. A minimum of four metallographic samples were taken from various areas of the sides and bottom of the parts to evaluate surface enrichment levels throughout the parts. These samples were etched with an oxalic acid stain etch which sensitively reveals slight increases in oxygen enrichment. The depth of enrichment was determined microscopically at 100X magnification.

The forming conditions and resulting surface enrichment levels as determined metallographically are summarized in Table 19. The techniques evaluated consistently maintained surface enrichment levels below 0.002 inch in depth, a level easily removed by chem-milling or pickling. Typically, it was observed that the top surface which was exposed only to argon and did not contact tooling, was extremely clean. The lower surfaces showed varying levels of surface enrichment with both argon and vacuum. See Figure 36 for an example of the surface conditions. Since the bottom surfaces contacted tooling, whereas the top surfaces did not, it is probable that the tooling was the primary source of the enrichment observed. Since the enrichment observed is of the interstitial type, the tooling must, therefore, be a source of oxygen and/or nitrogen, the most likely contaminants.

Based on these studies, it is considered that the use of argon only for SPF is preferable over vacuum since less equipment is required and the need for a perfect vacuum tight seal does not exist.

The use of an integral lip machined onto the sealing surface of the tooling is as effective as a titanium wire O-ring in providing a seal with the titanium sheet, and requires no maintenance. Such a lip would be less costly than the O-ring technique in the manufacture of parts and, consequently, was used for subsequent forming studies in this phase of the program.

Enrichment in the seal area was found to decay within about ¼ inch of the integral lip. For structural parts, it would be necessary to create this seal area outside the part configuration (e.g., in the trim area) or the part would require cleaning to remove this enrichment layer.

A problem was encountered during forming run No. 6. The tool sealing surface was reworked prior to this run, and a small burr was inadvertently left on some areas of the inside edges of the lower tool. This burr caused

66
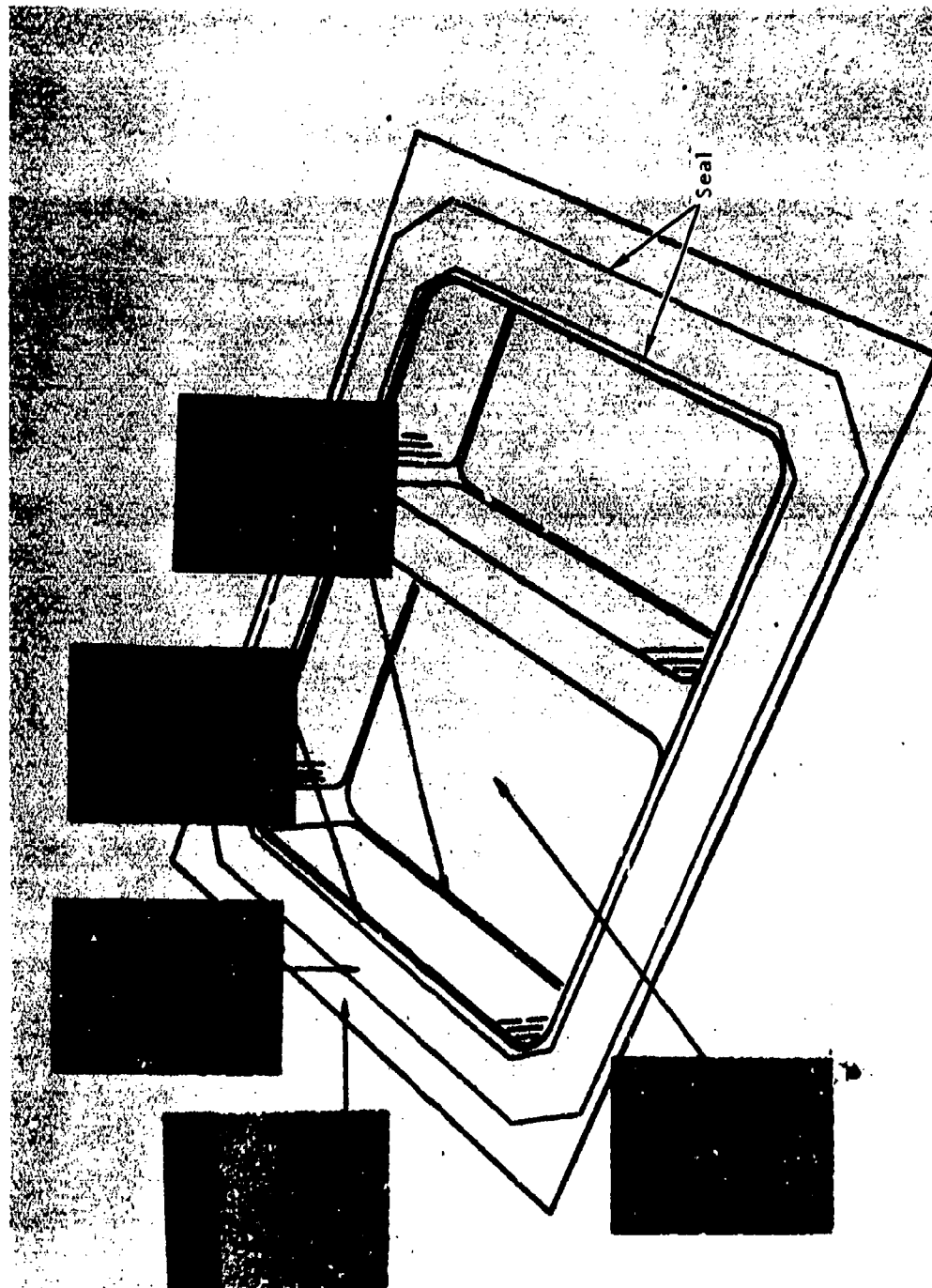
Figure 36. Example of typical formed bottom surface condition in part No. 12 formed with argon protection - photomicrographs at 100X, oxalic acid stain etchant used to reveal surface enrichment.

TABLE 19. RESULTS OF SURFACE ENRICHMENT CONTROL METHODS EVALUATION

Run No.	Environment		Vacuum level	Seal (Ti-tool)	Surface enrichment (in.)	
	Top	Bottom			Top	Bottom
1	Argon	Vacuum	7 - 10	Ti wire	None	0.0005
2	Argon	Vacuum	3 - 5	Ti wire	0.0003	0.0015
3	Argon	Vacuum	0.14 - 0.25	Double Ti wire	None	0.0010
4	Argon	Argon	-	Double Ti wire	None	0.0008
5	Argon	Argon	-	Double Ti wire	0.001	0.0015
6	Argon	Argon	-	Ti wire	None	0.0016
7	Argon	Argon	-	Double Ti wire	None	0.0019
8	Argon	Vacuum +argon flow	0.19 - 0.69	Integral lip	None	0.0019 - 0.003
9	Argon	Vacuum	0.03 - 0.15	Double integral lip with A channel	None	0.001
10	Argon	Vacuum	-	Double integral lip with A channel	None	0.008
11	Argon	Vacuum	0.03 - 0.18	Double integral lip with A channel	None	None
12	Argon	Argon	-	Double integral lip	None	None

the titanium sheet to tear in two areas during the initial pressure application of the forming run, and the forming run was terminated. These burrs were removed for subsequent runs, and no further tearing problems were encountered.

Part No. 10 also tore at the radius of the lower tooling. However, in this case, the full vacuum (effective 15 psi on top surface) was inadvertently drawn too rapidly in the lower tool chamber, which stressed the titanium sheet to a high level causing straining at a rate too high to achieve superplastic properties. A rerun of this test was conducted for part No. 11, except that the initial forming pressure (vacuum and argon) were applied slowly over a 30-minute period to reduce the strain rates imposed. This part formed without rupturing or other problems. Pressure control during the critical initial forming is more difficult with vacuum than argon, and this fact, coupled with the surface enrichment observations, support the value of using an argon gas system for forming.

PROCESSING CAPABILITY (TASK 3)

Forming tests conducted under this task were directed toward establishing the SPF forming capabilities of Ti-6Al-4V, utilizing forming process technology developed under tasks 1 and 2. Six different configurations were designed to provide a range of structural shapes for the forming studies. The three heats of Ti-6Al-4V selected for in-depth characterization in task 1 were utilized for most of these forming studies, and processing techniques established in task 2 were employed. The forming parameters were varied and correlated with tool configurations and corresponding Ti-6Al-4V superplastic properties.

The six configurations evaluated are shown in Figures 37 through 39. The lower dies for these configurations consisted of a common external die machined from 4130 plate with inserts placed into the external die to create the various configurations.

Concept I was created with an insert bar to produce a double pan configuration. This basic double pan configuration was utilized for evaluating forming characteristics. Concept II consisted of 4 rectangular bars placed in a picture frame configuration at the box sides thereby creating Z sections in the formed part. This configuration is found in many sheet metal formed parts. Major factors to concern in parts formed to this configuration are the requirements to form various radii in both concave and convex configurations at the sides as well as the development of the complex corners. Concept III utilized a male tool positioned in the center of the basic forming box to determine the effect of severe forming over corners of a male tool.

Concept IV consisted of an elliptical and a circular cavity machined through a 2-inch steel plate which is inserted into the basic forming box.
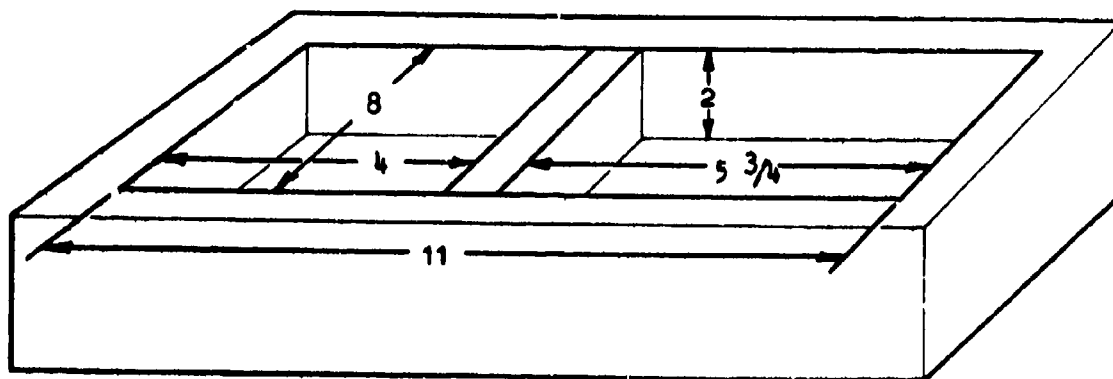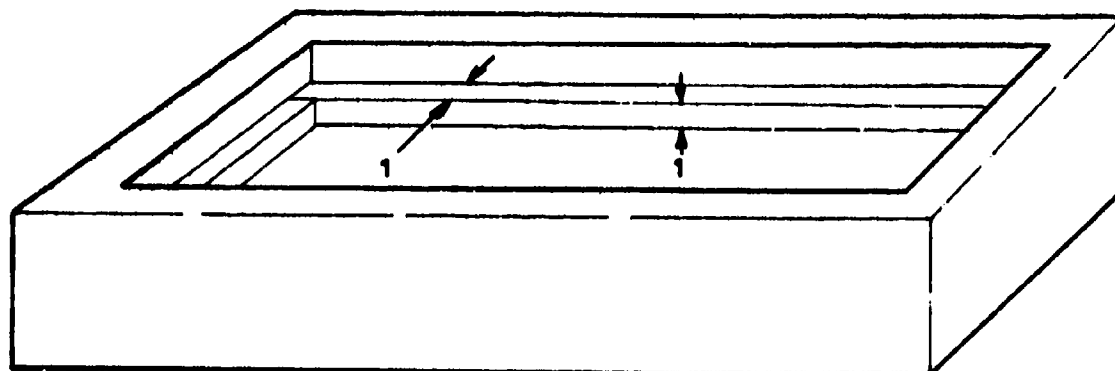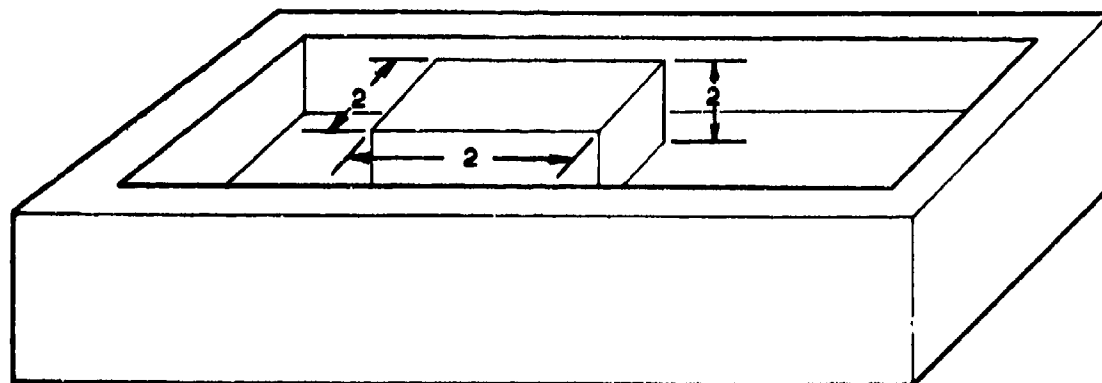
Figure 37. Tooling concepts to be used in task 3 superplastic forming studies.
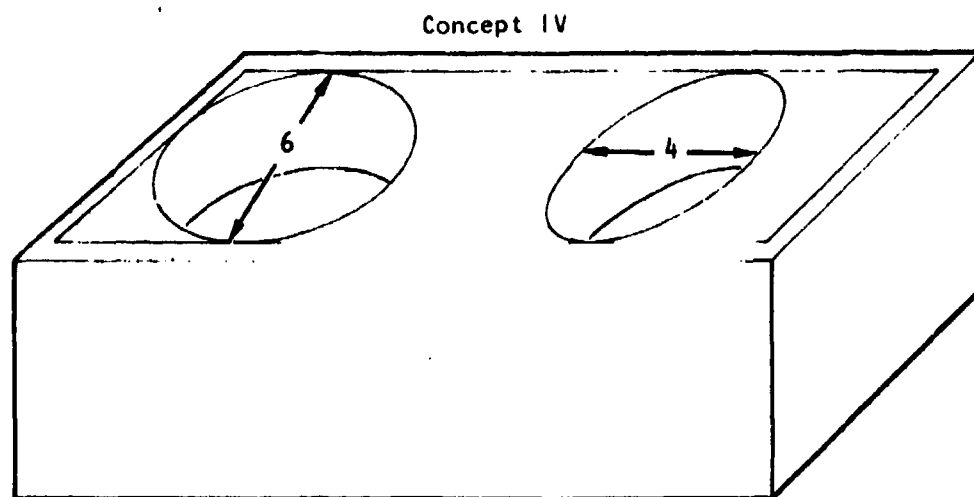
Concept IV

Figure 38. Tooling concept IV, used in task 3 superplastic forming studies.
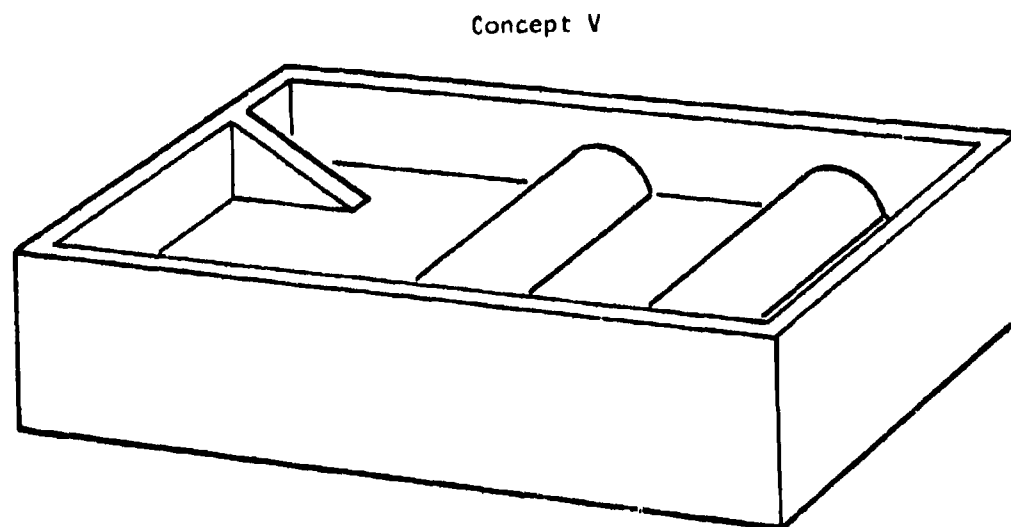
Concept V

Figure 38a. Tooling concept V, used in task 3, superplastic forming studies.

71
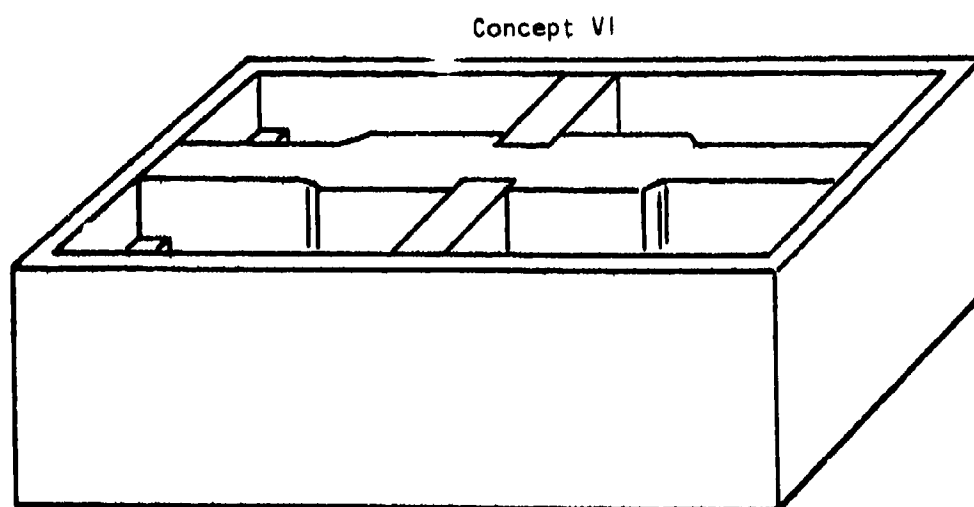
Concept VI

Figure 39. Tooling concept VI, used in task 3 superplastic forming studies.

72

Concept V consisted of a ramp and a series of half rounds inserted in the basic forming box. This configuration was a subscale part used to demonstrate the forming capability and parameters subsequently used for forming and nacelle forward center beam frame selected for phase II forming studies.

Concept VI was selected to demonstrate the applicability of the SPF process to forming multiple parts from a single sheet during a single forming operation. The configuration consists of joggles and steps positioned into the basic forming box to produce a four-cavity tool symmetrical about the center point.

A total of 25 parts were formed under this task per the six configurations. The forming parameters are summarized in Tables 20 and 21. Three materials characterized in task 1 were used for most of these forming studies (heats No. 295405, 301715, and G51126).

These three heats were selected to permit forming evaluation of the poorest superplastic properties as well as the best. Consequently, this effort was intended to provide information on the variability of SPF capabilities among these heats, and the relationship to their basic superplastic properties, as well as specific information on the forming of various configurations.

In addition to these materials used, other heats were selectively evaluated to provide additional information on the effects of metallurgical condition, superplastic properties, and gage.

FORMING PARAMETERS SELECTION

The forming parameters used for fabricating the various configurations were based on the superplastic properties of the titanium materials evaluated in task 1. Both the flow stress and strain rate sensitivity index as functions of strain rate were considered. The flow stress data provides a measure of the pressure required to form a given configuration and thickness, whereas the m characteristics indicate the suitability for superplastic forming.

The temperature selected for the process was 1,700° F. This temperature was selected because superplastic index (m) values were typically maximum, and the flow stress (σ) values were typically minimum, particularly at low strain rates. However, because of the wide temperature range over which superplasticity is typically observed for Ti-6Al-4V sheet, temperature range of 1,650° F to 1,750° F is considered suitable for the process, and provides latitude desirable for a manufacturing process.

The argon pressure applied to cause forming was linearly applied to a maximum level over a time period ranging from 20 minutes to 100 minutes. A slow pressure application is considered necessary to prevent forming too rapidly (too high a strain rate) which can result in low m values and, consequently,

73

TABLE 20. FORMING PARAMETERS UTILIZED DURING PHASE I,
TASK 3 PROCESSING CAPABILITY STUDIES

Run No.	Concept	Heat No.	Orientation[a]	Pressure (psi)	Time (min) Pressure applications	Time (min) Hold time
12	I	295405	L	45	30	90
13	I	301715	L	45	30	90
14	I	G51126	L	45	20	180
15	I	301715	LT	45	30	90
16	I	301715	L	45	58	120
17	I	G51126	L	45	104½	120
18	I	303182	L	45	104½	120
19	II	295405	L	45	30	90
20	II	301715	L	60	88	60
23	II	295405	L	45	30	90
24	II	K6838	L	60	88	90
21	III	301715	L	32	37	b
22	III	295405	L	25	20	b
25	III	304488	L	45	3	b

[a]Material orientation with respect to long direction of tooling
[b]Part ruptured

TABLE 21. FORMING PARAMETERS UTILIZED DURING PHASE I,
TASK 3, PROCESSING CAPABILITY STUDIES

Run No.	Configuration concept	Heat No.	Orientation[a]	Pressure (psi)	Time	
					Pressure applications (min)	Hold time (min)
26	IV	295405	L	45	30	90
PII-1	V	G602	L	70	123	120
PII-2	V	292661	L	85	133	180
PII-3	V	292661	LT	100	82	240
PII-4	V	292661	L	110	84	240
PII-5	V	292661	L	110	84	240
PII-6	V	292661	L	110	89	300
PII-7	-	303182	L	45	30	210
PII-8	-	295405	L	45	30	210
27	VI	301715	L	60	88	180
26	VI	304488	L	70	98	180

[a]Material orientation with respect to longitudinal direction of tooling.

loss of sur rplastic properties. The maximum pressure was varied from 45 psi to 110 psi, and the hold time at maximum pressure was varied from 1 to 5 hours.

Sixteen forming tests were conducted in which various material/parameter/configuration combinations were used, and resulting edge radii and thicknesses are summarized in Table 22. A detailed discussion of the forming characteristics is presented in the following paragraphs.

Concept I

Seven of the forming operations utilized this double-pan configuration. The detail layup of the forming assembly for concept I is illustrated in Figure 40. Heat 295405 which had been determined to be highly superplastic, formed easily (e.g., part No. 12) into the configuration with no problem, as shown in Figure 41. The sheet material was oriented with its rolling direction parallel to the long dimension of the tooling, and argon pressure was slowly increased to 45 psi over a period of 1/2 hour, then held at that level for 1-1/2 hours.

Heat 301715 (run No. 13) did not form satisfactorily when the same forming conditions were applied. The part ruptured as shown in Figure 42 at the upper edge of the small pan perpendicular to the rolling direction after being held at 45 psi for 30 minutes. Heat 301715 has been determined to be anisotropic with respect to its maximum strain rate sensitivity index, m_{max}, and the orientation of failure in this part corresponds to a relatively low m_{max} value of 0.61.

To directly assess the sensitivity of the forming capability of the material to its superplastic index, a second sheet from heat 301715 was again formed under the same conditions except that the sheet was rotated 90 degrees so that the long transverse direction (m_{max} = 0.84) of the sheet was exposed to the high plastic strain direction (part No. 15). This orientation was considered to be the most superplastic for this heat of material since the highest strain rate sensitivity was coincident with the highest strain direction, a condition which minimizes the chance of plastic instability and rupture. Forming for this test was conducted at 1,700° F, and the pressure was again applied slowly over 30 minutes to 45 psi and sustained at this pressure for 1-1/2 hours. The forming of this part was successful and the part formed into the double-pan configuration completely without a rupture as shown in Figure 43, indicating a direct relationship between measured superplastic characteristics and actual formability.

An additional forming test was conducted on heat 301715 to demonstrate that the rate of forming could be used to enhance the forming capability of this material (run No. 16). For this test, the longitudinal direction was again oriented in the high strain direction (the orientation which caused the sheet to rupture in the earlier test), but the rate of pressure application

76

TABLE 22. FORMING PARAMETERS AND RESULTING THICKNESS AND RADIUS MEASUREMENTS

Part No.	Configuration concept No.	Heat	Orientation [b]	Gas press. (psi)	Time (min)		Edge radius (in.)	Thickness (in.)		Comment
					Pressure Increase	Hold		Edge	Corner	
12	I	295405	L	45	30	90	0.156 / 0.156	0.021 / 0.020	0.015 / 0.012	5-1/2 in. wide section / 4 in. wide section
13	I	301715	L	45	30	90	0.625 / 1.375	0.031 / 0.032	0.030 / 0.032	5-1/2 in. wide section / 4 in. wide section
14	I	GS1126	L	45	20	—[a]	—	—	—	
15	I	301715	LT	45	30	90	0.156 / 0.156	0.024 / 0.022	0.015 / 0.015	5-1/2 in. wide section / 4 in. wide section
16	I	301715	L	45	58	120	0.125 / 0.125	0.025 / 0.020	0.014 / 0.015	5-1/2 in. wide section / 4 in. wide section
17	I	GS1126	L	45	104	—[a]	—	—	—	
18	I	303182	L	45	104	120	0.250 / 0.250	0.049 / 0.044	0.042 / 0.035	5-1/2 in. wide section / 4 in. wide section
19	II	295405	L	45	30	90	0.234 / 0.188	0.032 / 0.026	0.028 / 0.015	Upper step / lower step
20	II	301715	L	60	88	60	0.141 / 0.125	0.031 / 0.026	0.022 / 0.015	Upper step / lower step
23	II	295405	L	45 (1,600° F)	30	90	0.375 / 0.375	0.035 / 0.031	0.035 / 0.028	Upper step / lower step
24	II	K6838	L	60	88	90	0.205 / 0.188	0.035 / 0.031	0.031 / 0.022	Upper step / lower step
21	III	301715		32	37	—[a]	—	—	—	
22	III	295405		35	20	—[a]	—	—	—	
25	III	304488		40	35	—[a]	—	—	—	
26	IV	295405	L	45	30	90	0.219 / 0.219	0.030 / 0.030	—	Circular / Elliptical
P11-1	V	GS02	L	70	123	120	0.250	0.079	.067	
P11-2	V (run 1) (run 2)	292661	LT	85 / 85	133 / 133	188 / 188	0.188 / 0.078	—	—	Run 1 / Run 2, display part
P11-3	V	292661	L	100	82	240	0.125	0.062	0.042	
P11-4	V	292661	L	110	84	240	0.094	—	—	Display part
P11-5	V	292661	L	110	84	240	0.125	—	—	Display part
P11-6	V	292661	L	110	89	300	b	—	—	Display part
P11-7	—	303182	L	45	30	210	0.375	0.074	0.070	Singlepans for compression test specimens
P11-8		295405	L	45	30	210	0.141	0.031		
27	VI	301715	L	60	88	180	0.078 / 0.078 / 0.078 / 0.078	0.028 / 0.027 / 0.026 / 0.026	0.014 / 0.013 / 0.013 / 0.014	Pan A / Pan B / Pan C / Pan D
28	VI	304488	L	70	96	180	—	—	—	Display part

[a] Part ruptured during forming.
[b] Material orientation with respect to long dimension of part.

77
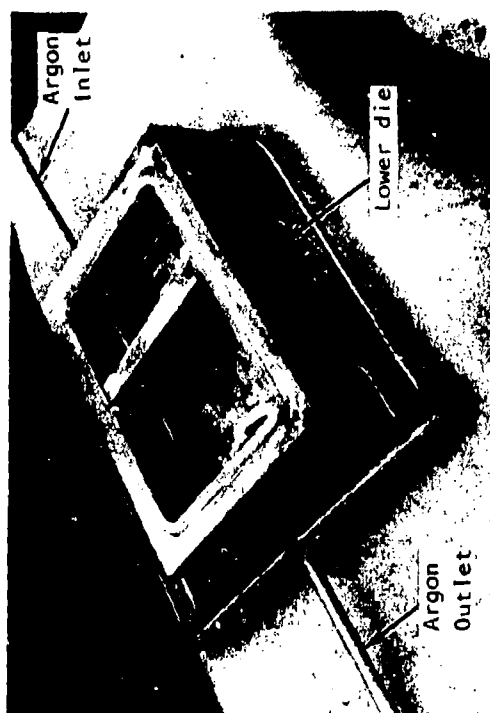
Figure 40. Concept I.

Figure 41.   Part No. 12, heat No. 295405, formed to configuration of concept 1.
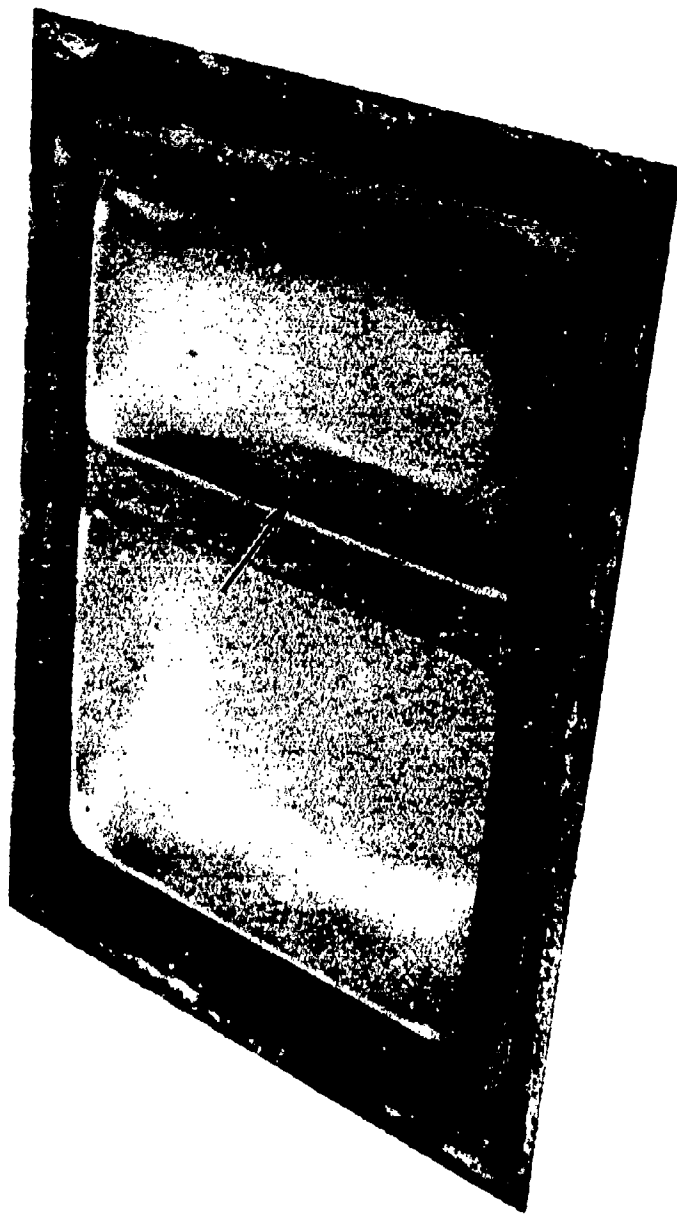
Figure 42. Part No. 13, heat No. 301715, formed to configuration of concept I. Part ruptured during forming (arrow).

Figure 43. Part No. 15, heat No. 301715, formed to configuration of concept 1. Ti-6Al-4V sheet turned 90-degrees from that of figure 20 to make high strain direction coincident with high m value.

was reduced so that the maximum pressure (45 psi) was achieved after 60 minutes as compared to 30 minutes for the previous unsuccessful test. In this test, the part satisfactorily formed into the die cavity, indicating that the slower rate of forming resulted in a higher m value.

The most difficult heat to form (of the six evaluated in phase I) was considered to be heat G51126. This was the heavier of the gages evaluated (0.100-inch thick) and exhibited the poorest combination of superplastic properties. This heat was formed to concept I for comparison to the other two heats formed.

When heat G51126 (run No. 14) was subjected to maximum forming pressure of 45 psi, attained in 1/2 hour, it failed in a similar manner to heat 301715, 45 minutes into the 1-1/2 hour hold cycle. The failure occurred in the small pan by necking just below the radius as shown in Figure 44. Heat G51126 had been found to exhibit low m_{max} values for both longitudinal (m_{max} = 0.69) and long transverse (m_{max} = 0.51) directions. The rupture in this part corresponded to straining in the longitudinal direction. Although rupture occurred in the small pan where highest strains are required, severe necking also occurred in a corresponding location of the large pan. Deformation inhomogeneities (corrugations), which had previously been observed with this material during high-temperature tensile tests formed also in this test and were orthogonal to the tear in the part.

A second run was conducted on this heat to determine if the reduced rate of forming would also prove successful for this material as it did for heat 301715. Since heat G51126 is thicker (0.100 inch) than 295405 or 301715 (both are 0.056 inch), the corresponding rate of pressure application and forming time were adjusted for the thickness so that forming conditions would be comparable to those used on the successfully formed 301715 part. Rupture again occurred prematurely during the forming cycle. The failure occurred near the upper radius of the larger of the two pan configurations and parallel to the longitudinal direction of the sheet. The recurring failures in heat G51126 are directly related to the low strain rate sensitivity indices (m_{max} = 0.63 and 0.51) which makes the material highly susceptible to plastic instability and not characteristic of most of the Ti-6Al-4V material. Failure to achieve adequate formability with this heat of material strengthens the correlation between superplasticity measurements and actual formability.

The final forming run utilizing the concept I configuration was accomplished with heat 303182, also 0.100-inch thick, to demonstrate that this thickness can be formed by the process. In contrast to heat G51126, heat 303182 exhibited high m_{max} values for both longitudinal (m_{max} = 0.84) and long transverse (m_{max} = 0.88) directions. As expected, the part (part No. 18) formed successfully, as shown in Figure 45.

The results of these forming tests substantiate the variations in superplastic characteristics determined in the process parameter study, and indicate

82
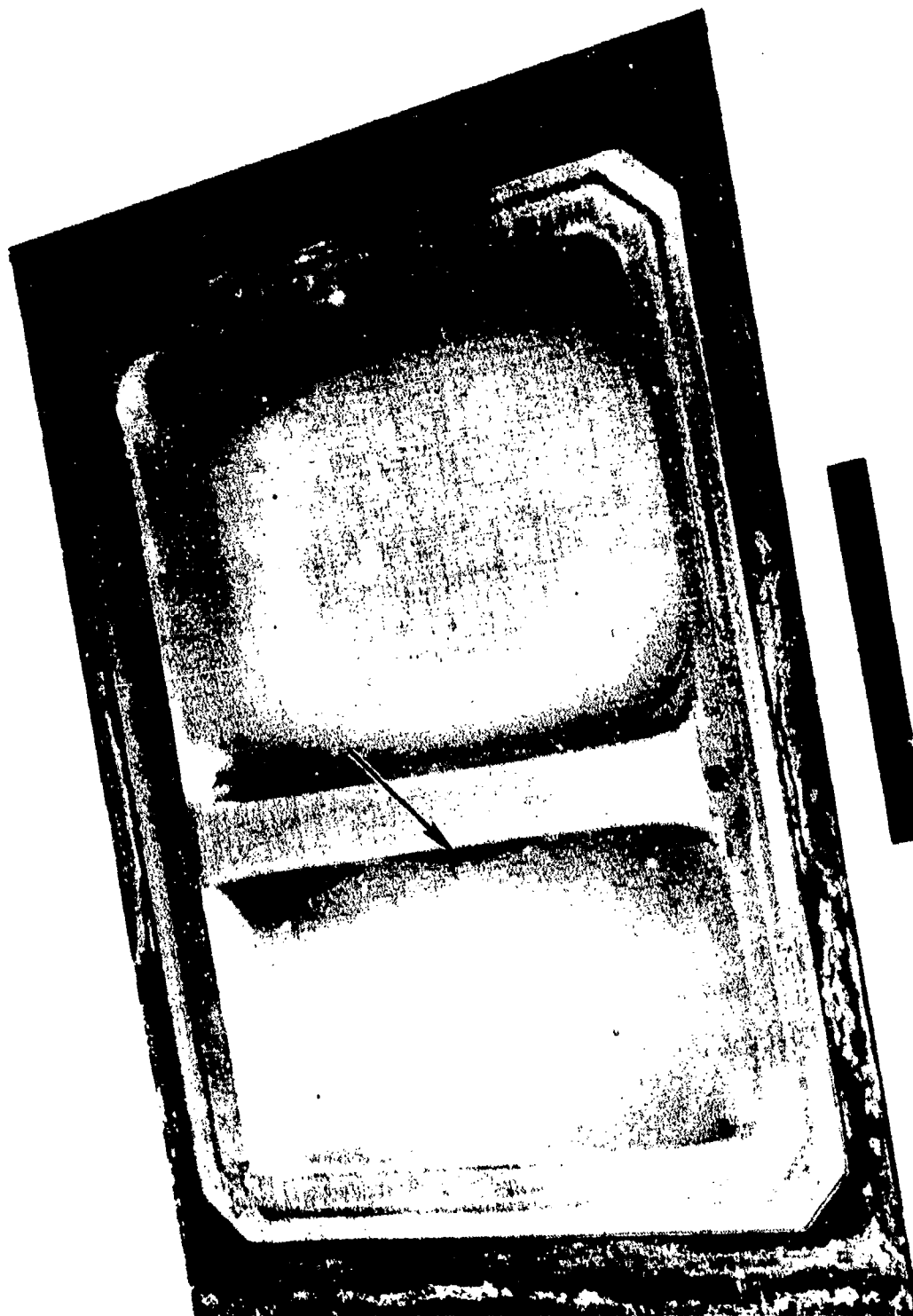
Figure 44. Part No. 14, heat No. G51126, formed to configuration of concept I. Part ruptured during forming (arrow).

83

Figure 45. Part No. 18, heat No. 303182 (0.100-inch thick) formed to configuration of concept I to demonstrate that forming limitations of heat No. GS1126 were not related to gage of material.

a high confidence that the superplastic properties can be used to accurately assess formability. The low strain rate sensitivity and correspondingly limited SPF characteristics of heat 651126 demonstrate that Ti-6Al-4V SPF applications, particularly where considerable plastic deformation is required, may require additional specification controls or a selection procedure (e.g., metallographic or high-temperature tensile) to assure superplastic properties. It is noteworthy, however, that of the six heats procured, only one exhibited low SPF properties, one was marginal, and four of the heats were shown to be highly superplastic.

Concept II

The concept II configuration was utilized to establish the requirements and limitations associated with forming edge and corner radii in a stepped side wall (Z cross-section sidewall). Four forming runs were conducted using this configuration from heats 295405, 301715, and K6838 (part No. 19, 20, 23, and 24.)

Heat 295405 was used to form part No. 19 (Figure 46) and No. 2.. Both parts were formed under identical pressure versus time forming profiles (1/2 hour to reach 45 psi, then hold for 1-1/2 hours) but with the forming temperature being 1,700° F for the former case and 1,600° F for the latter to evaluate the effect of temperature. Part No. 23 readily formed into the complex configuration although the resulting concave radii were larger than those formed under the same pressure/time parameters at 1,700° F. This test verified that this heat of material is sufficiently superplastic at 1,600° F to be formed into shapes requiring high tensile deformation, although longer times or higher pressures at 1,600° F are required to achieve the same degree of deformation (e.g., inside radii) as at 1,700° F because of the increased flow stress at the lower temperature.

Part No. 20 was formed from heat 301715 (Figure 47), a heat which had previously exhibited forming problems. The forming pressure for this part was increased to 60 psi with the time to reach this pressure level being increased to 1-1/2 hours to alleviate the tendency to failure by forming too rapidly (as demonstrated with the concept I parts). The hold time was 1-1/2 hours. Complete part formation was achieved with no evidence of tearing.

Test part No. 24 was formed from heat K6838 under 60 psi argon forming pressure at 1,700° F to provide a basis for evaluating the relationship between material property variations and forming parameters. The forming parameters were modified from those previously used with heat 295405 (part No. 19) to compensate for the higher flow stress characteristics of heat K6838 at 1,700° F. In the high strain direction (long transverse), the flow stresses for heat K6838 are an average of 30 percent higher than for heat 295405. The pressure was, therefore, increased from 45 psi to 60 psi (a 30-percent increase) to compensate for this difference in material properties. The hold time was the same as for part No. 23 (90 minutes).
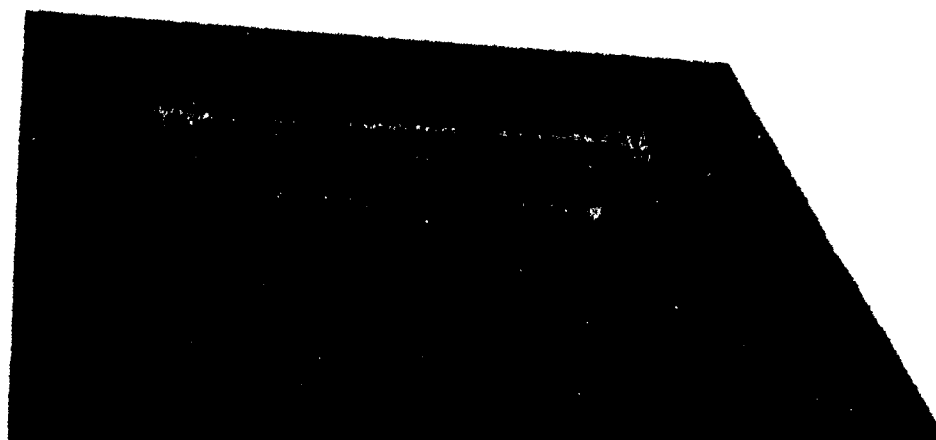
Figure 46.   Part No. 19, heat No. 295405, formed to configuration of concept II.
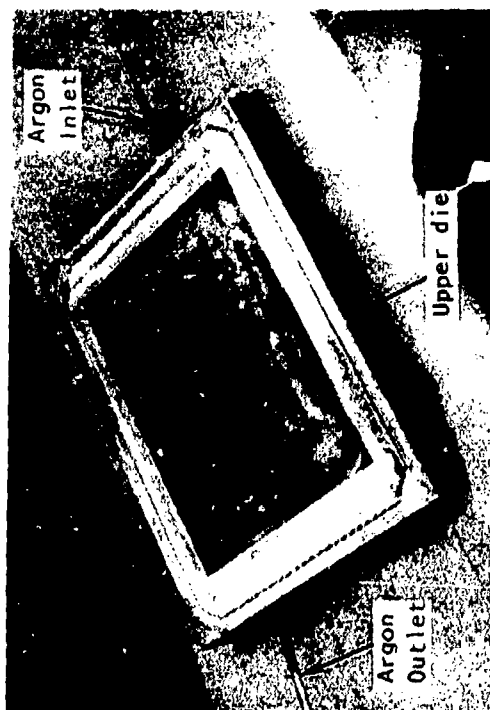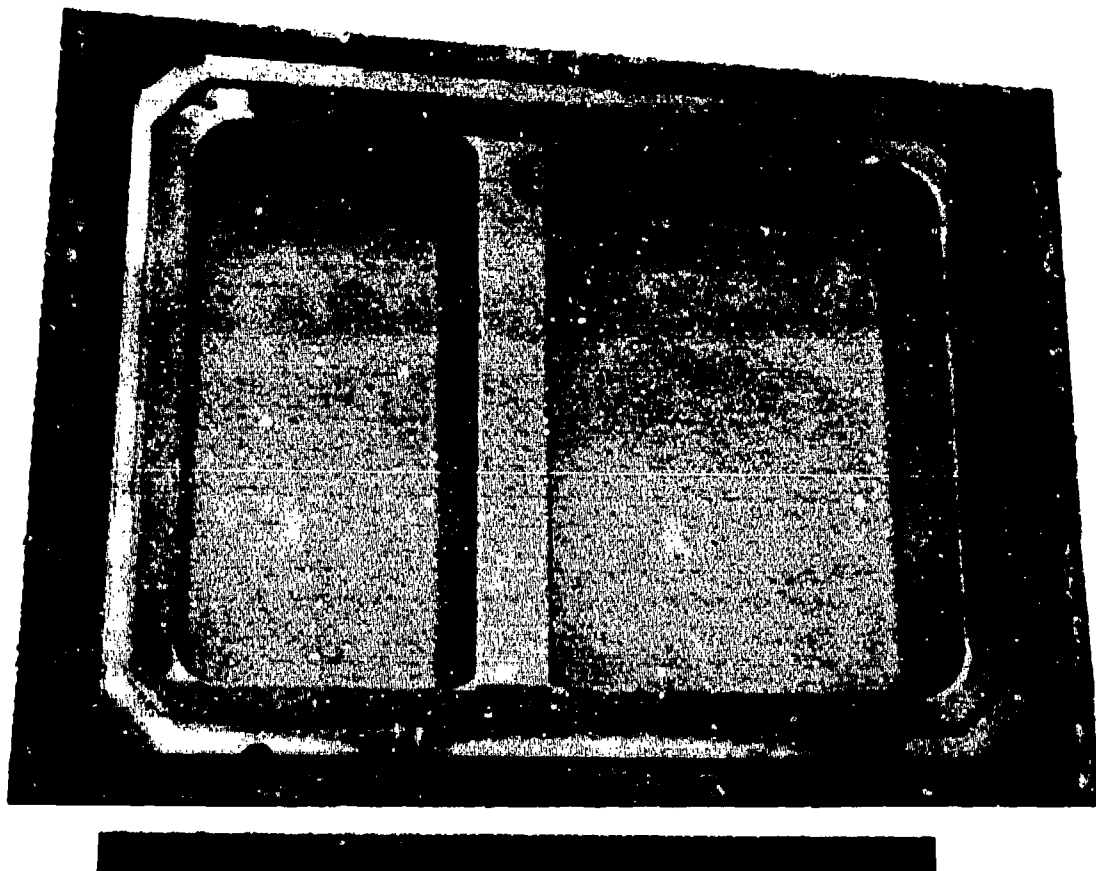

Figure 47.   Part No. 20, heat No. 301715, formed to configuration of concept II.

The rate of pressure application was not accelerated, however, and the time to reach the higher (60 psi) pressure level was, therefore, longer than for parts NO. 19 and 23. The extent of forming which occurs at the maximum pressure is much greater than that achieved during the pressure increase so that the longer time required to achieve the higher pressure is of lesser significance than the time at the maximum pressure. Part No. 24 exhibited comparable formability to part No. 19 as measured by the edge radius formed. This indicates that the process parameters can be adjusted to compensate for material property variability.

Concept III

Three forming operations were conducted with this configuration (parts No. 21, 22, and 25) from three heats of titanium (301715, 295405, and 304488, respectively). The tooling consisted of a 2-inch cubical steel insert placed in the bottom of the basic forming box (Figure 48).

The forming parameters planned for the first part (run No. 21) were intended to duplicate that of run No. 17, in which the concept I configuration was successfully formed. This part ruptured at 32 psi and 37 minutes into the forming cycle. Rupture which occurred at all four upper corners of the male insert, as shown in Figure 49, was attributed to the degree of plastic deformation required to form over the 90-degree insert corners. Prior to the next forming operation, alternate corners of the insert were radiused to 1/8 inch to reduce the tendency toward thinout at the corners. Heat 295405 was then subjected to a second forming cycle. Rupture again occurred, this time at 25 psi, 20 minutes into the forming cycle (part No. 22). Ruptures occurred only at the two sharp corners. The failures occurred as a result of severe deformation thinning at the corners of the male tool insert followed by rupture of the sheet material at the tool corners. A third part (No. 25) was, therefore, formed using the concept III configuration in which the titanium sheet was "reverse-formed" into an upper chamber to prestretch the sheet before forming over the tool block on the lower chamber.

Since rupture of parts 21 and 22 had occurred by high local tensile deformation, it was believed that a prestretching of the titanium sheet by forming into an upper tool cavity would permit more uniform deformation and, thereby, reduce the subsequent deformation necessary at the tool corners. However, the prestretched part wrinkled and distorted severely as it was formed into the lower chamber, and finally ruptured by tearing along one edge of the male insert tool. It is, therefore, concluded that severe forming over a small male tool is extremely difficult and would probably require a substantial radius on the tool corners.
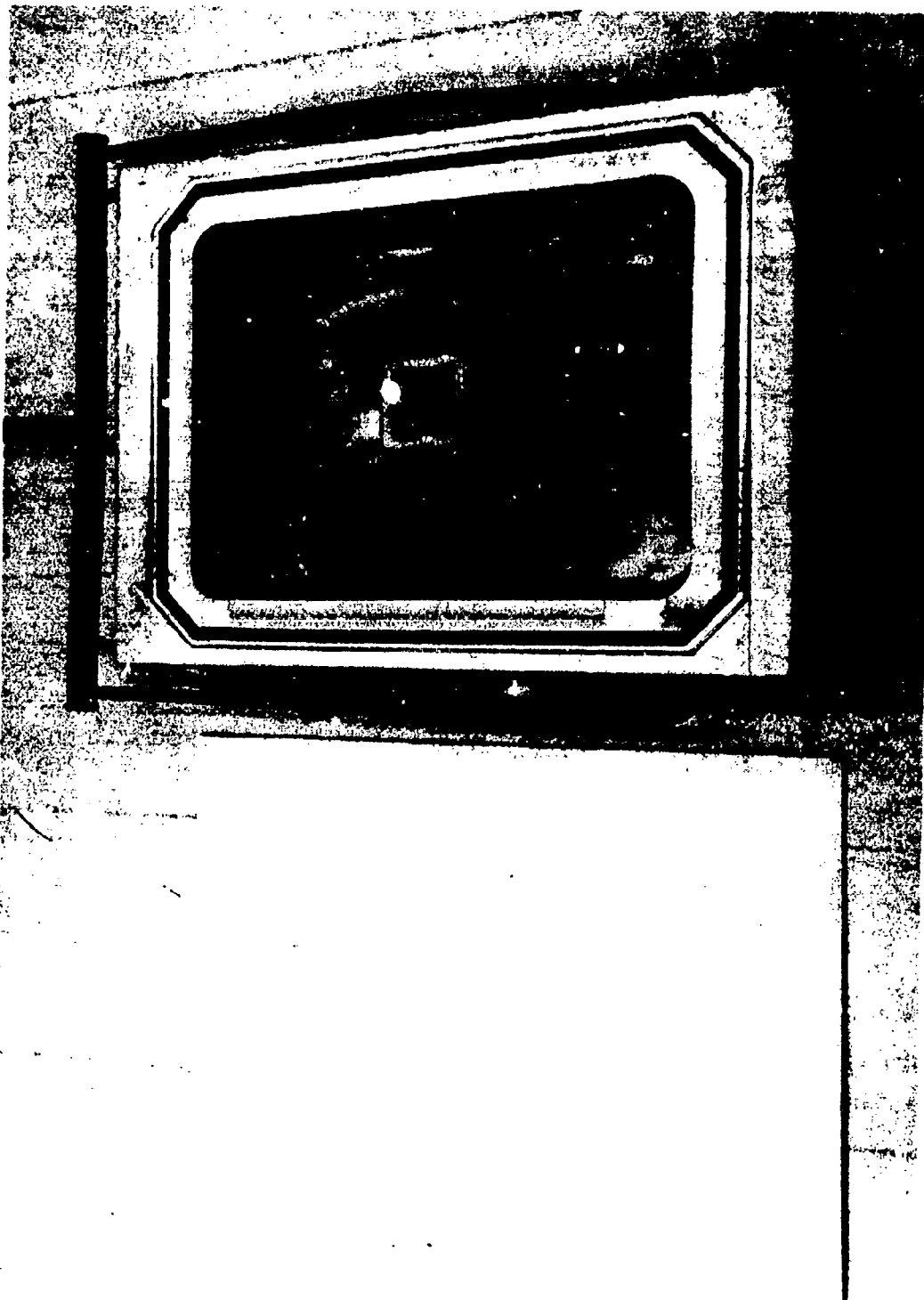
Figure 48. Concept III Configuration Tooling.

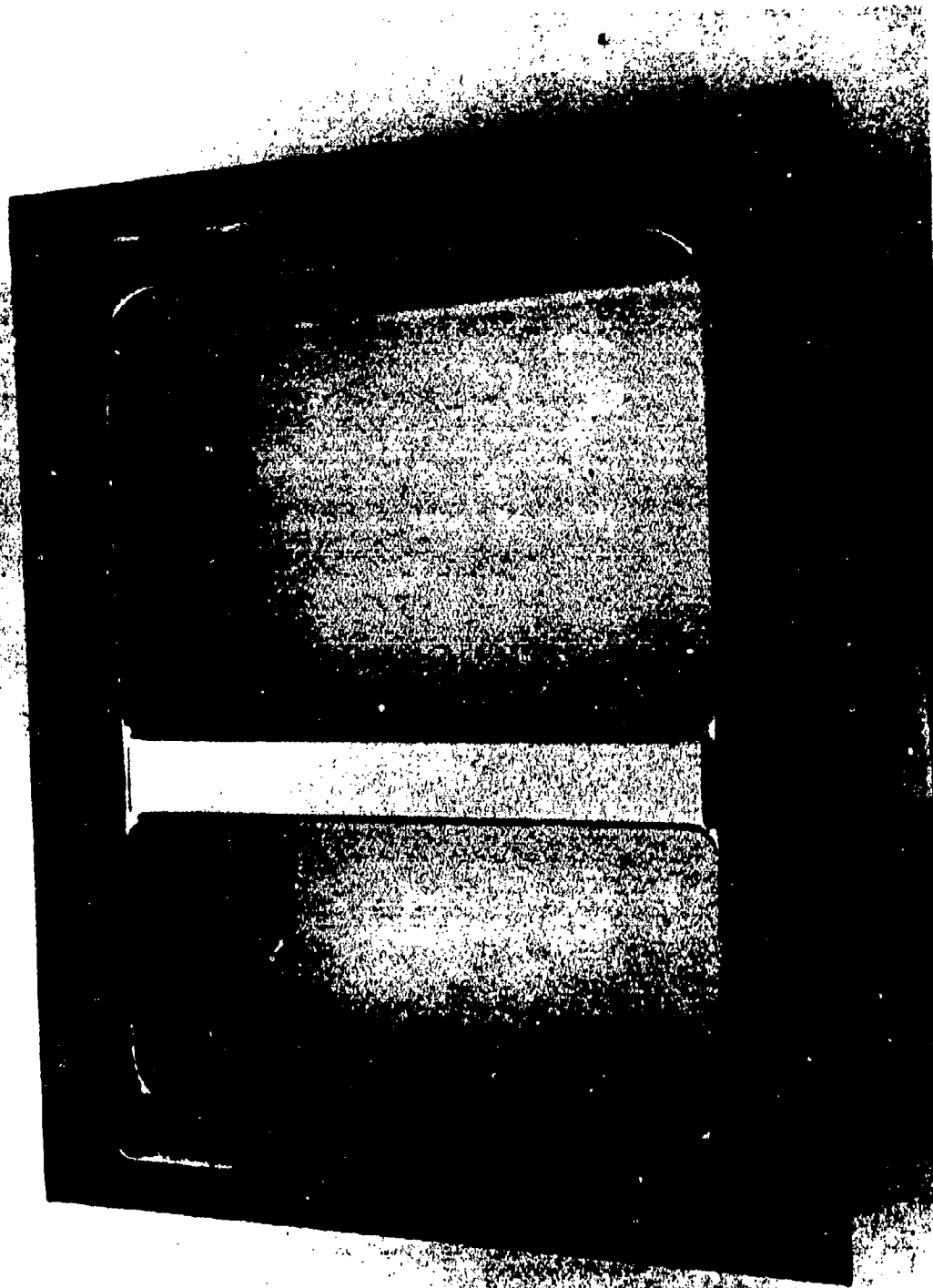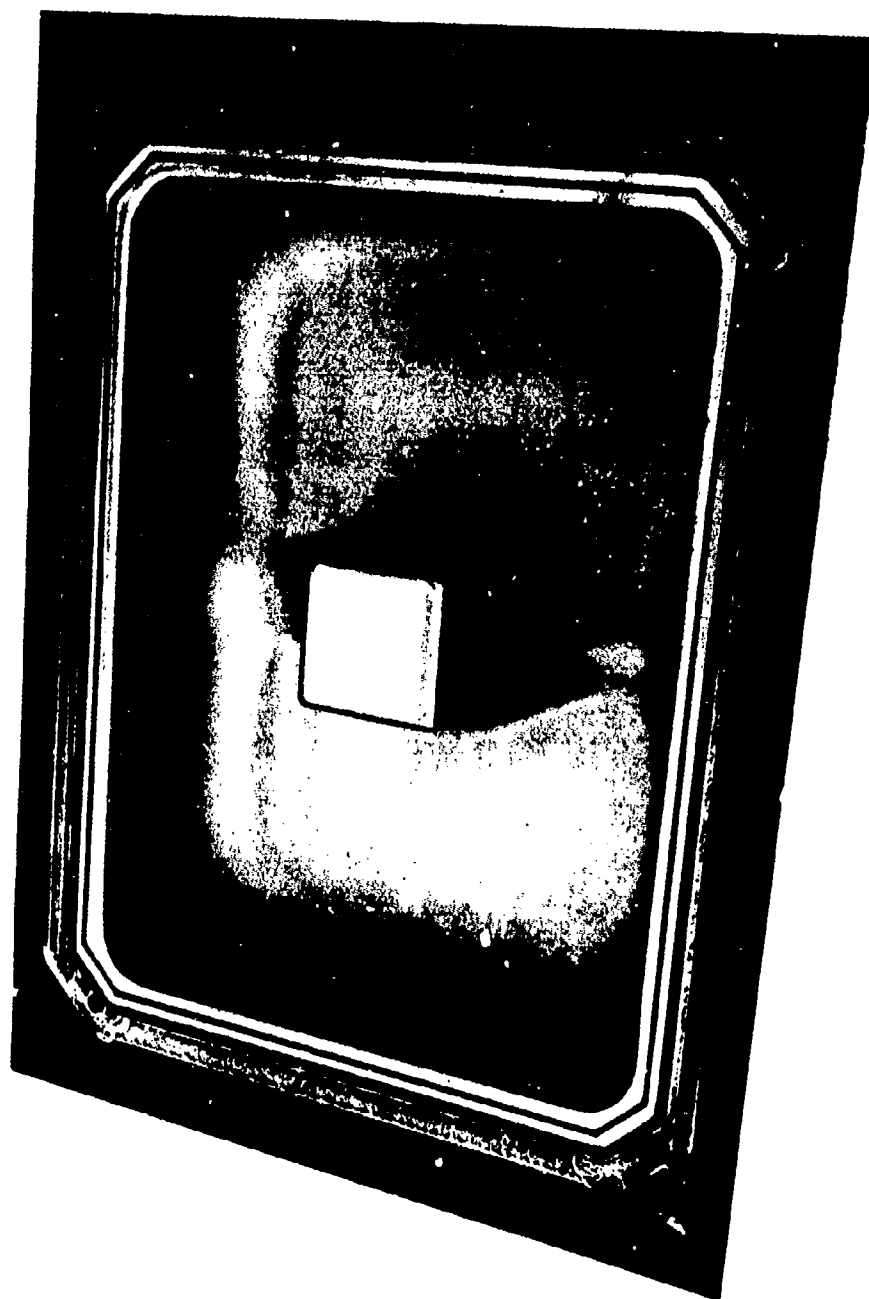Figure 49. Part No. 21, heat No. 301715, formed to configuration of concept III. Part ruptured during forming at upper corners of tool insert

Concept IV

The concept IV configuration was evaluated to establish the degree of thin-out and the resulting radii for material formed into circular and elliptical cavities. Process parameters developed for parts formed using the concept I and II configurations were utilized to form test part No. 26 (Figure 50) using the concept IV configuration. This part was formed from heat 295405 under 45 psi argon pressure for 2 hours at 1,700° F. The tooling configuration consists of a circular and an elliptical hole, each having a depth of 1 inch machined from 4130 steel plate. The part formed readily with no difficulties encountered in either forming or removal of the part from the tooling.

Concept V

A total of six parts were formed to this configuration. The subscale test parts formed to the concept V configuration have been used to evaluate parameters for forming the full-scale phase II part, to evaluate thickness profiles, and to determine the gage of the sheet required to meet formed part thickness requirements. These subscale parts represent the end sections of the nacelle forward center beam frame which is considered the most difficult section to form of the full-scale part. For these parts, 1/8-inch-thick Ti-6Al-4V sheet was required to be representative of the structural part and, therefore, additional material was used which was not characterized in task 1.

Part No. PII-1 was formed with beaded web configurations to demonstrate the capability for formed the beads into the side wall, a configuration which is structurally desirable. The resulting part was successfully formed.

A second configuration of interest was the ability to form a thin ramp section on one end of the part. This basic configuration was evaluated in parts PII-2 through PII-6 in which the beads were placed in various positions relative to the end ramp. Examples of these parts formed are shown in Figures 51 and 52.

Concept VI

The concept VI configuration was utilized to demonstrate the applicability of the process to simultaneous forming of multiple parts from a single sheet of titanium. Two parts were successfully formed to this configuration, using heats 301715 and 304488, as shown in Figure 53. The ease with which these complex, multiple-section, forming test parts were produced demonstrates the broad flexibility of the process.
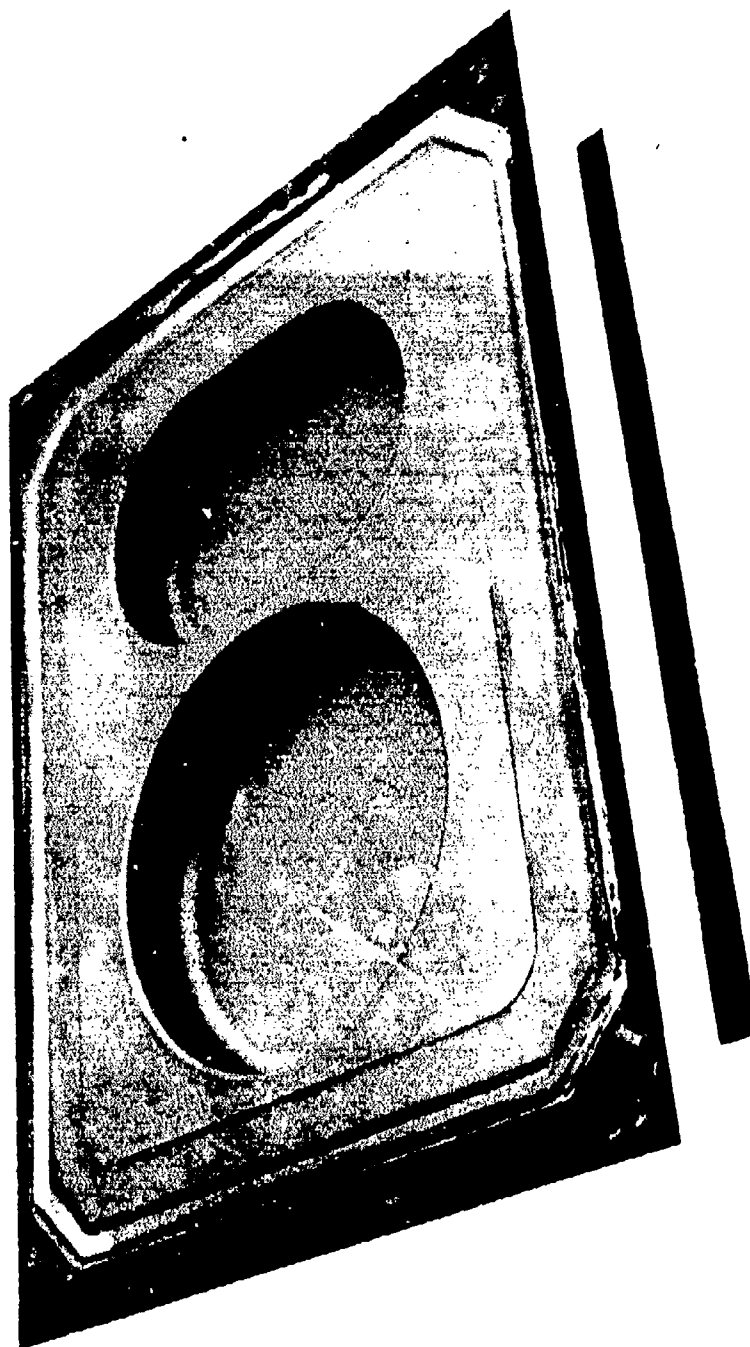
Figure 50. Part No. 26 superplastic formed in concept IV configuration.

91
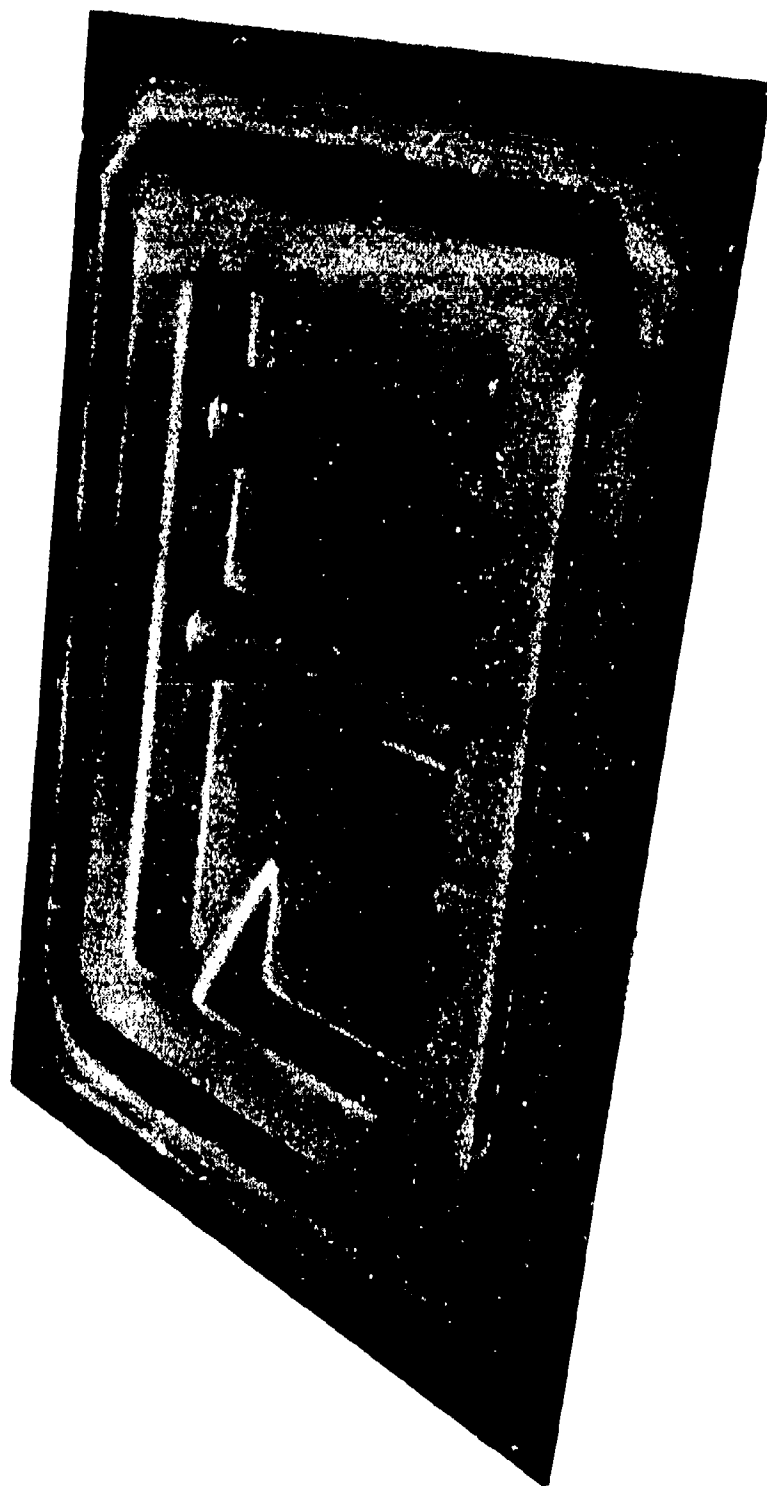
Figure 51. Superplastic forming a thin ramp section (Part No. PII-2).
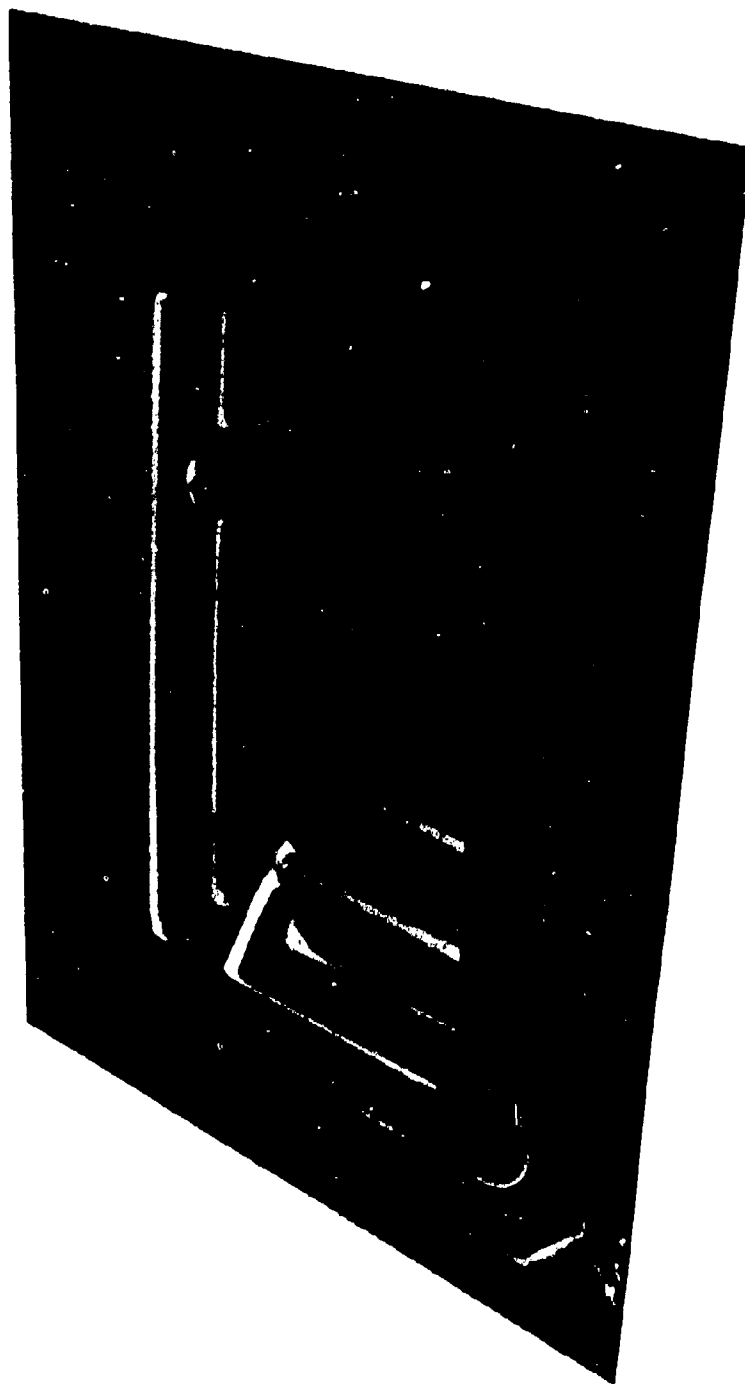
Figure 52. Part No. PII-6 formed to concept V configuration.

Figure 53. Part No. 28, concept VI configuration.

94

EVALUATION

Selected parts formed in task 3 were evaluated for dimensional characteristics, including thickness profiles and edge radii, and metallographic and mechanical property tests were conducted to provide a thorough evaluation of the metallurgical characteristics of the parts.

Thickness Profiles

Because of the large tensile deformation imposed on superplastically formed parts, the titanium diaphragm is generally reduced substantially in thickness. The thinning that results is a function of the severity of forming and configuration of the part being formed, and is of importance both to the design considerations and in the determination of starting stock thickness required to produce a given part. The basic thinning mechanism has been described analytically (Reference 3), and this analysis was considered along with the experimental measurements.

The analytical predictions are based on a thinning mechanism illustrated in Figure 54. In this mechanism, it has been assumed that the titanium diaphragm undergoes uniform thinning in those areas where the die is not contacted. In the first forming step (Figure 54b), the diaphragm forms freely and uniformly in the form of a bead until the bottom of the bead contacts the die bottom (Figure 54c). At this point, the area of the titanium diaphragm contacting the die no longer deforms, due to die friction, while deformation continues in the remaining areas where die contact has not been made Figure 54d). This mechanism results in a predicted thickness profile, as shown in Figure 55, in which a crown is present at the bottom center and the greatest thinning occurs at the corner radii. This mechanism also produces a flange thickness profile, as shown in Figure 56, which has the same thickness profile as the bottom. The analytical model developed for this thinning mechanism assumes a rectangular section, general in dimension, and semi-infinite in length (i.e., plane-strain condition).

Dimensional measurements were made on nine of the parts, and these resulting thicknesses checked against the analytical predictions. Examples of the thickness profiles for three basic pocket sizes, as shown in Figures 57 and 58. The pan dimensions are 4-inch wide by 2-inch deep, 5.75-inch wide by 2-inch deep, and 8-inch wide by 1-inch deep. These resulting profiles, both across the web and the sidewall, agree well with analytical predictions, indication that the mechanism of thin-out previously described is, in fact, accurate.

Of interest at this point was a prediction of thicknesses to be expected in the structural part (forward frame) to be fabricated in phase II and, therefore, thickness profile predictions were made for three widths of the part,
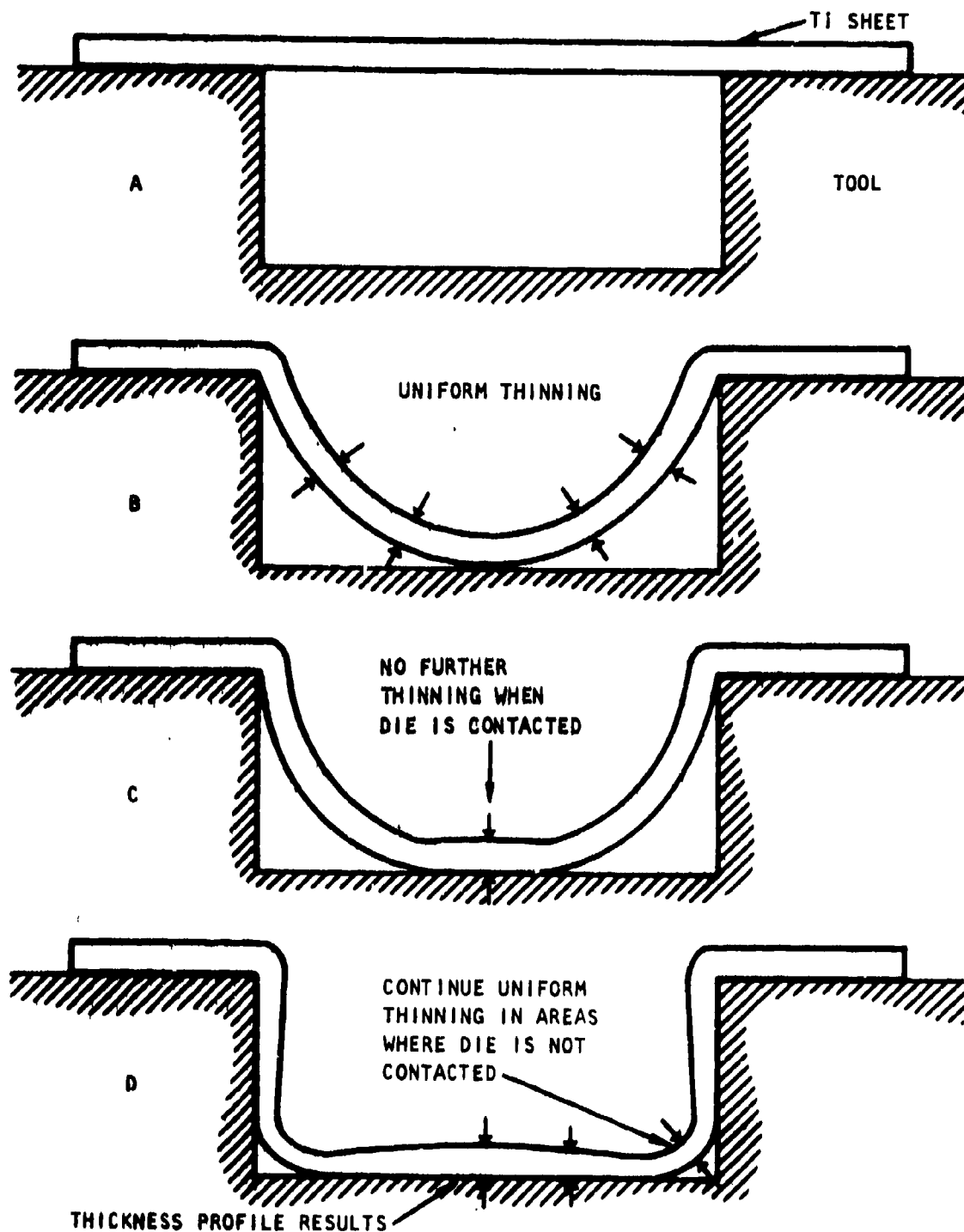
Figure 54. Thinning mechanisms assumed for die-cavity superplastic forming.

96
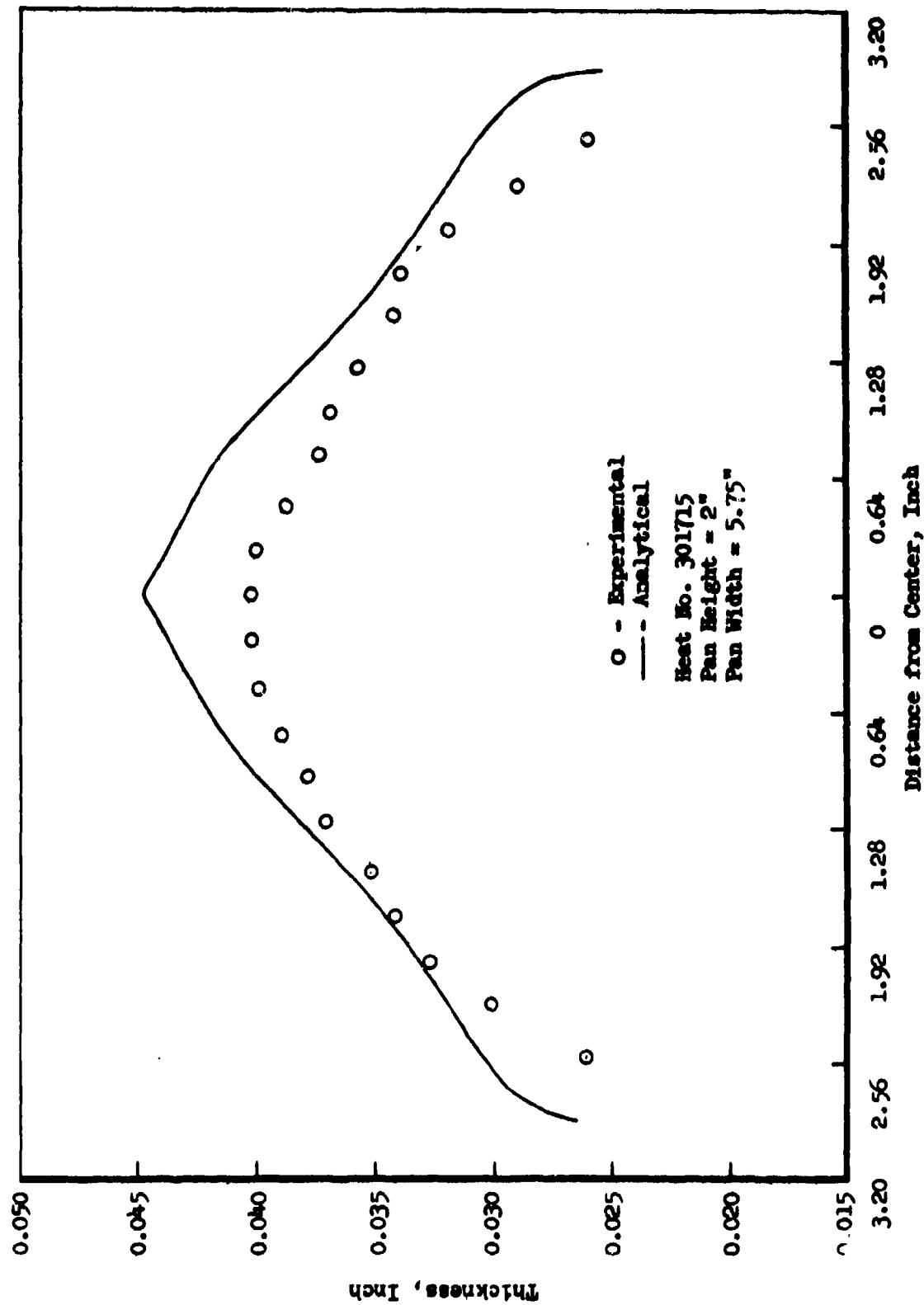
Figure 55. Comparison between predicted and measured web thickness profiles of part No. 15 formed from 0.058-inch-thick Ti-6Al-4V sheet material.

97
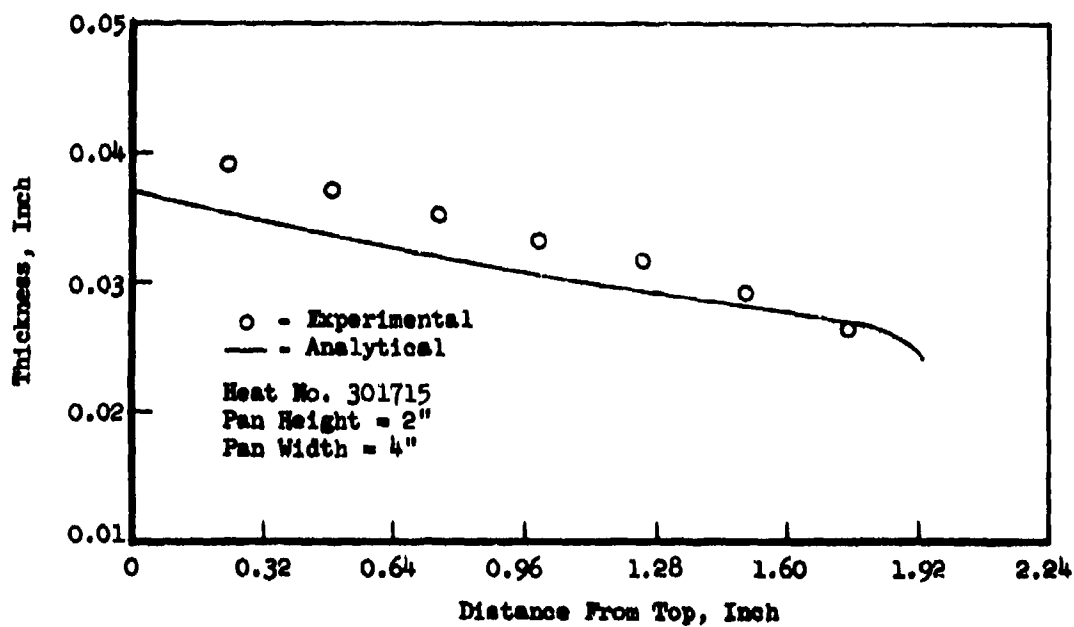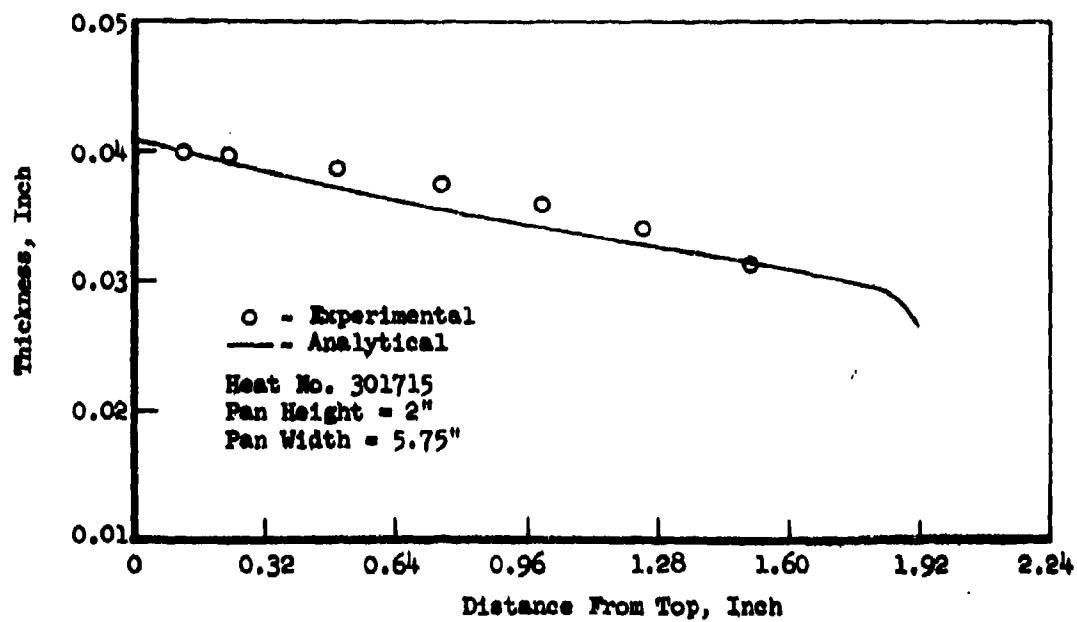
Figure 56. Comparison between predicted and measured flange thickness
profiles of part No. 15 formed from 0.058-inch-
thick Ti-6Al-4V sheet material.

Thickness profiles
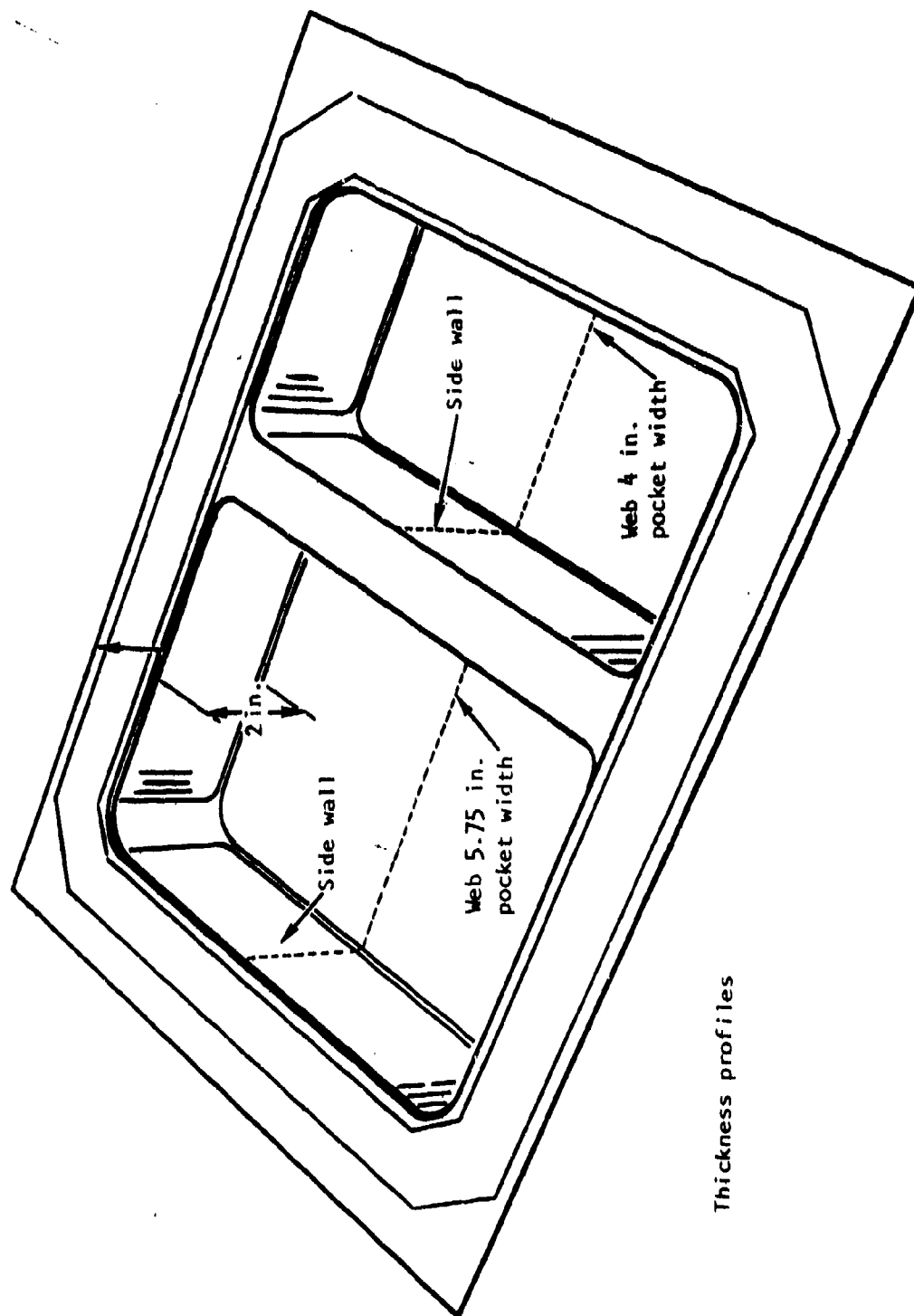
Figure 57. Location of thickness profile measurements for concept I part with 4-inch and 5.75-inch pocket widths.
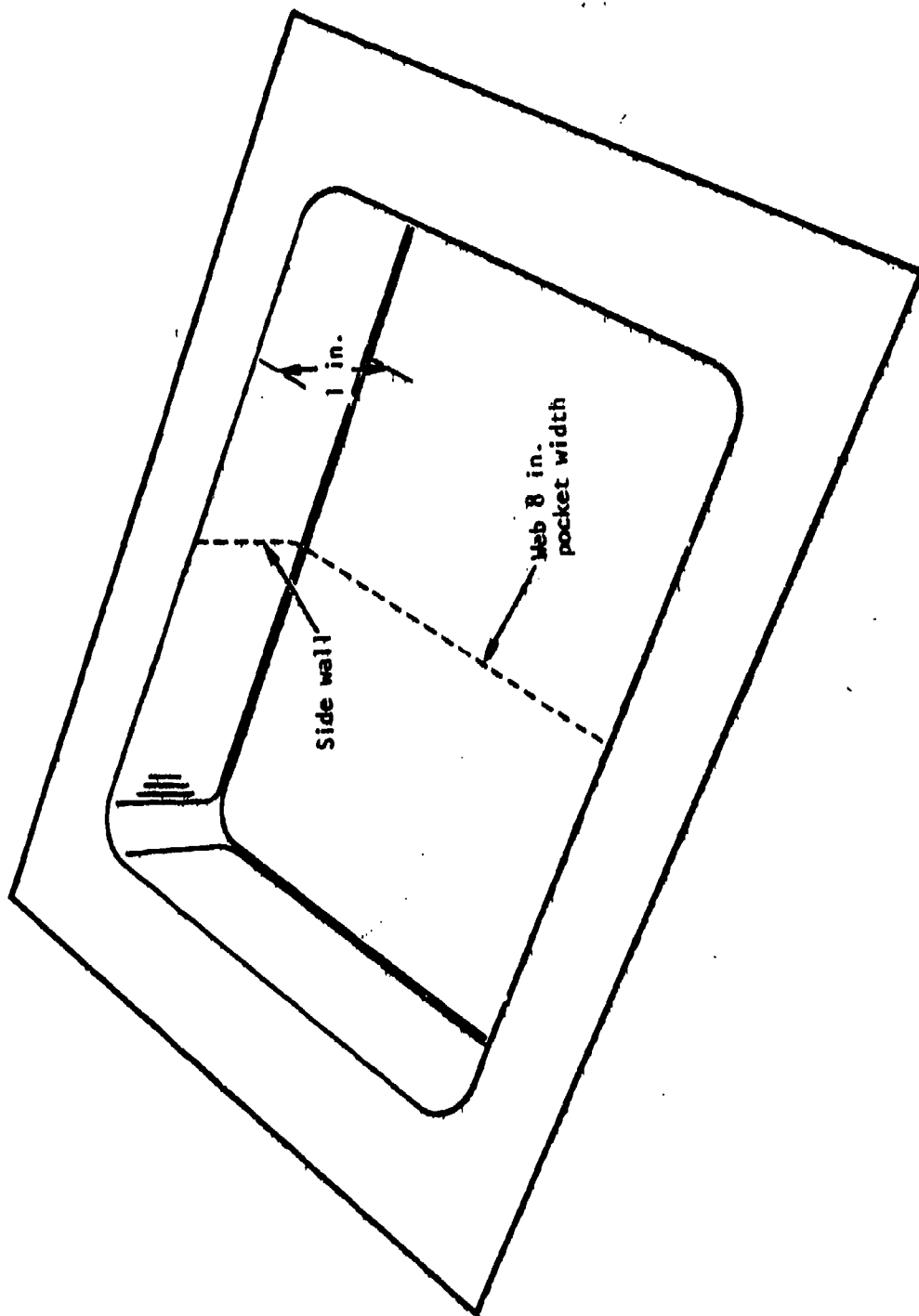
Figure 58. Location of thickness profile measurements for single pan configuration with 8-inch pocket width.

including extremes in width and an intermediate width (e.g., 3-inch, 4-inch, and 5-1/2-inch width with a 1-inch height). The results of these predictions are shown in Figure 59 for 1/8-inch starting gage.

An interesting result indicated by these calculations is that the minimum thickness at the edge radius does not noticeably vary with pocket width, even though the thicknesses elsewhere vary depending on width. This implies that a simple "rule of thumb" can be used to guide initial selection of the starting gage.

The corner thicknesses would be expected to differ from the edge thicknesses since the required amount of stretch in the corner should be greater. No correlation between edge and corner thicknesses was found, but the ratio of the corner and edge thicknesses is found to vary with edge radius formed as shown in Figure 60, where all available data from task 3 parts is included. No difference in thicknesses is observed unless the edge radius is less than about 0.5 inch, below which the difference increases as the radius decreases.

These results, combined with the capability for predicting thicknesses through the center of a typical rectangular section, provide excellent visibility as to thinning characteristics to be expected for a number of structural configurations.

Microstructural Evaluation

Selected parts were analyzed metallographically to determine surface condition and general microstructure characteristics in the formed titanium parts. The grain size of the titanium was measured to determine if any significant grain growth occurred during the forming operation. Metallographic samples were taken from five of the same parts that were subjected to tensile evaluation (parts No. 12, 15, 16, 19, and 20). Three areas representing three degrees of deformation of each part were evaluated:

* Location 1: Unformed flange area

* Location 2: Bottom center of formed pan

* Location 3: Edge radius of the pan

The results of the grain size measurements for these parts are presented in Table 23. Only a very slight increase in grain size is indicated for the deformed locations 2 and 3.

Part No. 18 was completely mapped using 26 metallographic specimens taken from both upper and lower surfaces of the formed part (Figure 61). The only regions within the formed part indicative of possible surface enrichment after being subjected to an oxalic acid strain etch were in the bottom flat surface

101
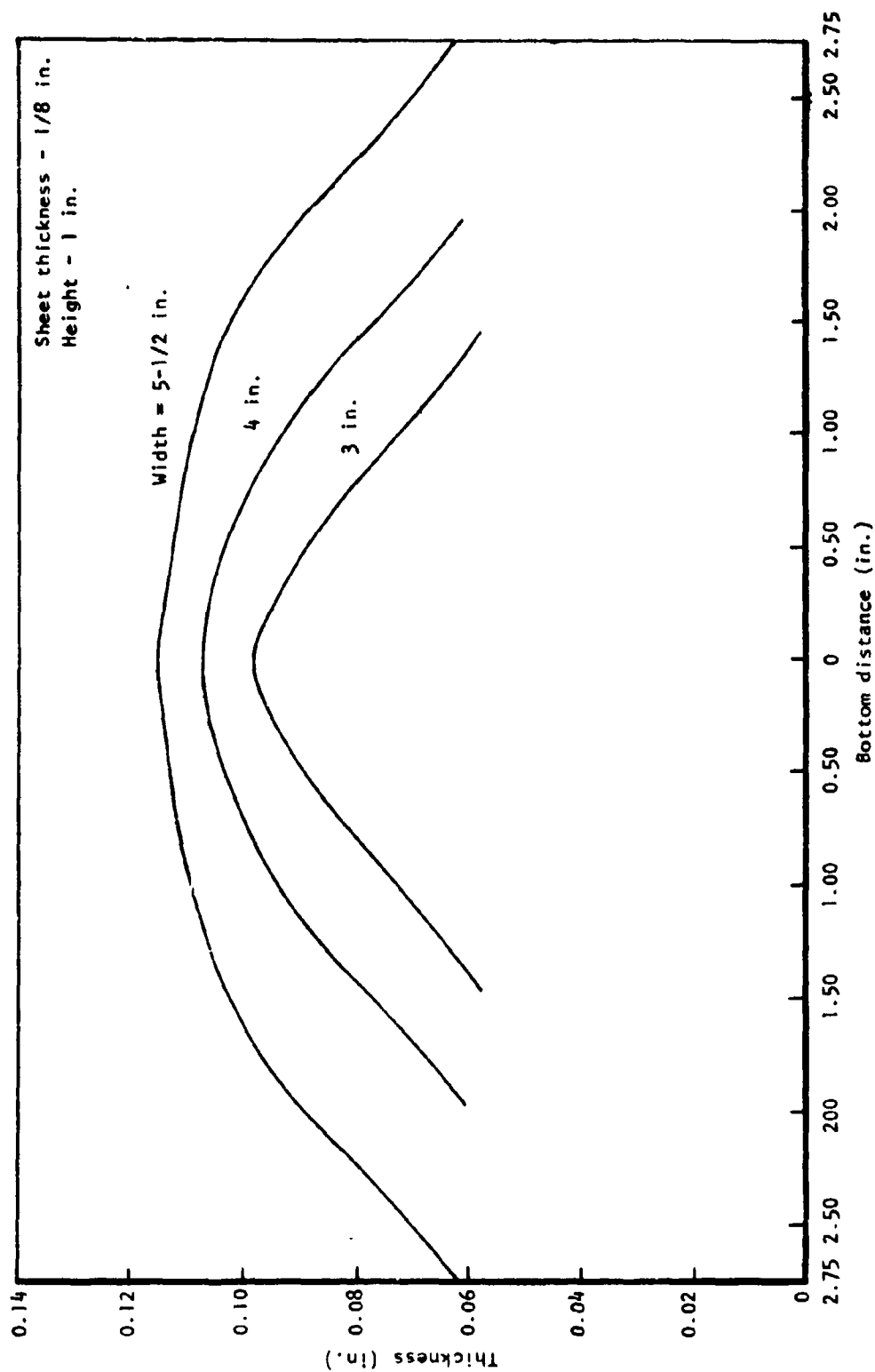
Figure 59. Computer-generated thickness profiles for three different widths of bottom web of nacelle forward center beam frame formed from 0.125-inch-thick Ti-6Al-4V sheet material.

102
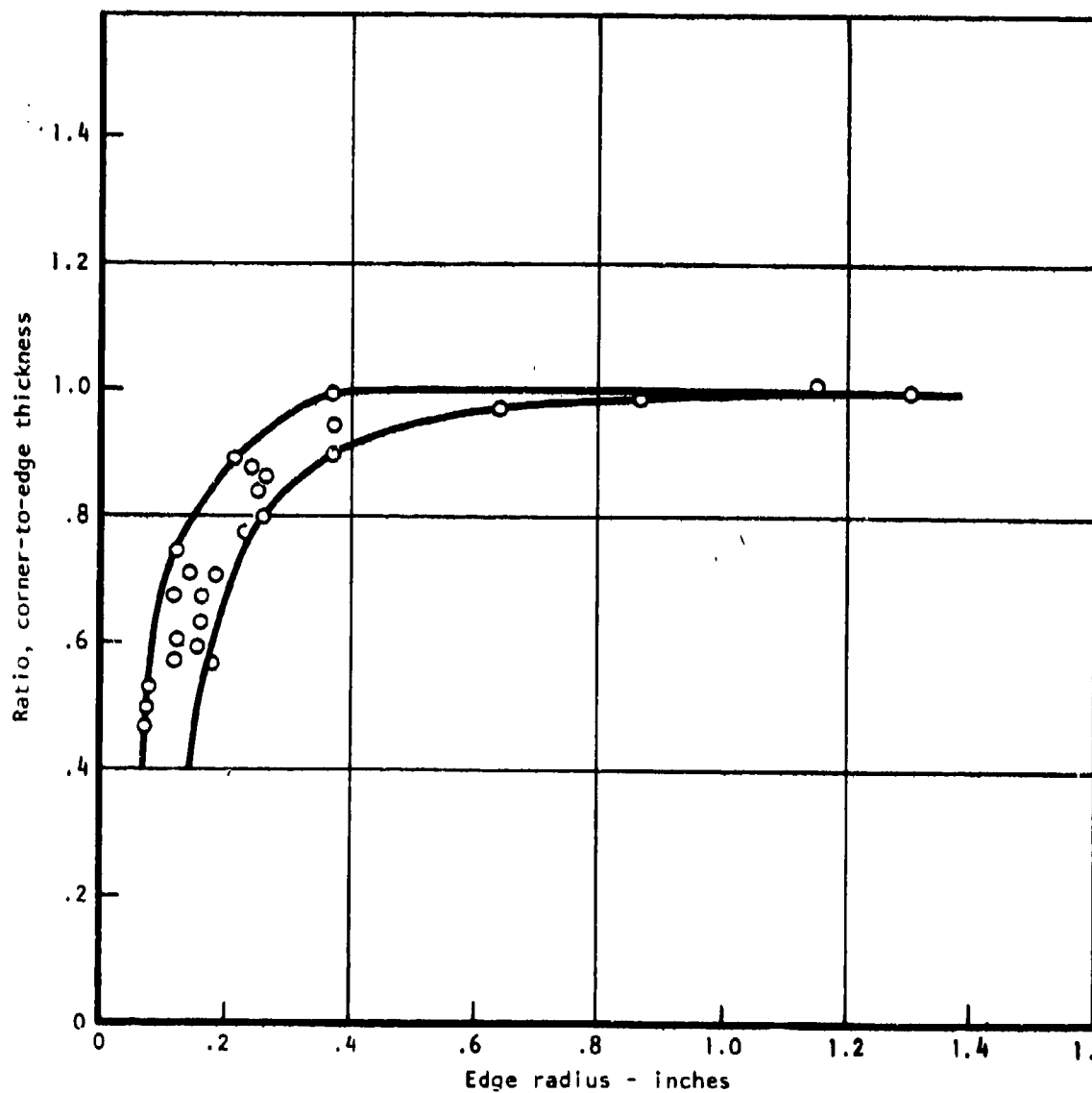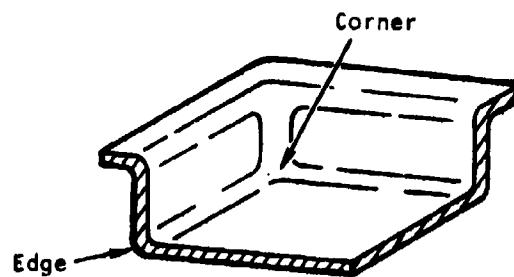
Figure 60. Effect of edge radius formed on ratio of corner-to-edge thickness.

TABLE 23.   GRAIN SIZE MEASUREMENTS OF PARTS FORMED
DURING PHASE I STUDIES

Part No.	Heat No.	Direction	Grain size (microns)		
			Location 1[a]	Location 2[b]	Location 3[c]
12	295405	LT	7.8	8.5	9.2
15	301715	L	6.4	7.4	7.9
16	301715	LT	7.7	7.9	8.7
19	295405	LT	8.0	8.8	9.0
20	301715	LT	8.0	8.3	8.6

[a] Unformed flange area
[b] Formed, bottom of pan
[c] Formed, edge radius

of the part (specimen 27, see Figure 62). This surface stain etch effect, usually indicative of oxygen and/or nitrogen enrichment, is present to a depth of about 2 mils. This level of enrichment can be readily removed by chemical means and does not constitute a problem. Specimen 23 (Figure 63) exemplifies the surface conditions of both surfaces throughout the rest of the part in which no edge effects or enrichment is evidenced. The areas outside the seal area display enrichment as depicted in specimen 1 (Figure 64). The metallography shows that the integral lip on the tooling provides a complete seal for eliminating enrichment from a formed part.

Mechanical Property Evaluation

Eight of the parts formed in task 3 were subjected to tensile and fatigue tests. The test specimens were taken from the part bottom web and side walls, and both L and LT directions were evaluated.

The eight parts evaluated represent three heats of Ti-6Al-4V alloy formed and three configurations:

1. The double pan (Figure 41)

2. The single pan with the Z-section, or stepped side wall (Figure 46)

3. A single pan without the Z-section.
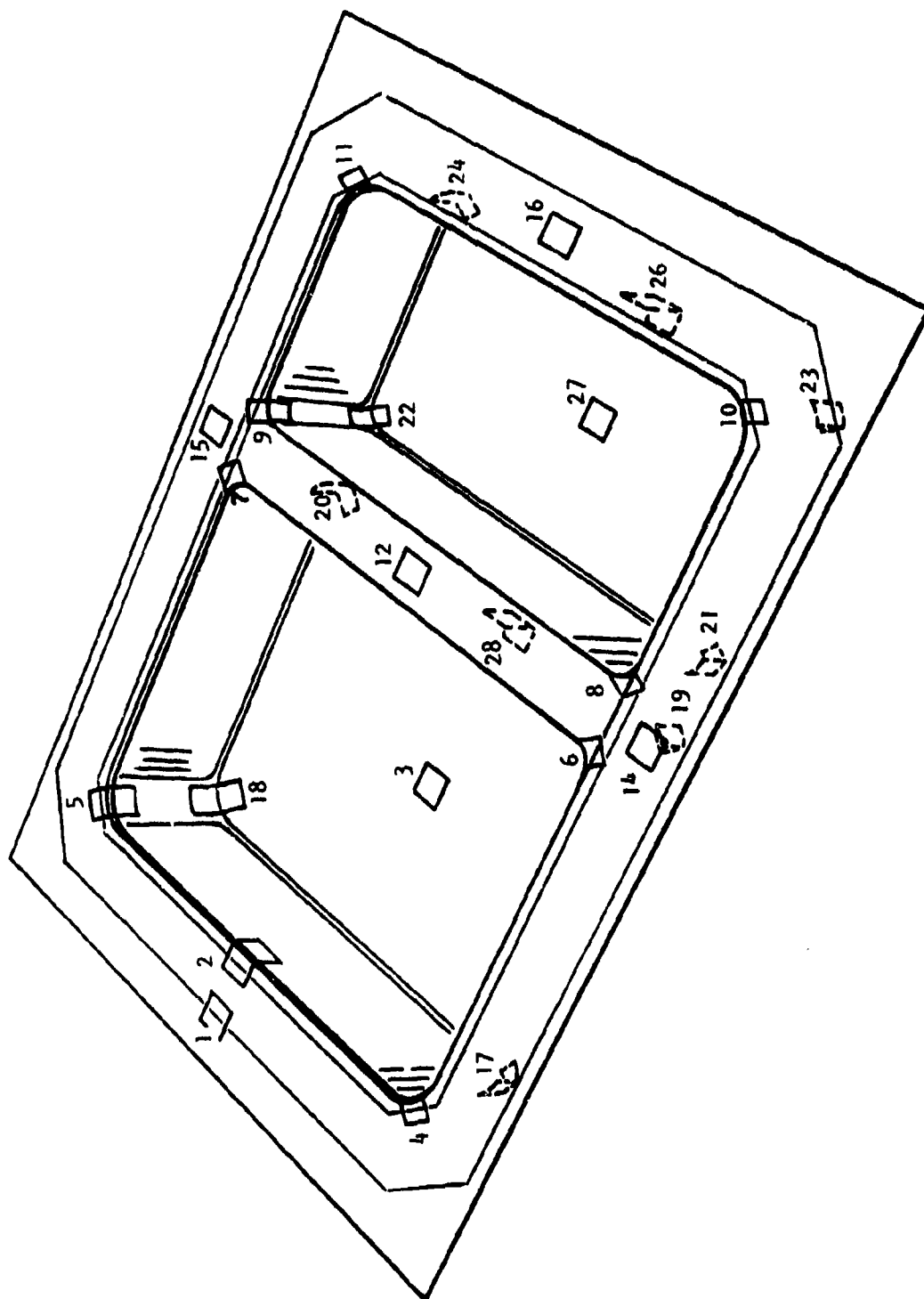
Figure 61. Location of metallurgical specimens in part No. 18.
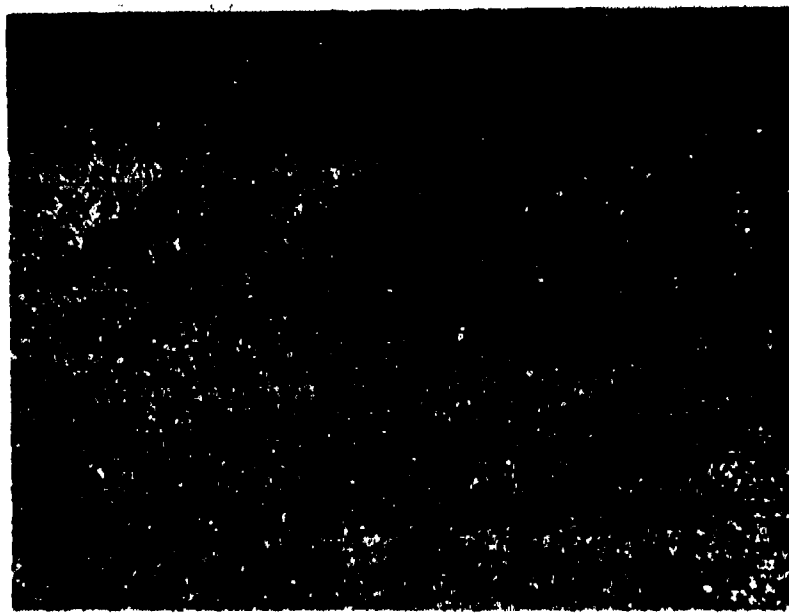
Top Surface   100X
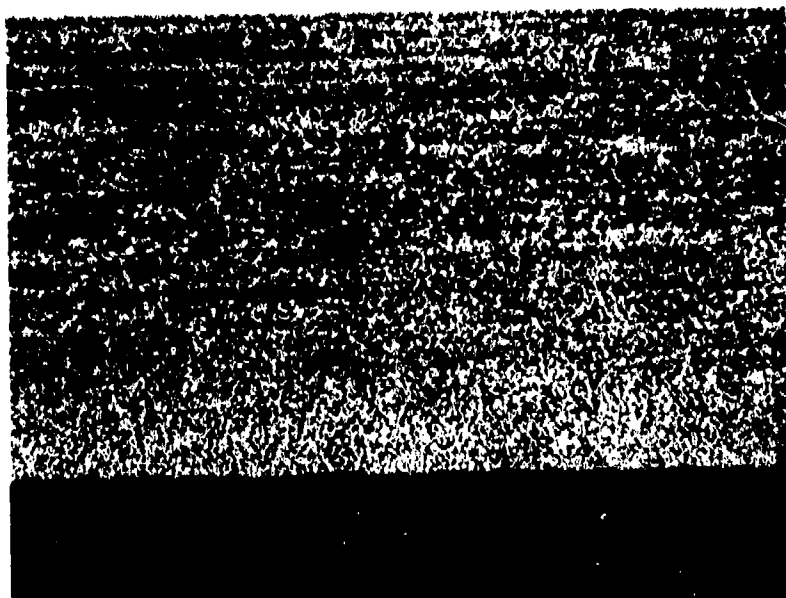
Bottom Surface   100X

Figure 62.   Surface conditions of specimen No. 27 from part No. 18.

Top Surface   100X
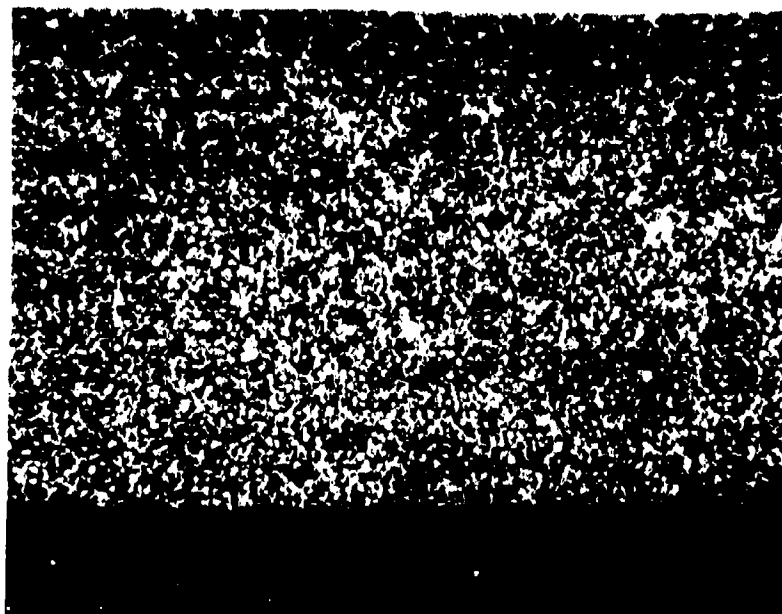
Bottom Surface   100X

Figure 63.   Surface conditions of specimen No. 23 from part No. 18.

Top Surface, Seal Area   100X

Bottom Surface, at Seal Area   100X

Figure 64.   Surface conditions of specimen No. 1 from part No. 18.

108

The size and thicknesses of the parts were such that test specimens were smaller and thinner than those used for as-received and thermally cycled material. The specimen configurations are presented in Figure 65. Whenever possible, the tensile specimens were machined with a 1-inch gage section.

The results of the tensile tests are presented in Table 24. The ultimate strength values are generally above 130 ksi, and yield strength values are generally above 115 ksi. Heat G51126, however, exhibited anomalous strength values, with those values for the L direction below corresponding values for the other two heats, and values in the LT direction are exceptionally high. This strength anisotropy of Heat G51126 is reflective of the as-received material, although the absolute values are lower.

A summary of average tensile properties is presented in Table 25 for as-received, thermally cycled, and superplastically formed to show the effect of processing. The trend, although exceptions are apparent, is for tensile ultimate to decrease from as-received to thermally cycled, and there is an indication, albeit not consistently observed, that the forming further reduces the ultimate slightly. The yield strength is also lower in thermally cycled condition than as-received, but in contrast to the ultimate strength, the yield strength after forming appears to be consistently lower than for the thermal cycle exposure only.

An effort was made to provide a rationale for understanding why the strength in the formed Ti-6Al-4V would be different than for thermally cycled. The major potential factors are grain size variations, and texturing effects during forming. A review of grain size measurements made in the previously discussed metallographic evaluation section shows no significant variation (e.g., increase) in grain size as a result of forming and, therefore, a grain size effect is not contributing to the observed yield strength variations.

The texture was determined for two heats (295405 and 301715) for the thermally cycled condition and superplastically formed. The results of this test revealed that the formed material was somewhat less textured than the thermally cycled material for both heats evaluated. A more intensive investigation would be required to establish the definite cause of the differences between the thermally cycled and formed materials, but for the purposes of developing and demonstrating the suitability of this process to structural applications, the properties of the superplastic formed material were employed and not considered to impair the application of the process.

The thicknesses of the parts formed in task 3 were not sufficient to permit compression testing because of buckling instability. Therefore, two additional pans were formed having a pocket depth of 1 inch to yield formed areas of sufficient thickness for machining compression specimens (>0.030 inch). The two parts were formed from heat No. 303182, part No. PII-7, and heat No. 295405, part No. PII-8, under identical forming conditions: 1,700° F at

	ℓ (in.)	a (in.)
A	2	1/2
B	3	1
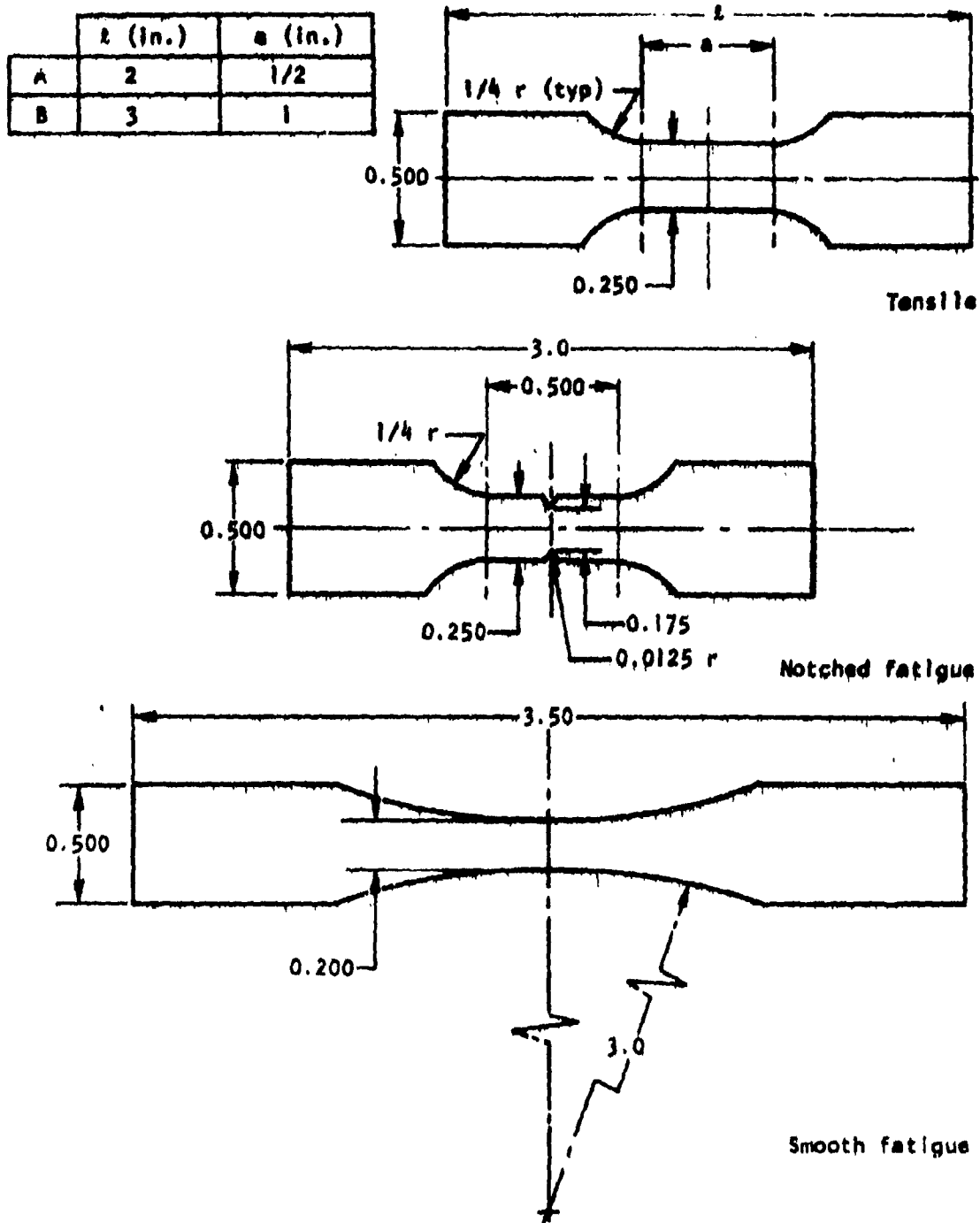
Figure 65. Specimen configurations used for evaluation of superplastically formed parts.

110

Heat No.	Test dir	Part No.	Specimen No.	Specimen thickness (in.)	Gage length (in.)	F_{tu} (ksi)	F_{ty} (ksi)	% elong
295405	L	12	T12-1	0.025	1/2	143.7	130.2	17
			T12-2	0.023	1/2	146.6	131.0	17
			C12-1	0.023	1	147.7	128.6	11
			C12-2	0.019	1	151.3	130.0	11
		19	T19-1	0.039	1/2	142.4	129.3	19
			T19-2	0.036	1/2	147.0	133.8	18
			C19-1	0.039	1/2	144.4	128.3	19
			NF19-1	0.038	1	145.9	131.9	14
			NF19-2	0.036	1	146.3	132.6	14
		23	NF23-1	0.035	1	144.8	127.3	13
			NF23-2	0.034	1	146.3	130.2	14
	LT	12	C12-4	0.029	1/2	135.6	120.5	17
			T12-6	0.027	1	139.0	116.6	12.5
301715	L	13	T13-1	0.037	1/2	141.9	128.5	17
			T13-2	0.036	1/2	138.5	123.6	17
			NF13-1	0.030	1	144.2	123.7	11
		15	T15-1	0.025	1/2	136.2	123.8	14
			T15-2	0.028	1/2	142.3	122.5	14
			C15-1	0.034	1/2	137.8	125.6	18
			C15-2	0.024	1	145.1	128.1	11
		16	T16-1	0.033	1/2	142.9	131.5	20
			C16-1	0.023	1	146.3	124.6	7
			C16-2	0.019	1	147.3	124.0	10
			NF16-1	0.026	1	145.6	126.1	12
			NF16-2	0.023	1	147.8	126.2	11
		20	NF20-1	0.043	1	135.1	123.8	14
			NF20-2	0.040	1	138.8	126.0	13
	LT	13	T13-4	0.055	1/2	130.6	114.0	17.5
		15	T15-3	0.035	1/2	132.3	116.9	14.5
			T15-4	0.032	1/2	136.4	114.8	12
			C15-3	0.022	1	140.2	118.0	7
			C15-4	0.018	1	139.3	113.6	5
		16	C16-3	0.024	1	141.8	114.4	10
			C16-4	0.032	1	137.3	114.6	11.5
			T16-3	0.026	1/2	130.3	114.4	18
			T16-4	0.030	1/2	136.8	121.1	14
			NF16-3	0.022	1	142.4	117.1	8
GS1426	L	14	T14-1	0.060	1/2	128.5	112.3	17
			T14-2	0.056	1/2	127.3	119.5	14
			NF14-1	0.051	1	125.0	110.7	12
	LT	14	T14-3	0.089	1/2	150.7	137.8	18

TABLE 25. AVERAGE TENSILE PROPERTIES OF TITANIUM SHEET MATERIAL IN AS-RECEIVED, THERMALLY CYCLED AND SUPERPLASTIC FORMED CONDITIONS (REF. TABLES 6, 8 AND 9)

Heat No.	Condition	L		LT	
		F_{tu} (ksi)	F_{ty} (ksi)	F_{tu} (ksi)	F_{ty} (ksi)
295405	As-received[a]	143.9	140.5	142.7	132.4
	Cycled	146.2	137.3	137.7	124.4
	Formed	146.0	130.3	137.9	118.6
301715	As-received[a]	141.3	139.0	138.7	132.9
	Cycled	138.2	127.6	133.1	121.5
	Formed	142.2	125.6	136.1	115.6
G51126	As-received[a]	145.3	128.4	157.6	150.4
	Cycled	131.4	122.0	153.0	143.8
	Formed	126.9	114.2	150.7	137.8

[a]Average of: 3 hr/1,650° F

3 hr/1,700° F

3 hr/1,750° F

112

45 psi argon pressure for 3-3/4 hours. The starting thickness for forming the two parts were 0.108 and 0.054 inch, respectively. The mechanical properties in compression are presented in Table 26. The average F_{cy} value in the longitudinal direction of the thermally cycled material is $15\Gamma.8$ ksi as compared to a value of 146.7 ksi for the superplastic formed material. F_{cy} values of 129.9 ksi were obtained for the thermally cycled material and 126.1 ksi for the formed material in the long transverse direction. This comparative effect is in agreement with tensile yield results previously discussed.

Fatigue specimens were machined from six different parts (No. 12, 15, 16, 19, 20, and 23) representing two heats (295405 and 301715) in both the notched and smooth condition. Fatigue life for as-received, thermally cycled and superplastically formed conditions are shown as a plot of $\%F_{tu}$ versus cycles to failure in Figures 66 and 67 and the data are included in Table 26. The fatigue results, for $K_t = 1$ and $K_t = 3$, do not reveal any differences in fatigue life for the three basic conditions evaluated.

These data are presented as $\%F_{tu}$ in order to normalize the stresses to the corresponding ultimate strengths, a standard practice for representation of fatigue data in design manuals such as MIL-HDBK-5.

Scatter bands are also presented for comparison which represent the observed range of fatigue data for Ti-6Al-4V alloy in the recrystallized annealed and diffusion bonded conditions. Both of these conditions involve thermal cycles to 1700F, and are therefore similar to the superplastic forming cycle. As can be seen in Figures 66 and 67, the fatigue data fall within these scatter bands and thus indicate that design fatigue life for super plastic formed parts is the same as that of the diffusion bonded or recrystallized annealed alloy.

113

TABLE 26. PROPERTIES OF Ti-6A1-4V SHEET MATERIAL
SUPERPLASTIC FORMED IN SINGLE-PAN CONFIGURATION

Heat No.	Thickness (in.)	K_t	Test Direction	Specimen	0.2% F_{cy}	% F_{tu}	To Failure
COMPRESSION							
303182	0.099		L	CII7-1	131.1		
	0.099		L	CII7-2	131.6		
	0.098		L	CII7-3	129.4		
	0.099		LT	CII7-4	147.0		
	0.098		LT	CII7-5	148.0		
	0.095		LT	CII7-6	145.4		
295405	0.049		L	CII8-1	146.1		
	0.049		L	CII8-2	149.0		
	0.049		L	CII8-3	144.9		
	0.049		LT	CII8-4	124.7		
	0.048		LT	CII8-5	127.1		
	0.047		LT	CII8-6	126.6		
FATIGUE							
295405	0.032	1	L	SF12-1		75	53,000
	0.028	1	L	SF12-2		75	58,000
	0.032	1	L	SF19-1		75	129,000
				SF19-1		75	673,000
	0.032	1	L	SF19-2		75	86,000
	0.035	1	L	SF23-1		75	89,000
	0.033	1	L	SF23-2		75	52,000
	0.020	3	L	NF12-1		50	8,000
	0.018	3	L	NF12-2		50	10,000
	0.026	1	LT	SF12-3		75	48,000
	0.025	1	LT	SF12-4		75	73,000
	0.025	3	lt	NF12-3		50	13,000
	0.021	3	LT	NF12-4		50	10,000
301715	0.030	1	L	SF15-1		75	21,000
	0.030	1	L	SF15-2		75	9,000
	0.029	1	L	SF16-1		75	1,430,000
	0.029	1	L	SF16-2		75	128,000
	0.032	1	L	SF20-1		75	1,437,000
	0.036	1	L	SF20-2		75	676,000
	0.029	3	L	NF15-1		50	10,000
	0.034	3	L	NF15-2		50	6,000
	0.030	1	LT	SF15-3		75	262,000
	0.029	1	LT	SF15-4		75	23,000
	0.029	1	LT	SF16-3		75	13,000
	0.028	1	LT	SF16-4		75	22,000
	0.031	3	LT	NF15-3		50	10,000
	0.026	3	LT	NF15-4		50	10,000

114
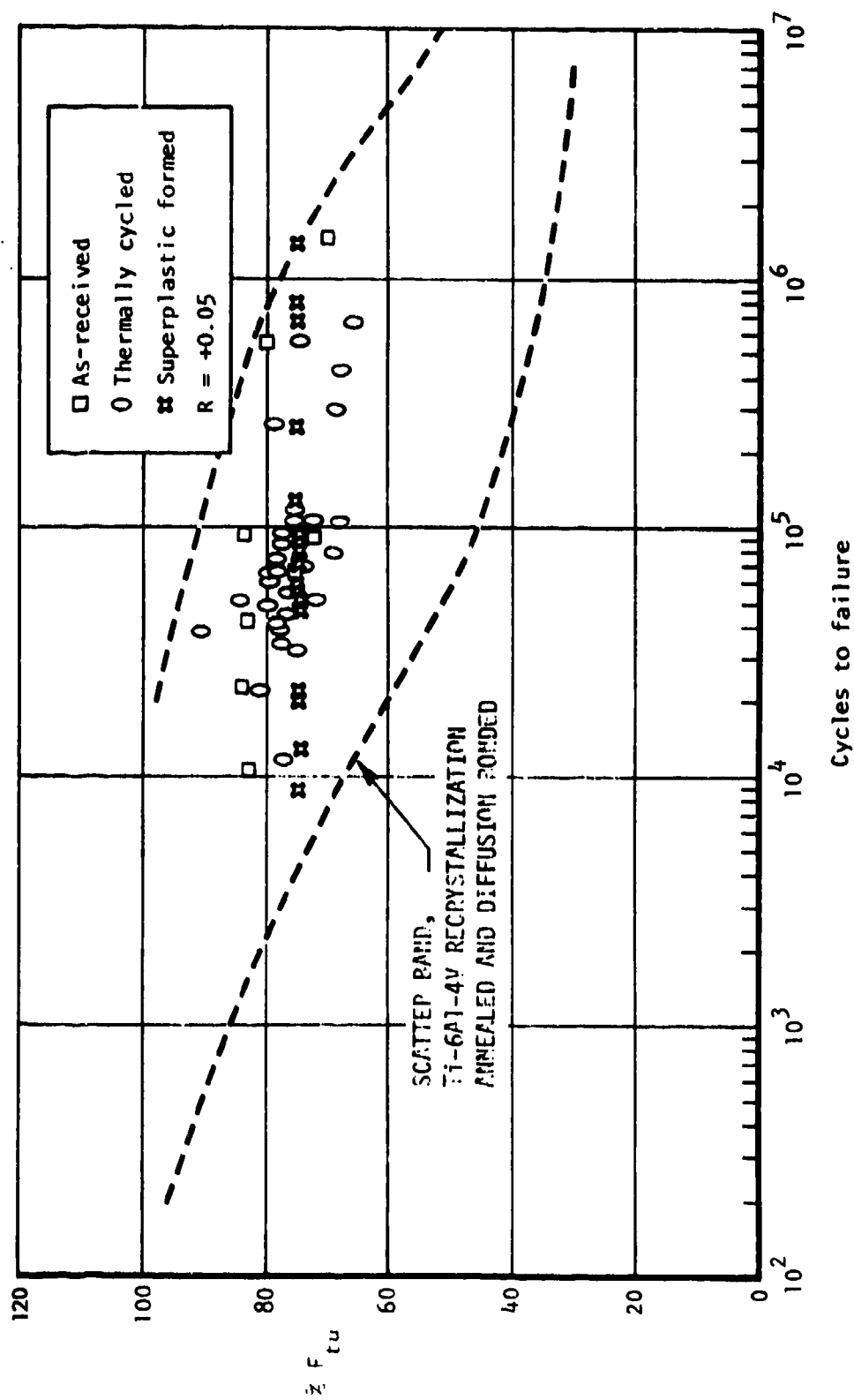
Figure 66. Smooth fatigue properties of as-received, thermally cycled, and superplastic formed Ti-6Al-4V sheet material used during phase I forming studies.

115
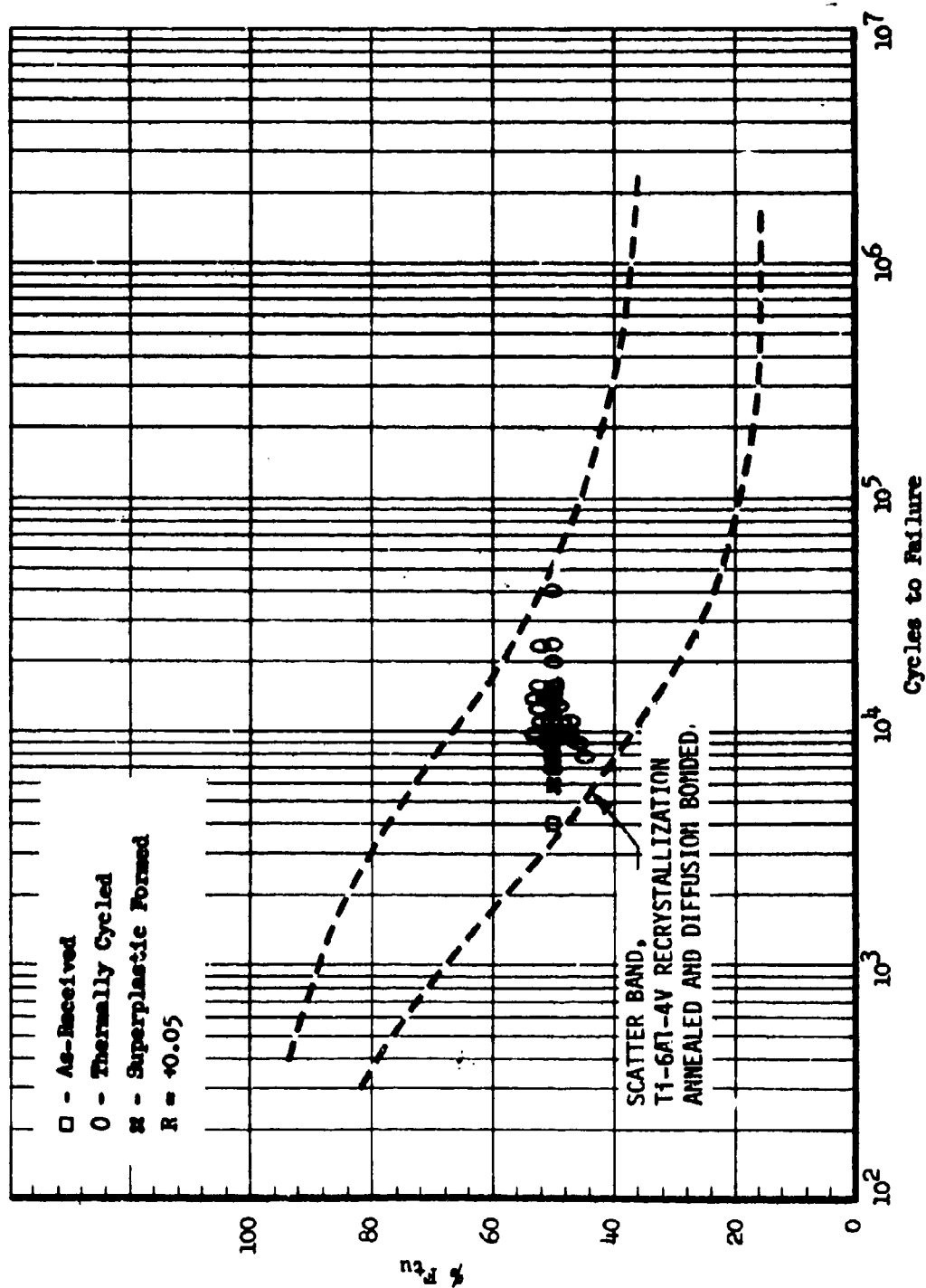
Figure 67. Notched fatigue ($K_t = 3$) properties of as-received, thermally cycled, and superplastic formed Ti-6Al-4V sheet material used during phase I forming studies

116

The objective of this phase of the program was to demonstrate the applicability of the superplastic forming (SPF) of titanium sheet to the fabrication of actual aircraft structural parts. The technology developed in phase I provided the baseline for the fabrication of the phase II aircraft components under manufacturing conditions.

COMPONENT SELECTION

Two sheet metal structural components of the B-1 aircraft were selected for fabrication during this phase of the program. One selection was made on the basis of completely redesigning an assembly into a monolithic structure, and the other was selected to demonstrate the SPF process on an existing design. The parts selected are sheet metal frames of titanium in the B-1 nacelle structure shown in Figure 68. The sheet metal frames separate and support the inboard and outboard engine compartments. The nacelle forward center beam frame is a Ti-6A1-4V sheet metal assembly utilizing eight separate parts mechanically fastened with 96 fasteners. These assemblies are used at eight different stations on each nacelle, making a total of 16 per aircraft. The current forming procedure encompasses the use of a steel hydropress die and preheated blanks. Two preforms are produced suitable for subsequent hot sizing which together yield the basic sheet metal section. Six individual parts are mechanically fastened to this section to provide the assembly. On the aircraft, 15 other similar assemblies are utilized, which, in conjunction with the assembly applicability to a one-piece formed part, influenced the selection. The second part selected is also in the same nacelle structure; however, a redesign was not contemplated, since the one-piece component would be formed to meet the existing die. This part also has a total of 16 applications. Thus, the SPF process would show applicability to a complex sheet metal component replacing an assembly and to a part normally formed by conventional means. The two components are shown in Figure 69.

COMPONENT DESIGN

The forward beam assembly, made up of eight individual parts, was redesigned into a one-piece component, eliminating seven parts and 96 fasteners. The one-piece design contains multiple stiffening beads throughout the web area to provide the stiffening elements and strength required, as shown in Figure 70. Return flanges around the part periphery were also included to provide the necessary attachment areas for surrounding structure. The redesign was predicated on the capability to superplastically form complex titanium sheet metal sections that could not otherwise be formed by conventional means. Subsequent to forming by the superplastic process, chemical

117
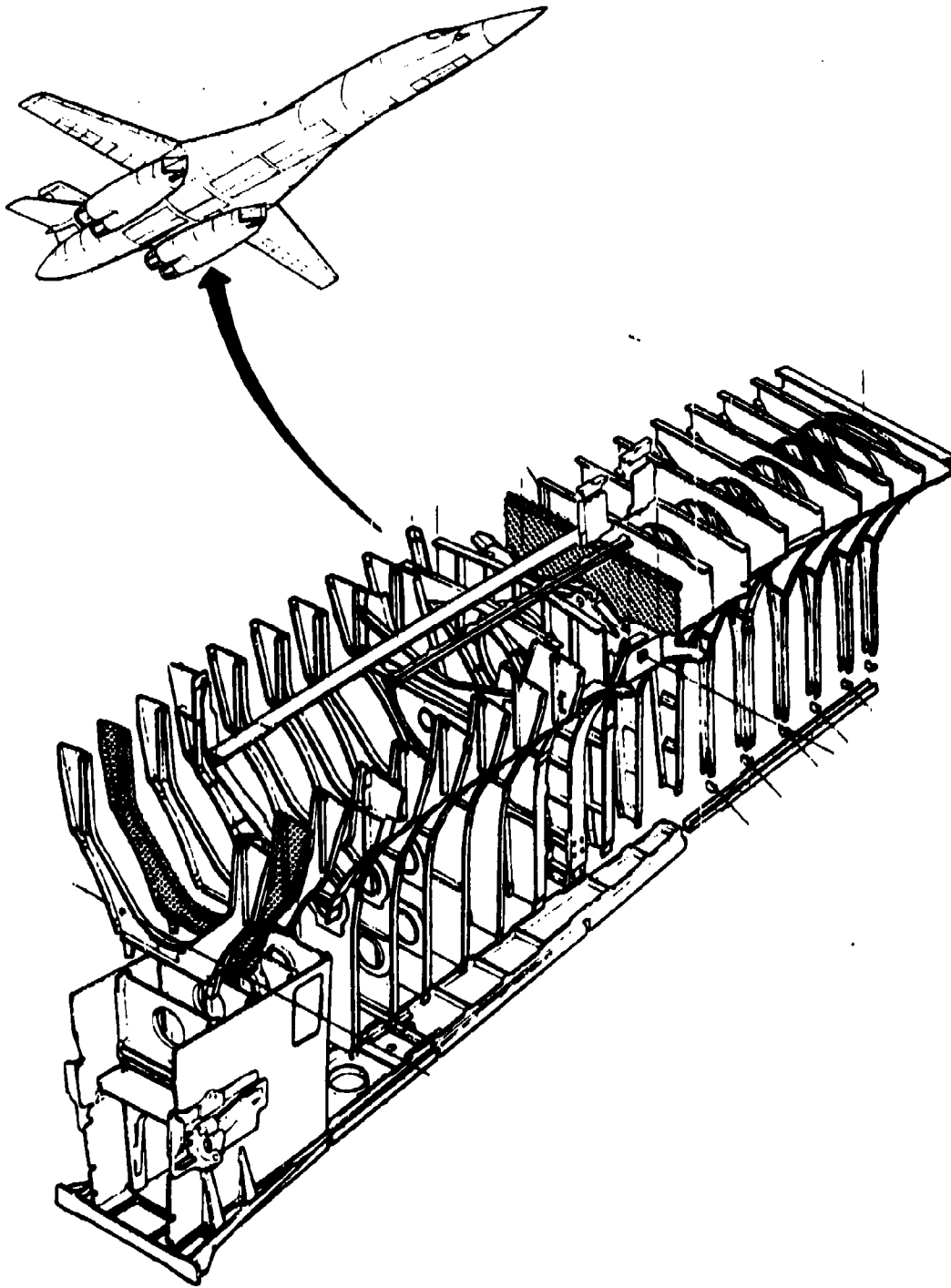
Figure 68.   Superplastic forming, nacelle applications.

118

Nacelle Aft
Center Beam Frame

Nacelle Forward
Center Beam Frame
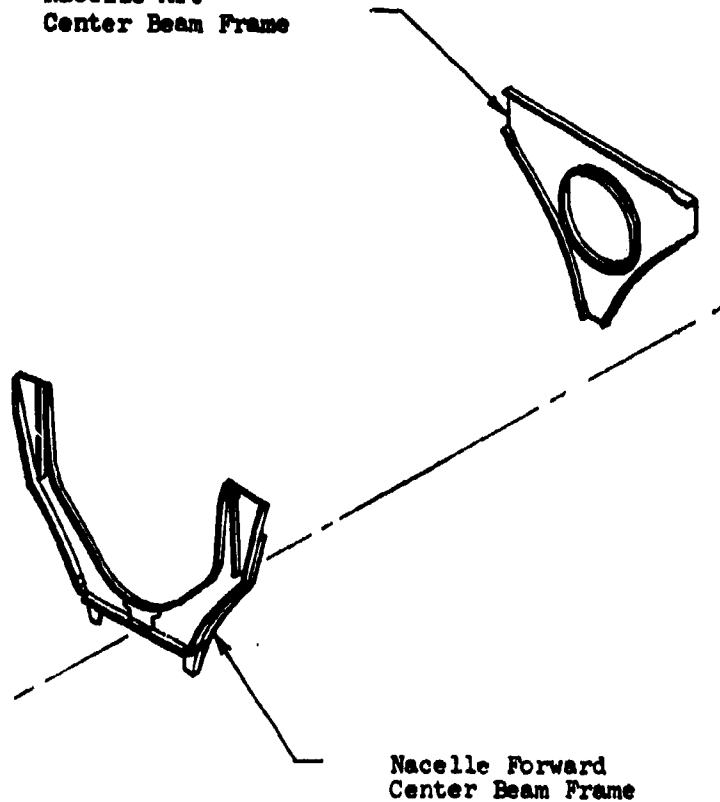
Figure 69. Selected phase II structural components to be formed.

milling of the part would reduce sheet thickness, achieving a lightweight
structure in the nacelle area and contributing substantially to overall weight
reduction.

MATERIAL CHARACTERIZATION

The Ti-6Al-4V sheet material for component fabrication was procured in
five heats to MIL-T-9046 requirements. Table 27 shows the chemical composi-
tion for the five heats of sheet products. Each heat was examined metallog-
raphically prior to procurement to assure that the microstructure was
consistent with that required for superplasticity as described in phase I.
In addition, the high-temperature (1,700° F) flow properties were also deter-
mined for each heat of material. Figure 71 shows the flow stress as a
function of strain rate for the five heats of materials in terms of maximum

119
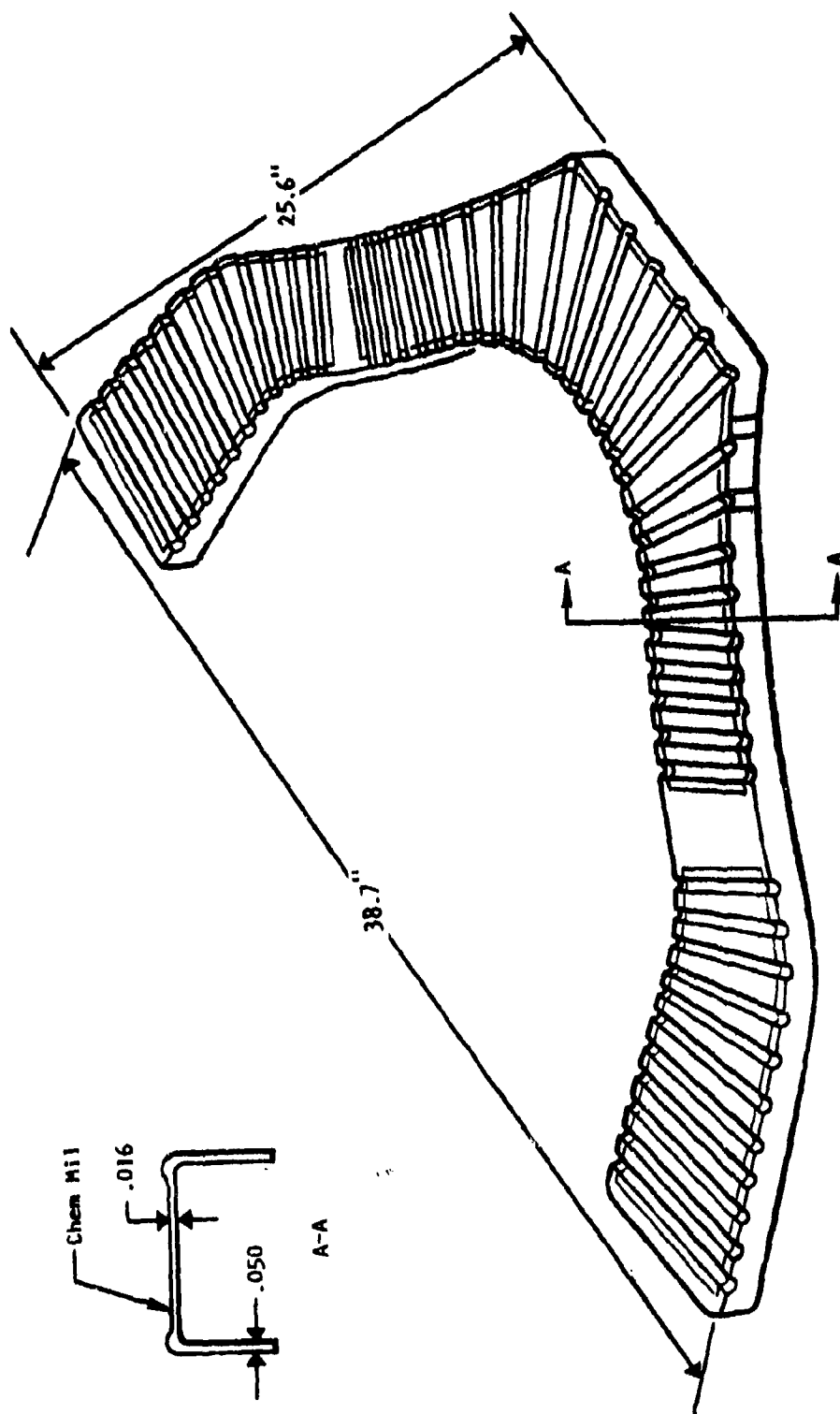
Figure 70. Redesigned nacelle forward center beam frame.

120

TABLE 27. CHEMICAL COMPOSITION OF Ti-6Al-4V SHEETS USED
IN PHASE II STUDIES

Heat No.	Size (in.)	Composition (wt %)						
		A	V	O	N	C	Fe	H
890033	0.125 x 60 x 115	6.3	4.1	0.132	0.010	0.02	0.16	0.0058
295866	0.125 x 60 x 152	6.3	4.0	0.137	0.011	0.02	0.16	0.0058
800620	0.125 x 60 x 152	6.2	4.1	0.125	0.130	0.01	0.16	0.0053
304488	0.060 x 48 x 95	6.1	4.1	0.116	0.009	0.02	0.20	0.0043
800630	0.080 x 36 x 96	6.4	4.1	0.135	0.015	0.01	0.17	0.0065

scatter, and the scatter are compared to those of the phase I heats. The
phase II materials possess flow properties generally in the lower region of
the phase I scatter band, which indicated that the forming parameters devel-
oped in phase I were suitable for the phase II material. The maximum strain-
rate sensitivity index (m_{max}) for the phase II material determined from the
slope of the flow stress versus strain rate curves ranged from 0.78 to 0.92,
indicative of suitable superplasticity for the five heats of materials, since
it was shown in the phase I study that good superplastic properties of the
sheet material is evident with m_{max} value about 0.7.

PROCESS PARAMETER SELECTION

The process parameters required to successfully form the nacelle forward
and aft beam frames were established on the basis of the preliminary forming
studies conducted under phase I, from the forming studies conducted on a sub-
scale part representative of a section of a frame, and from a comparison of
stress/strain-rate properties of the titanium alloys. These studies showed
forming parameters for a sheet of Ti-6Al-4V of 0.125-inch thickness required
for the forward frame. It was planned to begin with these parameters on the
initial full-scale part, and then increase pressure and decrease time until
optimum conditions were reached for a successfully formed part. The previous
tests on the material to be utilized had indicated suitable superplastic prop-
erties, leading to the conclusion that various pressures could be exploited.
Therefore, the initial forming trial on the forward frame was to utilize
90 psi pressure for 3 hours at 1,700° F, followed by necessary variations on
subsequent trials.

121
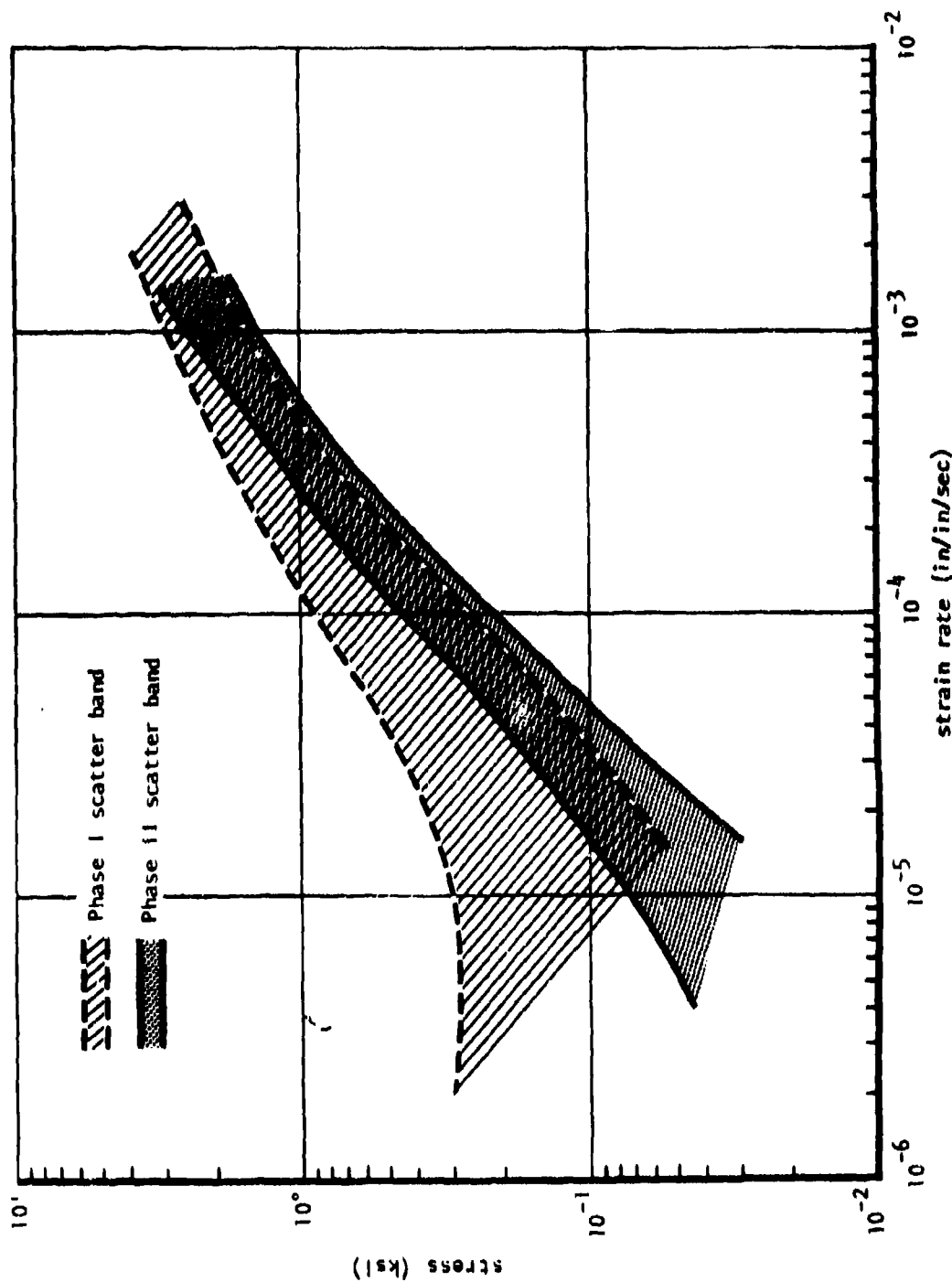
Figure 71. Comparison of flow stresses versus strain rates scatter bands between phase I and phase II heats.

122

TOOL DESIGN

Both male and female tool concepts were considered. The female tool configuration is the most suitable from the standpoint of attaining maximum material utilization. This concept, however, is the most difficult with which to achieve small edge and corner radii, since the material must flow into the cavity bottom after contact with the die side surface. Tooling material selected was based on studies conducted in phase I which determined candidate materials compatible with titanium at the forming temperature and which were low cost and readily available.

A female tool design was selected for the forward frame, on the basis of material utilization and ease of removal after forming. A male die was used in forming the aft frame, which provided the opportunity to evaluate both forms of dies.

NACELLE FORWARD CENTER BEAM FRAME

The tooling assembly for the forward beam fabrication consisted of 4130 steel upper and lower plates, 4140 steel central die with the cavity, and 1020 steel half-rounds and insert in the die cavity bottom. The upper and lower plates and the die insert are one piece each, while the die cavity plate was fabricated in four pieces. The multiple-piece die was utilized to facilitate easy disassembly after forming and provided for ease of part removal. A view of the die assembly is shown in Figure 72; the upper plate, showing the seal projection and argon gas cavity, is shown in Figure 73.

The six-piece die, including the bottom plate, was prepared for the forming trials by grinding the surfaces to provide a smooth, semipolished finish. Each of the die sections was mechanically fastened to the bottom plate, and rectangular steel bars were bolted to two sides to prevent movement during forming. The beaded insert plate laid free in the die cavity. Argon gas was introduced into the upper and lower portions of the die cavity through connections in the upper and lower plates and was exited through outlets below the center beaded plate and in the upper plate. The surface beneath the beaded plate was grooved to allow argon gas movement during forming and to prevent gas blockage at any point.

The titanium diaphragm being formed contacts the lower die assembly inside the peripheral seal and, therefore, this area was sprayed with graphite lubricant to prevent sticking problems as described in phase I. All other areas outboard of the formed part were sprayed with an yttrium-base material to prevent tooling members from adhering to one another. The seal lip was machined to within 3 inches of the die cavity, which allowed the use of a trimmed titanium sheet diaphragm close to the final part configuration.
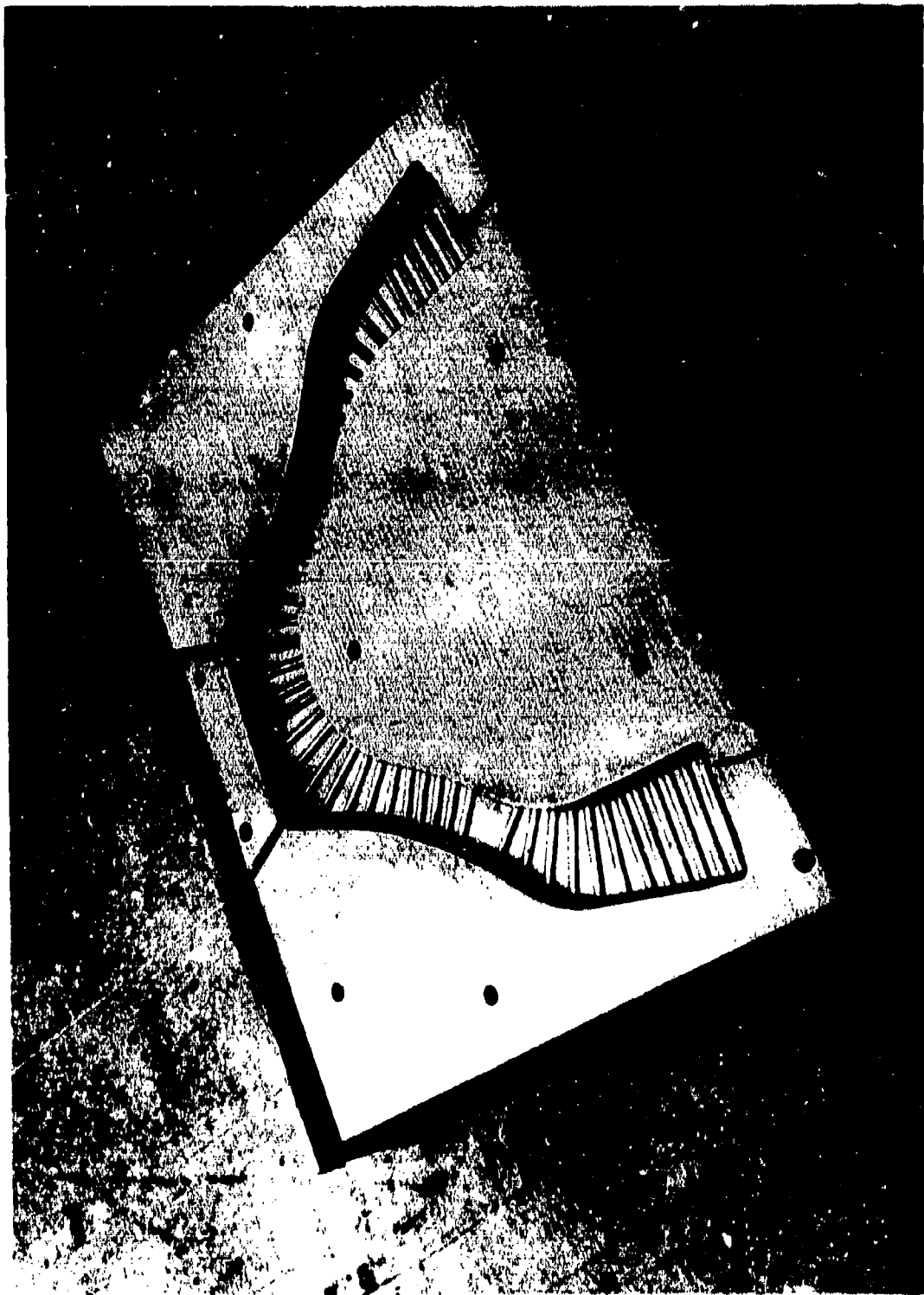
Figure 72. Multiple-piece female die utilized to form nacelle forward center beam frame configuration. (Note: Die pieces in photo applied in place, causing observable gaps.)

Figure 73. Upper plate showing argon gas cavity and seal lip projection (arrow).

125

The seal which held the titanium sheet diaphragm and contained the argon gas pressure was a machined lip on the upper plate and followed the periphery of the cavity as shown in Figure 73. The machined bead was 1/4-inch wide and 1/8-inch high. Applied pressure during heatup to 1,700° F forced the male bead seal against the titanium diaphragm and indented the titanium diaphragm sufficiently to affect the seal during forming and to hold the titanium diaphragm in place. Pressure to cause sealing was obtained using a conventional hydraulic press.

The completed tooling and titanium sheet assembly, shown in Figure 74, was placed between 4- by 6-foot ceramic heating platens and installed in a hydraulic press. The entire setup in the press is shown in Figure 75, with the electrical heating connections, the thermocouple hookup, and the argon gas connections. Thermocouples were embedded in the center die and the sides and center of the upper and lower plates. A continuous temperature recording was made during heatup, pressurization, and forming.

NACELLE AFT CENTER BEAM FRAME

A male tool was utilized for forming the nacelle aft center beam frame. The tooling utilized a male forming die of H-13 tool steel placed between two plates of 4130 steel. The die and plates were available and needed only slight modification for forming the aft frame. The large, heavy 4130 steel bottom plate utilized tiedown fasteners to position the center die. The center forming die was placed in the bottom plate, and additional plates were added to the side and central cavity, since only a short-part flange was required. The entire die and lower plate surface within the seal area was sprayed with graphite lubricant to prevent sticking, as shown in Figure 76. The upper plate, with an argon gas cavity, is shown in Figure 77. A seal was provided by using titanium wire (commercially pure) around the periphery of both the upper and lower plates. The titanium sheet diaphragm was placed between the two plates as shown in Figures 78 and 79. The completed assembly was placed between ceramic platens and installed in a hydraulic press with heating cables, thermocouple connections, and argon gas pressure tubing in a similar manner as in forming the forward frame.

COMPONENT FABRICATION

The procedure followed in forming the forward and aft frames included the following steps:

1. The titanium sheet diaphragm was cleaned and trimmed.

2. The tooling sections were firmly secured onto the bottom plate.

126

Figure 74. Completed tooling assembly - forward frames.
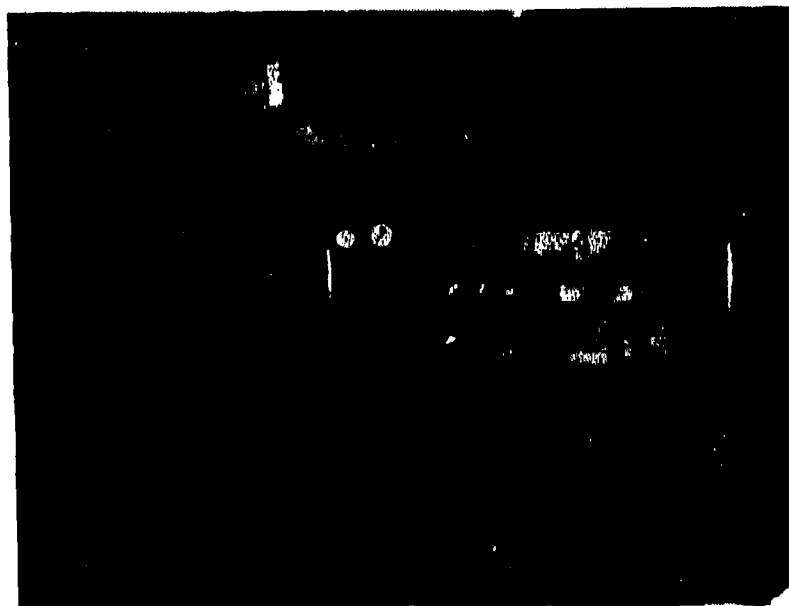
Figure 75. Press-installed forward frame tooling assembly.
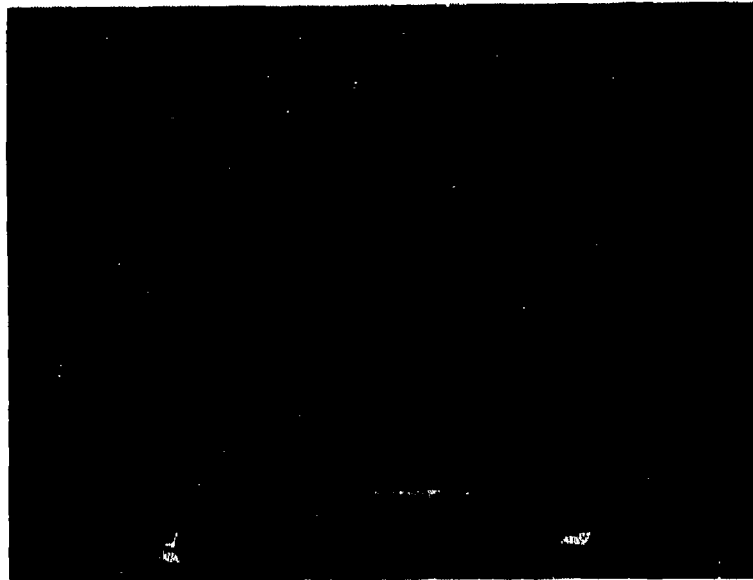
Figure 76.   Lower plate and die for nacelle aft frame forming.
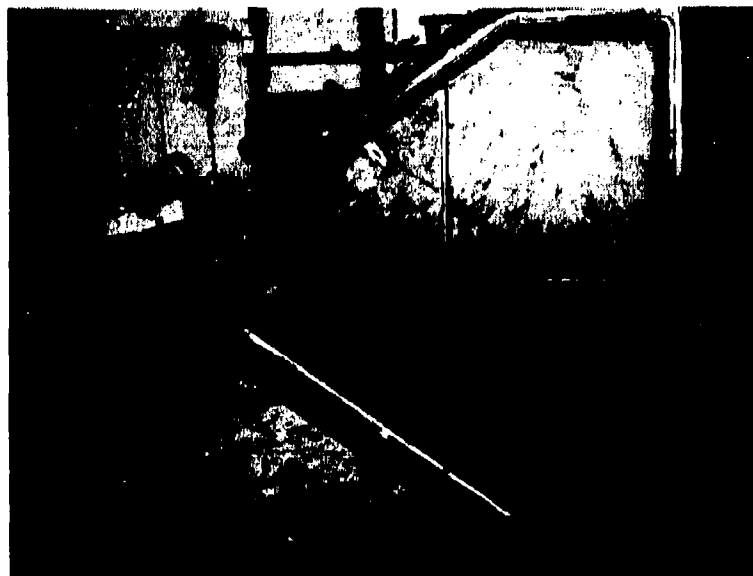
Figure 77.   Upper plate for nacelle aft frame forming.
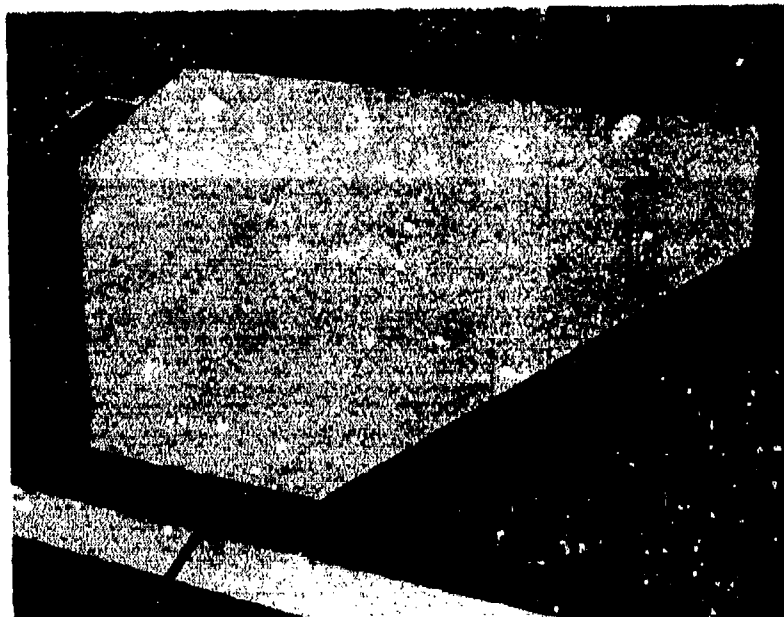
Figure 78. Titanium Diaphragm placed on bottom plate.

Figure 79. Completed tooling assembly for aft frame.

3. The tooling surfaces were sprayed with graphite lubricant inside the seal area.

4. The titanium sheet diaphragm was placed between the tooling. (For the aft frame, the titanium wire seal was placed on the plates prior to placement of the titanium diaphragm.)

5. The tooling was assembled and placed between ceramic heating platens in a hydraulic press.

6. The heating cables, thermocouple wires, and argon gas bottles were connected.

7. Heating of the platens was begun with continuous temperature recording and argon gas pressure applied (4 psi in the top cavity and 2 psi in the bottom cavity, typically). The slight positive gas pressure was applied to prevent influx of air during heatup. A higher pressure was applied to the top cavity to assure that the diaphragm did not pillow into the top cavity.

8. At a recorded temperature of 1,700° F (±50° F) of all thermocouples, the argon gas pressure in the top cavity was increased incrementally over a predetermined time period, to cause forming to occur.

9. The hydraulic press pressure was adjusted to maintain the seal and prevent significant leakage of the argon out of the upper die cavity.

10. When the forming pressure was reached, it was maintained for a pre-determined time period. (A typical time-pressure cycle is shown in Figure 80, showing a linear and a nonlinear method of reaching forming pressure.)

11. Forming of the titanium sheet diaphragm proceeded in a manner shown in Figure 54.

12. At the completion of the forming cycle, heating was terminated. Argon gas pressure was decreased to 4 psi in the top cavity, while 2 psi was maintained in the bottom cavity until the part was cooled to below 800° F.

13. The tooling was removed and disassembled.

14. The formed titanium part was trimmed to configuration and cleaned for inspection.
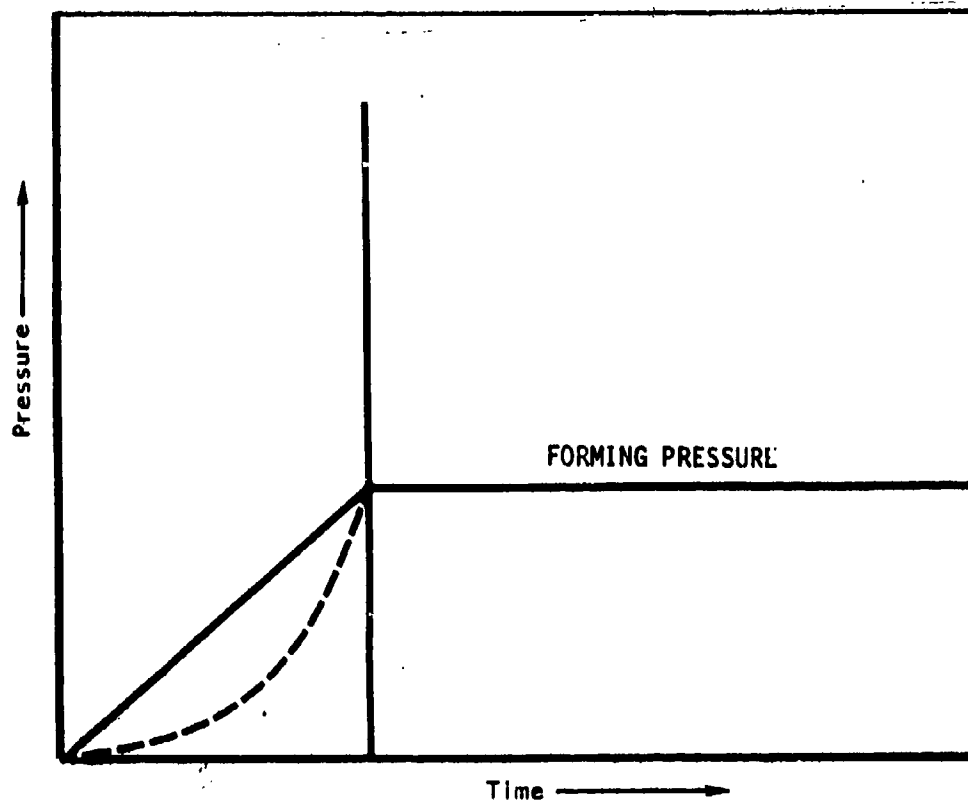
Figure 80. Time-pressure cycle.

NACELLE FORWARD CENTER BEAM FRAME FORMING RESULTS

A total of 11 forward frames were superplastically formed during phase II. Table 28 shows the forming runs, the parameters used, and the results. Seven titanium frames were successfully formed to provide the six required for Air Force Materials Laboratory evaluation. Bend radii, bead configuration, and joggle areas were well defined. All parts were formed at 1,700° F (±50° F) and varying argon pressures and times at pressure. No difficulty was experienced in maintaining proper temperature or argon gas pressure during forming, except in one instance when the hydraulic press malfunctioned.

During the application of argon gas pressure, the forming of the titanium sheet proceeded quickly, and the majority of the sheet metal deformation occurred during the first hour of reaching maximum forming pressure. The additional time at the forming temperature and pressure was necessary in order to obtain the final desired radius where the rate of forming is significantly slower.

131

TABLE 28. FORWARD FRAME PARAMETERS

Part No.	Temperature (°F) (During form cycle)	Argon gas pressure						Time at press. (hr)	Remarks
		Prior to form		During Form		After form			
		a	b	a	b	a	b		
FF-1	1,660-1,712	4	4	90	0.2	3	0.2	3	Part not fully formed in radii
FF-2	1,700-1,745	4	4	110	0.2	4	4	5	Part not fully formed in radii.
FF-3	1,700-1,750	4	4	130	2	4	4	5.5	Part not fully formed in radii.
FF-4	1,670-1,750	4	4	135	2	2.5	1.5	6	Part overformed in radii.
FF-5	1,680-1,745	4	4	150	2	4	2	5	Well formed.
FF-6	1,678-1,750	4	3.5	150	2	4	2	3	Well formed.
FF-7	1,680-1,744	4	4	150-155	2	4	2	2.5	Well formed.
FF-8-1	1,650-1,725	Free flow - Argon						-	No pressure from press.
FF-8-1 rerun	1,645-1,740	0.5	0.5	60	1	Free flow		10 min	Tube cracked - partially formed.
FF-8-2	1,690-1,745	1	0.5	150-155	0.75	0.75	0.75	3	Well formed.
FF-9	1,690-1,740	1	0.5	160	0.5	0.5	0.5	4.5	Well formed.
FF-10	1,675-1,745	2	0.5	160 165	0.5	1	1	2	Well formed
FF-11	1,635-1,745	2	1	160-165	0.5	-	-	4	FF-8-1 part reformed - well formed.

a Top surface

b Bottom surface

In the first three parts formed, the corner radii were larger than desired, and corrective action was taken to decrease these radii. It was determined that a contributing factor to this problem was the possibility of overheating this area, which could lead to higher material flow stresses, as demonstrated in phase I. Therefore, additional thermocouples were installed in the corner radii areas for part FF-4, and pressure-time combination was increased slightly. A tendency to overheat in this area was observed, but the temperature was maintained below 1,750° F throughout the forming cycle. The forming in this corner area on part FF-4 actually exceeded that required, thereby demonstrating that the temperature control was the primary source of the problem in forming the corner radii. Subsequent pressures were increased up to 165 psi, with an attendant decrease in holding time to 2-3 hours. This cycle produced well-formed frame configurations. Figure 81 shows the first five frames formed, and Figure 82 shows parts 6 through 10. The leg ends of parts 6 through 10, illustrating the tight radii and well-formed beaded areas, are shown in Figure 83.

During the forming of frame FF-8-1, the hydraulic press malfunctioned, resulting in complete loss of argon gas pressure and, therefore, no metal deformation. The part was rerun, and the argon gas inlet tube cracked, resulting in only partial forming, as shown in Figure 84. To demonstrate the feasibility of completing a partially formed part, FF-8-1 was subjected to another forming cycle and reidentified as FF-11. FF-11, at the same temperature and pressure as previous parts, resulted in an acceptable frame, as shown in Figure 85. This forming cycle on a partially formed part demonstrated the capability to complete the forming after an interruption in the forming cycle.

Metallographic Evaluation

Eight of the forward frames were examined metallographically for degree of surface enrichment. The specimens were taken from part prolongations inside the seal line and adjacent to the trim edge of the part. In addition, specimens were obtained from the body of one of the frames, FF-4, which was completely sectioned for mechanical and metallurgical testing. The specimens were polished and etched with an oxalic-HF acid etchant to reveal surface enrichment and general microstructure. The depth of the enrichment was measured microscopically and is summarized in Table 29. The specimen locations appearing as a numerical digit in Table 29 are identified in Figure 86, which is a sketch showing the forward frame and its prolongation after forming and before trimming. Specimens with identical numbers were those cut from the same area.

133
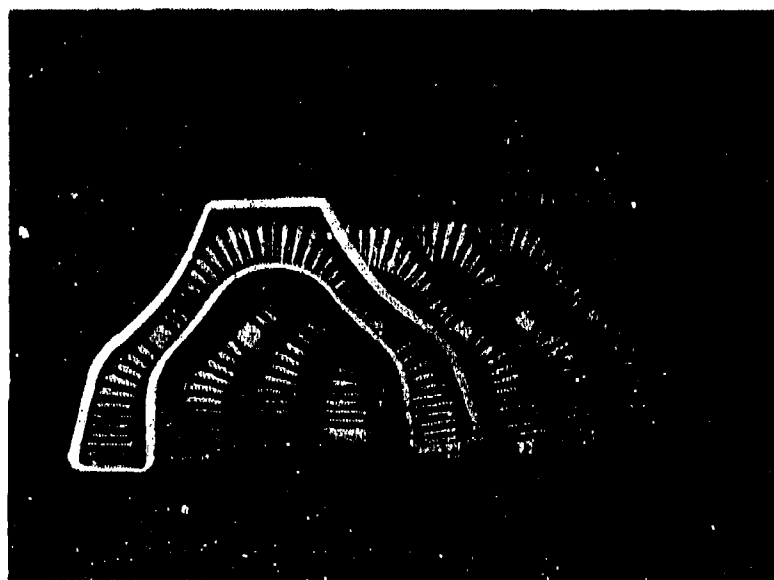
Figure 81. First five parts formed - nacelle forward center beam frame.
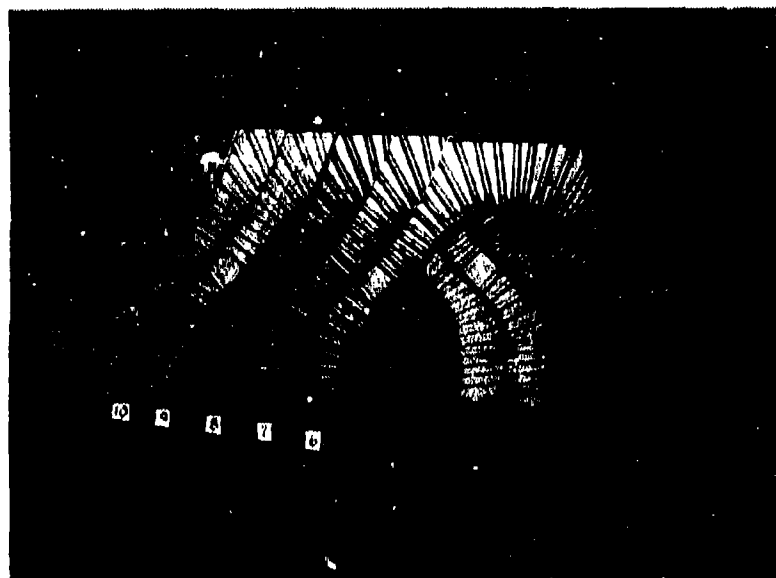
Figure 82. Nacelle forward center beam frame No. 6 through 10.

134

Figure 83. Forward frames No. 6 through 10 showing bead and radii definition.

135
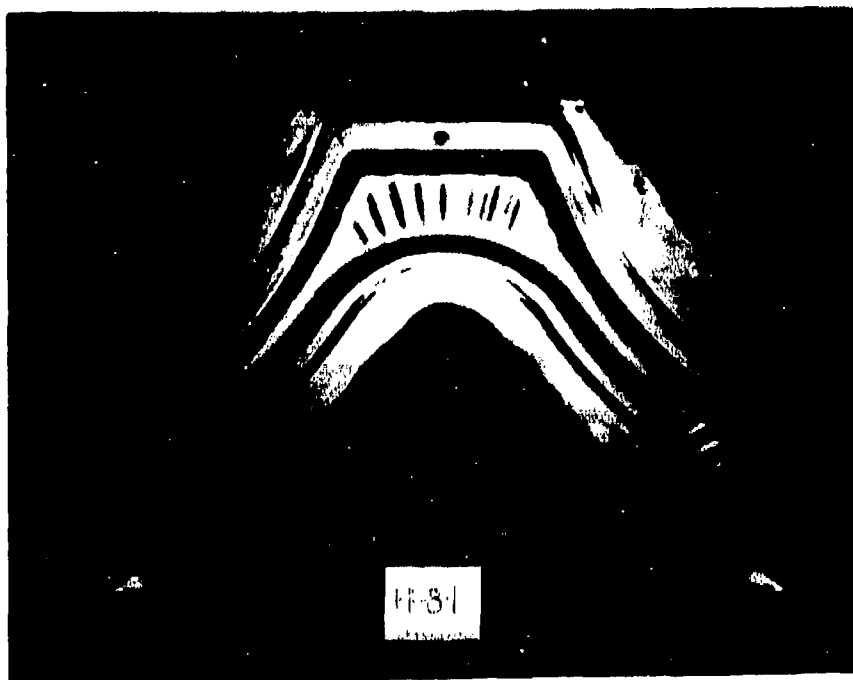
Figure 84. Partially formed forward frame No. FF-8-1.
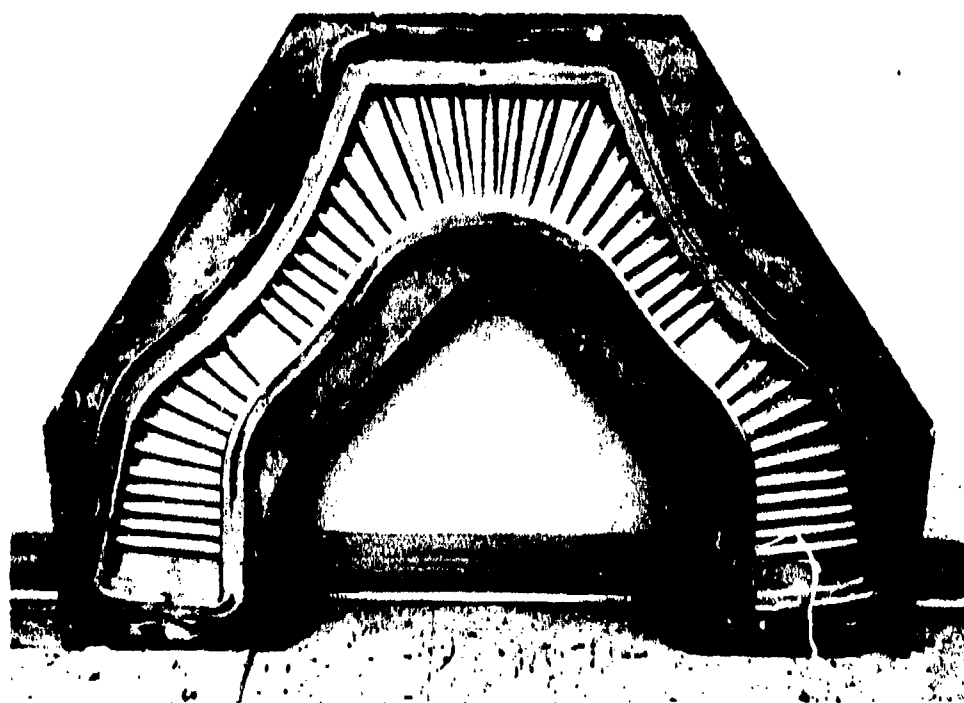
Figure 85. Fully formed forward frame No. FF-8-1 (reidentified as FF-11).

TABLE 29. NACELLE FORWARD CENTER BEAM FRAMES
SURFACE ENRICHMENT MEASUREMENTS

Sampling Area	Pack No.	Specimen Location (fig. 86)	Enrichment depth (in.)	
			Top surface	Bottom surface
Prolongation	FF-2	-1	Nil	0.007
		-2	↑	0.010
	FF-3	-1		0.007
		-2		0.010
	FF-4	-1		0.010
		-2		0.010
	FF-5	-1		0.010
		-2		0.007
		-3		0.005
		-4		0.010
		-5		0.010
		-6		0.006
		-7		0.007
	FF-6	-1		0.007
		-2		0.008
		-3		0.007
		-4		0.007
		-5		0.008
		-6		0.010
		-7		0.006
	FF-8	-1		0.010
		-2		0.007
	FF-9	-1		0.006
		-2		0.005
	FF-10	-1	↓	0.004
		-2	Nil	0.007
Body of frame	FF-4	-8	Nil	0.010
		-9	↑	0.008
		-10		0.008
		-11		0.007
		-12	↓	0.010
		-13	Nil	0.009

137
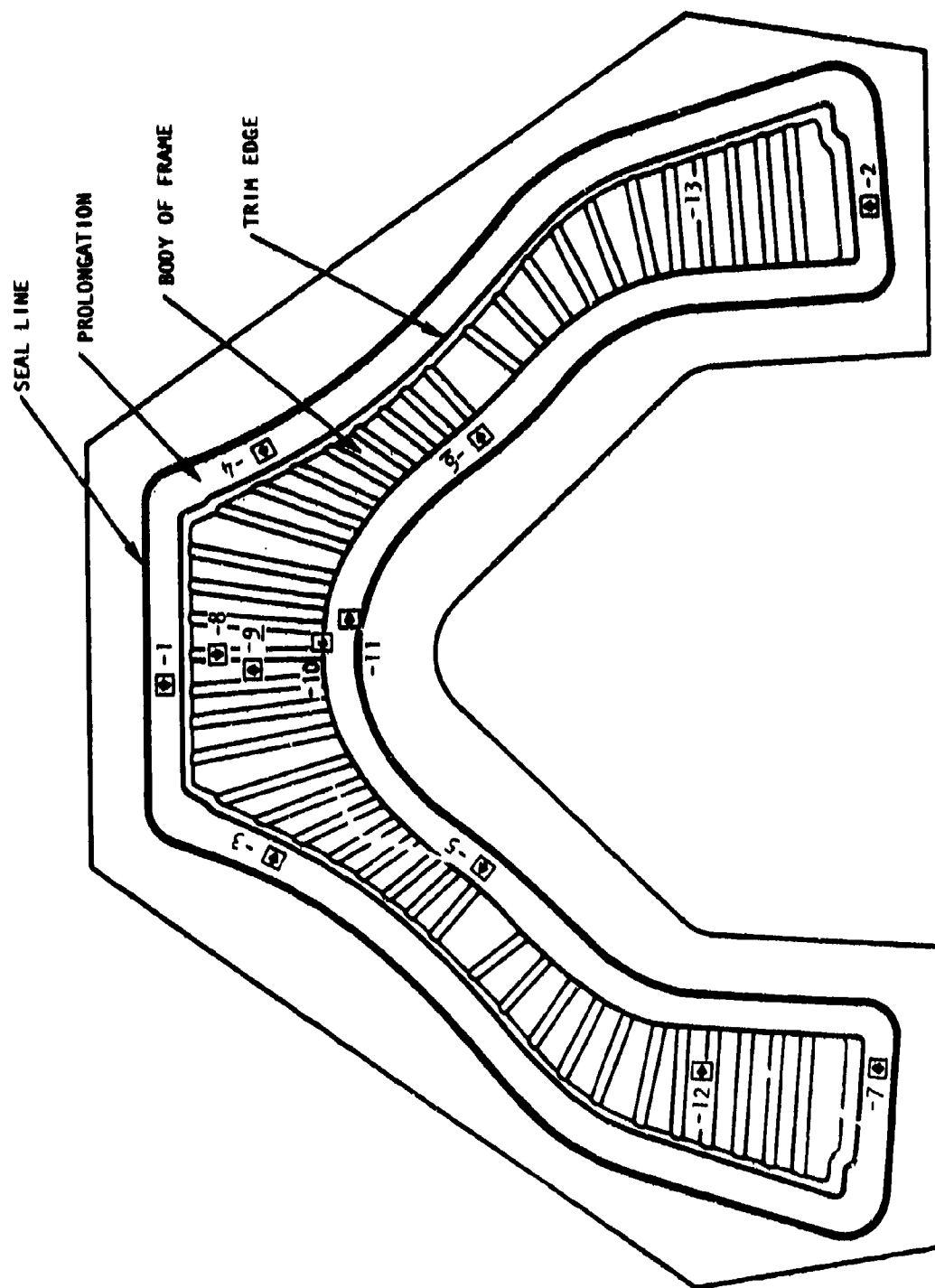
Figure 86. Locations of metallurgical specimens for surface enrichment measurements, nacelle forward center beam frames phase II.

As can be seen from Table 29, none of the top surfaces of any of the specimens showed evidence of enrichment, while all of the bottom surfaces showed varying degrees of enrichment, 0.004 to 0.010 inch in depth. Good correlation is observed between the trim area and part for FF-4, indicating that evaluation of such a prolongation will provide an adequate measure of production part surface condition. The level of enrichment observed can be readily removed by a chemical milling operation.

Figure 87 shows typical surface conditions of the specimens representing the part and prolongations. The enrichment, as can be seen from these photomicrographs, is the alpha stabilizing type, as evidenced by its light-etched equiaxed grains, and is most likely oxygen and/or nitrogen pickup. The source of the surface enrichment is considered most likely to be the stopoff compound used to facilitate part removal, although preliminary tests conducted with this material in phase I did not indicate enrichment. The reason enrichment was found in these parts and not in phase I parts is attributed to scale-up. The structural frames are considerably larger and were exposed to forming temperatures longer than the test parts of phase I. The stopoff compound is a mixture of collodial synthetic graphite and a volatile organic carrier. Since the graphite has been shown to be compatible with Ti-6Al-4V alloy, it is possible that the carrier in the mixture caused the enrichment.

CHEMICAL MILLING

Chemical milling was employed as a means to remove the surface enrichment and to prepare a complex contour for structural testing. The milling was performed in accordance with a Rockwell Process Specification which limits hydrogen pickup during milling to 50 parts per million (ppm) and the final cumulative hydrogen content of the part to 175 ppm.

Two frames, FF-2 and FF-3, were milled to a specified contour and thickness for the structural testing as shown in Figure 88, while six other frames, FF-5 through -10, were milled to remove 0.001 and 0.010 inch from the top and bottom surfaces, respectively. A selective area of milling, when required, was accomplished by masking the other areas with a spray-on compound. Coupons cut from the trim section of the parts were processed together, with the parts being chemical milled to determine the hydrogen pickup. Table 30 shows the results of interstitial content determinations for before and after the chemical milling. As can be seen from the table, the hydrogen pickup (27 ppm maximum) and the cumulative hydrogen content (66 ppm maximum) were well below the specification limits.
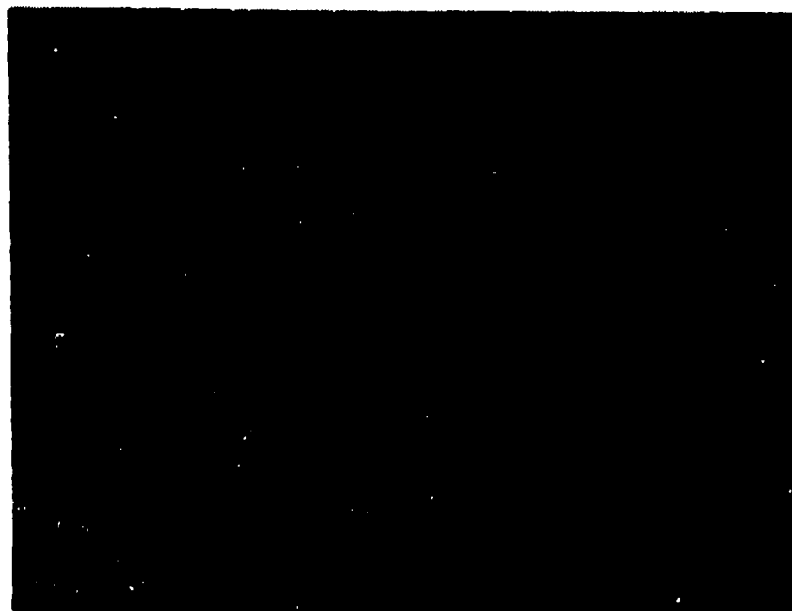
Top Surface   100X
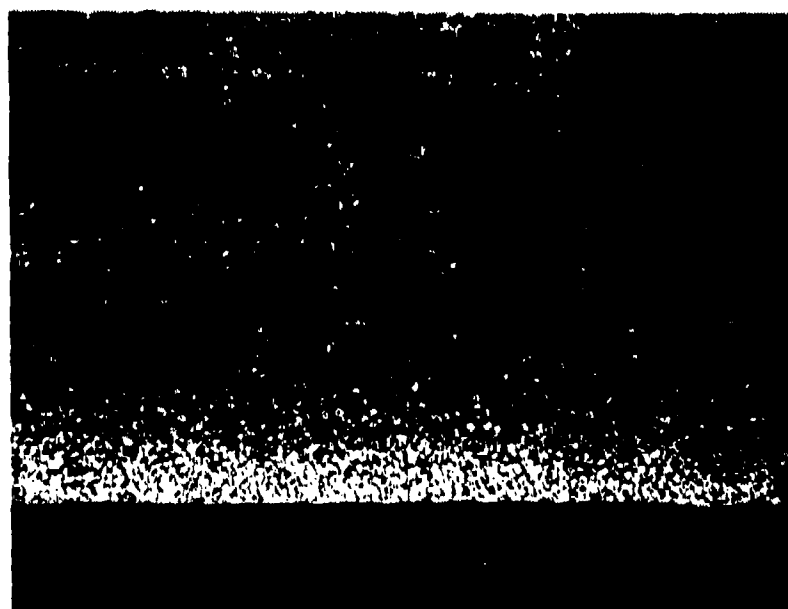
Bottom Surface   100X

Figure 87.   Surface conditions, typical of location 5, forward frame FF-6.
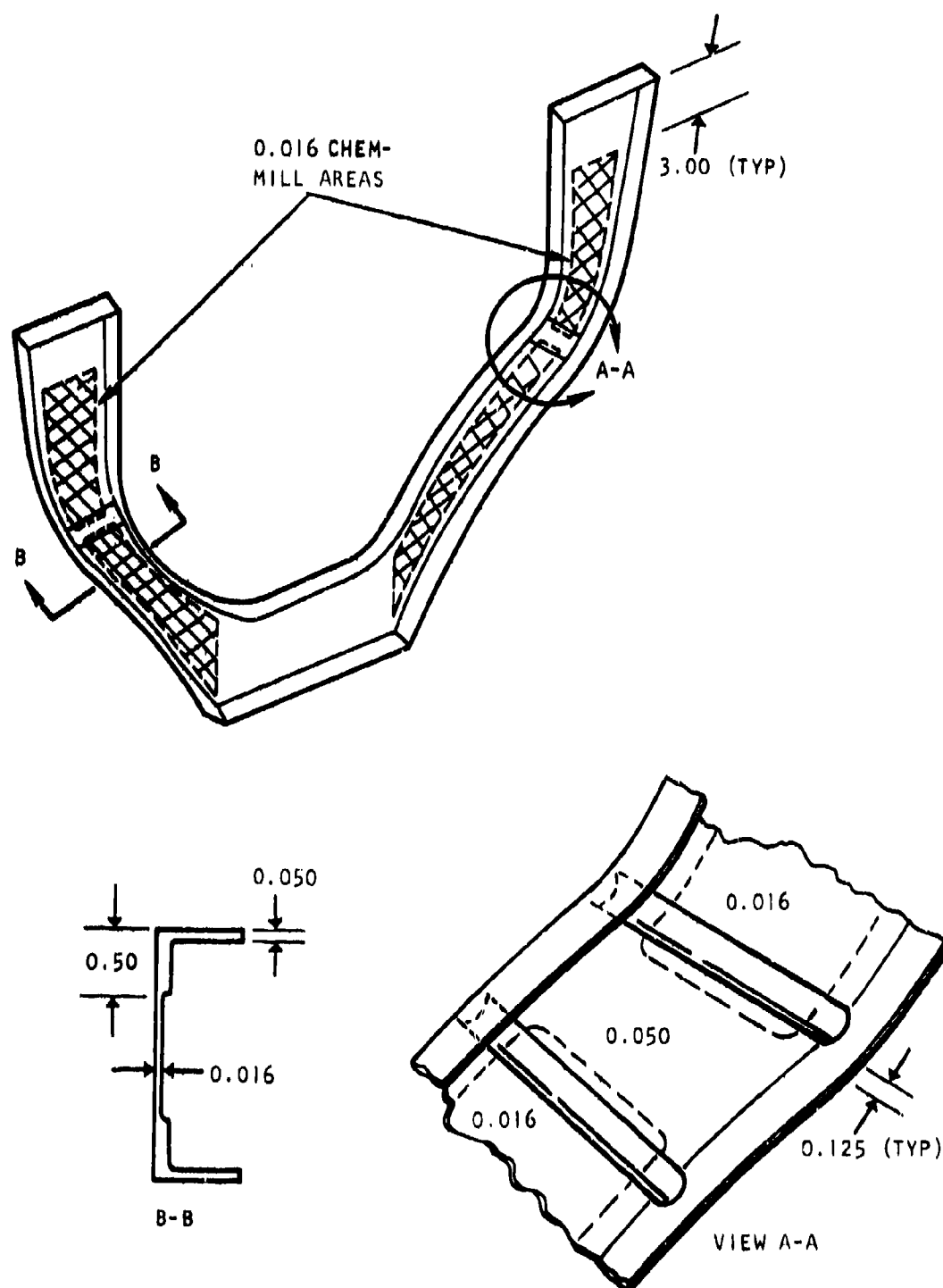
Figure 88. Chem-mill areas for frames structurally tested.

141

TABLE 30. HYDROGEN CONTENT BEFORE AND AFTER
CHEMICAL MILLING FORWARD FRAMES

Frame type	Frames chem-milled	H_2 contents (weight %)		
		Before CM	After CM	As received
Forward	FF-2* FF-3	0.0048	0.0063	0.0058
	FF-5* FF-6 FF-7 FF-8 FF-9 FF-10	0.0039	0.0066	0.0047

*H_2 levels were determined on a prolongation test coupon which accompanied the parts through the chemical milling process.

NACELLE AFT CENTER BEAM FRAME FORMING RESULTS

A total of 10 aft frames were superplastically formed during phase II. Table 31 shows the forming runs, the parameters used, and the results. Nine titanium sheet metal aft frames were successfully formed to provide the six required for the AFML. Bend radii, joggles, and flange configuration were well defined on all parts, attesting to the repeatability of the SPF procedure. All parts were formed at 1,700° (±50°) F and varying argon pressures and times at pressure. As with the forward frames, no difficulty was experienced in maintaining proper temperature or pressure during forming, with the exception of AF-3 where loss of seal occurred due to hydraulic press problems.

One aft frame, as formed and prior to trimming to final size, is shown in Figure 89. As can be seen, extensive forming of the titanium diaphragm into die cavities was necessary, with the tooling used, to obtain the final part. After trimming to the final configuration, the formed channels became prolongation material for subsequent testing. Aft frames 5 through 10 are shown in Figure 90.

142

TABLE 31. AFT FRAME PARAMETERS

Part No.	Temperature (F) (during form cycle)	Argon gas pressure						Time at press. (hrs)	Remarks
		Prior to form		During form		After form			
		a	b	a	b	a	b		
AF-1	1,635-1,765	4	4	45	0.2	4	0	2	Acceptable part.
AF-2	1,620-1,720	0.2	0.2	45	0.5	0.5	0.5	2.5	Not completely formed but acceptable for testing.
AF-3	1,650-1,735	3	2.5	30	2.5	-	-	-	Loss of seal - run aborted 40% formed.
AF-3 Rerun	1,620-1,740	3	2.5	100	1	0.5	0.5	0.5	New Ti sheet - acceptable part.
AF-4	1,645-1,750	2	0.5	100	0.5	0.5	0.5	1.5	Acceptable part.
AF-5	1,660-1,750	1	0.5	100-140	0.5	0.5	0.5	0.5	Acceptable part.
AF-6	1,600-1,750	2	1	125	0.5	1	1	10 min	Acceptable part.
AF-7	1,640-1,750	0.5	0.5	110	0.5	0.5	0.5	15 min	Acceptable part.
AF-8	1,650-1,750	3	3	120	1	1	1	6 min	Acceptable part.
AF-9	1,650-1,745	3	2	110	1	1	1	15 min	Acceptable part.
AF-10	1,660-1,750	3	4	110	1	3	3	15 min	Acceptable part.

[a]Top surface

[b]Bottom surface
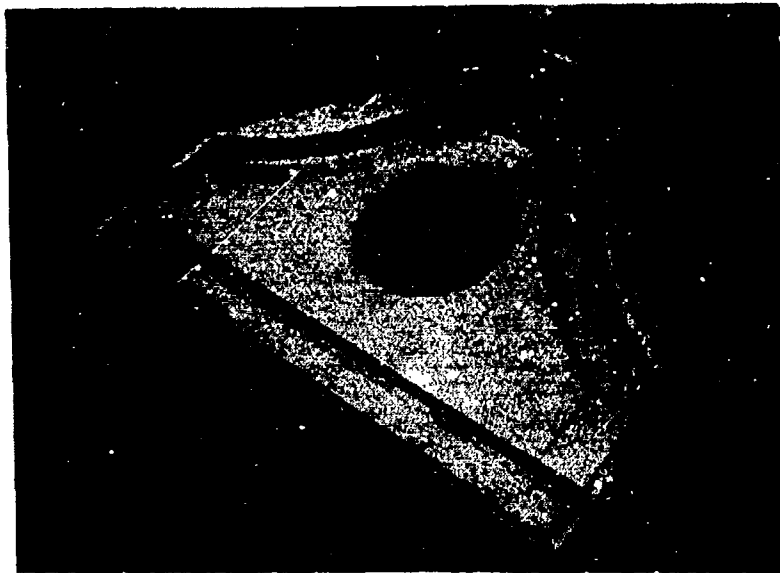
Figure 89. Nacelle aft frame - formed and prior to trim.
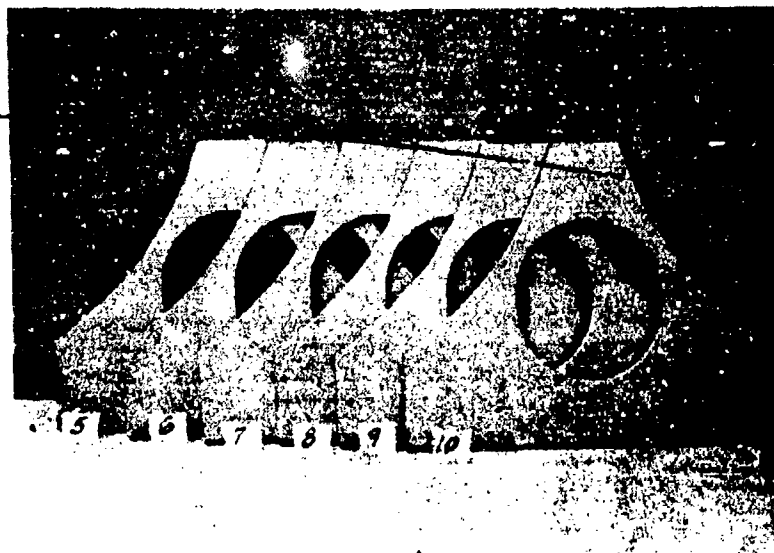
Figure 90. Nacelle aft frames No. 5 through 10.

SURFACE ENRICHMENT

All of the aft frames produced were sectioned in the prolongation area for surface enrichment measurements. In addition, two of the parts (AF-1 and AF-2) were examined within the frame bodies, which were also sectioned for mechanical testing. Table 32 shows surface enrichment depths measured on the specimens taken from prolongations and frame bodies. The specimen locations are identified in Figure 91. As can be seen from the table, the top surfaces were free from enrichment, while the bottom surfaces showed enrichment ranging from 0.004 to 0.008 inch, which is somewhat less than those found on the forward frames. A generally shorter forming cycle for the aft frames is believed to be the cause of the slightly shallower enrichment depth on these parts. The enrichment is also of the interstitial type, as described previously for the forward frames.

In Figure 92 are photomicrographs showing the conditions of microstructure typical of the specimens taken from various locations of the parts. The grain sizes and microstructures appear normal for superplastic formed Ti-6Al-4V sheet material.

CHEMICAL MILLING

Eight of the aft frames, AF-3 through AF-10, were chem-milled to remove the surface enrichment. The milling depths were 0.001 and 0.008 inch from top and bottom surfaces, respectively. The source and procedures used to chem-mill these frames were the same as those for the forward frames described earlier. AF-3 and AF-4 were chem-milled as a separate batch ahead of the others in order to meet the schedule for structural testing which utilized the two frames. The remaining six frames were chem-milled in a single batch and were inspected for variation in thickness reduction in different sections of the parts.

Table 33 shows the results of interstitial determination before and after the chem-milling. Again, the hydrogen pickup (27 ppm max) and the cumulative hydrogen contents (78 ppm max) were well below the limits specified. Table 34 summarizes the thickness reductions in chem-milling and at various sections of the six frames, AF-5 through AF-10. It is seen from the table that the variation in thickness reduction between parts was 0.002, 0.006, and 0.003 inch for web, radius, and flange sections, respectively. The larger variation in the radius is believed to be due to difficulty in obtaining thickness measurement in this area.

TABLE 32. NACELLE AFT CENTER BEAM FRAMES
SURFACE ENRICHMENT MEASUREMENTS

Sampling area	Pack No.	Specimen location	Enrichment depth (in.)	
			Top surface	Bottom surface
Prolongation	AF-1	-1	Nil	0.006
		-2		0.004
	AF-2	-1		0.005
		-2		0.003
	AF-3	-1		0.008
		-2		0.004
	AF-4	-1		0.008
		-2		0.005
	AF-5	-8		0.006
		-9		0.007
		-10		0.007
	AF-6	-8		0.008
		-9		0.006
		-10		0.005
	AF-7	-1		0.005
		-2		0.004
	AF-8	-1		0.005
		-2		0.005
	AF-9	-1		0.006
		-2		0.007
	AF-10	-1		0.006
		-2	Nil	0.004
Body of frame	AF-1	-3	Nil	0.008
		-4		0.006
		-5		0.008
		-6		0.008
	AF-2	-7	Nil	0.007
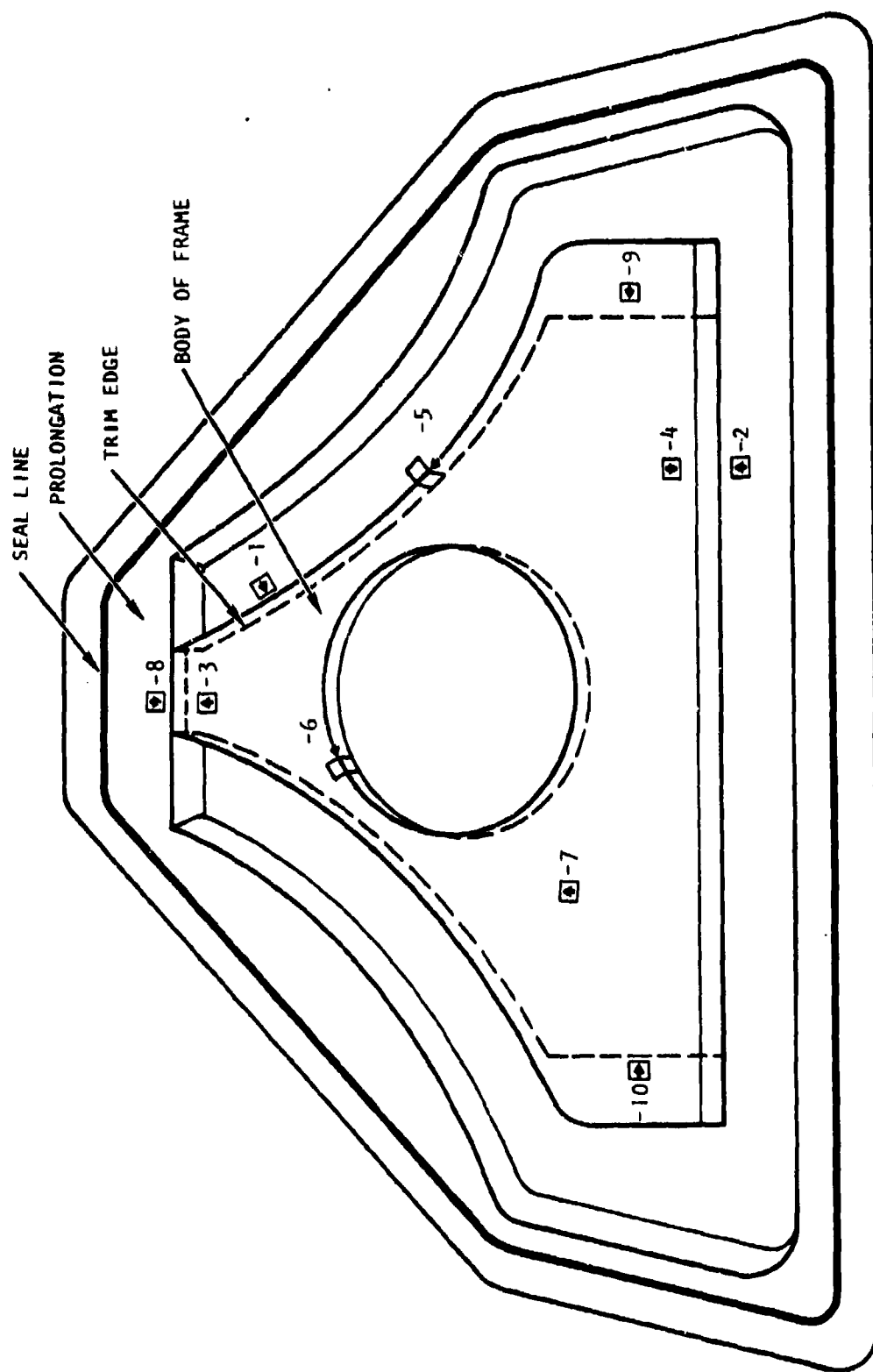
Figure 91. Location of metallurgical specimens for surface enrichment measurements, nacelle aft center beam frames (top view).

SEAL LINE
PROLONGATION
TRIM EDGE
BODY OF FRAME

-9
-5
-4
-2
-7
-7
-8
-3
-6
-7
-10

147
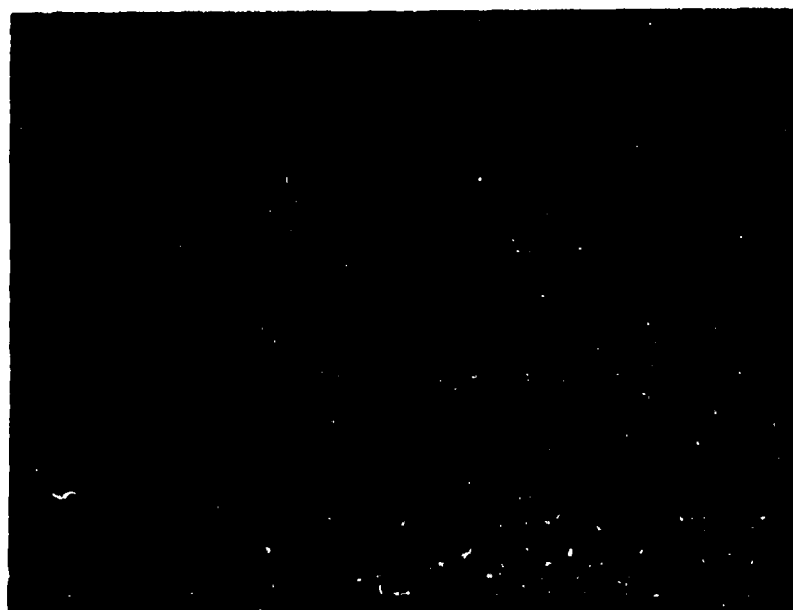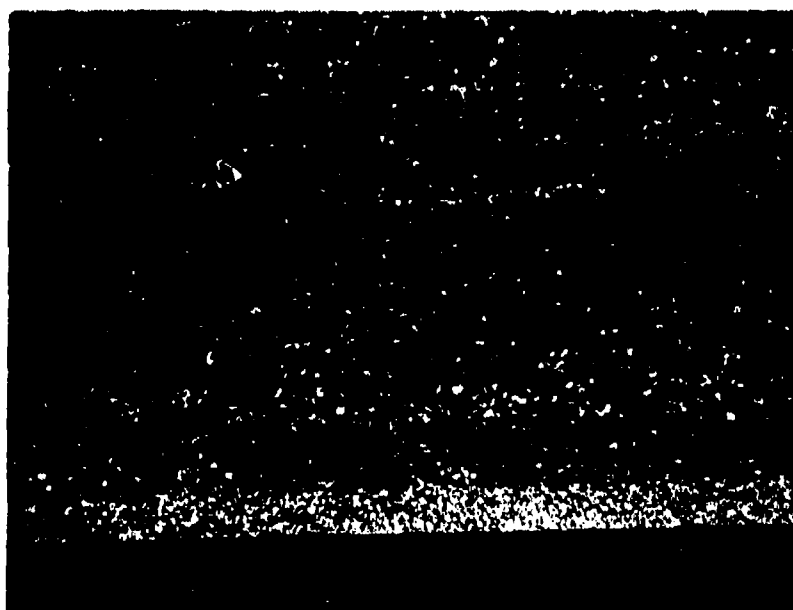
Top Surface   100X

Bottom Surface   100X

Figure 92. Surface conditions, typical of location 9, aft frame (AF-6).

TABLE 33. HYDROGEN CONTENT BEFORE AND AFTER
CHEMICAL MILLING AFT FRAMES

Frame type	Frames chem-milled	H_2 content (weight %)		
		Before CM	After CM	As received
Aft	AF-3 AF-4	0.0067	0.0052	0.0065
	AF-5 AF-6 AF-7 AF-8 AF-9 AF-10	0.0051	0.0078	0.0065

TABLE 34. SUMMARY OF CHEM-MILLING THICKNESS REDUCTION
FOR SIX NACELLE AFT FRAMES

Section	Part Areas*	AF-5	AF-6	AF-7	AF-8	AF-9	AF-10	Avg
Web	G1 Q Z W	0.009	0.008	0.008	0.006	0.007	0.009	0.0078
Radius	A A1 C1 I1 N	0.014	0.010	0.010	0.014	0.012	0.016	0.0126
Flange	B B1 D1 J1 O	0.010	0.012	0.012	0.012	0.012	0.013	0.0118

*Thickness reductions apply to similar thickness part areas
shown in Table 36.

DIMENSIONAL INSPECTION

NACELLE FORWARD CENTER BEAM FRAME

Thickness measurements were made through seven sections of the 10 forward frames as shown in Figure 93. Measurements were taken in the flange and web areas to establish thickness profiles for comparison to analytical predictions. The analytical predictions were based on the thinning mechanism illustrated in Figure 54, and as discussed previously. The analysis conducted for the various sections of the forward frames considered the actual width and depth dimensions of the die cavity at the respective sections and the starting gage of the Ti-6A1-4V sheet used.

Comparisons of the experimental and analytical thicknesses through three sections are presented as examples for the part bottom and flanges in Figures 94 and 95. The measured thickness profiles generally show good agreement with the predicted values. It is observed, however, that the bottom center thicknesses are consistently less than predicted for the wider sections as can be observed in Figure 94. The reason for this may be that some continued stretching occurs at this area even after the die is contacted, indicating that the die friction is being partially overcome. This effect diminishes as the section width decreases, in which case good agreement is observed. The greatest variance between predicted and observed values was sections F-F and G-G, near the end of the frame legs. That the observed thicknesses in these locations are less than predicted is understandable since the titanium diaphragm is being stretched into the part end as well as into the side flanges and is, therefore, a condition which conflicts with the assumption of a semi-infinite length to the rectangular section. Sections F-F and G-G of parts FF-1 through FF-3 were incompletely formed in the corner radii, thereby producing somewhat thicker sections in those areas than for the more fully formed subsequent parts. The flange thickness profiles are also reasonably well predicted as shown in the example in Figure 95.

Although some variations were observed, the results of the thickness measurements indicate that the analytical approach to predicting thinning is a valuable tool which can be used to determine the starting gage of sheet necessary to produce designated part thicknesses. For the forward frames fabricated, this approach was demonstrated to be suitable for selecting the starting sheet gage.

The overall dimensions of the forward frames were evaluated using a dimensional inspection test fixture, as shown in Figure 96, which permitted 16 points on the frames to be checked. The results of these tests revealed progressive dimensional changes from part to part which were generally consistent in direction and magnitude. These changes are summarized in Figure 97 where the average changes per part are illustrated.

150
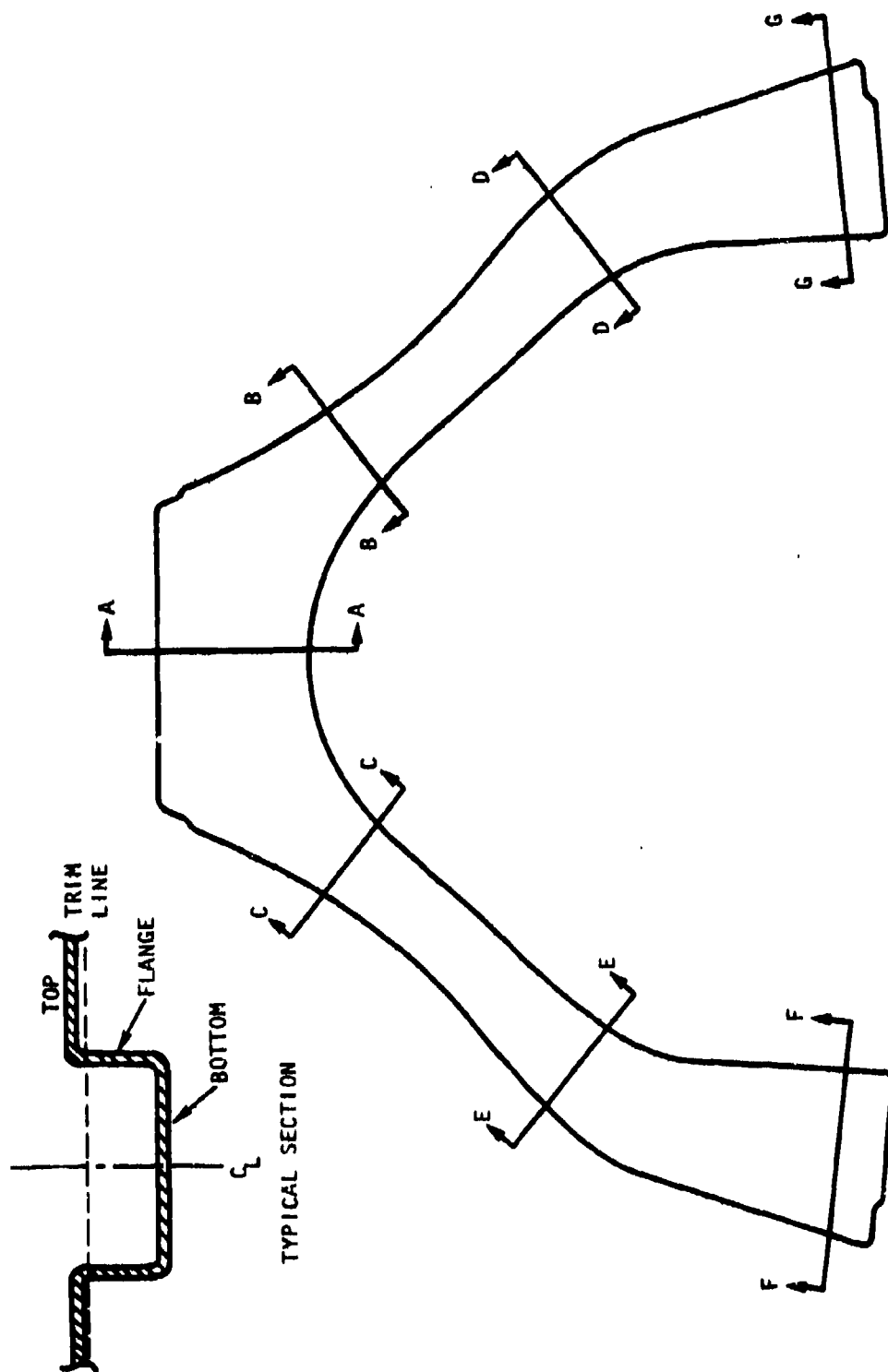
Figure 93. Forward frame section locations (where thickness profiles were determined).

151
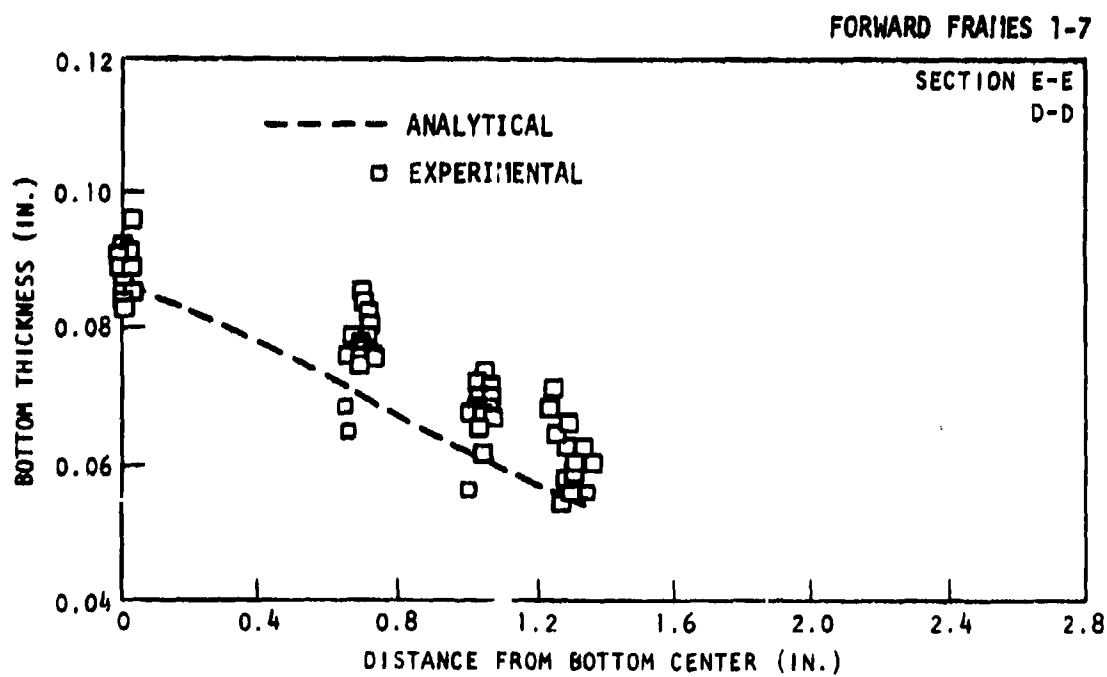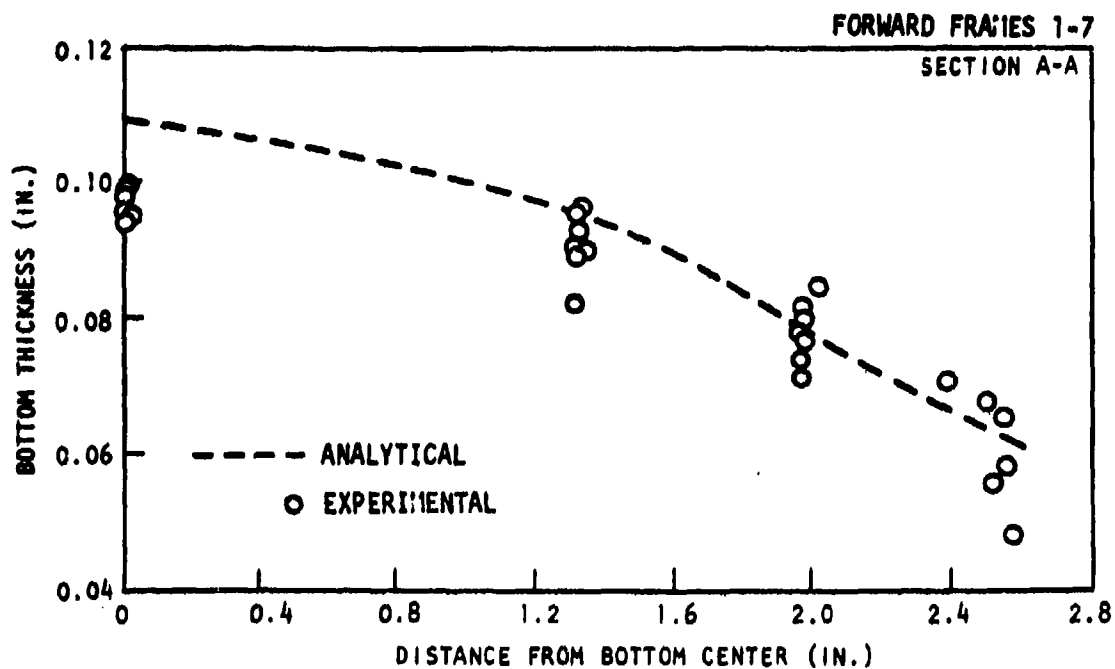
Figure 94.   Thickness profiles for bottom (web) areas of forward frames.
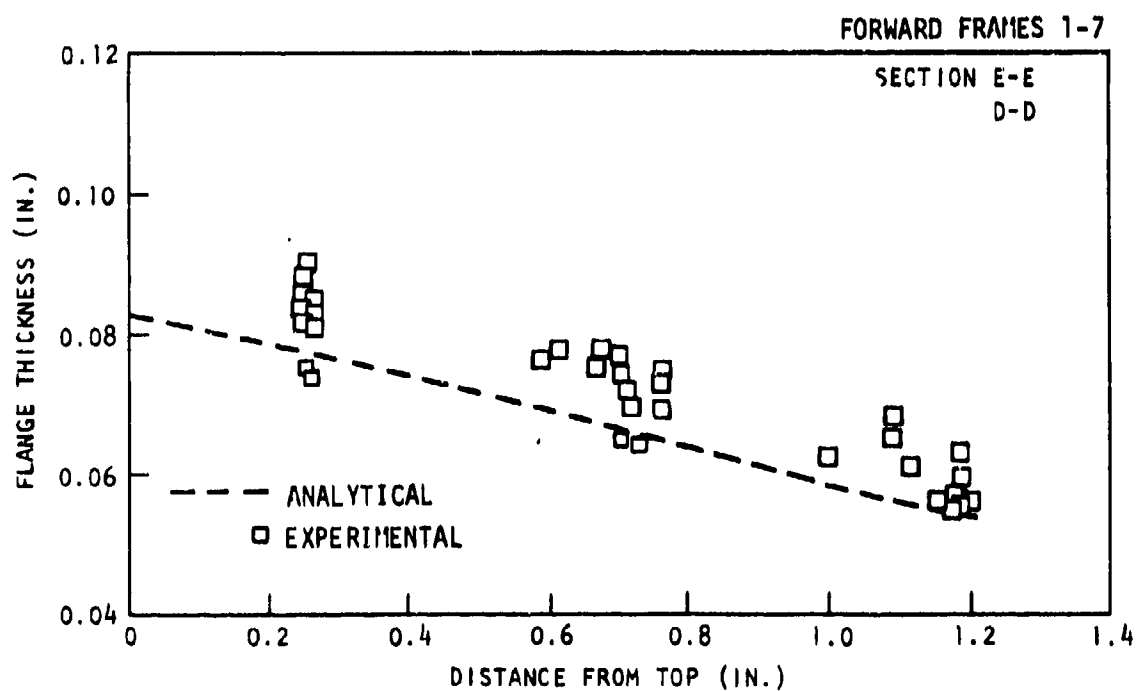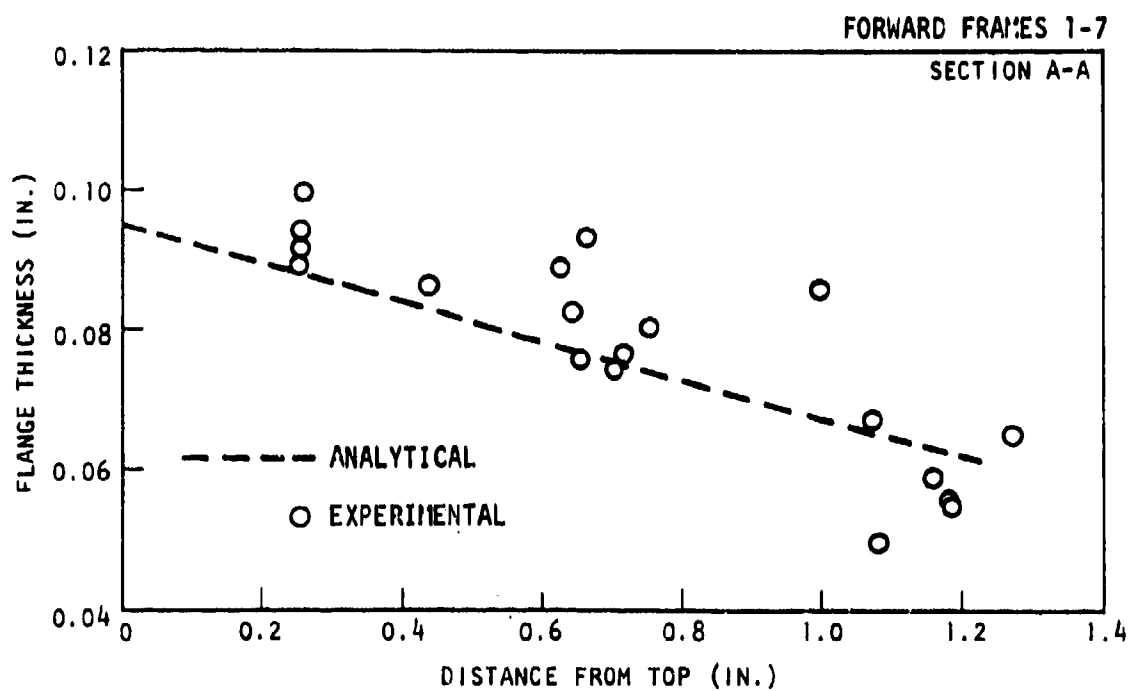
Figure 95. Thickness profiles for side flange of forward frames.

153

Figure 96. Forward frame dimensional inspection fixture.
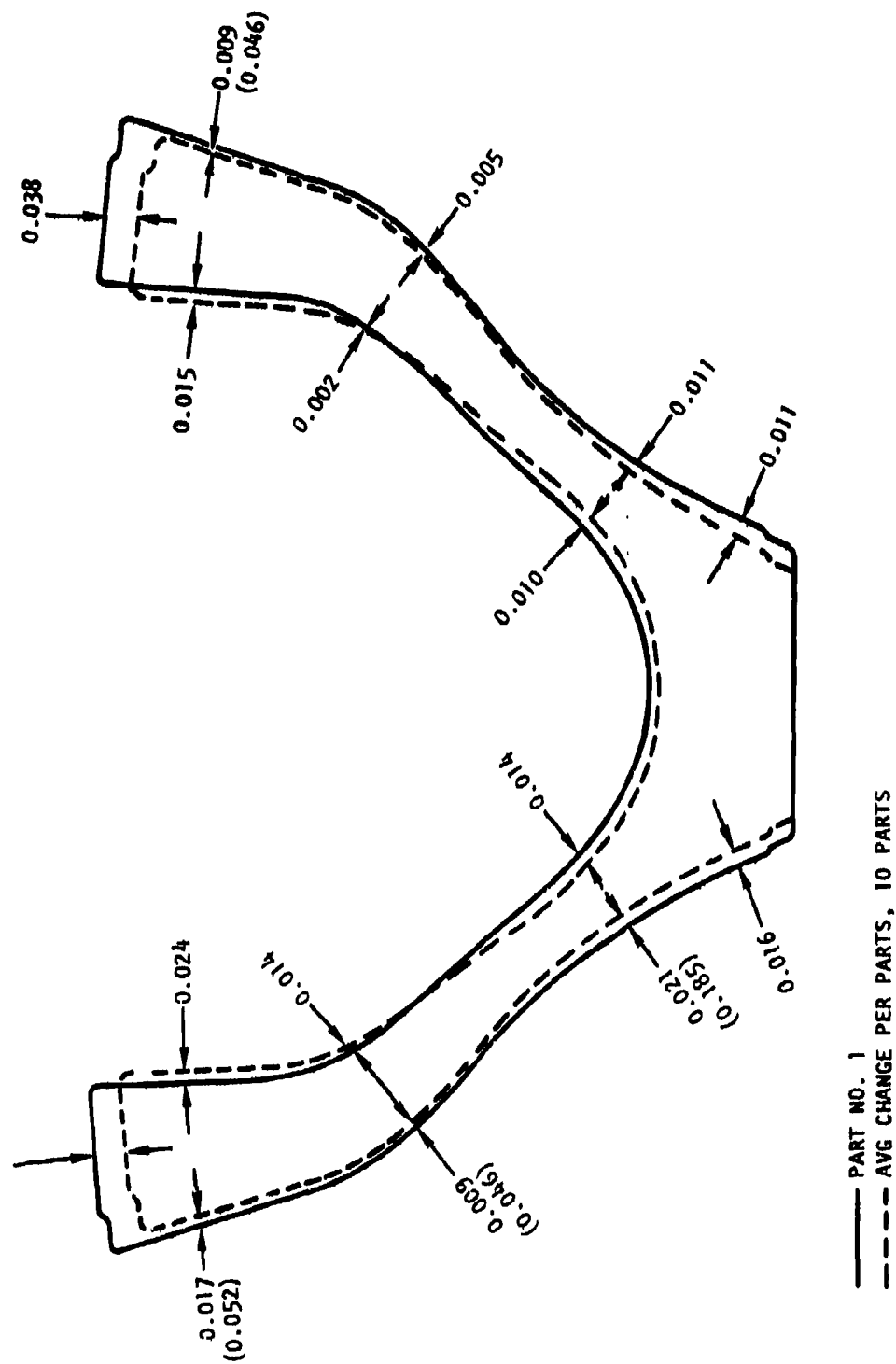
Figure 97. Dimensional changes observed in 10 forward frames (sketch exaggerated to show changes observed).

——— PART NO. 1
– – – AVG CHANGE PER PARTS, 10 PARTS

155

These changes were considered to be a result of corresponding dimensional changes in the tooling. The corresponding die sections were, therefore, measured to evaluate the amount of change between part No. 10 and 11. Punch marks were placed in the die to assure that the same areas were measured before and after the forming run. The points where measurement punch marks were made are shown in Figure 98. The results are summarized in Table 35 where corresponding average changes in parts 1 to 10 are also presented for comparison. The changes observed in the die dimensions during forming of part No. 11 follow the trend observed for the first 10 parts produced.

The cause of dimensional changes occurring in the die is believed to be primarily due to thermal gradients which develop during heatup and cool-down of the die assembly. Thermal data indicated that the periphery of the die assembly heats more rapidly than the interior which could cause compressive deformation in the hotter external edges of the tooling due to the differential expansion. A reverse thermal gradient on cool-down could further deform the tooling in the same direction since the cooler external edges could cause compression deformation in the hotter internal areas. Such dimensional changes in the tooling are consistent with the dimensional changes observed in the parts and tooling. Since such dimensional changes would not be tolerable in production parts, it is probable that large plan area superplastic formed parts will require higher hot strength alloys which will not deform under such thermal gradients. The use of a higher temperature alloy for a die was considered in the subsequent economic analysis and shows that it will not substantially affect cost savings for large quantities of parts typically required for volume production.

NACELLE AFT CENTER BEAM FRAME

Frame No. AF-3 through AF-10 were first dimensionally inspected to determine thickness profiles in web, radius, and flange areas. Figure 99 shows locations where the measurements were made. Results of the measurements for the seven frames were grouped into five areas where parts assumed identical superplastic thinning and are shown in Table 36. In general, the variation in the resultant thickness among frames in the same areas was ±0.0035 inch which was considerably less than those for the forward frames (generally ±0.009 inch). The simpler parts configuration of the aft frames that gave easy access to a more repeatable location for inspection is believed to be the cause for the improved thickness consistency.

To compare thickness profiles between the experimental results and the analytical predictions, four cases representing different cavity dimensions and degree of plane strain thinning were evaluated. Figure 100 shows locations of these cavities and corresponding dimensions. The analytically predicted thickness profiles for these locations and the actual thicknesses measured are compared in Figures 101 and 102. Using the sheet gage of 0.084 inch as a starting thickness, the analytical predictions were consistently lower than those

156
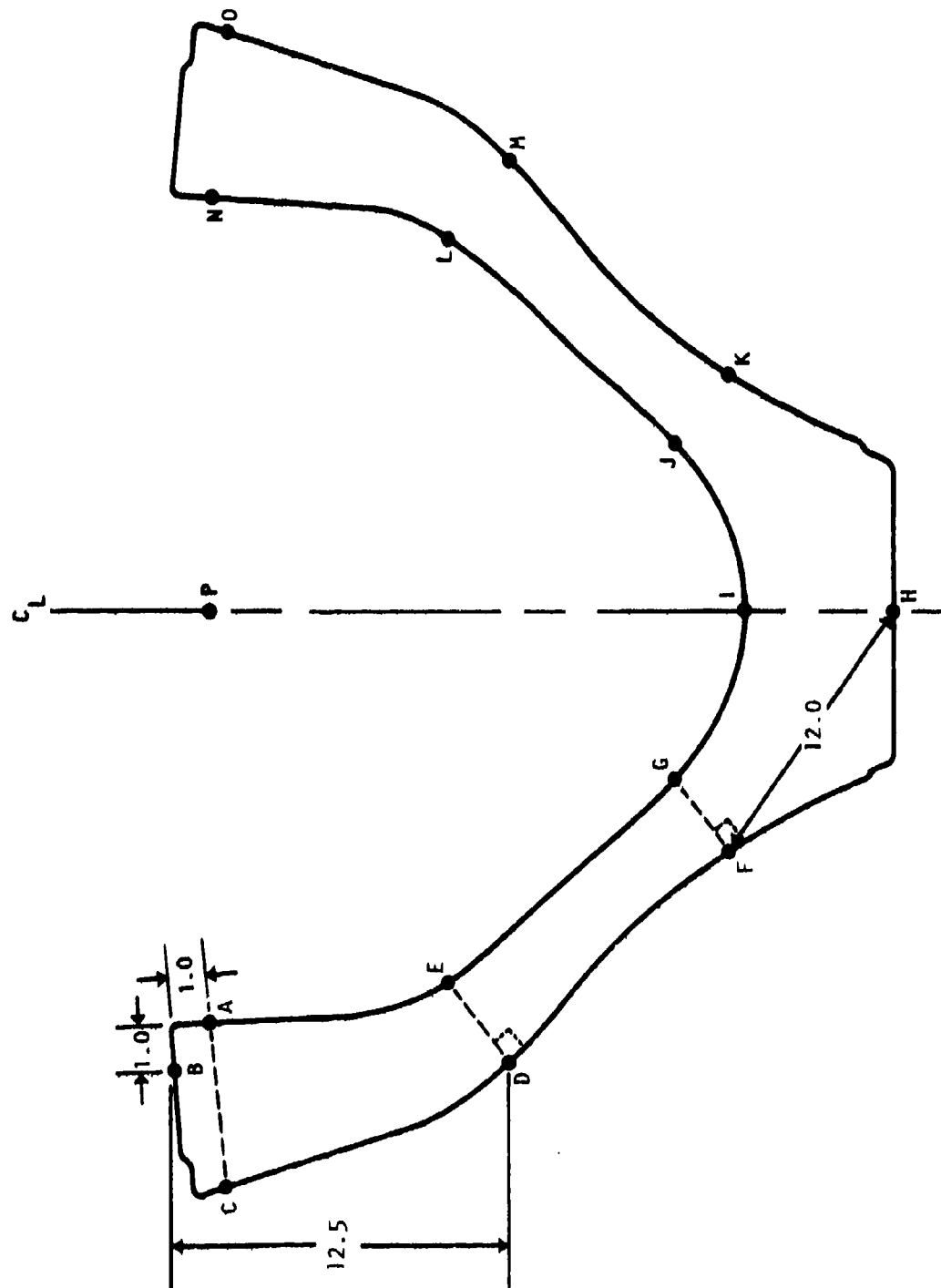
Figure 98. Die point locations where dimensional measurements where made.

157

TABLE 35. DIMENSIONAL CHANGES OF THE FORWARD FRAMES AND DIE

	Die location										
	A-N	C-O	D-E	F-G	J-K	L-M	N-O	C-A	E-L	D-M	F-K
Die change, parts FF-10 - FF-11	-0.050	-0.023	+0.004	-0.028	+0.010	+0.064	-0.004	-0.001	-0.046	-0.303	-0.001
Average part change	-0.039	-0.026	+0.005	-0.022	-0.020	+.006	+0.006	+0.006	-0.015	0.013	-0.032

Bottom view

Locations which have 2 letters: 1st letter
is measurement in radius, while 2nd letter
is for measurement at upper edge of flange

Figure 99. Inspection locations where thickness measurements
were made, aft frames.

159

TABLE 36. THICKNESS PROFILE ON NACELLE AFT FRAMES

Area	Location	Frame No.							
		3	4	5	6	7	8	9	10
Web	W	0.081	0.084	0.082	0.081	0.084	0.078	0.078	0.083
	Z	0.083	0.083	0.081	0.074	0.080	0.079	0.078	0.080
	G1	0.083	0.083	0.081	0.079	0.080	0.079	0.077	0.080
	K	0.085	0.081	0.080	0.083	0.079	0.077	0.076	0.079
	L	0.085	0.085	0.082	0.083	0.081	0.080	0.077	0.080
	M	0.082	0.083	0.079	0.083	0.081	0.079	0.076	0.079
	P	0.081	0.084	0.079	0.081	0.079	0.076	0.075	0.076
	Q	0.083	0.084	0.080	0.082	0.074	0.079	0.076	0.078
	R	0.082	0.083	0.079	0.082	0.080	0.076	0.073	0.079
	U	0.081	0.082	0.081	0.079	0.080	0.075	0.075	0.085
	V	0.083	0.083	0.082	0.081	0.079	0.077	0.077	0.083
	H1	0.082	0.082	0.082	0.080	0.076	0.076	0.077	0.080
	av	0.0826	0.0831	0.0807	0.0807	0.0794	0.0776	0.0763	0.0801
Radius 1	A	0.070	0.069	0.073	0.061	0.065	0.068	0.066	0.075
	C	0.072	0.069	0.072	0.059	0.073	0.069	0.066	0.073
	E	0.071	0.068	0.073	0.065	0.069	0.069	0.065	0.075
	G	0.072	0.068	0.069	0.074	0.072	0.069	0.068	0.072
	I	0.074	0.070	0.068	0.068	0.072	0.063	0.064	0.071
	N	0.075	0.074	0.072	0.065	0.076	0.075	0.071	0.076
	K1	0.069	0.071	0.072	0.071	0.072	0.068	0.064	0.071
	I1	0.069	0.089	0.071	0.072	0.068	0.067	0.063	0.070
	S	0.071	0.086	0.075	0.076	0.073	0.067	0.069	0.075
	av	0.0714	0.0738	0.0717	0.0679	0.0711	0.0683	0.0662	0.0731
Flange 1	B	0.050	0.053	0.051	0.052	0.056	0.054	0.054	0.056
	D	0.053	0.056	0.061	0.061	0.055	0.056	0.058	0.060
	F	0.053	0.055	0.053	0.052	0.058	0.056	0.059	0.059
	H	0.054	0.054	0.052	0.051	0.057	0.057	0.057	0.059
	J	0.053	0.055	0.048	0.046	0.054	0.051	0.053	0.054
	O	0.050	0.052	0.047	0.051	0.055	0.054	0.053	0.056
	L1	0.053	0.052	0.042	0.046	0.053	0.048	0.053	0.047
	J1	0.044	0.044	0.042	0.044	0.050	0.051	0.050	0.046
	T	0.048	0.052	0.049	0.048	0.054	0.052	0.052	0.053
	av	0.0509	0.0514	0.0483	0.0490	0.0547	0.0532	0.0543	0.0544
Radius 2	X	0.079	0.077	0.075	0.077	0.076	0.075	0.074	0.072
	C1	0.072	0.072	0.075	0.072	0.073	0.076	0.074	0.075
	E1	0.072	0.073	0.076	0.075	0.053	0.077	0.073	0.075
	A1	0.078	0.070	0.076	0.072	0.075	0.076	0.074	0.075
	av	0.0753	0.0730	0.0755	0.0740	0.0693	0.0760	0.0738	0.0743
Flange 2	Y	0.071	0.064	0.065	0.078	0.069	0.068	0.066	0.060
	D1	0.068	0.062	0.072	0.073	0.063	0.066	0.067	0.064
	F1	0.067	0.065	0.064	0.065	0.067	0.066	0.068	0.062
	B1	0.068	0.066	0.067	0.069	0.066	0.068	0.067	0.068
	av	0.0685	0.0643	0.0670	0.0713	0.0663	0.0670	0.0670	0.0635

160
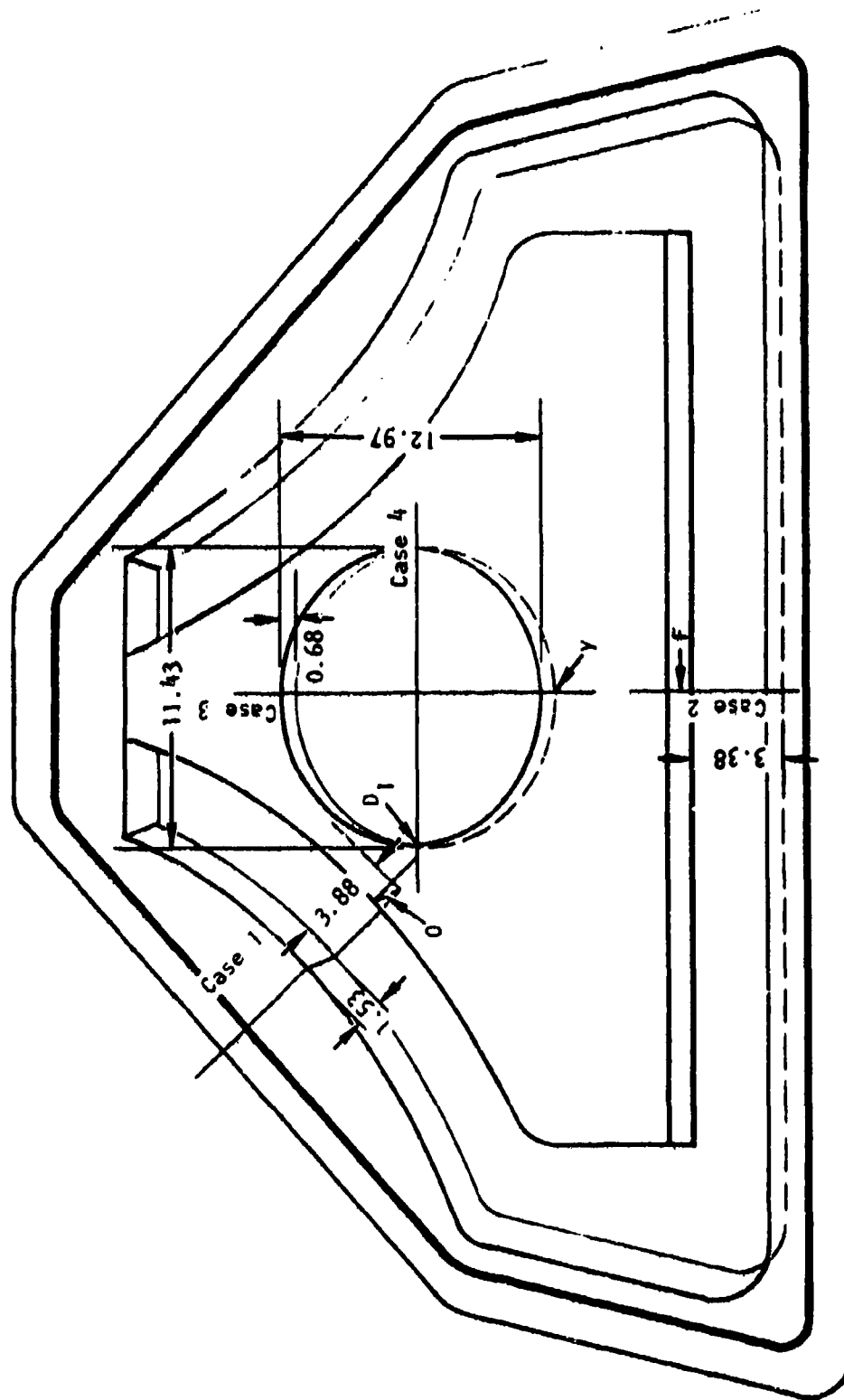
Figure 100. Location of cavities where thickness profiles were analytically predicted, aft frames.
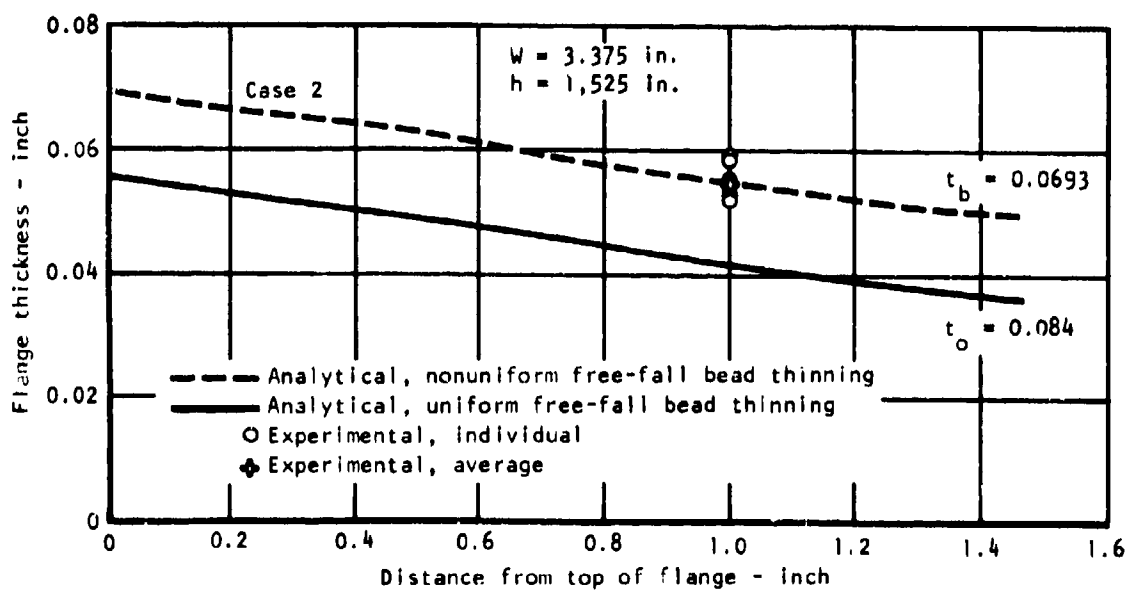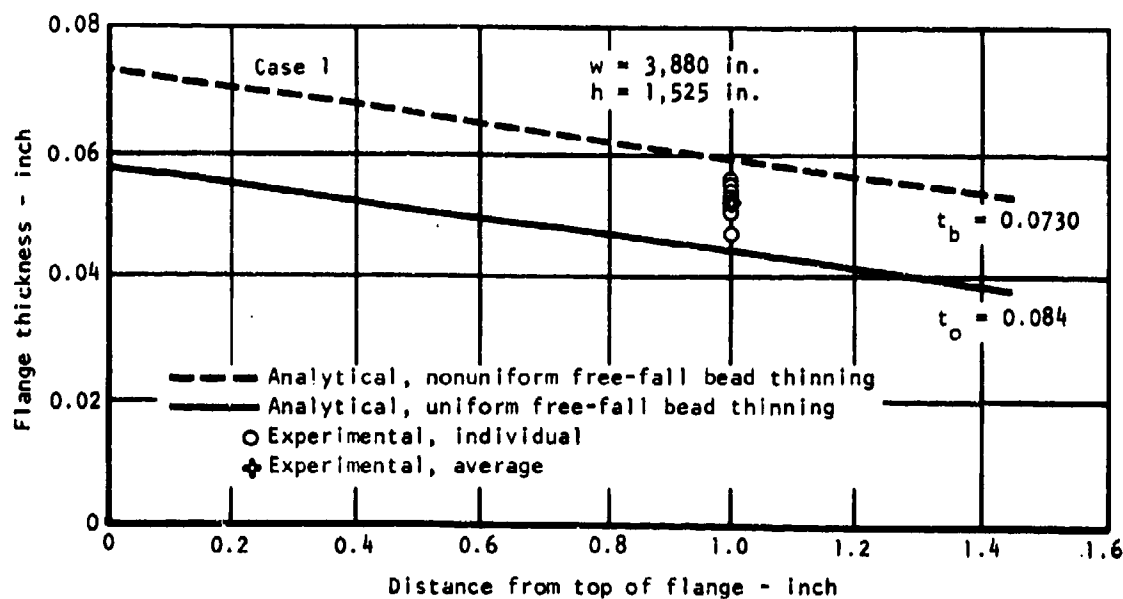
Figure 101. Thickness profiles, comparison of analytical prediction and experimental data, aft frames.
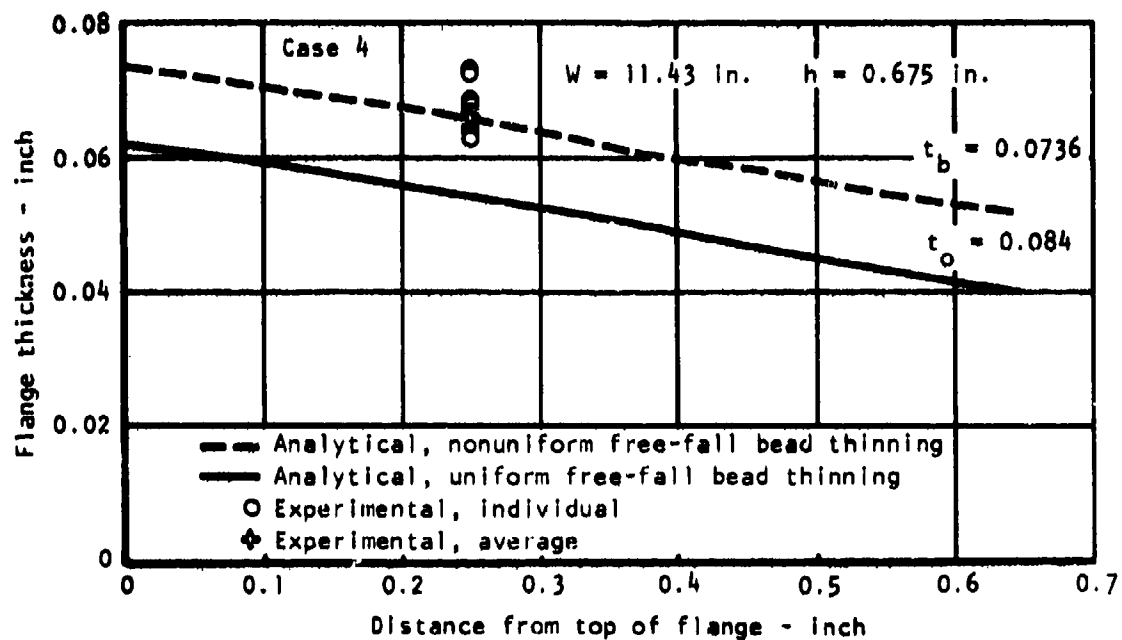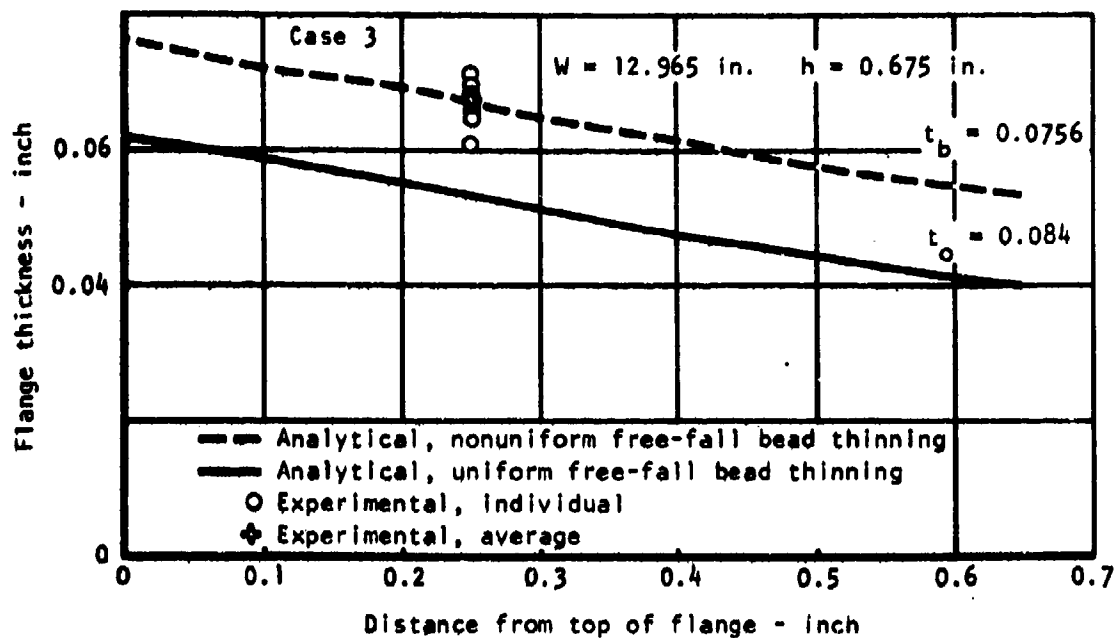
Figure 102. Thickness profiles, comparison of analytical prediction and experimental data, aft frames.

of the actuals by 0.009, 0.014, 0.014, and 0.012 inch for case 1, 2, 3, and 4, respectively. Cause of the larger deviations for the aft frames is likely to be due to plastic stretching of material beyond the edge of the die which would increase the amount of material being stretched and, therefore, decrease the amount of thinning necessary to form the pocket area.

Thickness profile in the flange area has a similar slope to that predicted, as shown in Figures 101 and 102, but the actual values are displaced to greater thicknesses by about 0.009 to 0.014 inch. This indicates that the thinning mechanism is basically as assumed in the analysis, but for more precise predictions of thicknesses, the model may need to be modified to account for secondary effects such as deforming material beyond the edge of the die cavity. The analytical predictions are, however, sufficiently close to the actual part thicknesses to be of distinct value in scoping the thin-out characteristics.

The overall dimensions were inspected for frames AF-3 through AF-10 using an inspection fixture shown in Figure 103. The fixture was so designed that the parts were centered at the center ellipse with a close-fit protruding plate in the fixture and gaps between fixed blocks and periphery of the parts were measured. The gaps represented relative size changes from part to part at locations opposite to where the fixed blocks were situated. Figure 104 is a sketch identifying each of the block locations. Results of the gap measurements at nine locations and for the eight frames are shown in Table 37, and Table 38 shows the calculated results of gap changes between the consecutively formed parts at each inspection point.

Because of the shape of the part, consistent positioning necessary for establishing comparative dimensional data was difficult to achieve, and the dimensional changes at each inspection point varied in a somewhat irrational manner as can be seen in Tables 37 and 38. In order to estimate the actual dimensional changes occurring between parts, the average of all dimensional changes were computed for each of the sequential parts fabricated. This was done since rotation or translation of the parts would cause gap increases in some areas and gap decreases in others, and averaging the dimensional variations should approximately cancel out these gap variations, leaving a measure of the real changes between parts. These average dimensional changes indicate dimensional changes of from -0.020 to +0.007 inch, with an average change for eight parts of -0.010 inch indicating a shrinkage of the outer part dimensions.

Additional inspection was conducted on frames No. AF-5 through AF-10 after they were chem-milled to establish the dimension across the minor axis of the center ellipse, diameter b of Figure 104. This dimension was measured using a precision ground radiused block to accommodate the fillets between web and flange at the inspection points. Results of the measurements are shown in Table 39. The trend for this dimension was consistent for all parts measured in that the diameter decreased when compared to the part formed previously. The amount of shrinkage varied from 0.008 to 0.043 inch which is considerably higher than that indicated for the outer dimensions of the parts.

164
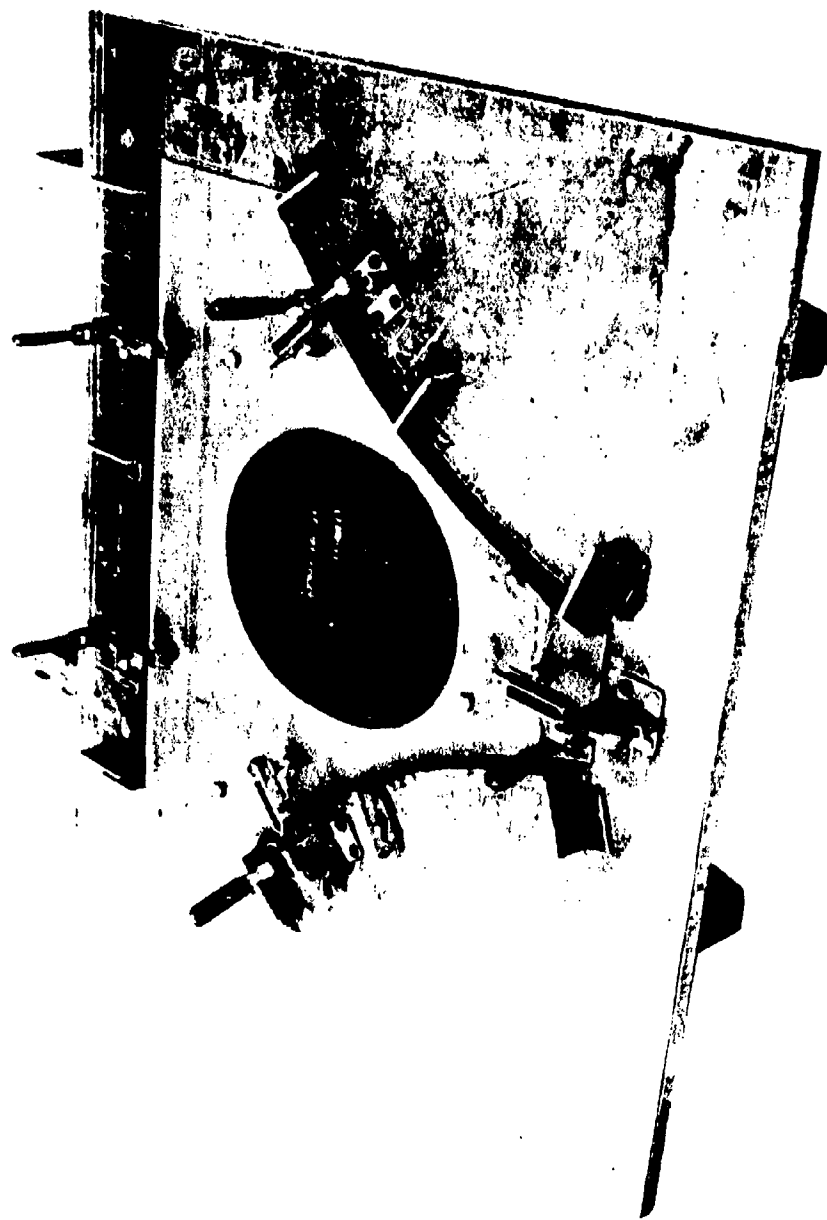
Figure 103. Inspection fixture used in determining overall dimensions of aft frames.

165
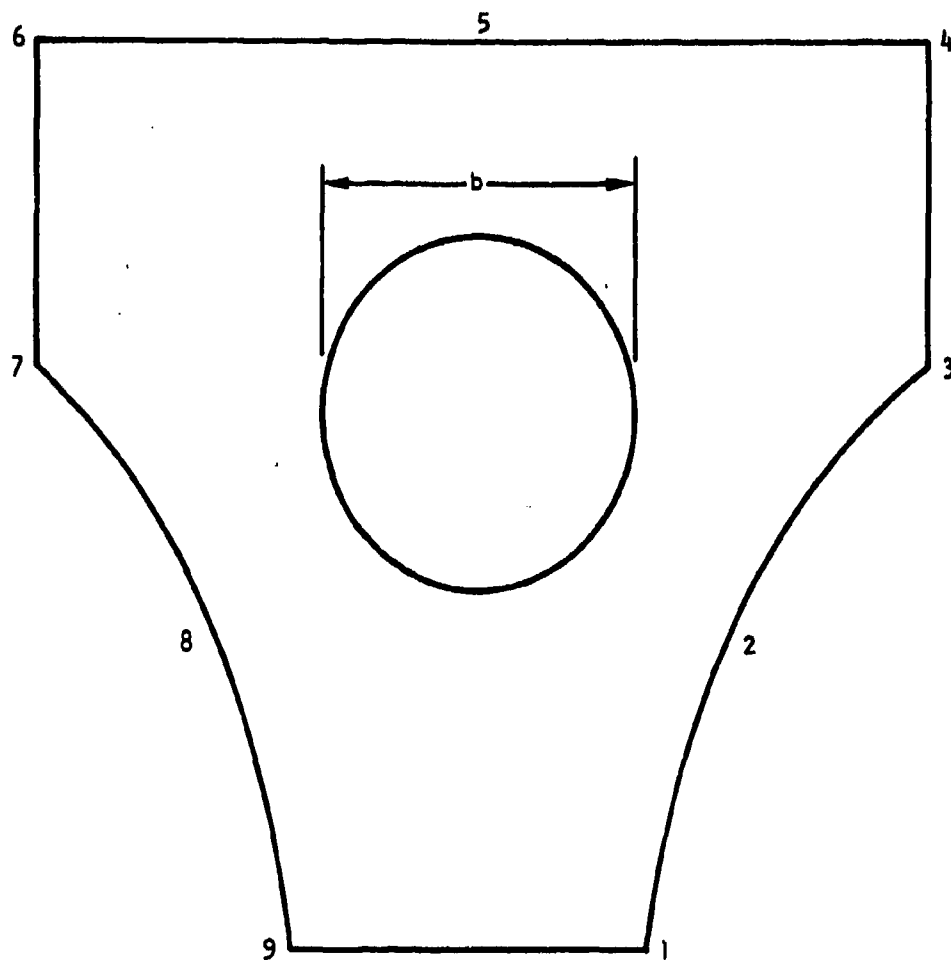
Figure 104. Locations of fixed reference points where gaps were measured, aft frames.

TABLE 37. OVERALL DIMENSIONS MEASURING FROM FIXED
POINTS INSPECTION FIXTURE

Location (fig. 104)	Nacelle frames							
	AF-3	AF-4	AF-5	AF-6	AF-7	AF-8	AF-9	AF-10
1	0.132	0.134	0.101	0.169	0.188	0.135	0.141	0.199
2	0.109	0.109	0.101	0.089	0.145	0.115	0.151	0.169
3	0.096	0.090	0.147	0.109	0.092	0.057	0.091	0.078
4	0.150	0.151	0.095	0.157	0.087	0.221	0.229	0.249
5	0.125	0.125	0.104	0.122	0.136	0.176	0.196	0.180
6	0.112	0.107	0.123	0.100	0.066	0.118	0.193	0.131
7	0.139	0.151	0.109	0.151	0.211	0.211	0.155	0.187
8	0.126	0.125	0.109	0.119	0.175	0.213	0.196	0.182
9	0.103	0.102	0.139	0.085	0.078	0.115	0.126	0.063

TABLE 38. DIMENSIONAL CHANGE FOR NACELLE AFT FRAMES

Location (fig. 104)	Dimensional change (inch)						
	3 → 4	4 → 5	5 → 6	6 → 7	7 → 8	8 → 9	9 → 10
1	-0.002	0.033	0.068	-0.019	0.053	-0.006	-0.058
2	000	0.008	0.012	-0.056	0.030	-0.036	-0.018
3	0.006	-0.057	0.038	0.017	0.035	-0.034	0.013
4	-0.001	0.056	-0.062	-0.030	-0.034	-0.008	-0.020
5	000	0.021	-0.018	-0.014	-0.040	-0.020	0.016
6	0.005	-0.016	0.023	0.034	-0.052	-0.075	0.062
7	-0.012	0.042	-0.042	-0.060	000	0.056	-0.032
8	0.001	0.016	-0.010	-0.056	-0.038	0.017	0.014
9	0.001	-0.037	0.054	0.007	-0.037	-0.011	0.063

TABLE 39. RESULTS OF DIMENSION/INSPECTION ON MINOR AXIS
OF CENTER ELLIPSE AND CORRESPONDING PART CHANGE

Description	Frame No.					
	AF-5	AF-6	AF-7	AF-8	AF-9	AF-10
b Dimension (inch)	12.600	12.5920	12.5580	12.5150	12.4770	12.4530
Shrinkage per part (inch)		0.0080	0.0340	0.0430	0.0380	0.0240
Shrinkage per part per inch		0.0006	0.0027	0.0034	0.0030	0.0019

The greater amount of shrinkage in the inner dimensions of the part may be caused by a combination of thermal gradient effects as observed for the forward frames and deformation caused by gas forming pressure used. The thermal gradients would tend to cause shrinkage throughout the die, whereas the gas pressure would be expected to cause shrinkage in the center ellipse, but expansion of the outer die edges. These two effects working in concert could lead to the dimensional changes observed.

The use of H13 alloy for the die, and the die design employed, did not prevent die deformation from occurring. It is, therefore, considered necessary that a better high-strength alloy be employed for production of parts using this process.

TEST AND EVALUATION

METALLURGICAL

The factors affecting material superplasticity and forming characteristics were evaluated in terms of microstructure in the as-received condition and for high-temperature flow properties. Table 40 summarizes the findings for the five heats of materials used in forming both the forward and aft frames.

First, in terms of microstructure, all but heat No. 890033 showed uniform grain size and were free from acicular or blocky alpha, as shown in Figures 105 through 108. The 890033 heat exhibited blocky alpha, which accounted for approximately 80 percent of the total volume. The blocky alpha did not adversely affect the superplasticity of the material, as indicated in phase I studies and as evidenced by the successful forming of the forward frame FF-1, which utilized material from heat 890033. Other microstructural variations,

168

TABLE 40. SUMMARY OF HIGH-TEMPERATURE FLOW PROPERTIES AND MICROSTRUCTURES
IN THE AS-RECEIVED CONDITION FOR FIVE HEATS OF Ti-6-4 ALLOYS
USED IN PHASE II

Heat No.	Orientation	m_{max} value	Flow[a] stress (ksi)	Acicular α	Blocky α	Avg grain size (μ)	Uniform grain size	Grain aspect ratio
890033	L LT	0.87 0.88	0.39 0.62	None	~80%	12.0	No	~5.0
295866	L LT	0.89 0.82	0.72 0.82	None	None	12.1	Yes	~3.5
800620	L LT	0.85[b] 0.92[b]	0.51[b] 0.45[b]	None	None	7.0	Yes	~4.0
304488	L LT	0.84 0.78	0.42 0.52	None	None	8.6	Yes	~1.0
800630	L LT	0.94[b] 0.90[b]	0.48[b] 0.55[b]	None	None	8.0	Yes	~2.5

[a] $\dot{\epsilon} = 1.67 \times 10^{-4}$ sec^{-1}

[b] Average of two tests

such as the average grain sizes varying from 8.0 to 12.1μ and the grain aspect ratio varying from 1 to 5, also did not appear to have a significant effect on the forming characteristic of the material. This is substantiated by the fact that the forming for all heats of material was accomplished using identical parameters.

The high-temperature flow properties were evaluated by comparing the m_{max} values and the flow stresses at a given strain rate of $1.67 \times 10^{-4} \times$ sec^{-1}. The m_{max} values varied between 0.78 and 0.94, indicating good superplasticity for all five heats of material. The heat 890033, which exhibited 80-percent volume fraction of blocky alpha, possesses m_{max} value (0.87 ~ 0.88), ranking between those of other heats that are free from the blocky alpha. This is another indication that the blocky alpha has no adverse effect on superplasticity of the material. The flow stresses varied between a narrow span of 0.39 ~ 0.82 ksi for the five heats of material, substantiating the formability of the materials, using an identical and low-forming pressure.

Figure 105. Microstructure of heat No. 295860 in as-received condition showing uniform grain size, free from blocky or acicular alpha, typical for materials used in phase II. Grain direction: (a) L, (b) LT, (c) ST, 250X.

170
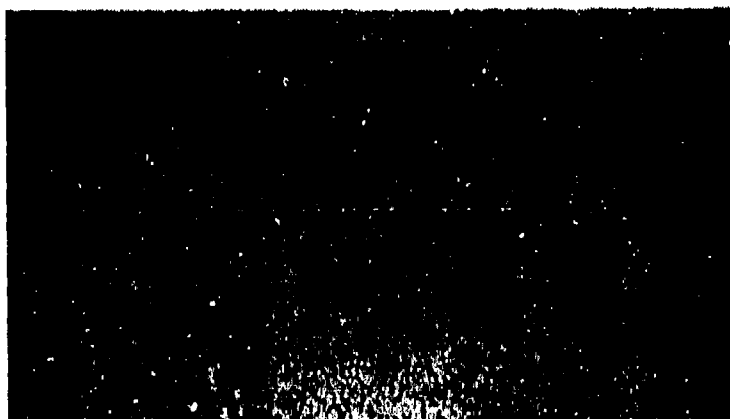
Figure 106. Microstructure of heat No. 800620 in as-received condition showing uniform grain size, free from acicular or blocky alpha, typical for materials used in phase II. Grain direction: (a) L, (b) LT, (c) ST, 500X.

Figure 107. Microstructures of heat No. 800630 in as-received condition showing block alpha. Grain directions: (a) L, (b) LT, (c) ST, 500X.

172

(a)
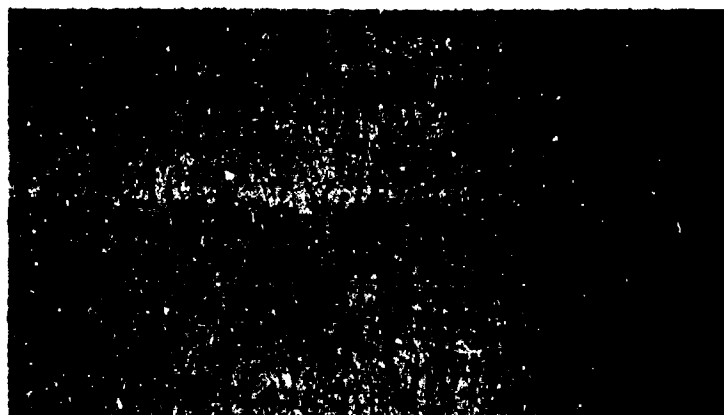
(b)
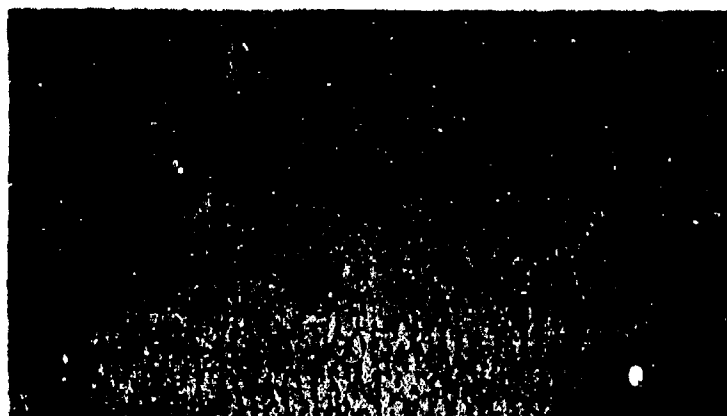
(c)
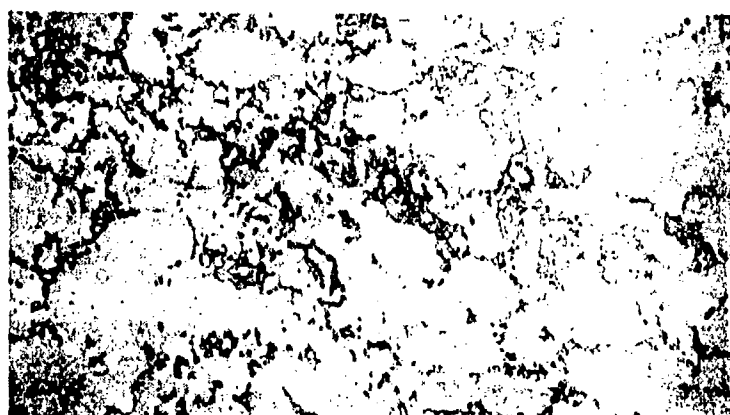
Figure 108. Microstructures of heat No. 890033 in as-received condition showing blocky alpha. Grain directions: (a) L, (b) LT, (c) ST, 500X.

The m_{max} value has been shown to be the best indicator for the superplasticity of the material, and the microstructural constituents that adversely affect the m_{max} values are the presence of acicular alpha and grain size in excess of 13μ. Therefore, the results of the testing conducted in both phase I and phase II indicate that metallographic evaluation can be effectively used to define and effectively screen Ti-6Al-4V materials for the SPF process.

MECHANICAL PROPERTIES

Tensile Test

Both the forward and the aft frames were tensile tested in the as-formed condition. The material used in forming the frames was tested in the as-received (mill annealed) condition and after thermal cycling at 1,700° F for 3 hours to form a base for determining the effects of superplastic forming. Table 41 summarizes the test results for the five heats of material used in forming the frames. Except for heat 295866, all heats were tested in the three material conditions and two grain directions. Heat 295866 was used to form two forward frames, FF-2 and FF-3, which were subsequently structurally tested. Therefore, mechanical testing was not conducted in the as-formed condition for this heat of material. Specimen locations for FF-1 and AF-11 are shown in Figures 109 and 110.

The tensile properties were compared in three conditions for each heat of material in each grain direction as shown in Figure 111. In general, the same trend was observed for all cases where both the tensile ultimate and yield strength decreased when materials were thermally cycled or superplastically formed, and is consistent with the observations of phase I. The forming appeared to cause more reduction than that of the thermal cycling. Statistically, material in the as-formed condition showed averages and standard deviation of 140.8(±4.6) and 126.4(±4.5) ksi ultimate tensile strength and tensile yield strength, respectively. The preceding calculations were carried out by mixing properties in both grain directions.

When reduced to design allowable A in accordance with MIL-HDBK-5 guidelines, the material showed A allowables of Ftu = 125.2 ksi and Fty = 111.3 ksi, which are in excellent agreement with design allowables developed for diffusion-bonded Ti-6Al-4V material. Since both the SPF and diffusion bonding processes involve heating to 1,700° F temperature for 2 to 3 hours and deforming material above recrystallization temperature (hot working), the equivalency in resulting tensile properties is to be expected.

Fatigue Test

For phase II materials, fatigue tests were conducted in two conditions - thermally cycled and as-formed. The as-superplastically formed specimens were

174

TABLE 41. SUMMARY OF TENSILE PROPERTIES FOR FIVE HEATS OF Ti-6A1-4V ALLOY USED IN PHASE II STUDIES (AS RECEIVED, THERMALLY CYCLED,[a] AND FORMED)

Matl Heat No.	Produced Frame No.	Grain dir	Specimen Cond	Specimen No.	Specimen Thickness (in.)	F_{tu} (ksi)	F_{ty} (2% ksi)
890033	FF-1	L	As-received	TAR1	0.122	144.5	136.0
				TAR2	0.122	144.8	137.4
			Thermally cycled	THT1	0.098	140.4	136.5
				THT2	0.100	145.8	137.5
			Formed FF-1	FF-1-1	0.048	146.0	131.6
				FF-1-2	0.040	144.8	129.0
		LT	As-received	TAR3	0.122	149.2	146.3
				TAR4	0.122	149.3	146.0
			Thermally cycled	THT3	0.101	146.9	141.0
				THT4	0.099	147.7	140.6
			Formed FF-1	FF1-3	0.054	143.4	128.0
				FF1-4	0.044	144.7	128.6
				FF1-5	0.035	142.6	124.6
				FF-6	0.042	141.6	124.1
295866	FF-2 FF-3	L	As-received	TAR-5	0.131	145.1	138.1
				TAR-6	0.121	144.8	138.2
			Thermally cycled	THT-5	0.107	139.3	133.6
				THT-6	0.107	140.3	134.1
		LT	As-received	TAR-7	0.131	144.7	138.6
				TAR-8	0.132	144.0	137.7
			Thermally cycled	THT-7	0.111	139.4	132.1
				THT-8	0.101	137.5	130.3

[a]1,700° F/3 hours, furnace cool

175

Matl Heat No.	Produced Frame No.	Grain dir	Specimen cond	Specimen No.	Specimen Thickness (in.)	F_{tu} (ksi)	F_{ty} (2% ksi)
800620	FF-4 through FF-10	L	As-received	TAR9	0.127	147.2	142.0
				TAR10	0.128	147.0	141.8
			Thermally cycled	THT9	0.127	145.6	138.9
				THT10	0.127	144.1	136.7
				THT11	0.128	143.5	135.8
				THT12	0.128	143.4	136.1
			Formed FF-4	FT-1	0.057	140.2	121.1
				FT-2	0.064	142.8	124.3
		LT	As-received	TAR-11	0.128	148.3	144.4
				TAR-12	0.127	148.4	144.8
			Thermally cycled	THT-13	0.128	142.6	134.6
				THT-14	0.128	143.7	135.2
				THT-15	0.128	143.7	135.2
				THT-16	0.128	142.9	134.9
			Formed FF-4	FT-3	0.062	139.9	.23.1
				FT-4	0.063	141.8	123.2
304488	AF-1	L	As-received	T41	0.056	145.3	143.0
				T451	0.056	145.5	142.8
			Thermally cycled	T47	0.060	144.2	137.9
				T410	0.060	148.5	137.7
			Formed AF-1	AF1-17	0.050	145.0	131.7
				AF1-18	0.051	146.7	133.2
		LT	As-received	T418	0.056	142.6	137.6
				T431	0.056	142.2	138.1
			Thermally cycled	T420	0.059	135.6	124.8
				T422	0.059	131.9	118.9

[a]1,700° F/3 hours, furnace cool

176

TABLE 41. SUMMARY OF TENSILE PROPERTIES FOR FIVE HEATS OF Ti-6Al-4V ALLOY USED IN PHASE II STUDIES (AS-RECEIVED, THERMALLY CYCLED[a], AND FORMED) (CONCL)

Matl Heat No.	Produced Frame No.	Grain dir	Specimen cond	Specimen No.	Specimen Thickness (in.)	F_{tu} (ksi)	F_{ty} (2% ksi)
304488 (cont)	AF-1	LT	Formed AF-1	AF1-9	0.049	131.3	119.1
				AF1-11	0.049	129.9	117.9
800630	AF-2 through AF-10	L	As-received	TAR-13	0.084	145.2	140.7
				TAR-14	0.084	146.1	141.4
			Thermally cycled	THT-17	0.084	144.0	135.9
				THT-18	0.084	141.0	132.1
				THT-19	0.085	141.3	132.6
				THT-20	0.085	140.3	131.5
			Formed AF-2	AF-3	0.081	138.1	128.5
				AF-4	0.081	137.0	126.7
		LT	As-received	TAR15	0.085	148.8	144.9
				TAR16	0.084	149.6	145.9
			Thermally cycled	THT21	0.085	144.1	135.9
				THT22	0.085	143.6	134.5
				THT23	0.083	145.5	135.9
				THT24	0.085	144.4	135.3
			Formed AF-2	AF2-1	0.080	139.1	130.6
				AF2-2	0.080	138.9	130.4

[a]1,700° F/3 hours, furnace cool
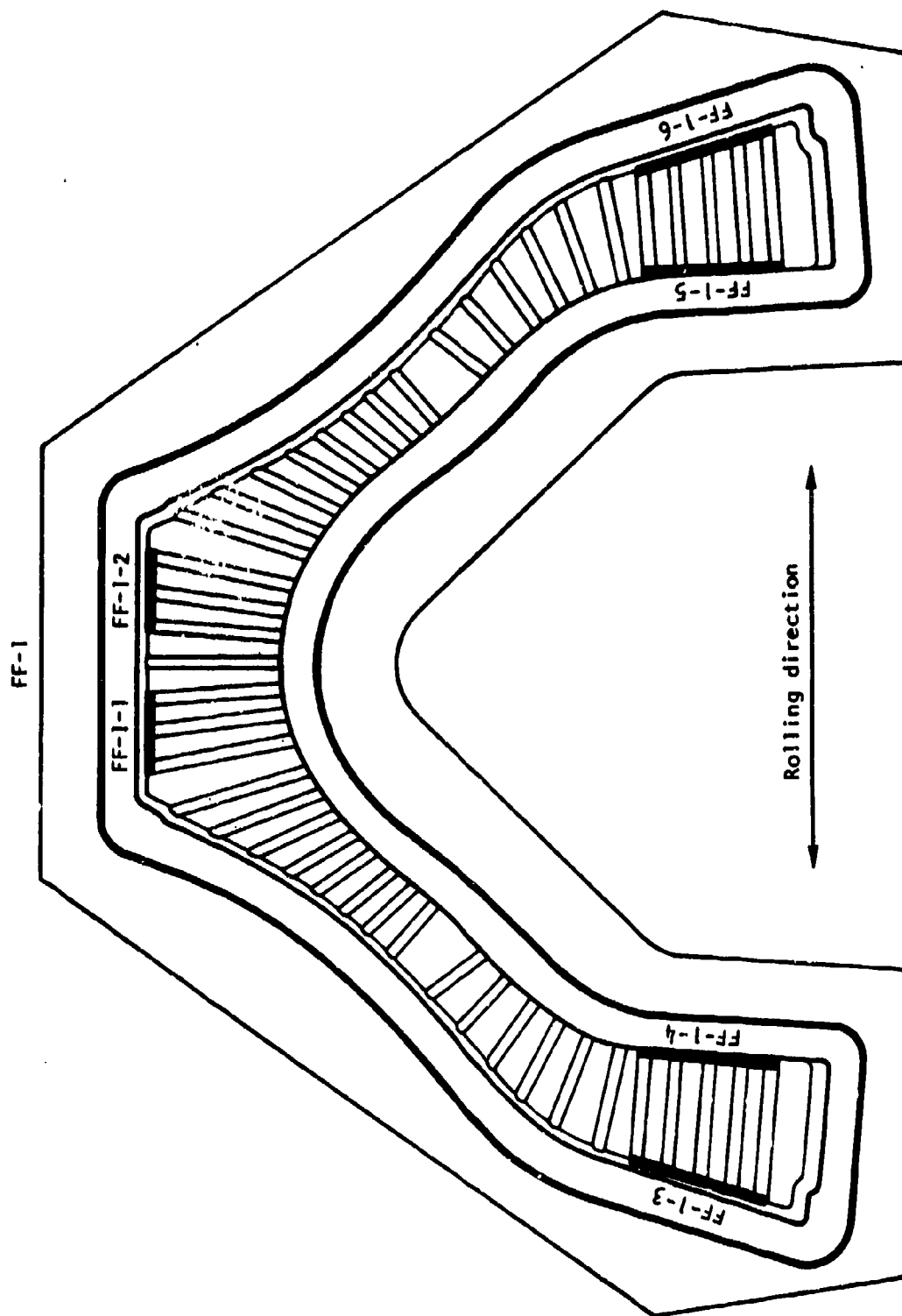
Figure 109. Location of tensile specimens taken from forward frame FF-1.

178
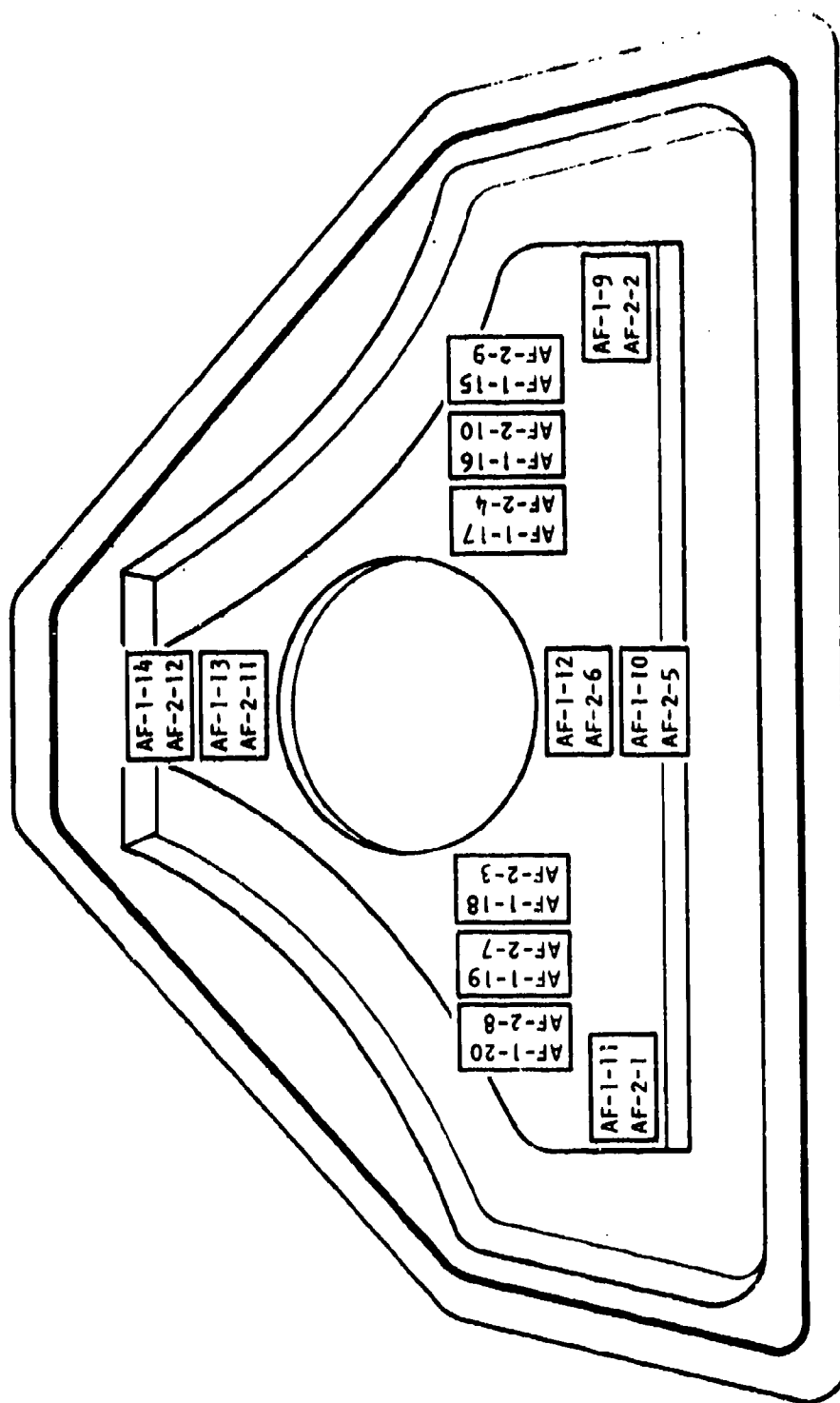
Figure 110. Locations of tensile and fatigue specimens taken from aft frames AF-1 and AF-2.
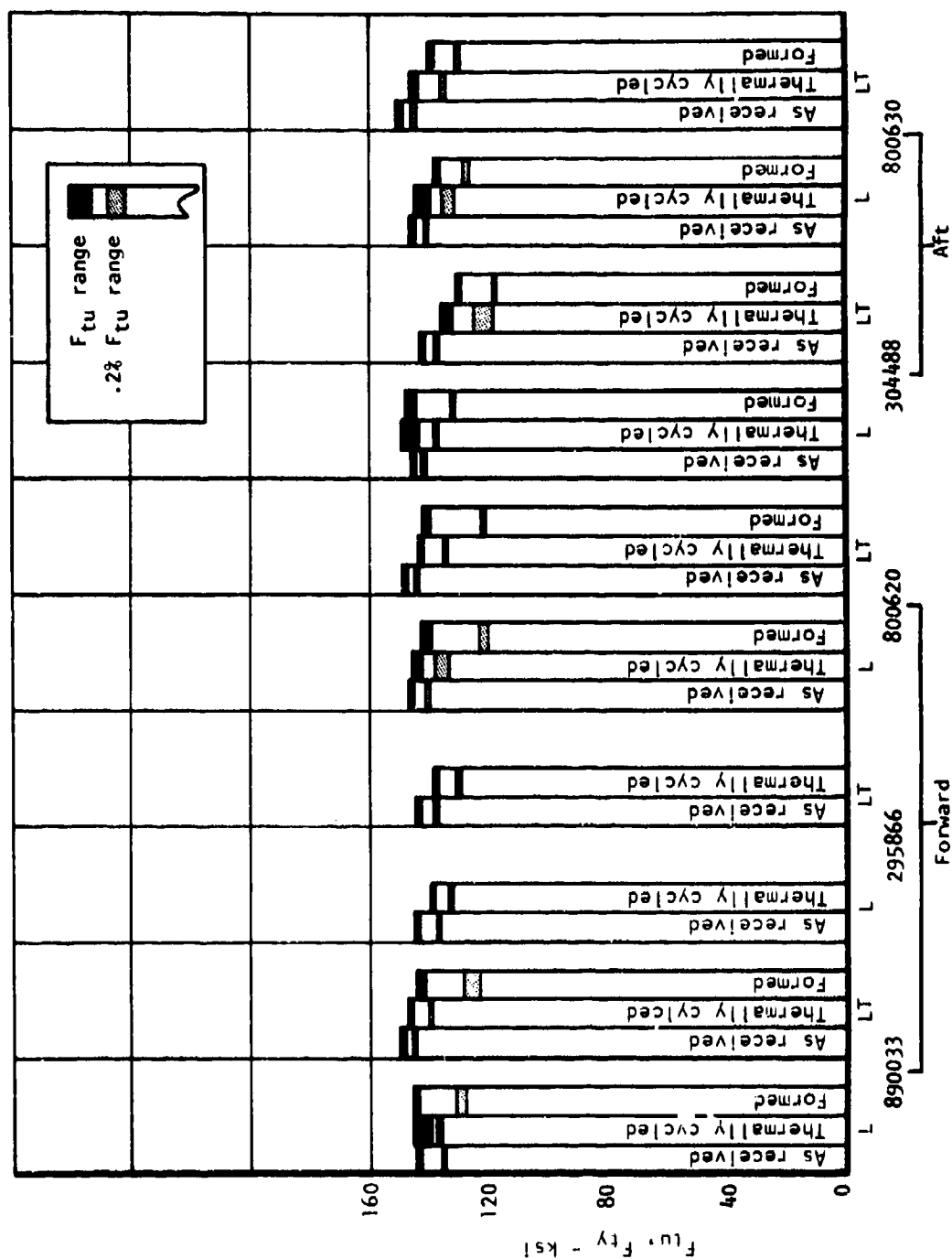
Figure 111. Effects of material conditions on tensile properties of five heats of 6Al-4V titanium alloy used in phase II forming studies.

taken from the aft frames only, since the beaded configuration of the forward frames did not provide a sufficiently large flat area for machining fatigue specimens. Sheet from each of the two heats used for the forward frames was therefore thermally processed in a furnace to simulate the forming cycle in order to obtain material for the fatigue test. Results of the fatigue tests are summarized in Table 42. Specimen locations for the as-formed condition are shown in Figure 110.

The results of the fatigue tests conducted on the superplastic formed material are presented in Figure 112. The data is shown in relation to phase I test results and to the scatter band typically observed for Ti-6Al-4V in the recrystallization annealed condition. As can be seen in Figure 112, the fatigue data for the superplastically formed material is consistent with prior results for this alloy.

STRUCTURAL TESTING

Forward Frames

Tᵂₒ of the forward frames were structurally tested under static loading to evaluate the buckling and crippling characteristics of the design, and to demonstrate the suitability of SPF for structural applications. The test was performed on the two nacelle forward center beam frames placed back-to-back to create a symmetric test configuration to simplify loading conditions and analysis. The static structural test was performed on forward frames No. 2 and 3, which were prepared by chemical milling to produce nominal thicknesses of 0.070 and 0.015 inch minimum values, as shown in Figure 88. The leg ends and the closed-top end remained in original thickness to provide support for the test fixtures. The test setup is shown in Figure 113. Instrumentation consisted of a single strain gage on each flange at the minimum section near the attachment to the test fixture. A total of six gages were installed to provide measurement of frame flange axial loads near the anticipated point of failure.

The procedure included the attachment of the two identical frames back-to-back to the test fixture shown in Figure 114. The loading jack was placed horizontally in the midplane separating the two frames. The frames were loaded in increments of 5,000 psi as monitored by an outer flange strain gage. When one side of the frames crippled, the frames were switched to test the opposite side of the two frames. The data recorded included hydraulic jack orientation and attachment location relative to the frames, all strain gage readings at each load increment, the vertical and horizontal deflections of the frames, the loading point for each loading increment, and all significant data and occurrences.

TABLE 42. SUMMARY OF PHASE II FATIGUE TEST RESULTS

Heat No.	Condition	K_t	Grain dir	Specimen No.	Specimen Thickness (in.)	Max stress % F_{tu}	Max stress ksi	R	Cycles to failure
890033	Thermally cycled at 1,700° F/ 3 hours, furnace cool. ♠	1	L	FHT1	0.0973	80	114.5	0.05	25,000
				FHT2	0.0978	80	114.5	0.05	30,000
			LT	FHT3	0.1010	80	117.8	0.05	8,000
				FHT4	0.0963	80	117.8	0.05	20,000
		3	L	FHT5	0.0980	50	71.6	0.05	6,000
				FHT6	0.1036	50	71.6	0.05	4,000
			LT	FHT7	0.1098	50	73.7	0.05	5,000
				FHT8	0.1085	50	73.7	0.05	4,000
295866	Thermally cycled at 1,700° F/ 3 hours, furnace cool ♠	1	L	FHT9	0.1052	80	111.8	0.05	17,000
				FHT10	0.1125	80	111.8	0.05	23,000
			LT	FHT11	0.1102	80	110.8	0.05	18,000
				FHT12	0.1163	80	110.8	0.05	6,000
		3	L	FHT13	0.1134	50	69.9	0.05	4,000
				FHT14	0.1091	50	69.9	0.05	6,000
			LT	FHT15	0.1110	50	69.3	0.05	6,500
				FHT16	0.1116	50	69.3	0.05	4,000
304488	Formed, AF1	1	L	AF1-16	0.0499	80	104.5	0.05	47,000
				AF1-20	0.0505	80	104.5	0.05	96,000
			LT	AF1-5	0.0346	80	107.6	0.05	21,000
				AF1-6	0.0343	80	107.6	0.05	17,000
				AF1-12	0.0491	80	116.7	0.05	34,000
				AF1-14	0.0497	80	116.7	0.05	31,000
		3	L	AF1-15	0.051	50	65.3	0.05	65,000
				AF1-19	0.0505	50	65.3	0.05	45,000
			LT	AF1-3	0.0336	50	67.3	0.05	16,000
				AF1-4	0.0318	50	67.3	0.05	18,000
				AF1-10	0.0503	50	73.0	0.05	23,000
				AF1-13	0.0506	50	73.0	0.05	2C,000
800630	Formed AF2	1	L	AF2-8	0.0818	80	110.1	0.05	22,000
				AF2-10	0.0815	80	110.1	0.05	28,000
			LT	AF2-6	0.0804	80	111.2	0.05	29,000
				AF2-12	0.0832	80	111.2	0.05	30,000
		3	L	AF2-7	0.0825	50	68.8	0.05	24,000
				AF2-9	0.0808	50	68.8	0.05	9,000
			LT	AF2-5	0.0805	50	69.5	0.05	15,000
				AF2-11	0.0814	50	69.5	0.05	17,000

♠Material thermally cycled in furnace to represent forward frames

a) Smooth Fatigue
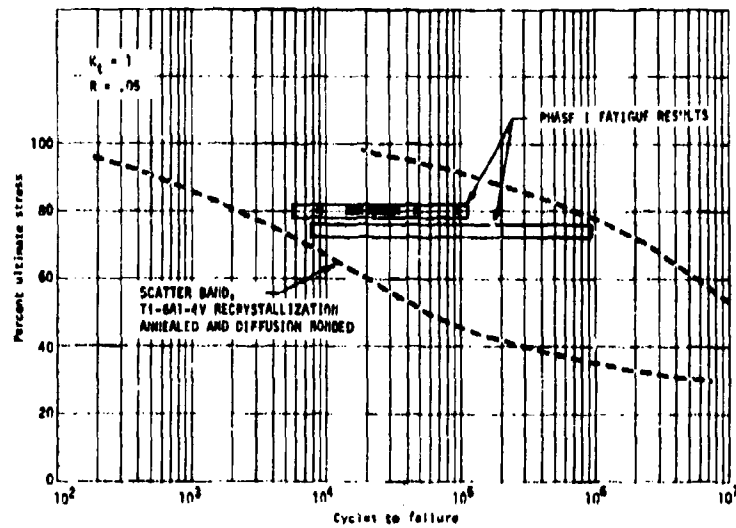
(Reference
Figure 66)

b) Notched Fatigue
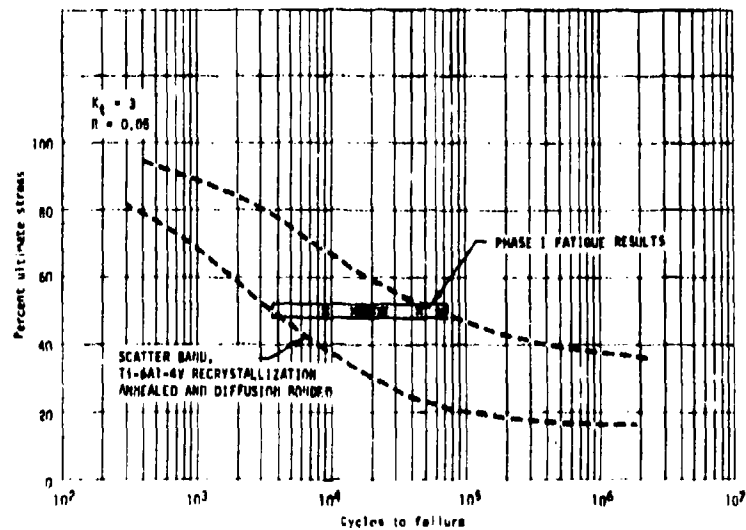
(Reference
Figure 67)

Figure 112. Effects of heat-treating and forming on fatigue properties
of Ti-6Al-4V alloy used in phase II studies.

183
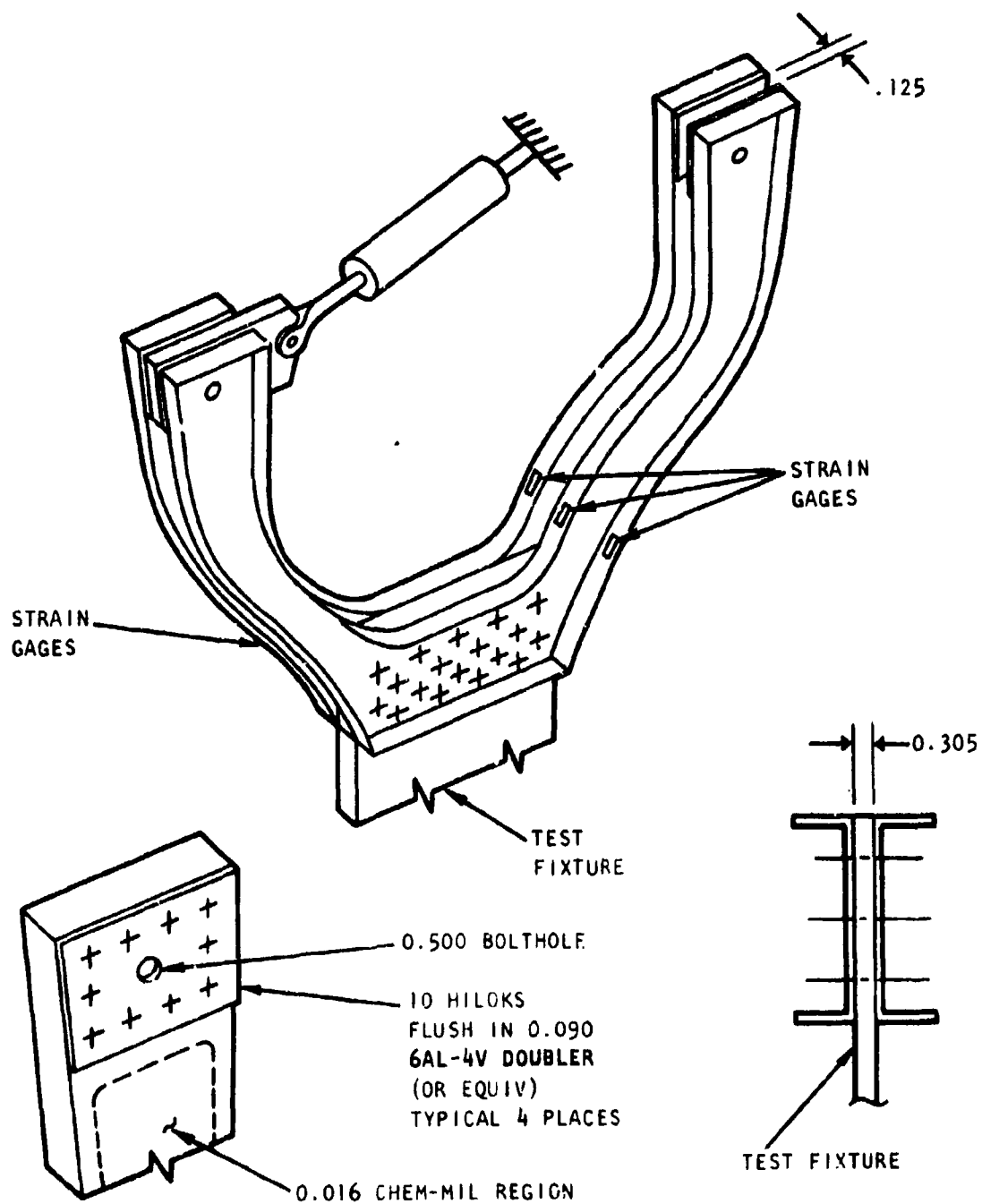
Figure 113. Test setup for structural test of forward frames.
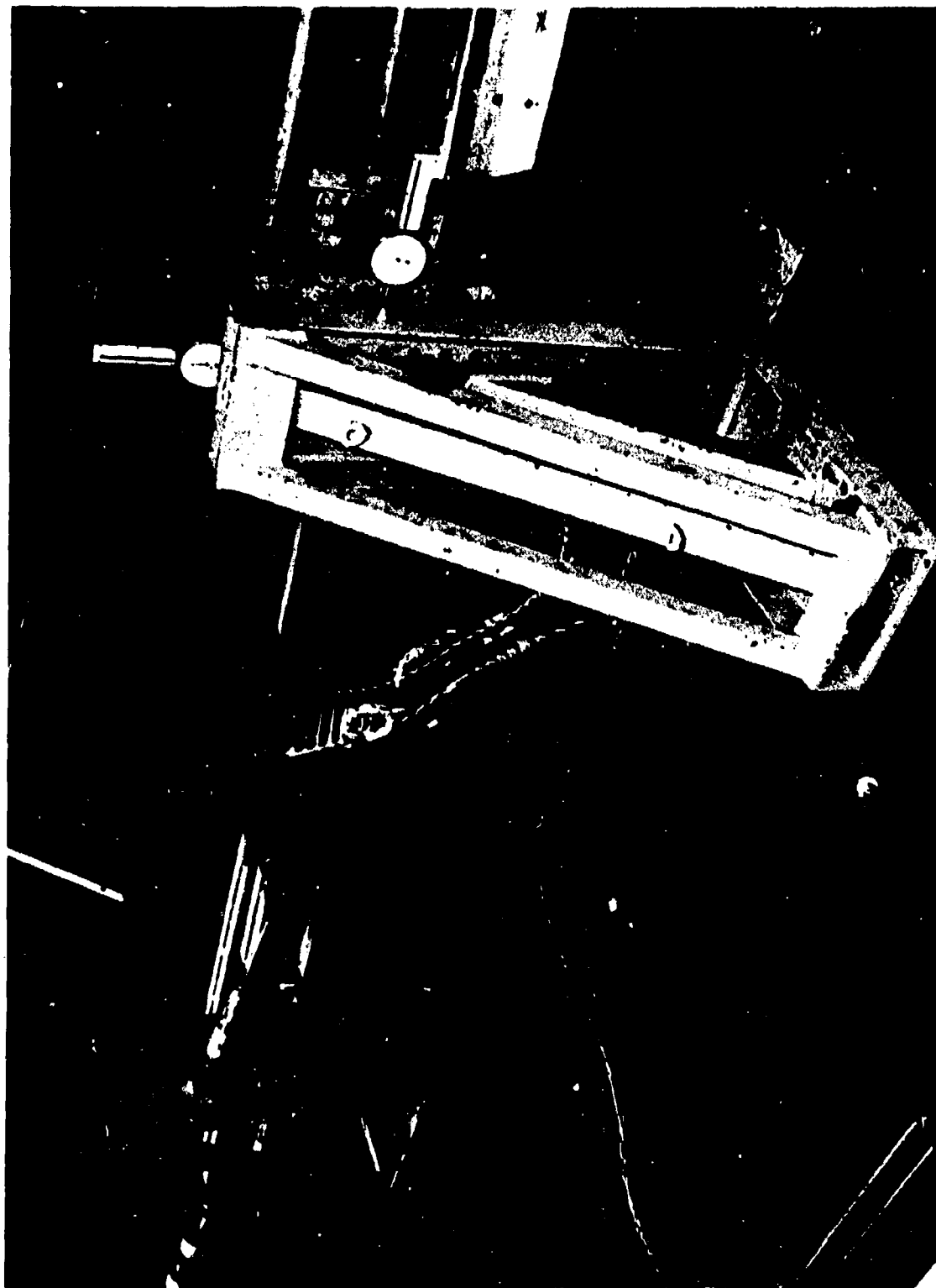
Figure 114. Static structural test fixture for forward frames.

The results of the static structural test are shown in Figure 115, which shows the buckling of the two frames at maximum load condition. When the load was released and the two frames returned to their original condition, cracking at the edge of the vertical flange occurred. Failure mode and location were as anticipated, and no buckling or wrinkling occurred in the beaded web area, demonstrating the suitability of this design configuration for reducing web thickness.

Stress analysis was conducted to determine if the bending stresses (f_b) at the time when frames showed instability were those of the anticipated compressive crippling strength of the structure (Fcc) predicted from material allowables, Fcy and Ec.

Considering a beam with a cross-sectional view, shown in Figure 116, which consisted of three effective structural elements, skin attachment and two flanges, the bending stress is expressed as:

$$f_b = LP \frac{C}{I_{NA}}$$

Where

    L = distance between loading point and test section

    P = load

I_{NA} = inertia at neutral axis

    C = distance between neutral axis and location where bending stress is measured

The neutral axis location and inertia can be determined using conventional stress analysis of:

$$C_a = \frac{\Sigma AY}{\Sigma A}$$

$$I_{NA} = \Sigma I_o + \Sigma AY^2 - (\Sigma A)(C)_a^2$$

Where

    Σ = summation

    A = areas of effective elements

Figure 115. Superplastic formed forward frame tested to failure.

187
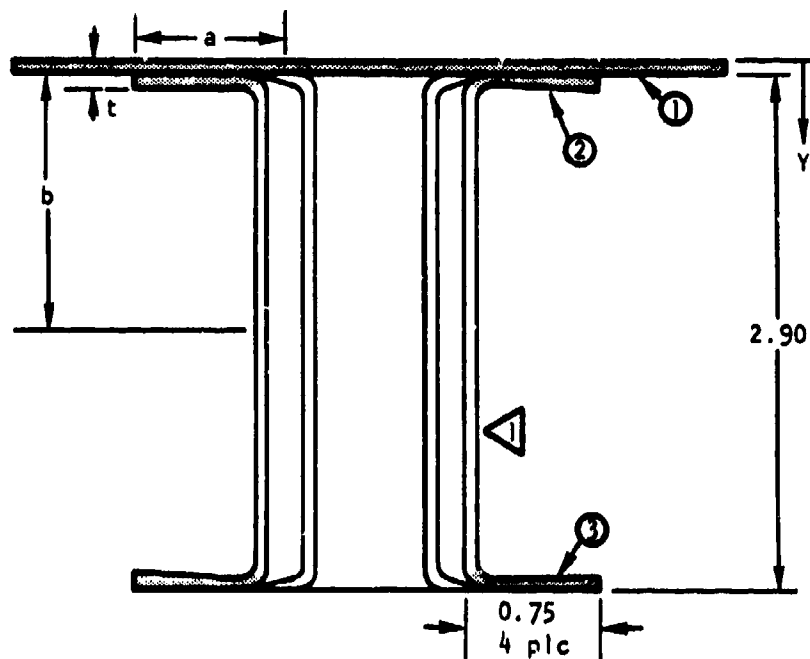
① Skin

② Effective element, flange 1 (Element 1)

③ Effective element, flange 2 (Element 2)

◁ Web and inner portions of flange
are ineffective in resisting bending
load

Figure 116. Test section of forward frames used in stress analysis showing
effective and noneffective elements.

Y = distances between measuring location and center of effective elements

$I_{\bullet}$ = inertia at section center

For the two forward frames tested, the preceding calculation yielded the following results for each of the two test conditions:

With skin (ELE 1)	Without skin (ELE 1)
C = 2.081 in.	C = 1.45 in.
I_{NA} = 0.617 in.^{4}	I_{NA} = 0.421 in.^{4}

The distance between the loading point and the test section was 17.4 inch measured from the test setup, and the failure loads were 1,095 and 920 pounds for the two legs tested with and without the skin, respectively. Therefore, the bending stresses are:

$$fb \text{ (with skin)} = 17.4 \times 1.095 \times \frac{2.081}{0.617} = 64.3 \text{ ksi}$$

$$fb \text{ (without skin)} = 17.4 \times 0.920 \times \frac{1.450}{0.421} = 55.1 \text{ ksi}$$

The cripple strength of a structure with a U-shape cross section can be predicted (Reference 4) when material properties, Fcy and Ec, are known and expressed as:

$$Fcc = K \sqrt{Fcy \, Ec}$$

where K is a function of the cross-section geometry or:

$$K = f \left(\frac{a+b}{2t} \right)$$

Where

a = flange length

b = web width

t = flange thickness

For the test section shown in Figure 116, the K-value obtained from Figure C 7.3, page C7.3, of Reference 4 was 0.044, or:

$$F_{cc} = 0.044 \sqrt{F_{cy} \; E_c}$$

Using the material property allowables of $F_{cy} = 117$ ksi and $E_c = 16.4 \times 10^3$ ksi, the predicted crippling strength was 60.9 ksi.

Comparisons between the structural tests and the predictions yielded the following relations:

$$f_b \text{ (with skin)} \quad > F_{cc}$$

$$f_b \text{ (without skin)} < F_{cc}$$

The preceding results indicated that the frames, when properly fixtured with a backup skin, had failed in a predictable manner consistent with this type of structure. The compression flange crippled, which, in turn, resulted in general beam instability.

Aft Frames

The structural tests were conducted on two aft frames, AF-3 and AF-4. The test method and setups were similar to those utilized for the forward frames, except that the aft frames were cut out at the top center section to provide for the fixture attachments in the loading area. Figure 117 shows the location of the cutout and the typical thickness profiles at test section after the frames were chem-milled for the structure tests. The tests included strain gaging at the anticipated buckling locations and incremental tension loading of each of the two legs until failure occurred.

The loading moment, measuring from the loading point in the test section, was 15.63 inch. Buckling had occurred at the anticipated test section at 569- and 599-pound loads for the two consecutive tests on the two legs of the frames. The failure mode, crippling of inner flanges before the occurrence of the general instability of the structure, indicated that the superplastic formed frames retained their structural integrity.

The stress analysis at the test section, shown in Figure 118 and utilizing the same approach used for the forward frames, yielded the following results:

$$C = 1.26 \text{ in.}$$

$$I_{NA} = 0.140 \text{ in.}^4$$

$$f_b \text{ (1st leg)} = 15.63 \times 0.569 \times \frac{1.26}{0.14} = 80.0 \text{ ksi (experimental)}$$

190
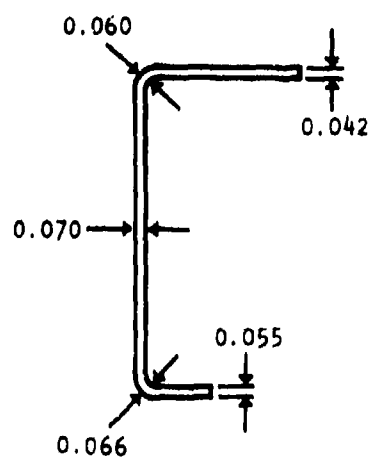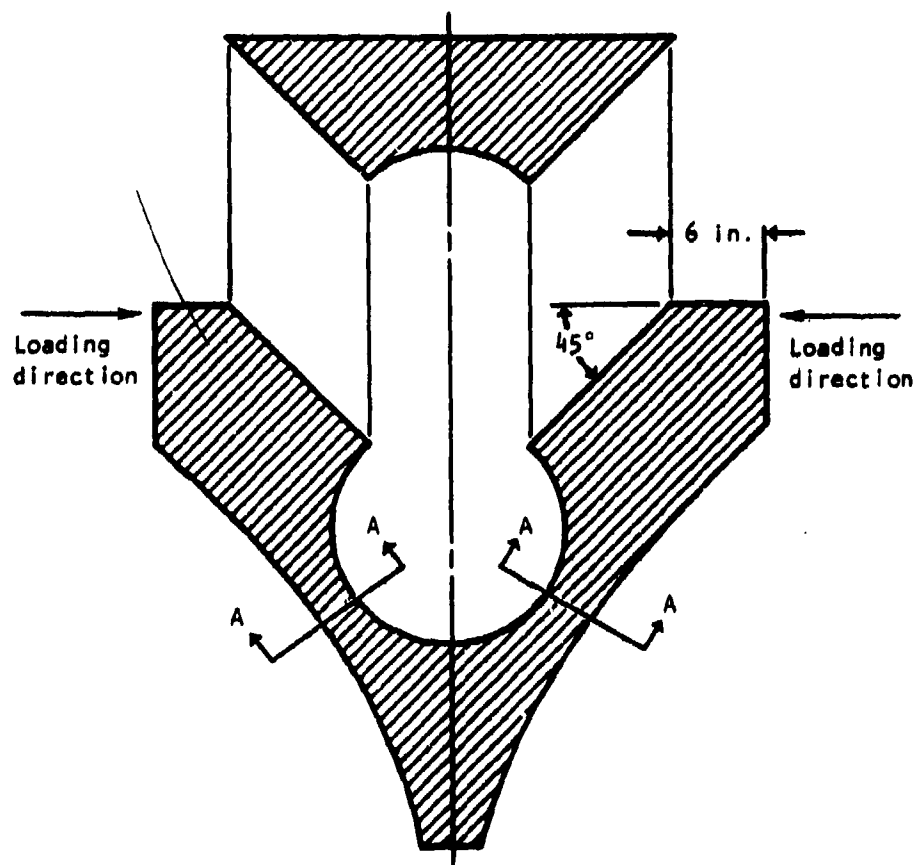
SECTION A-A

Figure 117. The cutout location and typical thickness profile at
test section of aft frames used in structural tests.
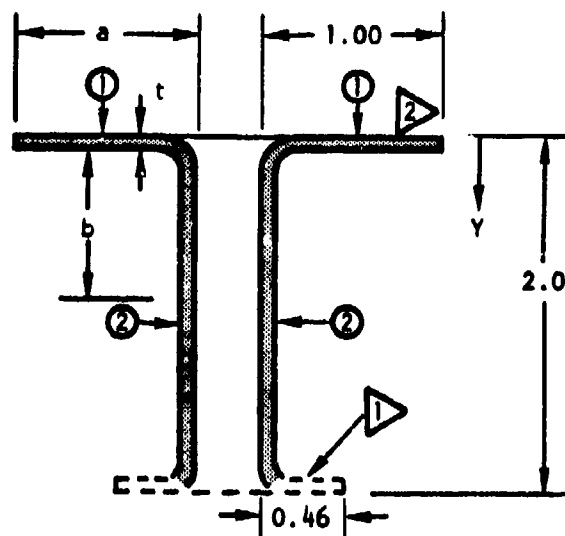
① Effective element, flange

② Effective element, web

▷1 The 6-inch radius of this flange makes it ineffective for resisting bending load

▷2 Skin element did not enter in calculation due to a shorter loading moment

Figure 118. Test section of aft frames used in stress analysis showing effective and noneffective elements.

$$f_b \text{ (2nd leg)} = 15.63 \times 0.599 \times \frac{1.26}{0.14} = 84.3 \text{ ksi (experimental)}$$

$$F_{cc} = 0.0575 \sqrt{117 \times 16.4 \times 10^3} = 79.7 \text{ ksi (predicted)}$$

It is evident that the bending stress at the time of instability is approximately equivalent to that of the predicted crippling stress, indicating that the frames had buckled in a predictable manner and were consistent with the beam structures produced by conventional methods.

ECONOMIC ANALYSIS

Cost trade-off studies were conducted with the object of establishing an economic comparison between forming a typical multidetail air vehicle components in one piece by SPF and the current practice of hot size forming of individual details and assembling them to complete the components. The various material utilization, processing, and tooling approaches used in this program were cost analyzed for comparison with cost elements for hot size forming and assembly of the comparable part. The trade study analysis was based on the technique of establishing a baseline cost for the separate elements of the current process by research of cost history for fabrication of typical air vehicle parts and by developing the cost element increments for SPF and cost tracking of the parts.

Two concepts of the application of SPF were considered. One was direct substitution, with no design changes for SPF from hot size forming to fabrication the major component of the assembly. The other concept included redesign to capitalize on the unique SPF capability to produce a monolithic part. Assembly of details was eliminated. Since SPF has the capability of forming parts in multiple in each cycle, the studies included a comparison of costs for two- and four-part simultaneous forming.

During the cost analysis, the following guidelines were assumed and utilized:

1. Production quantities for 241 air vehicles were assumed.

2. The development of the process was complete; therefore, no development costs were included.

3. The quality assurance costs were included as a percentage of fabrication labor cost.

4. A blended Wright learning curve slope of 69 percent from unit 1 to 3, 80 percent from unit 4 to 10, 85 percent from unit 11 to 50, and 90 percent from unit 51 and up was applied for projecting costs to production quantities.

193

5. The material costs included standard mortality and procurement factors.

6. The labor costs included setup prorated over a 12-ship relea e and a standard rework factor.

7. The tooling costs included a 108-percent cost-of-maintenance curve with tooling material calculated at a standard cost per hour of tool fabrication.

8. Labor hours were based on fabrication history for the hot size form concept and tracking of hours expended on the test parts for the SPF concept.

9. The cost calculations were derived by input of basic cost data to a computerized program.

10. Two-and-four-parts-per-forming-cycle labor hours were segregated to reflect the multiple effort prior to and including forming and the one-at-a-time operation subsequent to forming.

Nacelle Forward Center Beam Frame

The economic analysis for the nacelle forward frame was conducted as two separate studies. They included 1) fabrication of the frame using conventional hot size forming procedures and 2) fabrication of the frame using superplastic forming at rates of one, two and four parts per cycle. For the hot sizing operations, the individual parts shown in Fugure 119 make up the sheet metal assembly included in the cost trade study. A one-piece sheet metal part, redesigned to replace the assembly, was used for the SPF operations. The redesign incorporated integral return flanges and beads which replaced doublers, splice plates, stiffeners, and fasteners. This design also included selective chemical milling to obtain desired thicknesses and reduce weight. Figures 120 through 123 show the effect of quantity on cost for each of the four individual cost studies conducted and reflect the effect of the separate operations of fabrication, material, tooling, and purchased labor. A decrease in overall cost by utilizing SPF over hot size forming is indicated.

SPF of multiple parts simultaneously does not offer a significant additional cost decrease, and this is substantiated by Figure 124, which shows a direct comparison of the four studies. The figure does show a substantial cost reduction for superplastic forming of a one-piece reduction for superplastic forming of a one-piece frame by comparison to the conventional hot size forming approach.

194
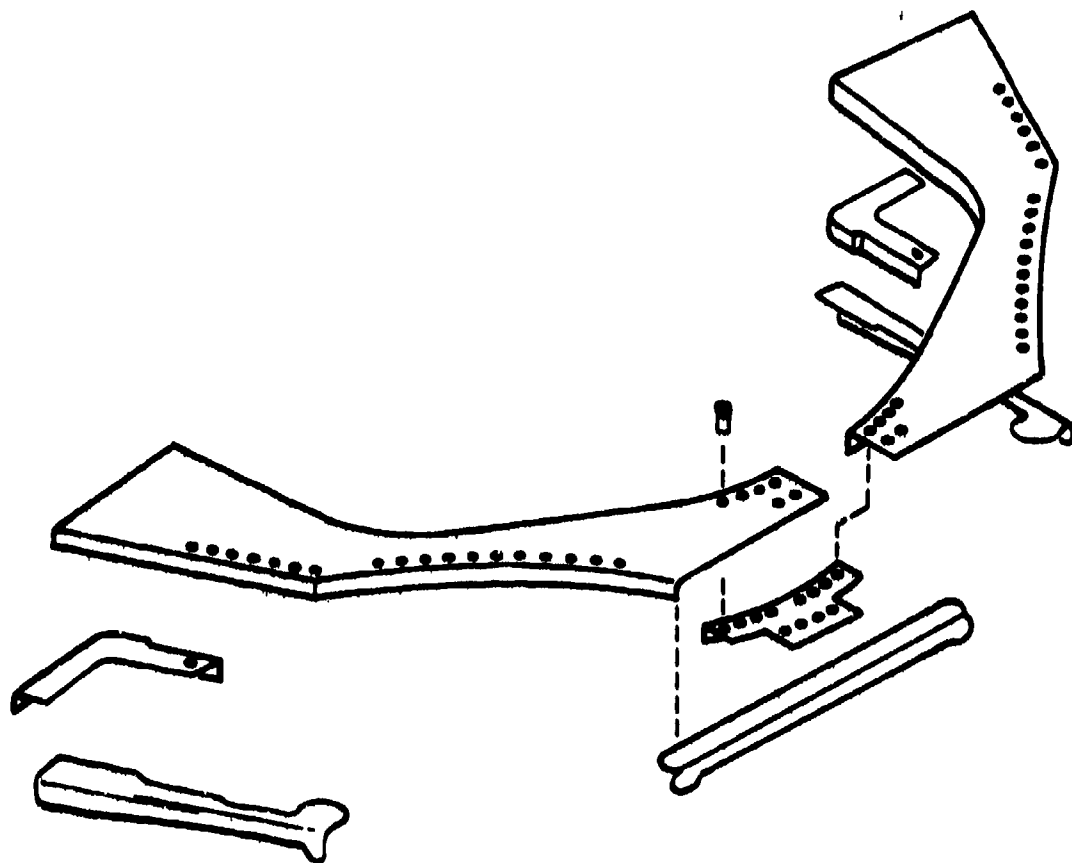
Figure 119.   Conventional design, nacelle forward frame.

195
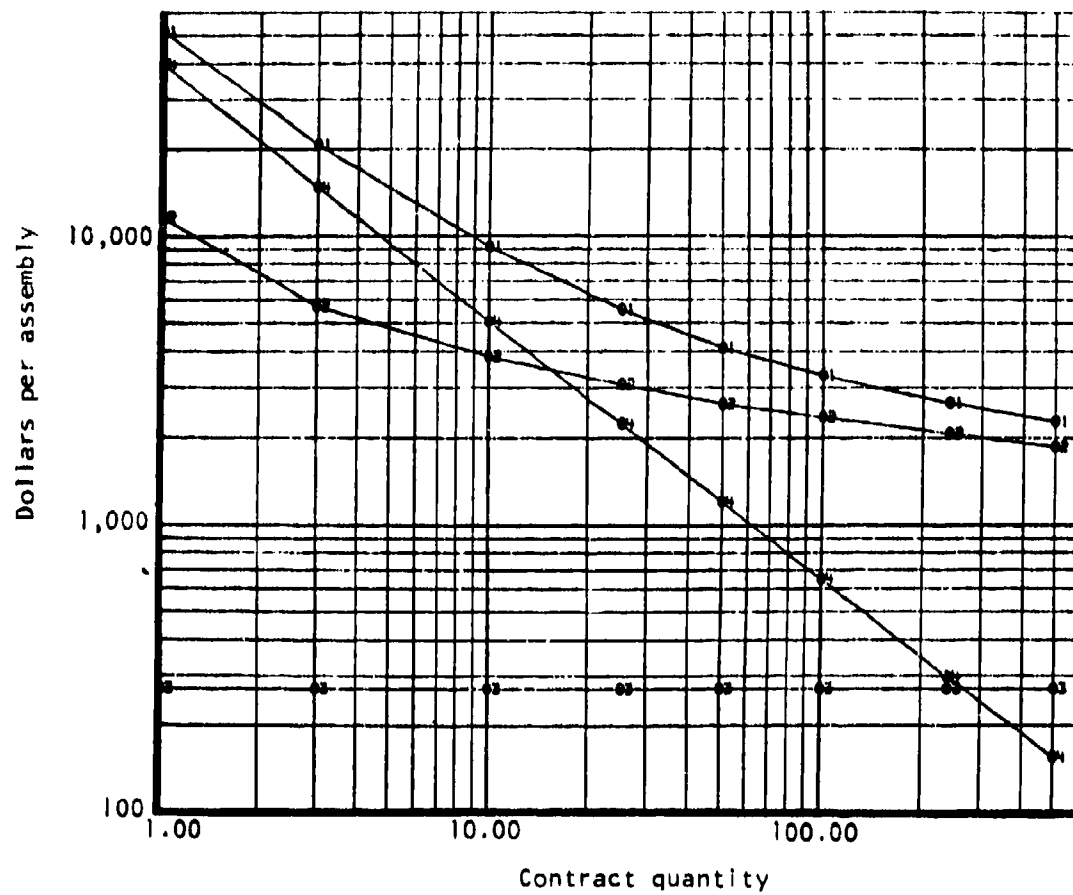
1. Total cost
2. Fabrication cost
3. Material cost
4. Tooling cost

Figure 120. Effect of quantity on cost - forward nacelle frame -
hot size form.

196

1. Total cost
2. Fabrication cost
3. Material cost
4. Tooling cost
5. Purchased labor cost
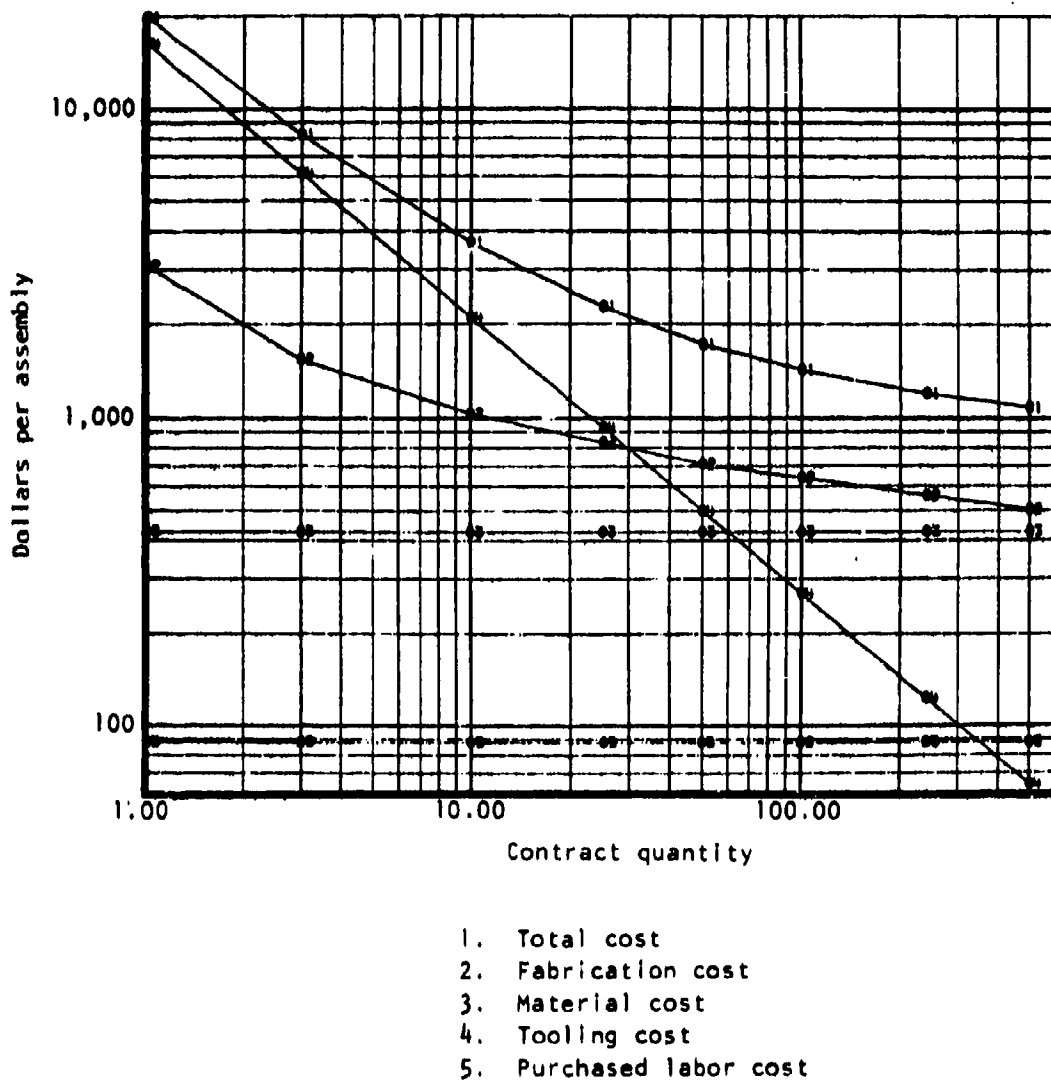
Figure 121. Effect of quantity on cost - forward nacelle frame - superplastic form
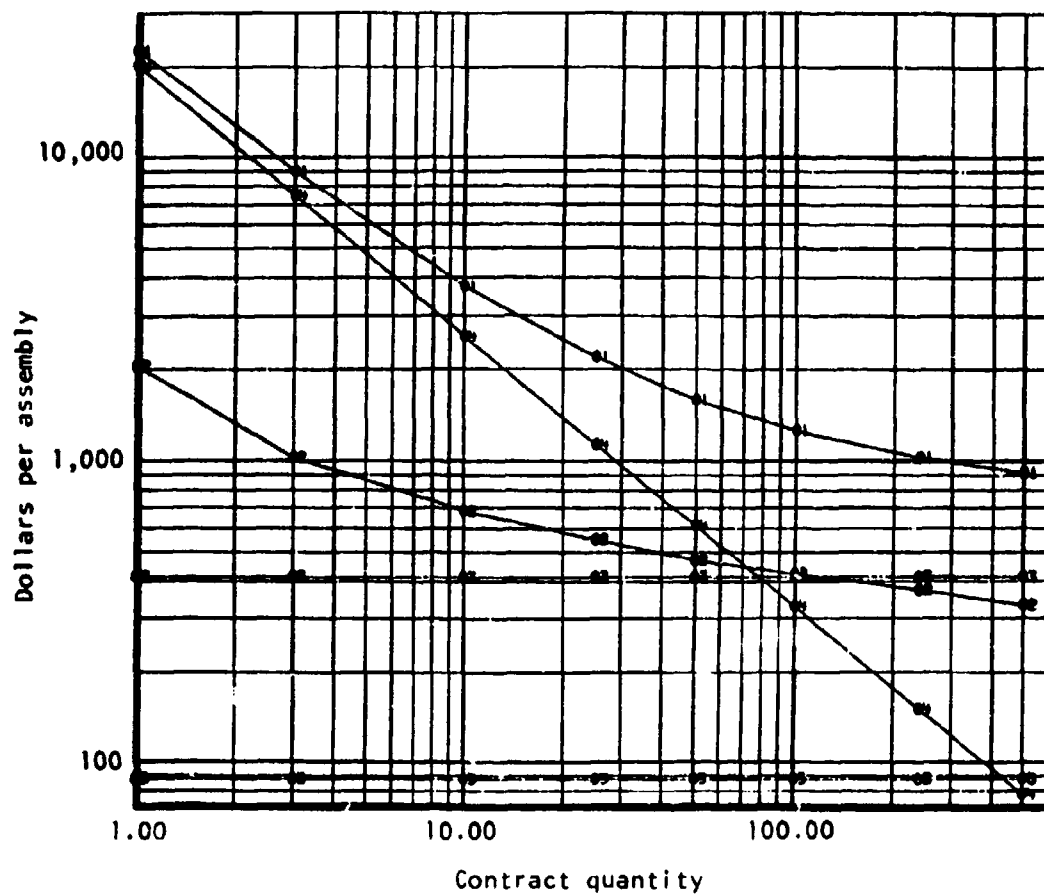
197

Figure 122. Effect of quantity on cost - forward nacelle frame - superplastic form two per cycle.
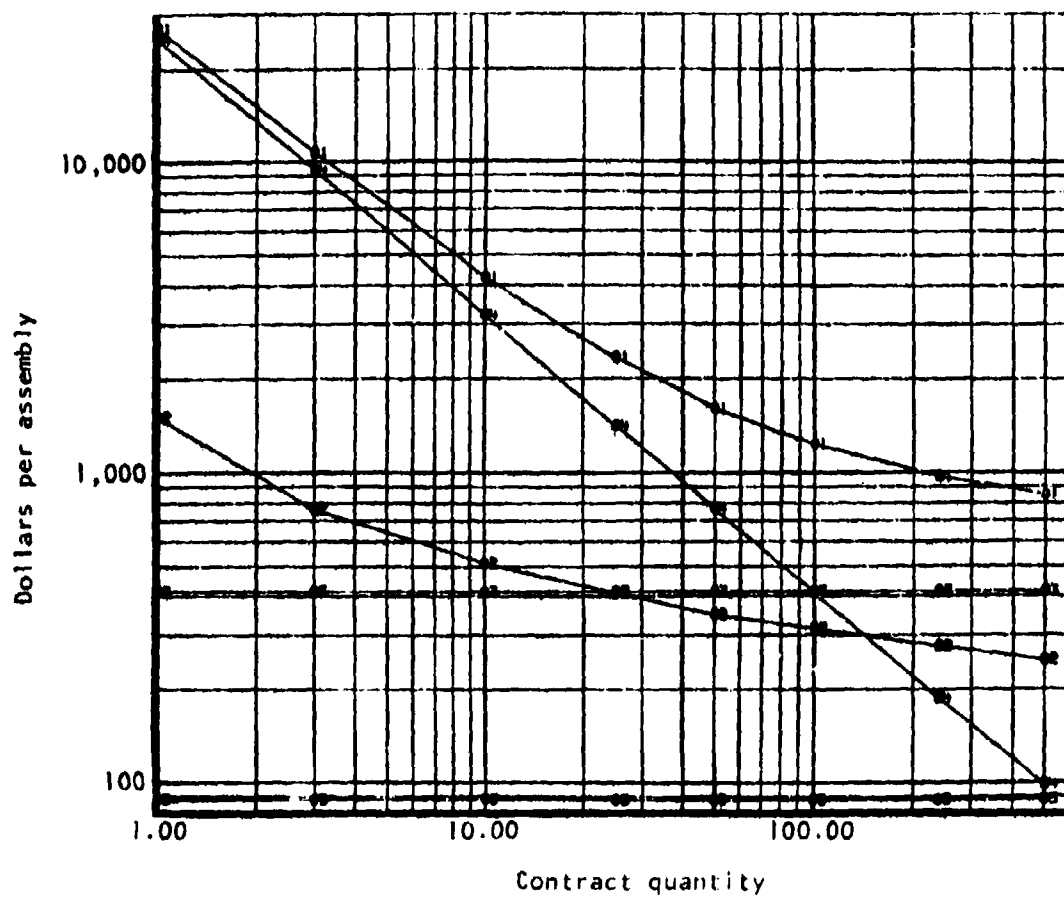
1. Total cost
2. Fabrication cost
3. Material cost
4. Tooling cost
5. Purchased labor cost

1. Total cost
2. Fabrication cost
3. Material cost
4. Tooling cost
5. Purchased labor cost

Figure 123. Effect of quantity on cost - forward nacelle frame - superplastic form four per cycle.
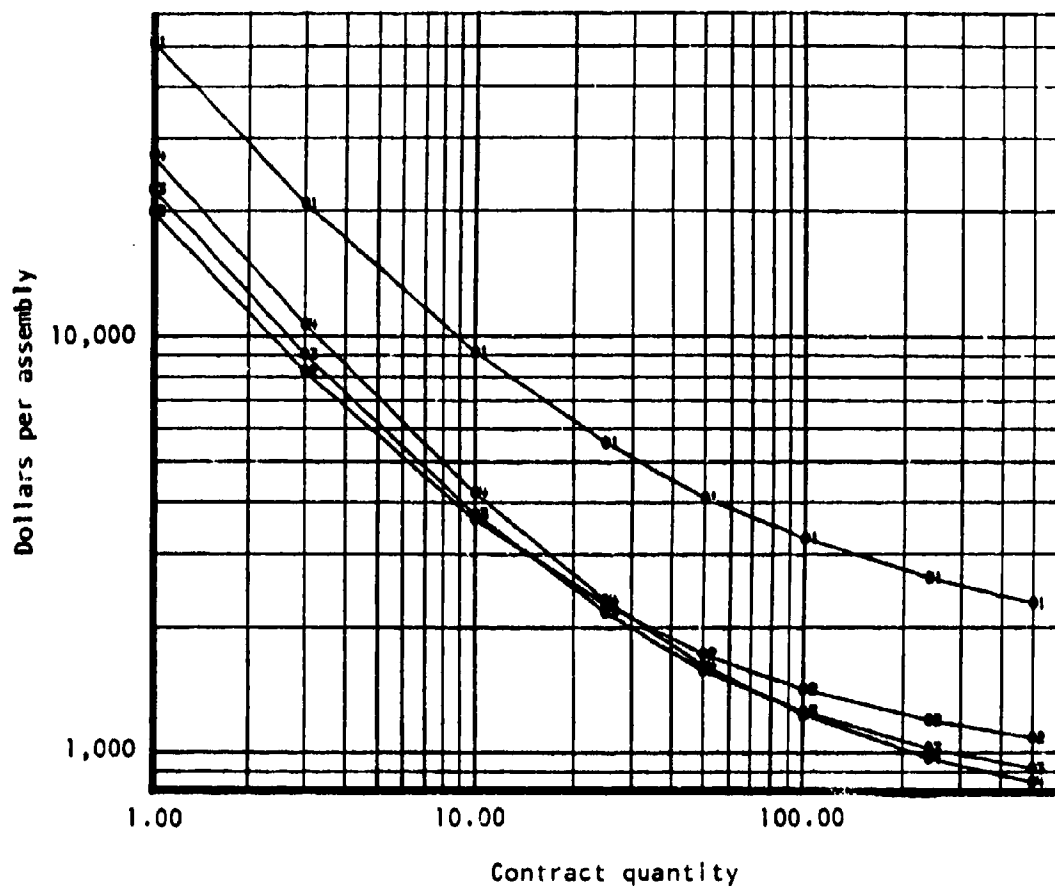
199

1. Hot size form
2. Superplastic form
3. Superplastic form two parts per cycle
4. Superplastic form four parts per cycle

Figure 124. Effect of quantity on cost - forward nacelle frame.

Nacelle Aft Center Beam Frame

The cost trade studies for the aft frame included several comparisons as follows:

Group A

1. The frame and a doubler, both preformed and hot sized

2. The frame superplastically formed, and the doubler preformed and hot sized

3. Two frames superplastically formed simultaneously, and the doubler preformed and hot sized

4. Four frames superplastically formed simultaneously, and the doubler preformed and hot sized

In the preceding cases, the assembly is completed by mechanically fastening the doubler to the frame. The result of the cost study is shown in Figure 125 and indicates an insignificant cost difference between SPF and hot sizing. This result was expected, since the frame or the frame assembly was not redesigned, but was considered in the comparison as an identical design.

Group B

1. The frame and a doubler, both preformed and hot sized

2. The frame was redesigned to incorporate integral return flanges and beads (shown in Figure 126), which replace doublers and fasteners, and was superplastically formed

3. Two redesigned frames superplastically formed simultaneously

4. Four redesigned frames superplastically formed simultaneously

In each of the preceding cases, the doubler and the mechanical fasteners were eliminated by the redesign. Chemical milling was employed in the beaded areas of the redesigned part to obtain desired thickness and reduce weight. Figure 127 shows the results of the study and indicates that hot sizing and SPF are similar in cost in low-quantity production, but based on a large quantity, the cost reduction for SPF becomes substantial.
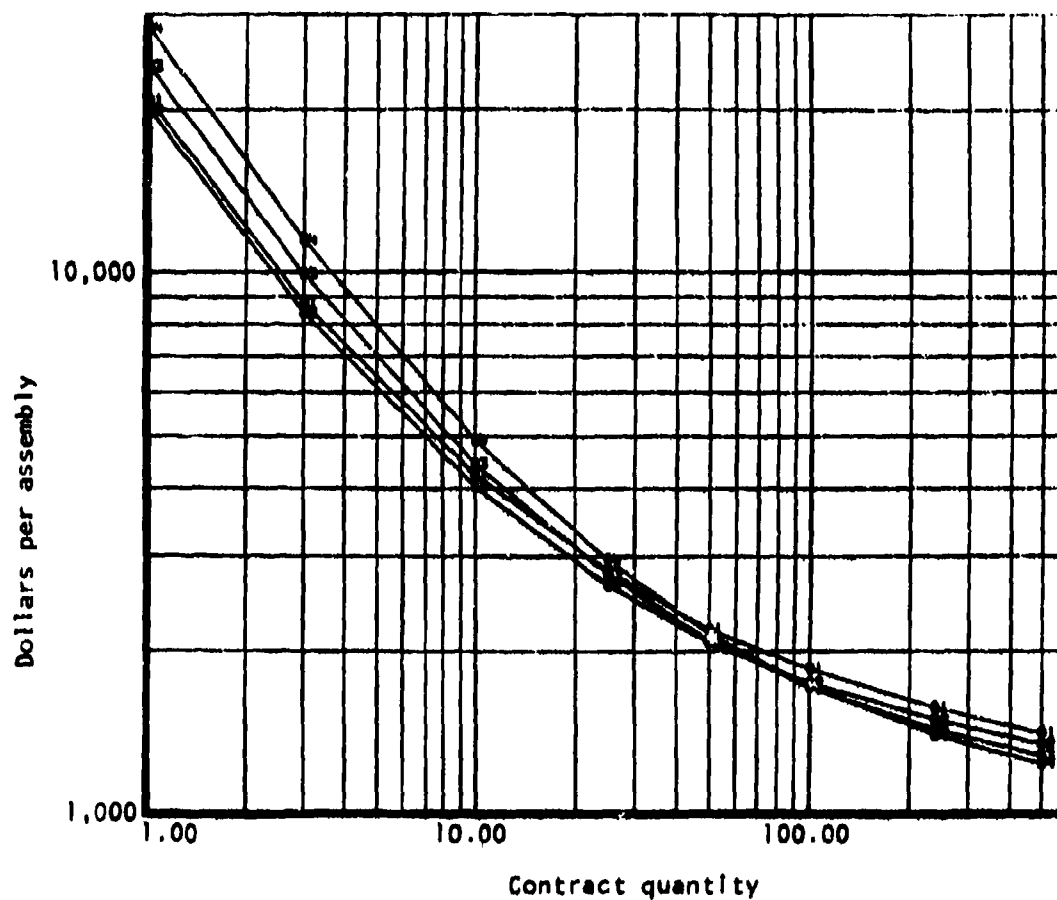
Figure 125. Effect of quantity on cost-aft fuselage frame.

1. Hot size form
2. Superplastic form
3. Superplastic form two parts per cycle
4. Superplastic form four parts per cycle

Conventional
design, nacelle
aft frame

Superplastic formed
design concept,
nacelle aft frame
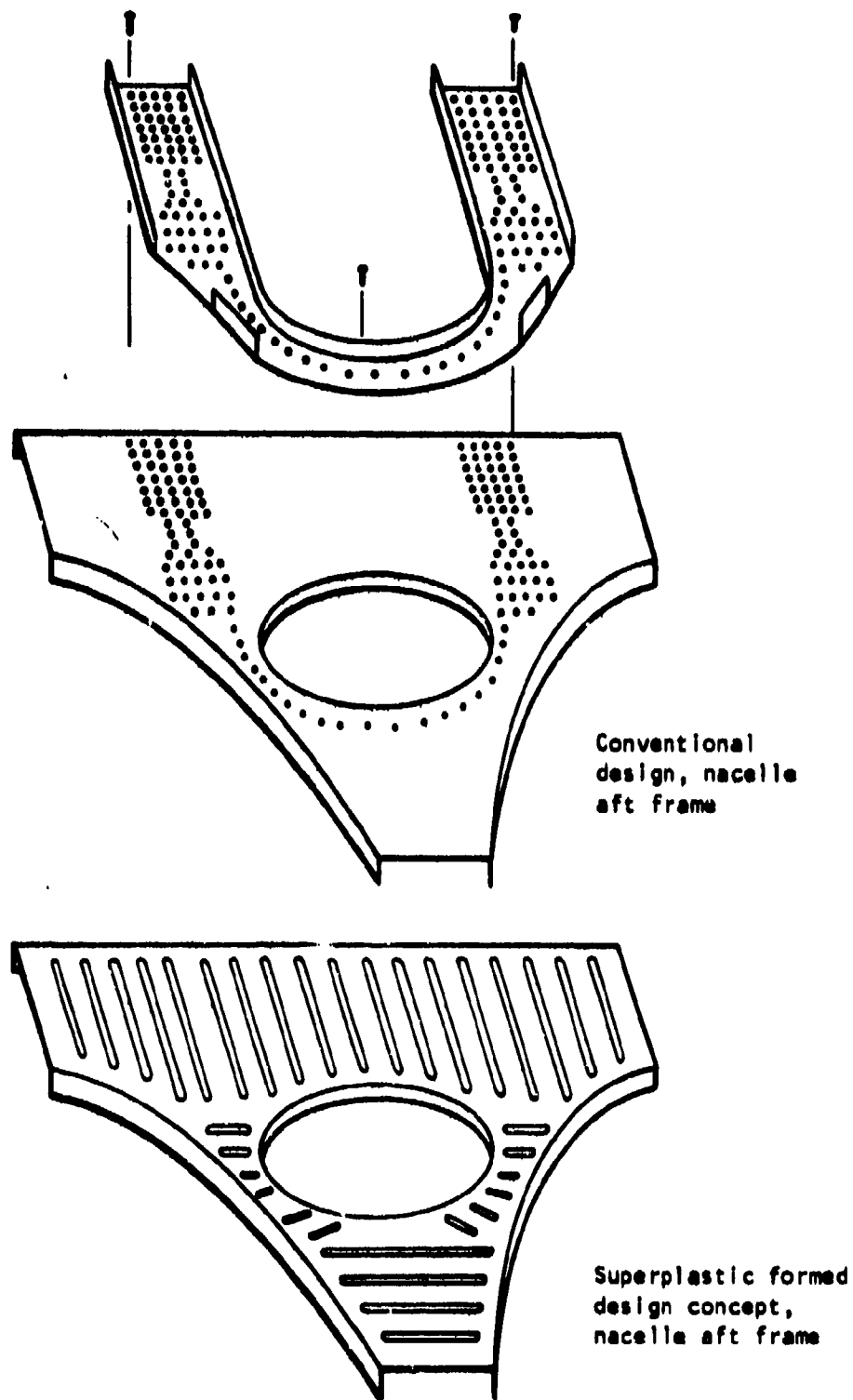
Figure 126. Aft frame redesigned.
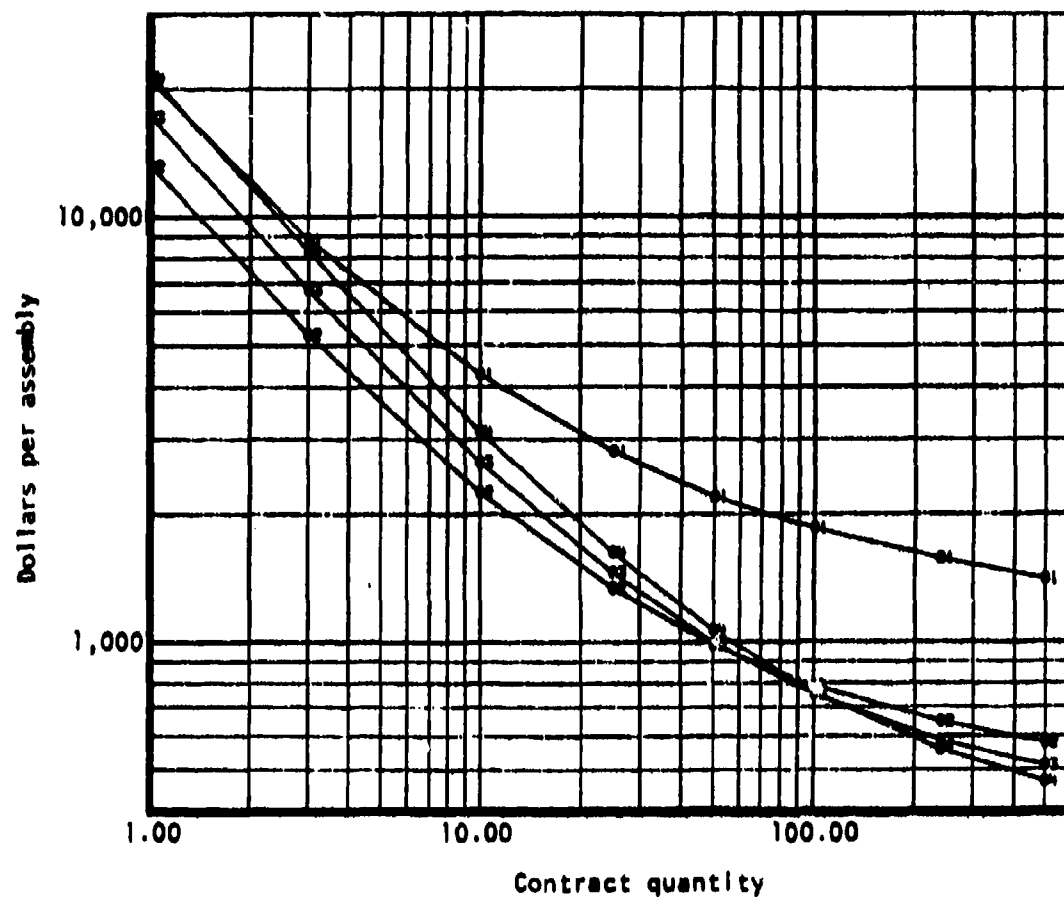
Figure 127. Effect of quantity on cost - aft fuselage frame.

Legend for figure:

1. Hot size form
2. Superplastic form
3. Superplastic form two parts per cycle
4. Superplastic form four parts per cycle

Axis labels:
- Vertical: Dollars per assembly
- Horizontal: Contract quantity

204

Superplastic forming a number of parts simultaneously does not appear to offer any cost advantages when small production quantities are considered. A small cost reduction in multiple forming is indicated when production quantity reaches a high level. As in the forward frame study shown in Figure 124 and in the aft frame study shown in Figure 127, a substantial cost reduction is offered by a complex one-piece part as a replacement for a multiple-piece assembly.

PHASE III - PROCESS EXTENSION

The objective of this phase of the program was to extend the phase II manufacturing process to demonstrate the applicability of the superplastic forming (SPF) technique to a titanium alloy other than Ti-6Al-4V. This was accomplished by fabricating and testing a second titanium alloy, utilizing the forward frame tooling and design.

ALLOY SELECTION

Alternate titanium alloys selected for this phase of the program were based on the criteria that material would be commercially available, be applicable to aircraft structures, demonstrate superplastic properties, have a strength-to-weight efficiency compared to Ti-6Al-4V, and be usable in the as-formed condition.

Beta titanium alloys were not under consideration as candidates, since Rockwell's experience has shown that these materials, although strain-rate sensitive at high temperatures, were only marginally superplastic. Values of m were generally less than 0.5.

Based on the aforementioned criteria, the titanium sheet alloys selected for screening tests for applicability to phase III activity were Ti-6Al-6V-2Sn, Ti-6Al-2Sn-4Zr-2Mo, and Ti-8Al-1Mo-1V.

MATERIAL CHARACTERIZATION

Specimens from each of the three materials (one heat for each alloy) were subjected to high-temperature tensile tests to establish the superplastic properties. The flow stresses of each alloy were measured under vacuum over a range of strain rates from 1.67×10^{-6} in./in./sec to 1.67×10^{-3} in./in./sec at three different temperatures (1,625°, 1,700°, and 1,775° F). These strain-rate ranges bracket the region in which maximum superplasticity was anticipated for these alloys. The data from these tests are shown in Table 43 and Figure 128.

Ti-6Al-2Sn-4Zr-2Mo exhibited the lowest flow stresses of the three alloys, as shown in Figure 129, a characteristic which is highly desirable in SPF, since lower pressures and/or shorter forming times would be possible. The maximum m value varied from 0.66 to 0.72, indicating that the material is in fact superplastic and should be suitable for forming the nacelle forward frame parts. Ti-8Al-1Mo-1V exhibited the highest m values of the three, but the flow stresses were higher than for Ti-6Al-2Sn-4Zr-2Mo. Ti-6Al-6V-2Sn exhibited comparatively low m values and higher flow stresses, a combination

206

TABLE 43. FLOW STRESS PROPERTIES OF THREE PHASE III
CANDIDATE ALLOYS AT THREE DIFFERENT TEMPERATURES

Titanium Alloy	Test temperature (° F)	m_{max}	Flow stress at m_{max} (ksi)
8-1-1	1,775	0.84	0.190
	1,700	0.77	0.272
	1,625	0.92	0.268
6-6-2	1,775	0.61	0.392
	1,700	0.47	0.312
	1,625	0.43	0.350
6-2-4-2	1,775	0.70	0.246
	1,700	0.72	0.192
	1,625	0.66	0.540

which made this alloy less desirable for forming the structural parts.
Ti-6Al-2Sn-4Zr-2Mo was selected over Ti-8Al-1Mo-1V because of its lower flow
stress and because it is considered to be of greater potential interest for
airframe applications.

PROCESS PARAMETER SELECTION

The process parameters established for SPF Ti-6Al-2Sn-4Zr-2Mo were
selected on the basis of the stress-strain rate properties determined for this
material. These properties showed similar behavior to the Ti-6Al-4V material
used to fabricate the forward frames in phase II. The forming parameters
selected for this phase were therefore the same as for the forward frames pre-
viously produced.

TOOLING

The tooling assembly used for fabricating the forward frame of Ti-6Al-
2Sn-4Zr-2Mo was the same tooling used in phase II. No modifications were
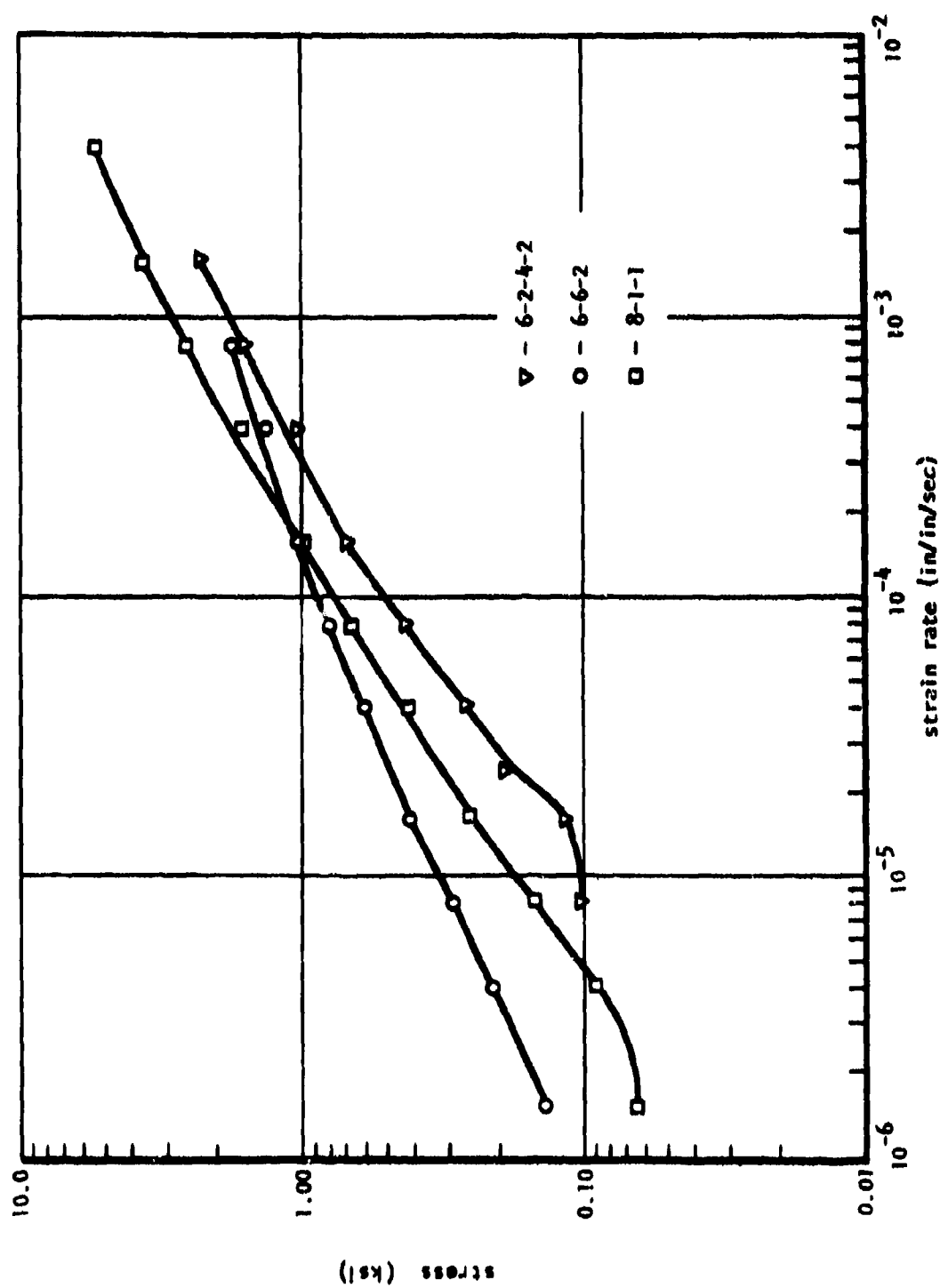
Figure 128. Flow stress–strain rate curves of candidate alloys for phase III forming studies at 1,700° F.

208
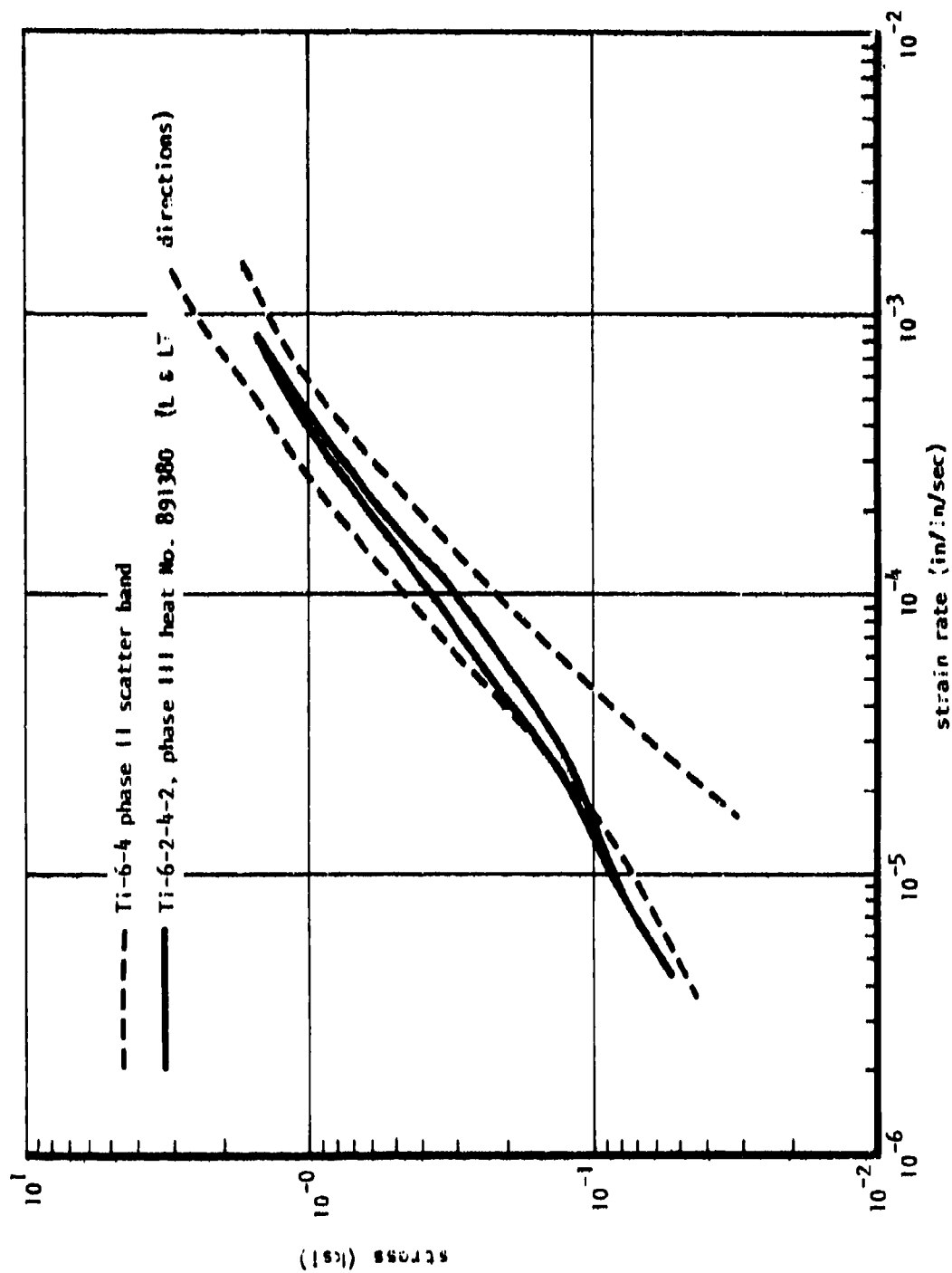
Figure 129. Comparison of high-temperature flow properties between Ti-6-4 and Ti-6-2-4-2 alloys.

209

necessary, with the exception of general refurbishment and verification of the required configuration through a template check.

COMPONENT FABRICATION

The fabrication procedure for the phase III part was conducted in the same manner as the fabrication of the phase II parts. The same equipment and forming cycles were utilized, and a total of three nacelle forward frames were superplastically formed with Ti-6Al-2Sn-4Zr-2Mo. Table 44 shows the parameters used for the forming runs, and the results. The resulting formed parts substantiated the suitability of the forming parameters selected, and demonstrated that the process can be extended to other titanium alloys on the basis of high-temperature superplastic properties.

Ti-6Al-2Sn-4Zr-2Mo forward frames were successfully formed to provide two parts for structural test and one part for destructive tests. The configurations were well defined, using parameters identical to phase II. Parts FF-12 and FF-14 were trimmed, cleaned, and chemical milled in preparation for structural test.

Forward frame 13 exhibited a somewhat larger fillet radius than required for structural test in the narrow sections of the part legs. This was the result of lower temperatures in those areas which was caused by temperature control difficulties encountered with this part, and is not related to the formability of the alloy used. The problem could be rectified by a

TABLE 44. PHASE III FORWARD FRAME PARAMETERS

Part No.	Temperature (° F) (during form cycle)	Argon Gas Pressure						Time at press. (hr)	Remarks
		Prior to form		During form		After form			
		Top	Bottom	Top	Bottom	Top	Bottom		
FF-12	1,700-1,745	1	1	165	0.5	1	0.5	2.5	Well formed
FF-13	1,630-1,750	1	1	165	1	5	3	0.75	Part not fully formed in radii
FF-14	1,660-1,745	1	1	165	1	5	3	1.25	Well formed

re-forming cycle, as was demonstrated for part FF-11. It was determined that the large radii would not interfere with or influence destructive test and evaluation; therefore, the part was used for this purpose.

METALLOGRAPHIC EVALUATION

The surface enrichment was examined in the prolongation section for all three frames produced. In addition, samples were taken within the body of frame FF-13, which was cut for mechanical properties evaluation. Results of the enrichment depth measurements are shown in Table 45 and specimen locations are identified in figure 130. It can be seen from Table 45 that the top surfaces were free from any enrichment. The bottom surface showed 0.004- to 0.006-inch enrichment in the prolongation area as well as in the frame body. Except for the shallower depth, this is also the characteristic observed for the forward frame formed in phase II.

TABLE 45. PHASE III NACELLE FORWARD BEAM FRAME SURFACE
ENRICHMENT MEASUREMENTS

Sampling Area	Part No.	Specimen location	Enrichment top surface	Depth (in.) bottom Surface
Prolongation	FF-12	-5	Nil	0.005
		-6	Nil	0.005
	FF-13	-1	Nil	0.006
		-2	Nil	0.005
		-5	Nil	0.004
		-6	Nil	0.006
	FF-14	-1	Nil	0.004
		-2	Nil	0.006
Body of frame	FF-13	-8	Nil	0.004
		-9	Nil	0.005
		-10	Nil	0.004
		-12	Nil	0.006

211
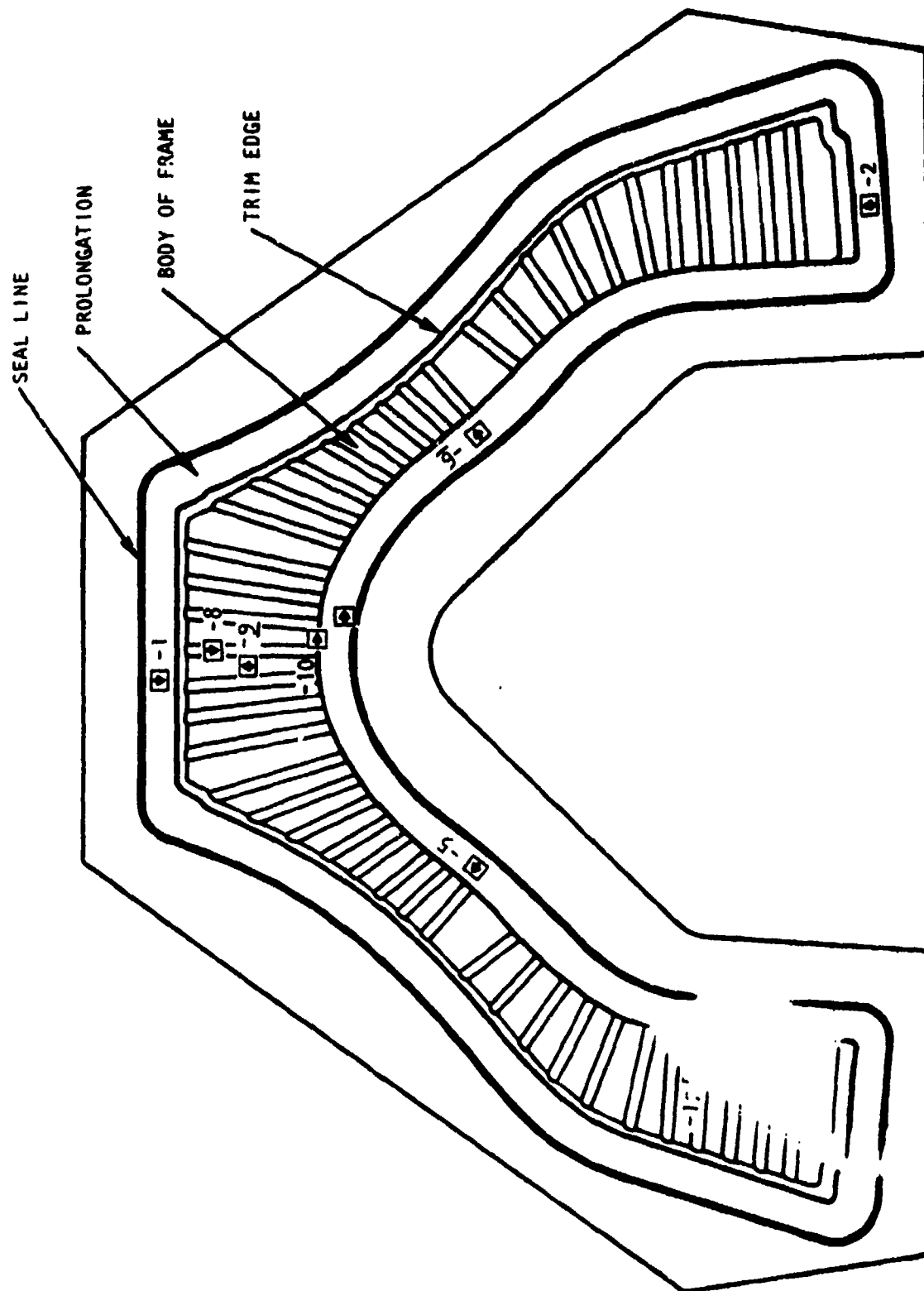
Figure 130. Locations of metallurgical specimens for surface enrichment measurements, nacelle forward center beam frames, phase III.

CHEMICAL MILLING

Frames FF-12 and -14 were chem-milled to remove the surface enrichment and to produce the desired contour for the structural testing. The source and processing procedures were the same as those used in chem-milling phase II parts. Results of interstitial content determinations for the coupons before and after the chem-milling are shown in Table 46. The hydrogen pickup was only 8 ppm, and the cumulative hydrogen content was 49 ppm, which were well below the maximum allowed by the specification. Final thicknesses in the web and flange areas of section B-B were 0.021 and 0.025 inch, respectively, somewhat thicker than the 0.016-inch thickness permissible in the beaded web area. The stresses in the structural testing were, therefore calculated based on this actual thickness in the test area.

DIMENSIONAL INSPECTION

Frames FF-12 and FF-14 were dimensionally inspected for thickness profiles at the locations shown in Figure 93, which were the same as for phase II forward frame inspection location. Results of the thickness measurements and overall dimensions are shown in Tables 47 and 48. Comparisons between analytically predicted profiles and those of the actual measurements are shown in Figures 131 through 134. Except for bottom thicknesses of sections FF and GG, the analytical predictions were in good agreement with those of the experimental measurements. Sections FF and GG showed thicknesses generally 0.010 to 0.020 inch lower than those predicted. The discrepancy was anticipated because of the close proximity to the end flanges as discussed in phase II.

TABLE 46. HYDROGEN CONTENT BEFORE AND AFTER CHEM-MILLING - PHASE III

Frame type	Frames chem-milled	H_2 contents (% of weight)		
		Before CM	After CM	As rec'd
Forward	FF-12 FF-14	0.0041	0.0049	0.0051

213

TABLE 47. THICKNESS PROFILES AND WEB WIDTH FOR TWO NACELLE FORWARD
FRAMES PRODUCED UTILIZING Ti-6-2-4-2 ALLOY SHEET

| Section | Frame No. | Thickness (in.) | | | | | | | Web Width |
		t1	t2	t3	t4	t5	t6	t7	
A-A	AF-12	0.080	0.074	0.066	0.041	0.040	0.073	0.083	5.263
	AF-14	0.085	0.084	0.077	0.062	0.062	0.081	0.086	5.230
B-B	AF-2	0.073	0.069	0.059	0.038	0.043	0.069	0.079	3.115
	AF-14	0.075	0.072	0.061	0.057	0.059	0.071	0.081	3.075
C-C	AF-12	0.075	0.069	0.062	0.038	0.045	0.068	0.082	3.195
	FF-14	0.072	0.067	0.059	0.051	0.050	0.069	0.078	2.904
D-D	FF-12	0.077	0.072	0.063	0.051	0.050	0.068	0.073	2.790
	FF-14	0.077	0.069	0.063	0.058	0.055	0.067	0.070	2.812
E-E	FF-12	0.081	0.075	0.065	0.051	0.050	0.064	0.074	2.775
	FF-14	0.074	0.069	0.063	0.055	0.052	0.065	0.072	2.760
F-F	FF-12	0.082	0.072	0.062	0.045	0.050	0.073	0.083	5.218
	FF-14	0.084	0.080	0.059	0.048	0.047	0.072	0.080	5.258
G-G	FF-12	0.080	0.073	0.062	0.039	0.038	0.071	0.079	5.235
	FF-14	0.078	0.075	0.063	0.052	0.045	0.072	0.078	5.248

TABLE 48. OVERALL DIMENSIONS FOR THREE FORWARD FRAMES
PRODUCED UTILIZING Ti-6-2-4-2 ALLOY

| Location | Gap (in.) | | | Location | Gap (in.) | | |
	FF-12	FF-13	FF-14		FF-12	FF-13	FF-14
1	0.255	0.251	0.249	11	0.367	0.376	0.377
2	0.299	0.291	0.309	12	0.242	0.248	0.209
3	0.315	0.331	0.340	13	0.258	0.212	0.131
4	0.360	0.386	0.390	14	0.274	0.265	0.188
5	0.249	0.345	0.366	15	0.441	0.502	0.555
5	0.167	0.122	0.112	16	0.264	0.249	0.273
7	0.219	0.249	0.213	17	0.322	0.347	0.359
8	0.305	0.339	0.303	18	0.322	0.341	0.336

Figure 131. Comparison of analytical and experimental flange thickness profiles; FF-12 and FF-14; sections AA, DD and EE.
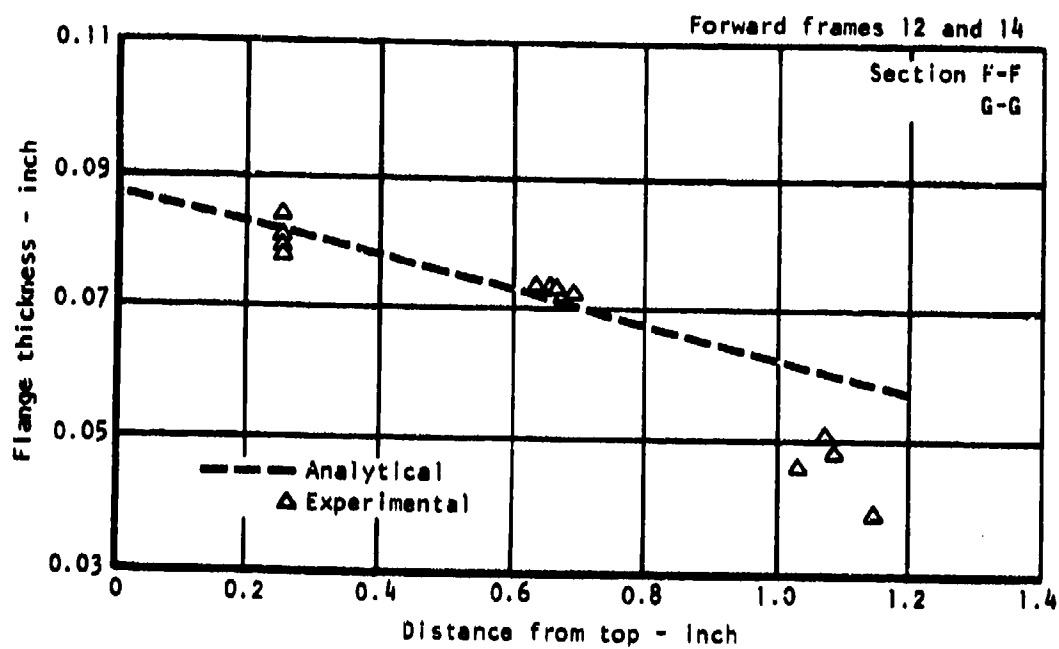
Figure 132. Comparison of analytical and experimental flange thickness profiles; FF-12 and FF-14; sections FF, GG, BB and CC.
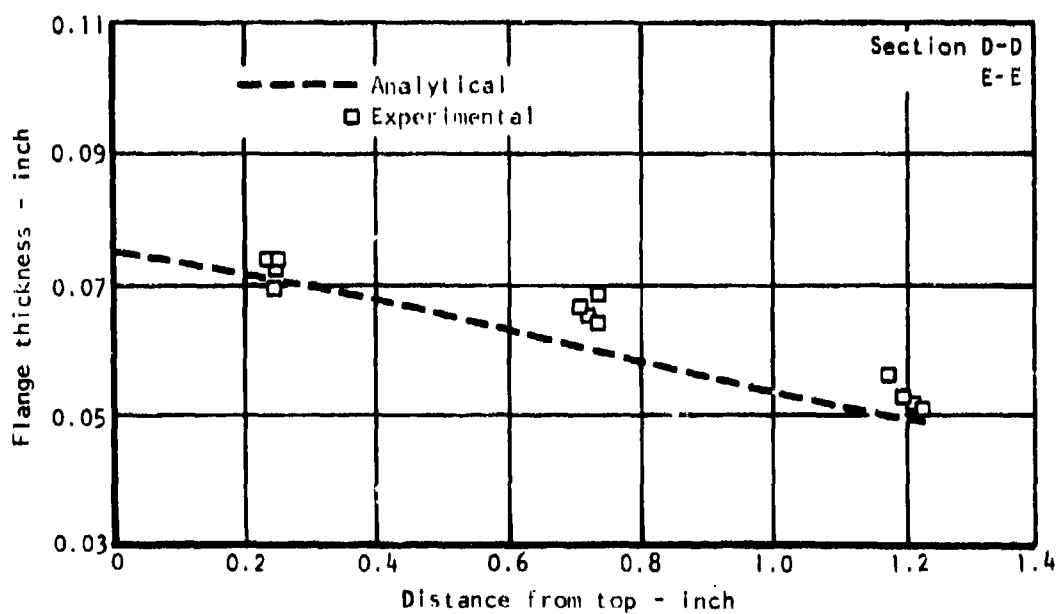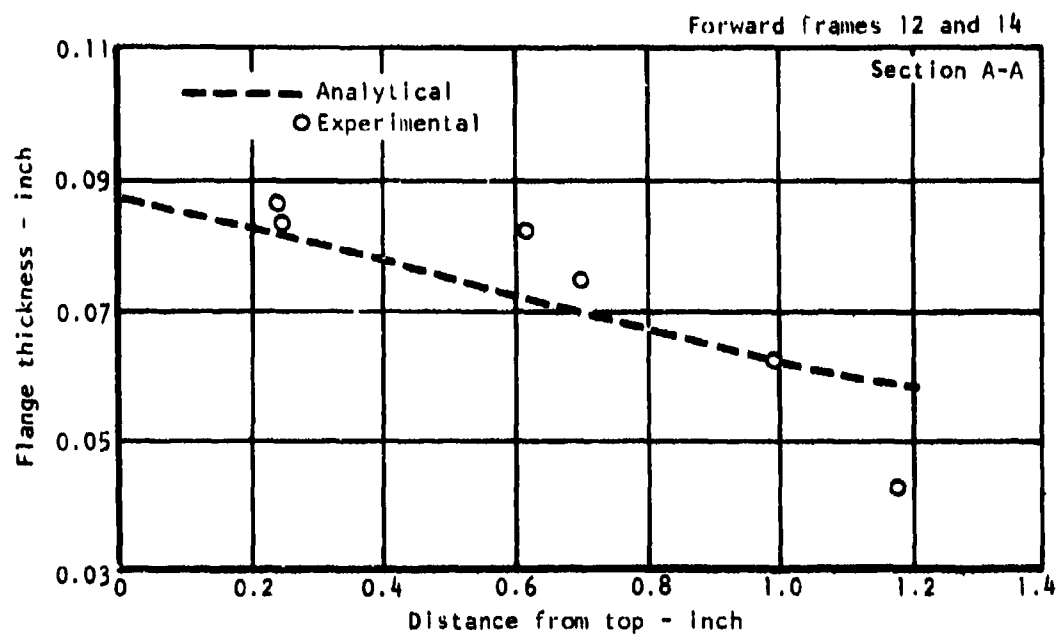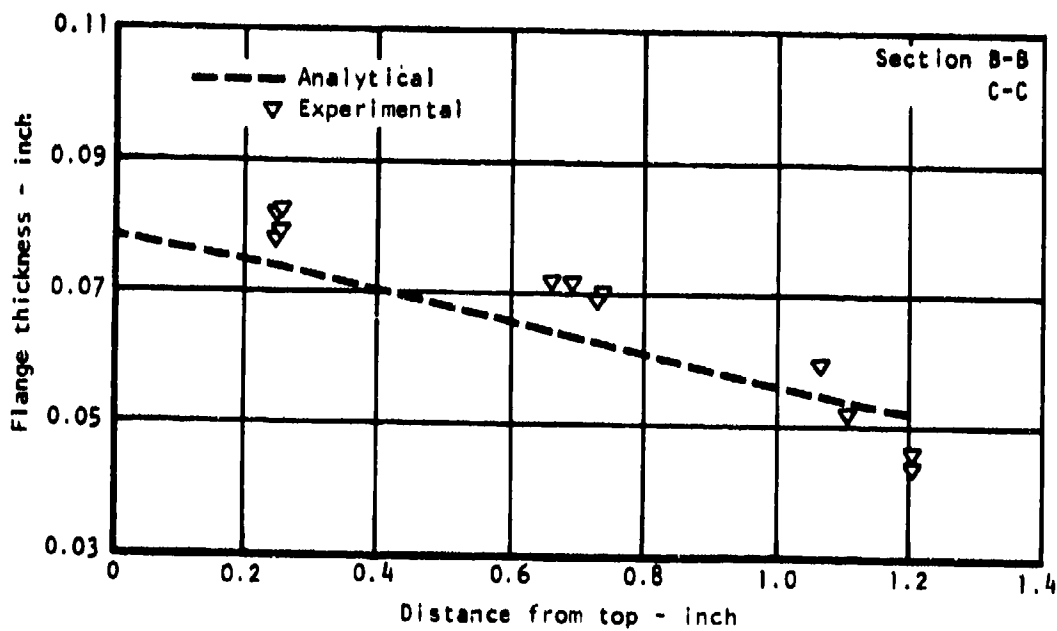
216
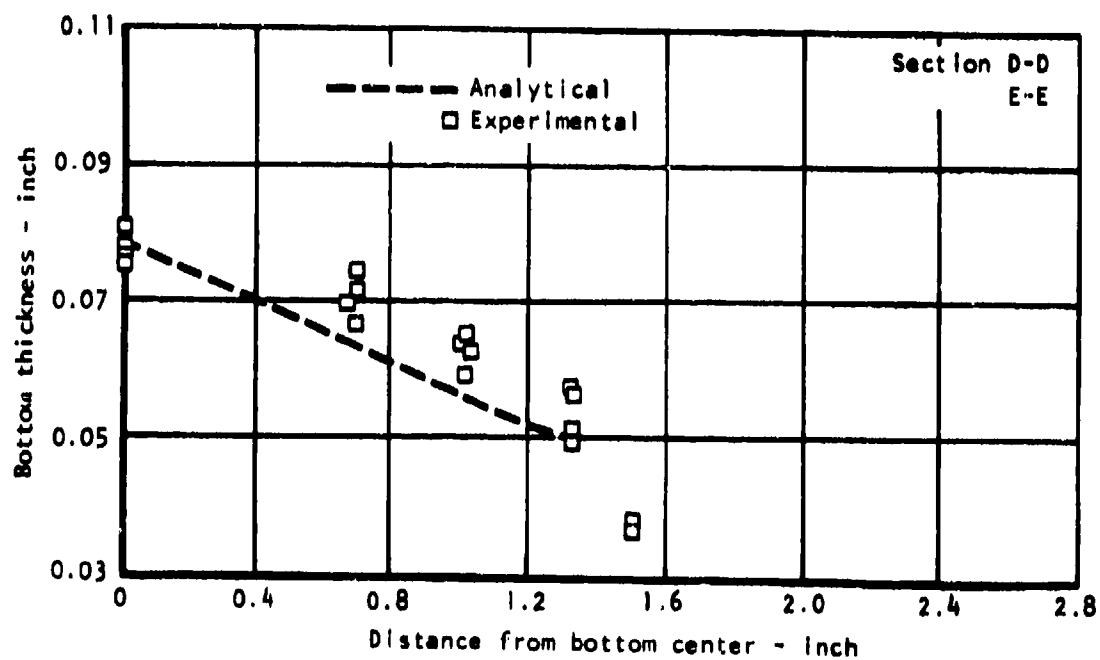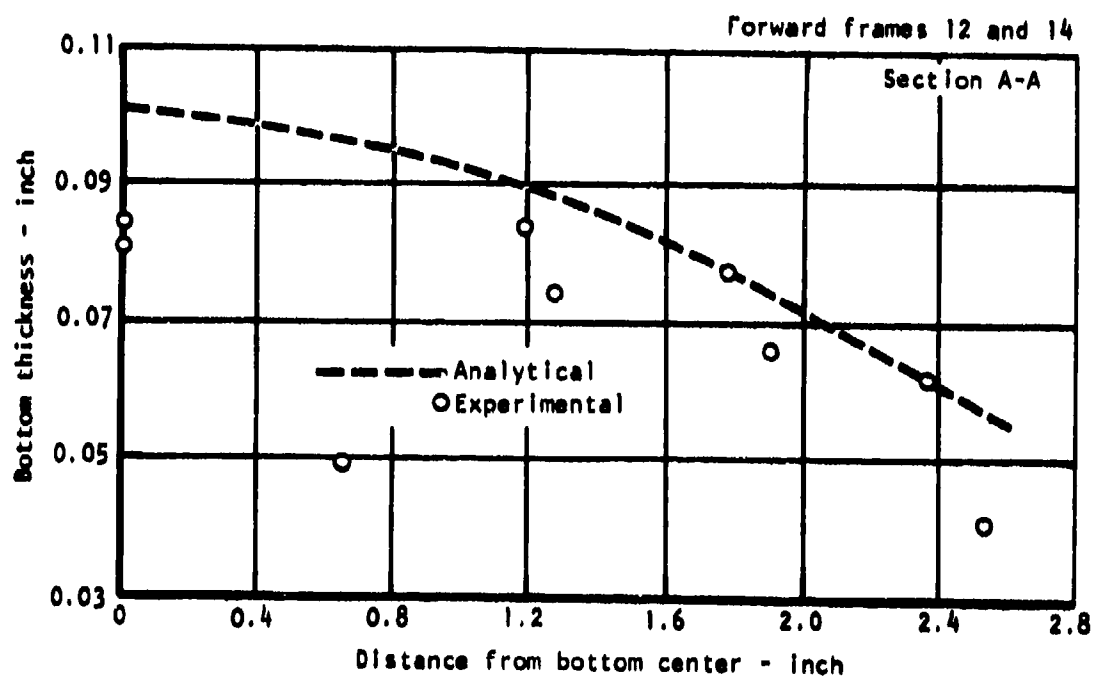
Figure 133. Comparison of analytical and experimental bottom thickness profiles; FF-12 and FF-14; sections AA, DD and EE.

217
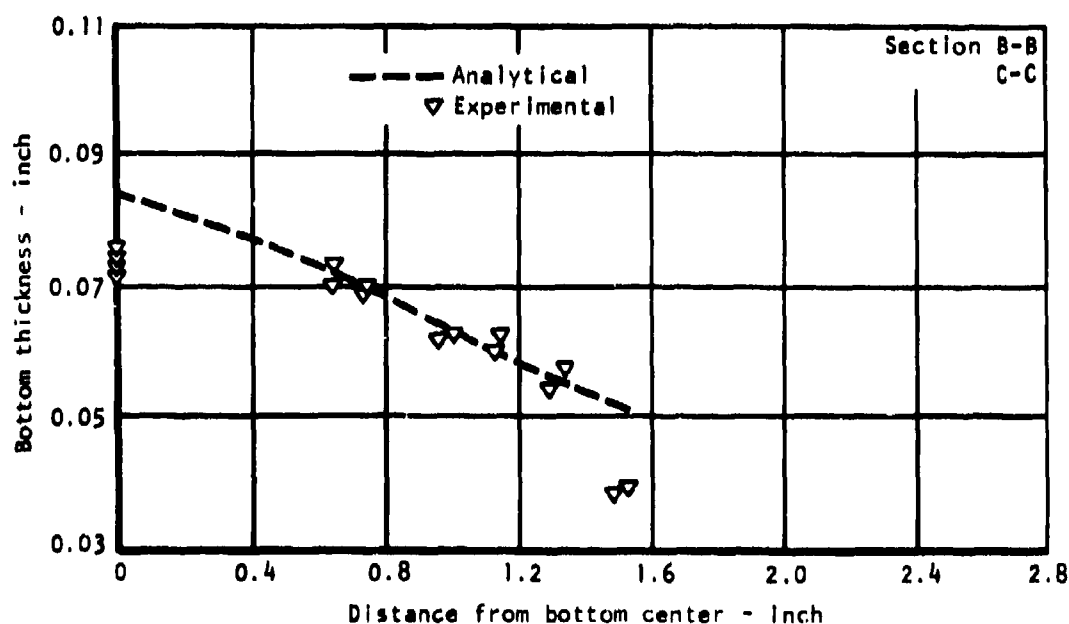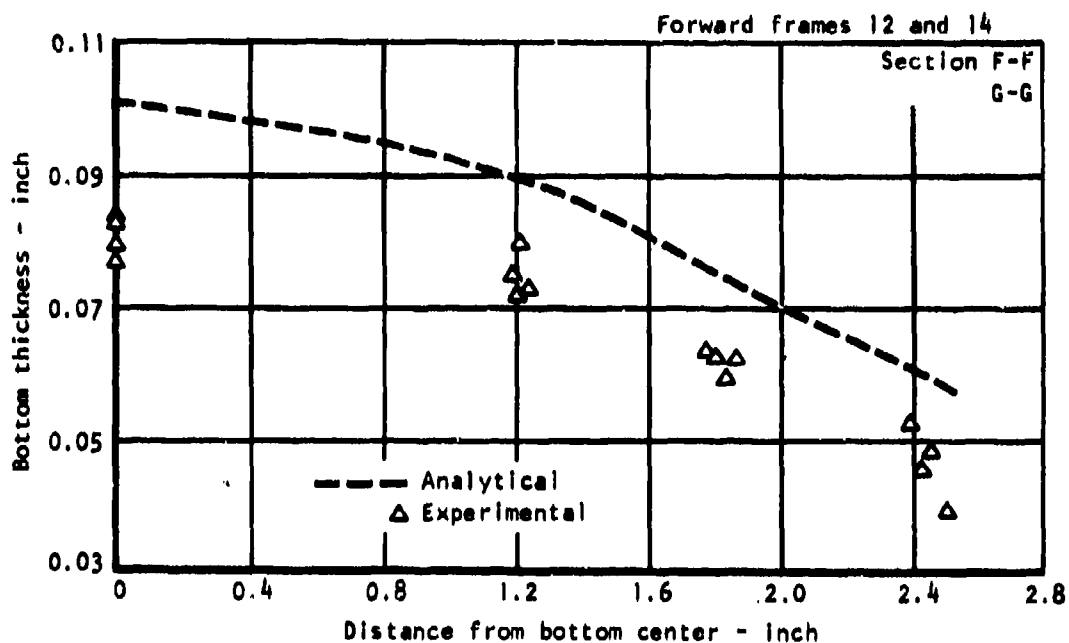
Figure 134. Comparison of analytical and experimental bottom thickness profiles; FF-12 and FF-14; sections FF, GG, BB and CC.

The overall dimensions for the three frames FF-12, -13 and -14 were measured employing the same procedures and inspection fixture used in inspecting phase II forward frames. Results of the measurements are shown in Table 48. Locations of the inspection points shown in the table are identified in Figure 135. The relative size changes between the three frames were calculated from Table 48 measurements and are summarized in Table 49. Adapting the method used in determining phase II forward frame dimensional changes, the average changes for the three phase III frames are illustrated in Table 49.

TABLE 49. DIMENSIONAL CHANGES FOR THE THREE FORWARD FRAMES PRODUCED UTILIZING Ti-6-2-4-2 ALLOY

Location	Dimensional changes (in.)		
	FF-12 - FF-13	FF-13 - FF-14	Avg
1	0.004	0.002	0.003
2	0.008	-0.018	-0.005
3	-0.016	-0.009	-0.013
4	-0.026	-0.004	-0.015
5	-0.096	-0.021	-0.059
6	0.045	0.010	0.028
7	-0.030	0.036	0.003
8	-0.034	0.036	0.001
11	-0.009	-0.010	-0.010
12	-0.006	0.036	0.015
13	0.046	0.081	0.064
14	0.009	0.077	0.043
15	-0.061	-0.053	-0.057
16	0.015	-0.024	-0.005
17	-0.025	-0.012	-0.019
18	-0.019	0.005	-0.007
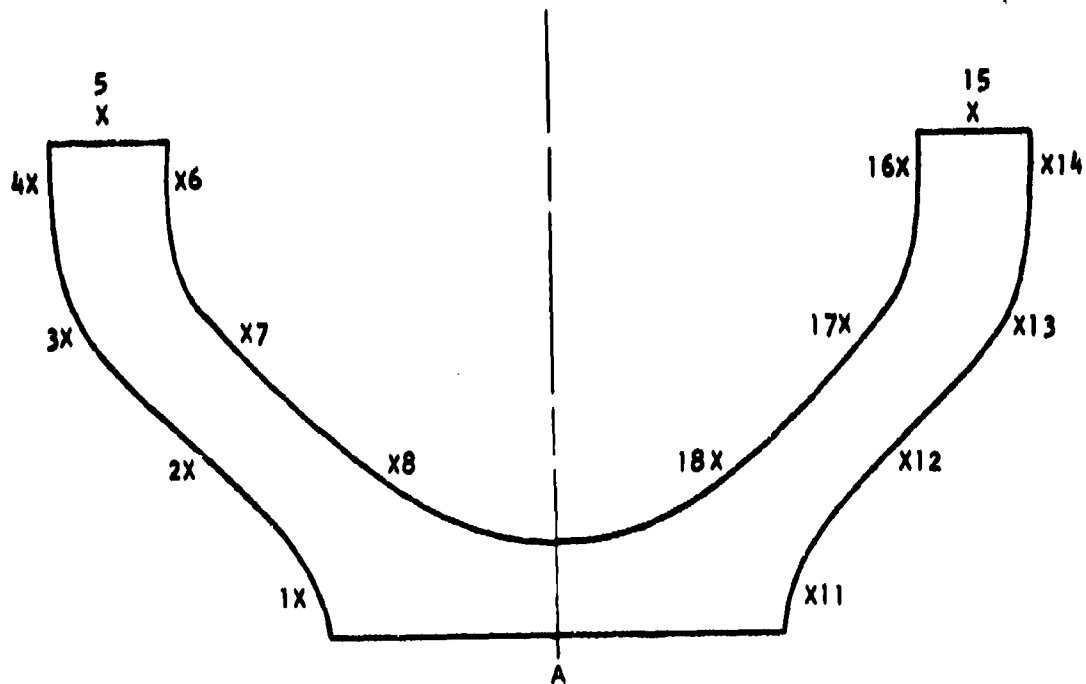
Figure 135. Location of inspection points for gap measurements, phase III, forward frames.

TABLE 50. SUMMARY OF HIGH-TEMPERATURE FLOW PROPERTIES AND
MICROSTRUCTURE IN THE AS-RECEIVED CONDITION FOR Ti-6-2-4-2
ALLOY USED IN PHASE III

m_{max} value			Avg grain size			
Heat No.	Orientation	Flow stress*	Acicular α	Blocky α	Uniform grain	Grain aspect ratio
8913180	L	0.76 - 0.51	None	None	Yes	~ 7
	LT	0.77 - 0.53				
*$\dot{\epsilon}$ = 1.67 x 10^{-4} sec^{-1}						

The overall dimensional changes between forming runs are comparable to
those observed for the Ti-6Al-4V frames (phase II), as would be expected,
since the same die and processing procedures were used.

TEST AND EVALUATION

METALLURGICAL

The heat of material used in forming phase III frames was examined in
the as-received condition for its microstructural characteristics and high-
temperature properties. In addition, the microstructure in the thermally
cycled (1,700° F) condition was also examined. Microstructures in the as-
received condition are shown in Figure 136 and in the thermally cycled con-
dition, in Figure 137. The high-temperature flow stress versus strain-rate
curves for the two grain directions are shown in Figure 138. Table 50 sum-
marizes criteria that affect the superplasticity of the material.

It is seen from the preceding that the material possesses uniform
microstructure and fine-grain size (5.1) without the presence of acicular
or blocky alpha. Extensive cold reductions in sheet rolling is evidenced
by the high grain aspect ratio of approximately 7. The heavy reduction did
not appear to have any effect on the forming characteristics at 1,700° F,
since the thermally cycled condition exhibited microstructure with complete
recrystallization (equiaxed grain), as shown in Figure 137. The strain-rate
sensitivity indexes for the two grain directions were 0.76 and 0.77, indicat-
ing that the material possessed adequate superplasticity at 1,700° F. This
was substantiated by the successful forming of the three forward frames
utilizing this heat of material.

(a)

(b)
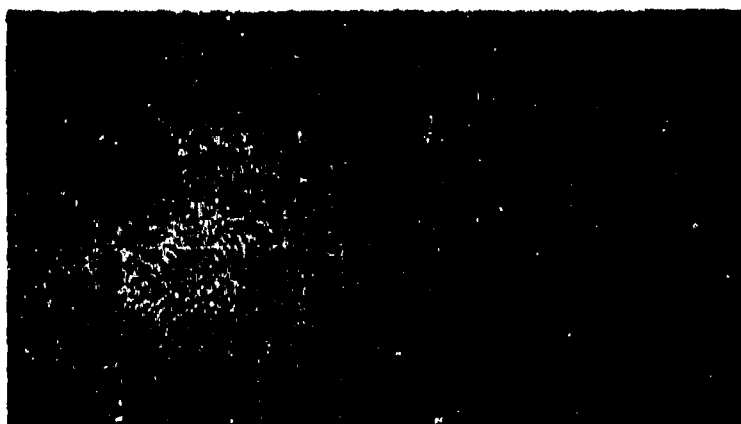
(c)

Figure 136. Typical microstructure of Ti-6-2-4-2, heat No. 891380 in
as-received condition showing uniform and fine grains.
Grain direction: (a) L, (b) LT, (c) ST, 500X.
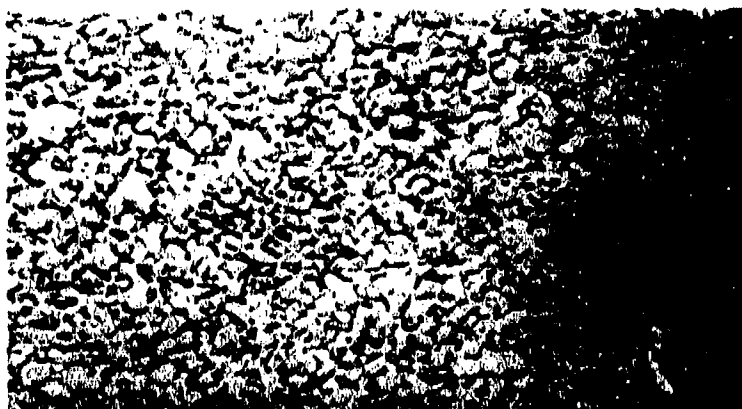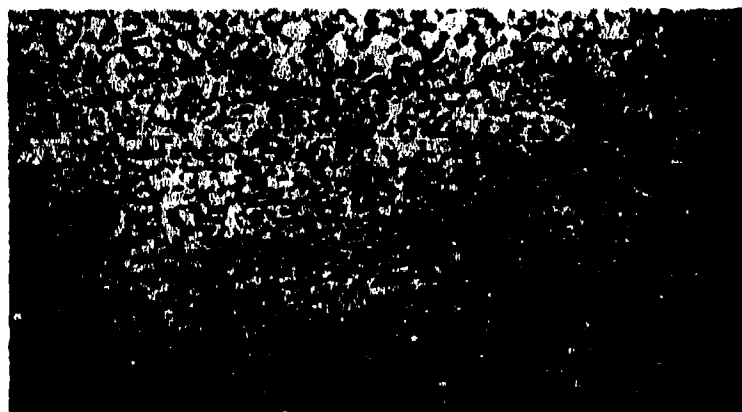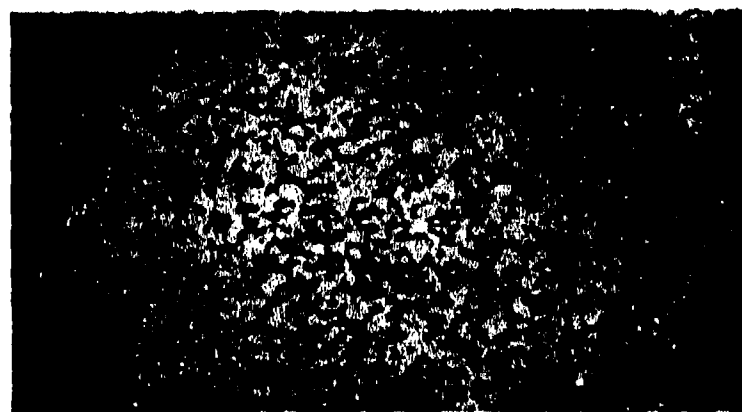
Figure 137. Typical microstructure of Ti-6-2-4-2, heat No. 891380 in
thermally cycled (1,700° F - 3 hours) condition showing completely
recrystallized grains. Grain direction: (a) L, (b) LT, (c) ST,
500X.
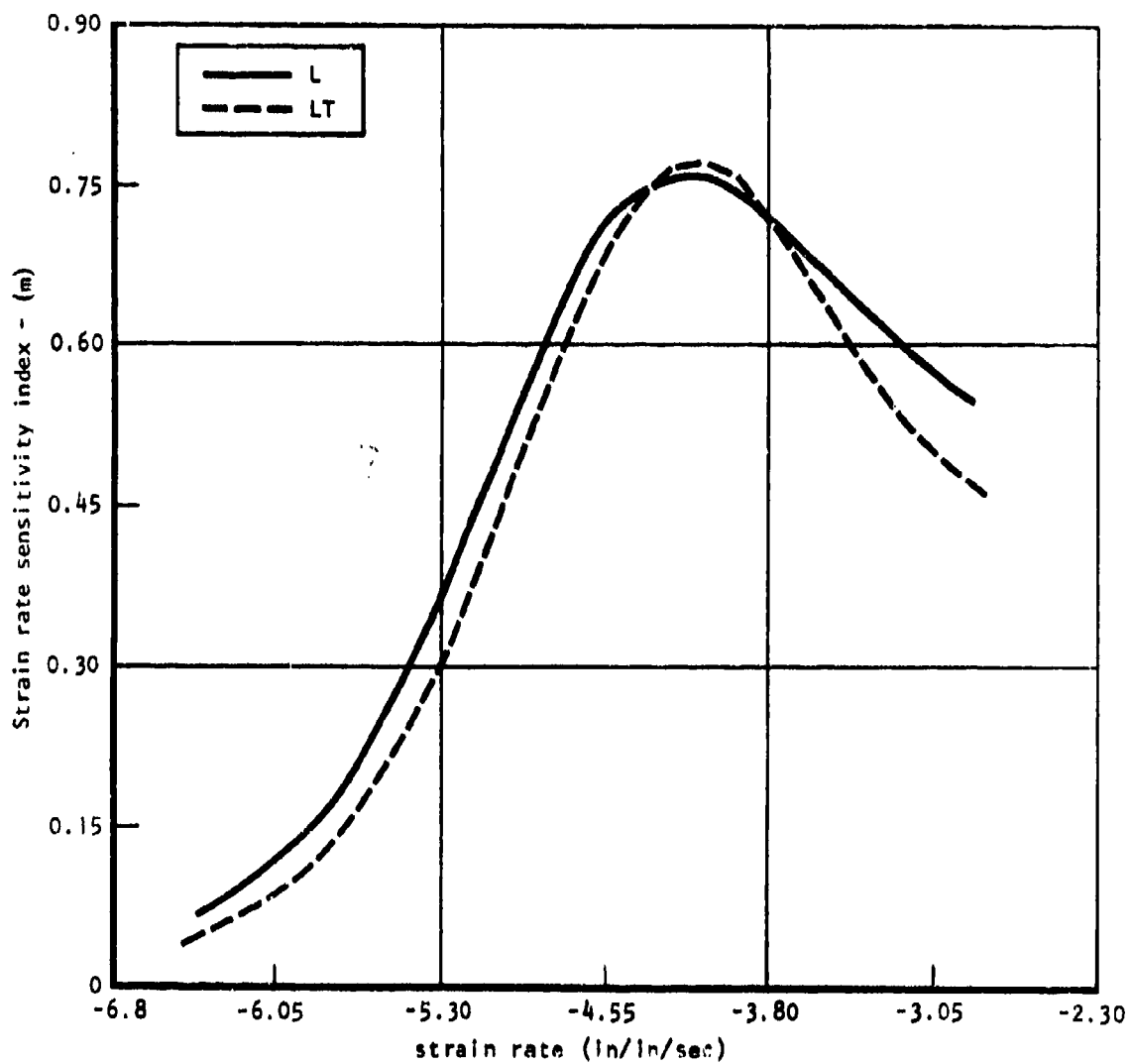
Figure 138. Strain rate sensitivity as a function of strain rate at 1,700° F for Ti-6-2-4-2 material (HT No. 891380) used in phase III study.

MECHANICAL PROPERTIES

One of the three frames produced, FF-13, was sectioned for mechanical property evaluations which included tensile, compression, and fatigue tests. In addition, material in the as-received and in the 1,700° F thermally cycled conditions were also tested for their mechanical properties, which formed a basis for the evaluation of the effect of the SPF. Tables 51 through 53 show the results of the mechanical properties tests in tension, compression, and fatigue, respectively. Figure 139 identifies specimen locations taken from the forward frame FF-13. The mechanical properties in the three material conditions are graphically compared for each grain direction, as shown in Figure 140.

The trend in tensile behavior is similar to that observed for Ti-6Al-4V, in that the strength of the thermally cycled and formed material was less than that of the as-received. However, the properties of the formed material are somewhat higher than those of Ti-6Al-4V.

The compressive yield strength also showed the same trend as that of the tensile yield strength, except that the quantities were somewhat higher. In the as-formed condition, the compressive yield strength falls within the scatter band for the tensile yield strength, indicating that no Bauschinger effect developed due to the SPF.

The fatigue properties evaluated in terms of failure cycles under constant-amplitude cycling stress showed that the as-formed condition was at least as good or better than those of the as-received condition. The fatigue properties for the thermally cycled condition was comparable to that of the as-received condition.

In general, the effect of SPF on mechanical properties of the Ti-6-2-4-2 alloy showed the same trend, but differed slightly in quantities when compared to those of Ti-6-4.


STRUCTURAL TESTS

Two of the frames, FF-12 and FF-14, were structurally tested to determine the effect of SPF on structural integrity of the frames made of Ti-6-2-4-2. The frames were first chem-milled to the test contours identical to those for the phase II forward frames shown in Figure 88. The test setups and procedures were also identical to those of the phase II, as shown in Figure 113.

225

TABLE 5i. TENSILE TEST RESULTS ON Ti-6-2-4-2 ALLOY IN THREE CONDITIONS: AS-RECEIVED, THERMALLY CYCLED, AND SUPERPLASTIC FORMED

Matl heat No.	Produced frame No.	Grain dir	Specimen condition	Specimen No.	Specimen thickness (in.)	F_{tu} (ksi)	F_{ty} (2% ksi)	Elongation %	Gage length
891380	FF-12	L	As received	T1	0.114	147.2	143.0	13	2
	FF-13	L	As received	T2	0.112	149.6	145.2	12	2
	FF-14	LT	As received	T5	0.116	148.7	145.3	12	2
		LT	As received	T6	0.113	150.7	149.0	11.5	2
		L	1,700° F/ 3 hr	T3	0.088	142.2	137.2	15	2
		L	1,700° F/ 3 hr	T4	0.085	145.0	136.7	15	2
		LT	1,700° F/ 3 hr	T7	0.088	143.3	138.6	14	2
		LT	1,700° F/ 3 hr	T8	0.069	143.2	136.8	14	2
		L	Formed	FT1	0.051	140.2	132.3	16	1
		L	Formed	FT2	0.065	143.8	137.5	14	1
		LT	Formed	FT3	0.062	142.6	136.1	14.5	1
		LT	Formed	FT4	0.052	140.9	130.5	14	1

226

TABLE 52. COMPRESSION TEST RESULTS ON Ti-6-2-4-2 ALLOY IN THREE
CONDITIONS: AS-RECEIVED, THERMALLY CYCLED,
AND SUPERPLASTIC FORMED

Heat No.	Condition	Grain dir	Specimen No.	Thickness (in.)	2% F_{cy} (ksi)	EC 10^6 (psi)
891380	As received	L	C9	0.115	151.3	17.0
		L	C10	0.112	150.3	18.1
		LT	C13	0.116	162.1	19.0
		LT	C14	0.113	165.8	19.2
	1,700° F/3 hr	L	C11	0.095	139.8	18.3
		L	C12	0.096	140.7	18.2
		LT	C15	0.095	144.6	19.3
		LT	C16	0.095	148.1	19.5
	As-formed (FF-13)	L	FC-5	0.060	133.0	17.3
		L	FC-6	0.050	136.3	17.9

227

TABLE 53. FATIGUE TEST RESULTS ON Ti-6-2-4-2 ALLOY IN
THREE CONDITIONS: AS-RECEIVED, THERMALLY CYCLED,
AND SUPERPLASTIC FORMED

| Heat No.	Condition	K_t	Grain dir	Specimen No.	Specimen thickness (in.)	Max stress			Cycles to failure
						% F_{tu}	ksi	R	
891380	As received	1	L	S17	0.117	80	118.7	0.05	44,000
			L	S18	0.115	80	118.7	0.05	47,000
			LT	S21	0.116	80	119.8	0.05	37,000
			LT	S22	0.115	80	119.8	0.05	18,000
		3	L	N25	0.116	50	74.2	0.05	12,000
			L	N26	0.115	50	74.2	0.05	9,000
			LT	N29	0.115	50	74.9	0.05	10,000
			LT	N30	0.115	50	74.9	0.05	5,000
	1,700° F/ 3 hr	1	L	S19	0.096	80	114.9	0.05	32,000
			L	S20	0.096	80	114.9	0.05	24,000
			LT	S23	0.093	80	114.6	0.05	41,000
			LT	S24	0.091	80	114.6	0.05	63,000
		3	L	N27	0.091	50	71.8	0.05	11,000
			L	N28	0.098	50	71.8	0.05	19,000
			LT	N31	0.097	50	71.6	0.05	20,000
			LT	N32	0.089	50	71.6	0.05	12,000
	As-formed FF-13 (trim area)	1	L	FS-10	0.067	80	113.5	0.05	175,000
			LT	FS-9	0.097	80	113.5	0.05	188,000
		3	L	FN-8	0.083	50	71.0	0.05	14,000
			LT	FN-7	0.078	50	71.0	0.05	20,000
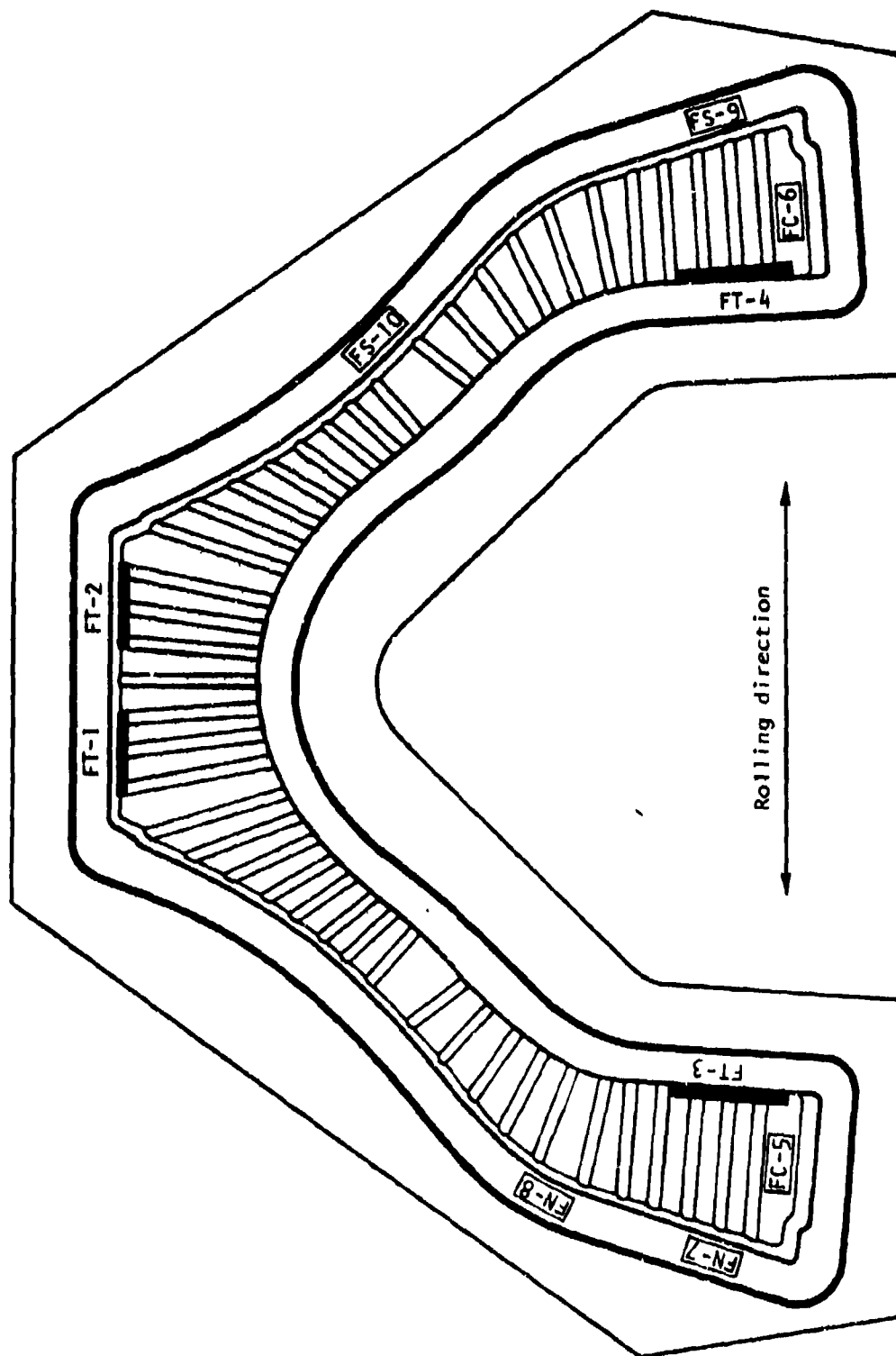
Figure 159. Mechanical test specimen locations taken from forward frame FF-15 (Ti-6-2-4-2 alloy, phase III).
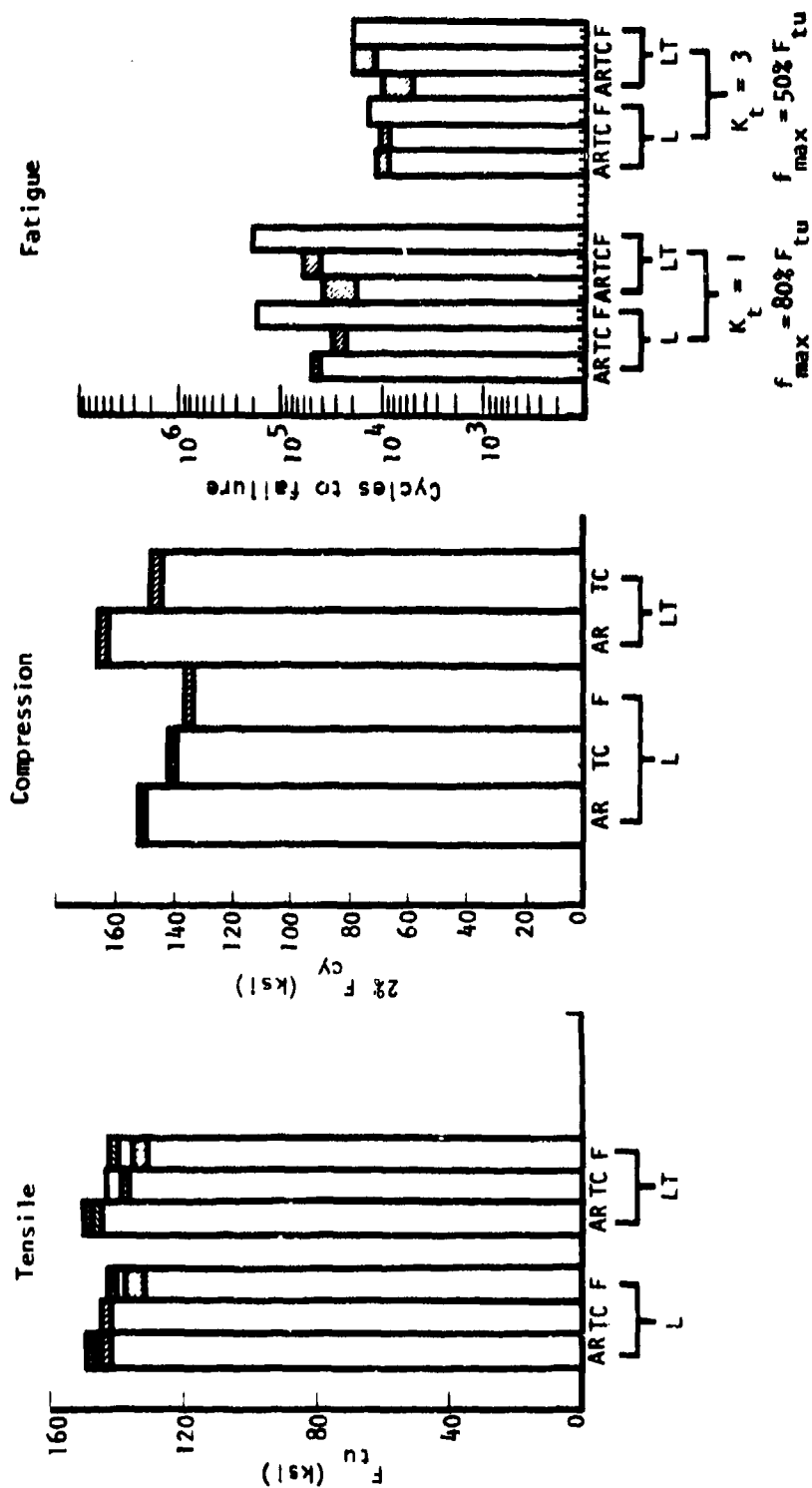
Figure 140. Comparison of mechanical properties for Ti-6-2-4-2 alloy in three conditions: as-received (N.A.), thermally cycled at 1,700° F, and superplastic formed.

For the two tests conducted on each of the two legs, the frames buckled in the anticipated location of the compressive flange before the structure showed general instability. This is consistent with the results obtained for the phase II frames which were made of Ti-6-4, indicative of the suitability of SPF extended to the new alloy.

The buckling loads for the two consecutive tests were 1,050 and 1,100 pounds calculated from the load gages used in the test setups. Using the approach used in analyzing phase II forward frames for its bending stresses and the predicted crippling strength yielded the following results:

$$C = 2.081 \text{ in.}$$

$$I_{NA} = 0.617 \text{ in.}^4$$

$$fb \text{ (1st leg)} = 17.4 \times 1.05 \times \frac{2.081}{0.617} = 61.62 \text{ ksi}$$

$$fb \text{ (2nd leg)} = 17.4 \times 1.10 \times \frac{2.081}{0.617} = 64.6 \text{ ksi}$$

$$Fcc = 0.044 \sqrt{117 \times 16.4 \times 10} = 60.9 \text{ ksi}$$

The preceding results demonstrate that the frames had crippled in a predictable manner and were consistent with results described earlier in phase II tests.

CONCLUSIONS

PHASE I

1. Ti-6Al-4V titanium alloy sheet having a uniform fine grain structure, a low grain aspect ratio, and the absence of acicular or blocky alpha exhibits good superplastic properties.

2. 6Al-4V titanium alloy sheet containing a heavily banded microstructure with acicular alpha exhibits poor superplastic properties, unsuited for forming parts which require substantial elongation.

3. A constitutive equation relating strain rate to flow stress provides an excellent representation of experimental data and can be used to compute a continuous function of strain-rate sensitivity index, m, as a function of strain rate.

4. The capability for forming deep drawn parts in Ti-6Al-4V sheet is directly related to the maximum strain-rate sensitivity index, m_{max}.

5. Ti-6Al-4V with a maximum strain-rate sensitivity index, m_{max}, of greater than 0.70 can be deep-drawn into sections at least 2 inches deep.

6. Argon gas contained within a mechanically sealed die will adequately protect exposed titanium surfaces and will provide the superplastic forming medium for titanium sheet at 1700F.

7. Thinning which occurs in unrestrained areas of the sheet during superplastic forming, essentially ceases on contact with the tooling resulting in a predictable and reproducible thickness profile.

8. The mechanical properties of superplastically formed Ti-6Al-4V sheet are comparable to those exhibited by other fully recrystallized products and, as such, are lower than for the as-received material in the mill annealed condition.

PHASE II

1. The capability of the superplastic forming process significantly exceeds that of the prior state-of-the-art conventional titanium forming processes.

2. The full potential of superplastic forming can be best achieved by designing to the process capabilities, which can result in more efficient design, fewer parts, lower cost, and lighter weight structure.

3. Superplastic forming of large frames designed for conventional hot size form is cost competitive with the conventional process.

4. Ti-6Al-4V sheet material can be superplastically formed into large complex die configurations up to at least 0.125 inch thickness with properly selected forming parameters.

5. An analytical model that assumes thinning only in free-forming sections and plane strain deformation will accurately predict thickness variations on full-scale parts in superplastic forming.

6. Dies made of 4140 or H13 steels will result in part dimensional deviations due to die material shrinkage during the 1,000F forming cycle. Better high temperature die materials will be required for production of parts with close-tolerance requirements.

7. Ti-6Al-4V sheet surface enrichment of 0.004 to 0.010 inch can occur as a reaction between the titanium and the die stop-off or lubricant on the lower part surface. The upper part surface exposed only to argon is not enriched.

8 Surface enrichment of the titanium sheet after forming is easily removed by chemical milling.

9. Superplastic forming of titanium sheet will produce structural elements capable of carrying equivalent loads as those produced by conventional processing.

PHASE III

1. Superplastic forming can be extended to other titanium alloys displaying superplastic characteristics, such as Ti-6Al-2Sn-4Zr-2Mo.

2. Identical superplastic process parameters can be utilized to form dissimilar titanium alloys possessing similar superplastic flow properties.

3. Mechanical, structural, and metallurgical properties and dimensional characteristics of Ti-6Al-2Sn-4Zr-2Mo superplastically formed sheet will behave similarly to Ti-6Al-4V superplastically formed sheet.

1. Paton, N. E., Rockwell International Science Center, unpublished data.

2. Lee, D., and Backofen, W. A., Trans Metallurgical Society of AIME, Vol. 239, 1034, July 1967.

3. Hamilton, C. H., Mills, J. A., "Superplastic Forming of Titanium Structures," AFML Technical Report IR-794-3 (IV), January 1974.

4. Bruhn, "Analysis and Design of Flight Vehicle Sturctures".

APPENDIX A

PROCESS SPECIFICATION FOR
SUPERPLASTIC FORMING OF TITANIUM SHEET

1. SCOPE

1.1 This specification establishes the requirements for elevated temperature superplastic forming of titanium alloy parts using material procured to specification MIL-T-9046 Type III, Composition C, D, or G. It includes material and processing requirements and quality requirements for the formed part.

2. APPLICABLE DOCUMENTS AND MATERIALS

2.1 Applicable Documents. The following documents, of the latest issue in effect, form a part of this specification to the extent specified herein. In the event of a conflict between the documents referenced herein and the contents of this specification, the contents of the specification shall be considered a superseding requirement.

Specifications

   Military

   MIL-S-5002   Surface Treatments and Inorganic Coatings for
                       Metal Surfaces of Weapons Systems

   MIL-C-81769   Chemical Milling of Metals, Specification for

   MIL-I-6866   Inspection, Penetrant Method of

   MIL-T-9046   Titanium and Titanium Alloy, Sheet, Strip and Plate

   MIL-A-18455   Argon, Technical

   American Society for Testing and Materials

   ASTM E-8   Tension Testing of Metallic Materials

3. REQUIREMENTS

3.1 Material. Titanium for superplastic forming shall be procured to MIL-T-9046, Type III, Composition C, D, or G, annealed.

3.2 <u>Surface Preparation</u>. The surfaces of the titanium alloy detail(s) prior to forming shall be cleaned in accordance with MIL-S-5002.

3.2.1 After cleaning per 3.2, titanium alloy detail(s) shall be suitably protected from contamination until the forming layup operation.

3.3 <u>Equipment</u>

3.3.1 <u>Heating Equipment</u>

3.3.1.1 Heating platens shall be capable of maintaining temperatures in the working zone within $\pm$50F of the indicated temperature. Temperatures shall be controlled by automatic and recording pyrometers or potentiometers.

3.3.1.2 Thermocouples shall be utilized to monitor and control part temperature

3.3.2 <u>Argon Gas</u>

3.3.2.1 The argon gas used for superplastic forming shall conform to MIL-A-18455. The moisture content or oxygen content of the argon shall not exceed 8 parts per million and the dew point shall be -80F or lower.

3.3.3 <u>Vacuum Systems</u>

3.3.3.1 The vacuum system used in superplastic forming titanium shall be capable of producing a vacuum gage reading of 1×10^{-4} TORR or better. The vacuum gage shall be installed in the evacuation line between the pack assembly and the cold trap or equivalent.

3.3.3.2 The vacuum system shall be capable of effectively removing condensible vapors, such as water vapor and mechanical and/or diffusion pump oil vapors, from the vacuum atmosphere in the assembled pack. The means to accomplish this must be at least equivalent in effectiveness to a liquid nitrogen cold trap.

3.4 <u>Tooling</u>

3.4.1 Forming tools shall have a surface finish of 125 RHR or finer and shall be free from scale, hydrocarbons and other foreign matter which might cause contamination of the formed part.

3.4.2 The tooling may be coated with 0.0003 to 0.0008 inches of dry graphite lubricant and should be a smooth adherent film free of pin holes, blisters and runs.

3.4.3 The forming chamber of the tooling shall be sealed from the atmosphere sufficiently to maintain a vacuum of 10^{-3} TORR.

3.5 Forming Parameters

3.5.1 Either vacuum or differential argon pressure forming may be used to obtain forming pressure.

3.5.2 Forming parameters of temperature, inert gas pressure, vacuum and time shall be controlled by documented procedures.

3.5.3 Argon Pressure Forming

3.5.3.1 Surfaces of parts shall be protected by an argon atmosphere during heatup. Free flow of argon shall be present on both sides of the material to be formed above a temperature of 800° F.

3.5.3.2 The rate of argon gas pressure increase to the maximum forming pressure shall be such that the maximum pressure is not reached earlier than 30 minutes after initiation of forming.

3.5.4 Vacuum Forming

3.5.4.1 Vacuum applied after reaching forming temperature shall reach 1×10^{-3} TORR or better within 30 minutes after first application of vacuum.

3.5.5 Maximum forming temperature shall not exceed 1750° F.

3.5.6 After forming has been accomplished the vacuum or argon atmosphere shall be maintained until the temperature drops below 800° F.

3.6 Following forming, surface enrichment shall be removed by chemical milling in accordance with MIL-C-81769 or by conventional machining. A minimum of 0.010 inch shall be removed from the surface contacting the tooling.

3.6.1 The surface of formed parts shall be free of cracks when examined per 4.6.2

3.7 Mechanical Properties

3.7.1 Superplastic formed parts shall conform to the mechanical property requirements of Table I when tested in accordance with 4.6.1.

TABLE I

MECHANICAL PROPERTIES

Ultimate Tensile Strength-Min. (ksi)	Yield Strength at 0.2% Offset-Min. (ksi)	Elongation in 4D or 2 In.-Min. (%)
125	115	10

3.7.2 Metal Thinning Due to Superplastic Forming

3.7.2.1 Metal thin-out in sheet metal parts due to superplastic forming is acceptable provided the thickness in the formed area is not less than 75% of the specified gage, except as noted in 3.7.2.2.

3.7.2.2 When closer thickness control is required or additional thinout is permitted, the minimum allowable thickness shall be noted on the drawing.

4. QUALITY ASSURANCE PROVISIONS

4.1 Responsibility for Inspection. Unless otherwise specified, the supplier is responsible for the performance of all inspection requirements specified herein. The supplier may utilize his own facilities or any commercial testing laboratory approved by the Procuring Agency. The Procuring Agency reserves the right to perform any of the inspection requirements set forth in this specification where such inspections are deemed necessary to assure that the product conforms to the specification requirement.

4.2 Acceptance. Compliance with the requirements of this specification shall be assured by detailed operating procedures and inspection requirements.

4.2.1 Inspection Record. An inspection record shall be maintained for each superplastic formed part and shall accompany each part through processing, and inspection.

4.3 **Equipment Approval**. The following shall be approved and/or calibrated prior to their use in the superplastic forming process: temperature measuring equipment, vacuum measuring instruments, vacuum valves, vacuum pumps, thermocouple locations, press and pressure gages.

4.4 **Temperature Measurements**. The temperature measuring system shall be capable of detecting any deviations from the pack assembly temperature. The temperature and time at temperature shall be monitored by control thermocouples placed between the heat source and the pack assembled unit and the temperature shall be recorded on a multipoint potentiometer chart.

4.5 **Process Verification**

4.5.1 Prior to production superplastic forming, a process verification part, i.e., the first part fabricated of a particular type design after the forming tool design and the manufacturing and process sequence have been established, shall be evaluated to determine compliance with all the requirements of this specification. Evaluation for surface enrichment and mechanical properties shall be made on coupons cut from the part and prolongations.

4.5.2 Acceptance of superplastic formed parts shall not be permitted until process verification part has met all requirements of this specification.

4.5.3 The process shall be subject to requalification when changes are made in processing parameters, tooling, etc.

4.6 **Test Methods** (Process Verification and Production Parts)

4.6.1 **Tensile Testing** - Tensile testing shall be in accordance with ASTM E-8.

4.6.2 **Penetrant Inspection**. Penetrant inspection shall be in accordance with MIL-I-6866.

4.6.3 **Metallurgical Evaluation**. Mounted metallographic samples shall be etched and examined to evaluate depth of enrichment.

5. PREPARATION FOR DELIVERY

Not applicable.

6. NOTES

6.1 Definitions

6.1.1 Superplastic forming is a process in which the titanium sheet material is heated to elevated temperatures and its shape substantially changed by maintaining a pressure differential by applying a vacuum on one side of the titanium sheet and a positive pressure (argon gas) on the opposite side, or an argon pressure differential, causing the titanium sheet to fill the die cavity and take the shape of the tooling within the cavity.